The novel role of mitochondrial morphology in cardioprotection

Thesis submitted by

Sang Bing, Ong

BSc (1st Class Hons) MSc (Merit)

For the degree of

Doctor of Philosophy

Faculty of Biomedical Sciences, Division of Medicine

University College London (UCL)

The Hatter Cardiovascular Institute

University College London Hospital & Medical School
67 Chenies Mews, UCL
London, WC1E 6HX. UK.

September 2010

Declaration

I, Sang Bing Ong, confirm that the work presented in this thesis is my own. Where information has been derived from other sources, I confirm that this has been indicated in the thesis. Construction of adenoviral constructs containing mitochondrial-targeted photo-activatable green fluorescent protein (mtPA-GFP) was performed by Dr. Sapna Arjun, who is a postdoctoral fellow in our laboratory. Isolation of rat endothelial cells was performed by Dr. Sean Davidson, Senior Research Fellow in our laboratory. Preparation of heart slices for electron microscopy was done by Mr. Mark Turmaine of the Electron Microscopy Unit in UCL. The *in vivo* work has been performed by another postdoctoral fellow in our laboratory, Dr. Shiang Yong Lim.

Mr. Sang Bing Ong

This thesis is dedicated to my nanny, who took care of me with love and tenderness when I was little, but passed away due to heart failure in the year 2010

Abstract

Background– Mitochondria are able to change their morphology by undergoing either ‘fusion’ to form elongated interconnected networks or ‘fission’ to generate fragmented disconnected mitochondria. We investigated whether changes in mitochondrial morphology influence susceptibility of the heart to ischaemia-reperfusion injury (IRI). We hypothesised that promoting mitochondrial fusion protects the heart against IRI by inhibiting mitochondrial permeability transition pore (mPTP) opening. **Methods/Results**– Mitochondrial fusion was induced in a HL-1 cardiac cell line by: 1), over-expressing Mitofusin 1 or 2 (known mitochondrial fusion proteins) or $Drp1_{K38A}$ (a dominant negative mutant form of Drp1, a known mitochondrial fission protein), 2), using the drug *mdivi-1* (a Drp1 small molecule inhibitor) and 3), over-expressing or pharmacologically activating Akt1 (a known pro-survival kinase involved in growth and proliferation). Promoting mitochondrial fusion decreased mitochondrial permeability transition pore (mPTP) sensitivity and reduced cell death following simulated IRI (SIRI). In contrast, inducing mitochondrial fragmentation by over-expressing hFis1 (a known mitochondrial fission protein), enhanced cell death following SIRI but had no effect on mPTP opening. Treatment with *mdivi-1* decreased mPTP sensitivity and reduced cell death in both HL-1 cells and adult murine cardiomyocytes following SIRI, and reduced myocardial infarct size in the adult murine heart. Elongated adult cardiac mitochondria (4-6 μM) were observed using electron and confocal microscopy in adult murine hearts and these were increased with *mdivi-1* treatment prior to ischaemia.

Conclusions–For the first time we show that modulating mitochondrial morphology can influence the susceptibility of the heart to IRI. We show that inducing mitochondrial fusion protects the heart against IRI. These findings provide a novel pharmacological target for cardioprotection.

Acknowledgements

I would like to express my sincerest thanks to my supervisors, Dr. Derek Hausenloy and Professor Derek Yellon for selecting me to be a Biotechnology and Biological Sciences Research Council (BBSRC) – Hatter Foundation - Dorothy Hodgkin Postgraduate Award (DHPA) scholar in the Hatter Cardiovascular Institute, hence allowing me to undertake doctoral studies in the United Kingdom.

For Dr. Derek Hausenloy, my primary supervisor, special thanks for always being there for me, for coaching and guiding me throughout the duration of my PhD, for always caring for me, giving me opportunities to attend conferences, co-author papers and participate in exchange research programmes, and always giving me a smile whenever you turn around upon hearing me knocking on your office door and last but not least, for allowing me to study the role of mitochondrial morphology in cardioprotection.

For Professor Derek Yellon, my secondary supervisor, without whom the Institute would not be able to flourish, prosper and attain the level of greatness as it currently enjoys. I thank you personally for the weekly supervision slots, allowing me to voice my concerns and opinions, for allowing me to participate in my first ever international mitochondrial meeting in the United States which served as an important source of inspiration and most important of all, for sourcing the other half of the funding to pair up with the matching fund from the BBSRC to create a DHPA for me.

I also thank Dr. Sean Davidson for imparting to me all the research skills needed for this study, for always teaching me patiently, never once losing his temper and always helping me out whenever I encountered problems in my project and most importantly, showing me a good example of how a senior or mentor should be when teaching the juniors scientists.

I am also extending my thanks to other scientists or principal investigators whom I met during the course of my PhD in London; Dr. Gyorgy Szabadkai (UCL) for kindly being the examiner for my MPhil/PhD upgrade, Professor Michael Duchen

(UCL) for allowing me to use his Wellcome Trust-funded confocal microscopes when I first started my PhD, Mark Turmaine of the UCL Electron Microscopy Unit for kindly processing the adult murine hearts for electron microscopy (EM) imaging, Professor Jim Downey (University of South Alabama) for kindly reviewing my CV in the American context, Professor Luca Scorrano (University of Geneva) for providing me with the plasmids needed, allowing me to visit his laboratory in Geneva and collaborating on the Akt project as well as Dr. Asa Gustafsson (UC San Diego) for kindly providing me with my first postdoctoral appointment in advance.

I thank the members of the laboratory who have helped me in various aspects of the project, Sapna, Suma, Max, Hilary, Louise, Marta, Cara, Vikram, Abi and all the past and present research and clinical fellows. To my brothers, Ging and little Geng, who have been a source of joy, food-source, information point and willing listener to me, I thank both of you. To Rachel Tan, my good friend from Singapore, who is also studying for a PhD at UCL, I am glad to be able to share opinions and troubles with her. To all the students who have worked with me on some of these projects – Gary, Annie, Jie Hann, Martin, Uma and Rachel, it has been fun to teach and learn with them. To my friends working in Mayling and Wong Kei restaurants in London, I appreciate you all for constantly providing extra food for me.

To my fiancée, Shel-Hwa Yeo, who is also a PhD student at the University of Otago in New Zealand, I express sincerest love, gratitude and thanks to her for being so understanding and patient with me, for being so brave and independent hence allowing me to focus on my work without having to worry about her, chatting to me every weekend and for sharing all about life in NZ with me.

Last but not least, I thank my parents and God who kindly brought me to this world, brought me up, nurtured, taught and educated me and always being there for me.

TABLE OF CONTENTS

TABLE OF FIGURES

Chapter One: GENERAL INTRODUCTION

Chapter Three: GENERAL METHODS

Chapter Four: MODULATION OF MITOCHONDRIAL MORPHOLOGY IN CARDIAC CELLS

Page

Chapter Five: PROTECTING THE HEART AGAINST ISCHAEMIA-REPERFUSION INJURY BY MODULATING MITOCHONDRIAL MORPHOLOGY Page

Chapter Seven: LINKING PRO-SURVIVAL KINASES TO CARDIOPROTECTION VIA MITOCHONDRIAL DYNAMICS Page

LIST OF TABLES

Chapter One: GENERAL INTRODUCTION

LIST OF ABBREVIATIONS

The following is a list of abbreviations used in this thesis:

%	percentage
AAR	area-at-risk
ADP	adenosine diphosphate
AIF	apoptosis-inducing factor
Akt	cellular Akt/protein kinase B
AMI	acute myocardial infarction
AMP	adenosine monophosphate
AMPK	AMP-activated protein kinase
ANF	atrial natriuretic factor
ANOVA	analysis of variance
ANT	andenince nucleotide translocase
APAF-1	apoptosis protease-inducing factor 1
APD	action potential duration
ATP	adenosine triphosphate
ATPase	ATP synthase
Bad	Bcl-XL/Bcl-2-associated death promoter
Bax	Bcl-associated X protein
BDM	2, 3 – butanedione monoxime
BSA	bovine serum albumin
Ca^{2+}	calcium ion
caAkt	constitutively-activated Akt
CaMK	calcium/calmodulin dependent protein kinase
cAMP	cyclic adenosine monophosphate
CARD	caspase-recruitment domain
CAT	carboxyatractylate
cBiMPS	Sp-5,6-Dichloro-cBIMPS
Cdk1	cyclic dependent kinase 1
Cl^-	chloride
CLSM	confocal laser scanning microscopy

CMV	cytomegalovirus
CsA	ciclosporin A
CypA	cyclophilin A
CypD	cyclophilin D
Cys	cysteine
Da	Dalton
DIABLO	direct IAP-binding protein with low pI
DKO	double knock-outs
DMSO	dimethyl sulphoxide
DNA	deoxyribonucleic acid
2-DOG	2-deoxyglucose
Drp1	dynamin-related protein 1
ECG	electrocardiogram
EDTA	ethylenediaminetetraacetic acid
eNOS	endothelial nitric oxide synthase
EPO	erythropoietin
ER	endoplasmic reticulum
Erk	extracellular signal-regulated MAPK
ETC	electron transport chain
FAD	flavin adenine dinucleotide
FMN	flavin mononucleotide
Fzo	*fuzzy onions*
GED	GTPase effector domain
GFP	green fluorescent protein
GLP	glucagon-like peptide
GSK	glycogen synthase kinase
GTP	guanosine triphosphate
H^+	hydrogen ion/proton
HCO^-_3	hydrogen carbonate ion
HEPES	4-(2-hydroxyethyl)-1-piperazineethanesulfonic acid
hFis1	human fission protein 1
HPO^-_4	hydrogen phosphate ion
H_2O	water
iNOS	inducible nitric oxide synthase

IMM	inner mitochondrial membrane
IPC	ischaemic preconditioning
IPost	ischaemic postconditioning
IP_3R	inositol trisphosphate receptor
IR	ischaemia reperfusion
IRI	ischaemia reperfusion injury
K^+	potassium ion
K_{ATP}	ATP-sensitive potassium channel
kDa	kilodalton
LAD	left anterior descending
LV	left ventricular
M	molar
MABP	mean arterial blood pressure
MAPK	mitogen activated protein kinase
mdivi-1	mitochondrial division inhibitor 1
MEF	mouse embryonic fibroblast
Mfn1	mitofusin 1
Mfn2	mitofusin 2
Mg^{2+}	magnesium ion
Mgm1	mitochondrial genome maintenance 1
MI	myocardial infarction
min	minutes
$mitoK_{ATP}$	mitochondrial KATP
mM	milimolar
µM	micromolar
mPTP	mitochondrial permeability transition pore
mRNA	messenger RNA
mtPA-GFP	mitochondrial-targeted photo-activatable green fluorescent protein
mtRFP	mitochondrial-targeted red fluorescent protein
Na^+	sodium ion
NADH	nicotinamide adenine dinucleotide
NADPH	nicotinamide adenine dinucleotide phosphate
NFAT	nuclear factor of activated T-cells

NGF	nerve growth factor
nm	nanometres
NO	nitric oxide
NOS	nitric oxide synthase
NRF1	nuclear respiratory factor 1
OMM	outer mitochondrial membrane
OPA1	optic atrophy 1
PAO	phenylarsine oxide
PARL	presenilin associated rhomboid-like protease (PARL)
PB1	perfusion buffer 1
PB2	perfusion buffer 2
PCI	primary coronary intervention
PDGF	platelet-derived growth factor
PDK	3’-phosphoinositide-dependent protein kinase
pEGFP	plasmid-enhanced green fluorescent protein
PGC-1alpha	peroxisome proliferator-activated receptor-gamma coactivator 1 alpha
PI	propidium iodide
PI3K	phosphatidyl inositol 3’-OH kinase
PKA	protein kinase A
PKB	protein kinase B
PKC	protein kinase C
PPIase	peptidyl prolyl transisomerase
P70S6K	70-kDa ribosomal protein S6 kinase
RISK	reperfusion injury salvage kinase
RNA	ribonucleic acid
ROI	region of interest
rpm	revolution per minute
ROS	reactive oxygen species
RyR	ryanodine receptor
SEM	standard error of mean
Ser	serine
SfA	sanglifehrin A
sIR	simulated ischaemia reperfusion

sIRI	simulated ischaemia reperfusion injury
SMAC	second mitochondrial activator of caspases
SO^{2-}_4	sulphate ion
SR	sarcoplasmic reticulum
TFAM	transcription factor A, mitochondrial
Thr	threonine
TMRM	tetramethyl rhodamine methyl ester
TTC	triphenyltetrazolium chloride
2-DOG	2-deoxyglucose
UK	United Kingdom
UV	ultraviolet
VDAC	voltage-dependent anion channel

LIST OF PUBLICATIONS

The following is a list of publications arising from the thesis:

ORIGINAL RESEARCH ARTICLES (peer-reviewed)

1. *Sang-Bing Ong*, Sapna Subrayan, Shiang Y Lim, Derek M Yellon, Sean M Davidson, Derek J Hausenloy. 'Inhibiting mitochondrial fission protects the heart against ischaemia/reperfusion injury.' ***Circulation*** 2010: 121 (18): 2012 – 2022.

REVIEWS (peer-reviewed)

1. *Sang-Bing Ong*, Derek J. Hausenloy. 'Mitochondrial morphology and cardiovascular disease.' ***Cardiovascular Research*** 2010. *In press*.

2. Derek J. Hausenloy, *Sang-Bing Ong*, Derek M. Yellon 'The mitochondrial permeability transition pore as a target for preconditioning and postconditioning.' ***Basic Research in Cardiology***. 2009: 104 (2): 189 – 202.

ABSTRACTS (peer-reviewed)

1. *SB Ong*, S Arjun, SY Lim, DM Yellon, SM Davidson, DJ Hausenloy. Modulating mitochondrial dynamics as a novel cardioprotective strategy. ***Heart*** 2010: 96 (11) Suppl 1: A10 – A 11

2. *SB Ong*, S Arjun, SY Lim, DM Yellon, SM Davidson, DJ Hausenloy. Keeping your mitochondria in shape to protect your heart. ***J. Mol. Cell. Cardiol***. 2010: 48 (5) Suppl 1: S167 – S168

3. Mocanu MM, *Ong SB*, Mukherjee UA, Davidson SM, Yellon DM, Hausenloy DJ. PTEN inducible kinase-1 (PINK1): A novel mitochondrial target for myocardial protection. ***Eur J Heart Failure*** 2009: 8 (Suppl 2): ii1–ii826

4. Hausenloy DJ, *Ong SB*, Davidson SM, Yellon DM. Changing the shape of mitochondria protects the HL-1 cardiac cell against simulated ischaemia-reperfusion injury. ***Eur J Heart Failure*** 2009: 8 (Suppl 2): ii1–ii826

5. *SB Ong*, SM Davidson, DM Yellon, DJ Hausenloy 'Mitochondrial fusion by genetic or pharmacological manipulation protects against ischaemia-reperfusion injury.' ***Heart*** 2009: 95(Suppl I): E

6. *SB Ong*, SM Davidson, LK Ho, DM Yellon, DJ Hausenloy 'Mitochondrial fusion protects against ischaemia-reperfusion injury.' ***Heart*** 2009: 95 (4): e1

Young Research Worker's Prize (Finalist), British Cardiovascular Society (BCS) 87th Annual Conference & Exhibition, 1 – 3 June 2009, ExCeL, London UK.
SB Ong - 'Keeping mitochondria in shape for cardioprotection'

Chapter One: GENERAL INTRODUCTION

1.1 Epidemiology of Coronary Artery Disease

Cardiovascular disease is the leading cause of death worldwide. It is responsible for over 200,000 deaths per year in the United Kingdom and was the cause of 17.5 million deaths in the year 2005, according to the World Health Organisation [1, 2]. It has been estimated that the overall money spent on tackling cardiovascular disease in the UK amounts to 30.7 billion pounds per year with 47% of this for health care, followed by 27% for productivity losses due to mortality and morbidity, and the remaining 26% to informal care-related costs [3]. Therefore, it is essential that cardiovascular research be carried out to explore every avenue for improving the treatment of cardiovascular disease.

Cardiovascular disease in general, refers to the diseases of the heart and circulatory system, with the prevalent form of cardiovascular disease being coronary heart disease and cerebrovascular disease [4]. Cardiovascular disease has a pathogenetic pathway that is complex in nature and is triggered by various environmental factors such as smoking, diet, sedentary lifestyle, alcohol, diabetes and obesity [5, 6]. Modern scientific research has established that cardiomyocyte death caused by prolonged coronary artery occlusion is the major and most acute form of cardiovascular disease [5, 7]. The occluded coronary artery is unable to provide sufficient oxygen and nutrient supply to the myocardium, causing the tissue to become ischaemic and infarct [7] (details in Section 1.2.1.1). Following an episode of ischaemia or restriction of blood supply, revascularisation of the infarcted tissue results in ischaemia-reperfusion injury (IRI) which leads to subsequent myocardial infarction, cardiac arrhythmias and contractile dysfunction [8, 9] (details in Section 1.2.1.2). Cardiomyocytes are terminally differentiated and difficult to replace once dead, hence causing loss of function to the myocardium and finally a diseased heart [5]. The death pathway involves either apoptosis, a highly regulated programmed cell death mechanism or necrosis, a highly detrimental, unregulated form of cell death [5, 10]. Apoptosis can be differentiated from necrosis based on the amount or levels of adenosine triphosphate (ATP), a coenzyme responsible for transferring energy within cells, available. The occurrence of apoptosis relies on the presence of a high amount

of ATP whereas necrosis occurs when the ATP is scarce [11]. These different forms of cell death will be discussed in greater detail in Section 1.2.3.

The major cause of cardiovascular morbidity and mortality - acute myocardial IRI is discussed in the following section (see Section 1.2).

1.2 Myocardial Ischaemia-Reperfusion Injury

Myocardial reperfusion injury is a term used to depict the injury to the heart culminating in cardiomyocyte death, caused by restoration of coronary blood flow after a prolonged blockage. Occlusion of the coronary artery will lead to progressive damage over time with changes in the contractility, metabolism and ultrastructural features of the myocardium [12-15]. Ischaemia-reperfusion injury has been the subject of much debate, specifically as to whether the period of ischaemia is the main cause of cell death or whether the period of reperfusion exacerbates the injury inflicted during ischaemia and causes cell death [16]. In laboratory animals, reperfusion generally has to be initiated within 20 minutes of the onset of ischaemia to prevent the occurrence of necrosis and permanent damage as prolonged ischaemia will lead to only modest or non-functional recovery [12]. Nevertheless, recent studies have used a 30 minute ischaemia protocol with varying durations of reperfusion, depending on whether a Langendorff-perfused heart [17-19] or *in vivo* infarct model [20, 21] is used as the endpoint of interest. The concept of reperfusion injury was founded on the basis of experimental results showing a higher abundance of cell death following ischaemia-reperfusion compared to ischaemia alone. In a study by Vanden Hoek *et al* using chick cardiomyocytes and propidium iodide staining for demarcation of cell death, they found that there was 17% of cell death in the group of sustained ischaemia versus 73% of cell death in the reperfused group when 4 hours ischaemia and 4 hours of reperfusion were compared to 1 hour ischaemia and 3 hours reperfusion. Ischaemia alone causes cell death due to deprivation of oxygen [22]. Apart from causing deleterious global injury, reperfusion also triggers a myriad of inflammatory effects which exacerbate the local insult [23-25]. In the following section 1.2.1, we will explore the different metabolic and biochemical changes that occur during ischaemia and reperfusion.

1.2.1 Pathogenesis of Ischaemia-Reperfusion Injury

1.2.1.1 Metabolic & Biochemical Consequences of Myocardial Ischaemia

Complete occlusion of the coronary artery due to the formation of a thrombus at a site of atherosclerotic rupture deprives the cardiac tissue of oxygen. The deprivation of oxygen causes uncoupling of oxidative phosphorylation by impairing the electron flow through the respiratory chain leading to an accumulation of Nicotinamide adenine dinucleotide hydrogenase (NADH) and flavin adenine dinucleotide hydrogenase (FADH) and subsequent termination of ATP production [13, 14]. The impaired electron flow causes the collapse of mitochondrial membrane potential as the electrochemical gradient across the inner mitochondrial membrane is no longer maintained [26]. The remaining ATP is then hydrolysed by the F_0F_1-ATPase causing the accumulation of catalytic metabolites such as hypoxanthine which can be oxidised to release free radicals [27]. The lack of ATP and oxygen causes the cells to utilise anaerobic glycolysis instead of aerobic respiration for ATP production [13, 14, 28]. The process of glycolysis causes a build-up of lactic acid, hence accumulating H^+ ions in the cytosol. The decrease in intracellular pH activates the Na^+/H^+ exchanger to remove the cytosolic protons but inadvertently causes accumulation of Na^+ ions [13, 14, 28]. The Na^+/K^+-ATPase which is responsible for removal of the Na^+ ions is inactivated because of the lack of ATP and increasing intracellular phosphate (P_i) [13, 14, 28]. The increasing levels of Na^+ triggers the Na^+/Ca^+ exchanger to function in reverse, causing accumulation of intracellular Ca^{2+} while removing the Na^+ [29]. The high levels of cytosolic Ca^{2+} results in mitochondrial accumulation of Ca^{2+} via the mitochondrial Na^+/Ca^{2+} exchanger and transfer of Ca^{2+} from endoplasmic reticulum (ER) [30]. In summary, following a period of sustained myocardial ischaemia, there is a decrease in intracellular pH (< 7.0), elevated levels of intracellular Ca^{2+} and [P_i], and ATP depletion.

1.2.1.2 Metabolic & Biochemical Consequences of Myocardial Reperfusion

Following ischaemia, the restoration of blood flow re-oxygenates the ischaemic cardiac tissue. This reperfusion causes repolarisation of the mitochondrial membrane

potential and subsequent re-activation of the respiratory chain [30], triggering the production of reactive oxygen species (ROS) and oxidation of NADH/FADH [12, 16, 23, 31, 32]. Reperfusion also leads to the wash-out of lactic acid, which restores the physiological pH. The levels of calcium drops initially but is then restored via the activation of the Ca^{2+}-uniporter by recovery of the mitochondrial membrane potential [33, 34]. The different factors and changes which takes place during ischaemia and the onset of reperfusion convenes to mediate cell death by triggering the opening of the mitochondrial permeability transition pore (mPTP) [23, 31, 35], a crucial mediator of cell death which will be discussed in greater details in Sections 1.2.2.4 and 1.7.

1.2.2 Mediators of Lethal Myocardial Ischaemia-Reperfusion Injury

In this section, we will explore in greater detail the individual changes happening during ischaemia and reperfusion that ultimately lead to lethal myocardial IRI.

1.2.2.1 Re-oxygenation & production of reactive oxygen species (ROS)

Re-oxygenation or re-vascularisation itself is a potent mediator of IRI. The respiratory chain in the mitochondria is re-initiated following oxygenation and thus leading to ROS generation by xanthine oxidase (O-form) which is derived from xanthine dehydrogenase (D-form) through a conformational change [36]. ROS is a general term encompassing molecules including superoxide (O_2^-), peroxynitrite ($ONOO^-$), singlet oxygen (O^-), and hydroxyl (OH^-) [37]. The process of hypoxia and pathological conditions such as cardiovascular diseases triggers an elevated level of xanthine oxidase, particularly in the endothelial cells lining the blood vessels of the heart [38]. During the conversion of hypoxanthine to xanthine and xanthine to uric acid, oxygen is used as an electron acceptor, producing $O_2^{\bullet-}$ and hydrogen peroxide (H_2O_2) as side products [36, 37].

Another source of ROS is the NADPH oxidase originating from neutrophils or the superoxide produced from eNOS/iNOS [39]. The non-phagocytic NADPH oxidases are termed as the NOX family, which comprises of seven isoforms: NOX1, NOX2 (formerly gp91phox), NOX3, NOX4, NOX5, and dual oxidases 1 and 2 (DUOX1 and DUOX2) [37, 40]. These isoforms are transmembrane proteins with

subunits located in both the cytosol and cellular membrane [40]. Upon binding of the subunits to each other to form a functional isoform, the transmembrane complex is able to transport electrons across the membrane to reduce O_2 to $O_2^{\bullet -}$ [37]. The evidence supporting the role of NOX in tissue damage following myocardial infarction remains debatable but there are studies detecting an enhanced expression level of NOX in patients with myocardial infarction or coronary heart disease [41-43].

eNOS is a homodimer comprising of two monomers which consist of both a reductase domain and an oxygenase domain [44, 45]. The reductase domain is crucial for binding of NADPH, FAD, and flavin mononucleotide (FMN) while the oxygenase domain is responsible for carrying a prosthetic heme group for proper dimerisation of both monomers. The oxygenase domain binds (6R)-5,6,7,8-tetrahydrobiopterin (BH_4), molecular oxygen, and the substrate l-arginine to become a fully functional enzyme complex [44, 45]. eNOS catalyses an electron transfer within the reductase domain from NADPH via the flavins FAD and FMN to the heme in the oxygenase domain [46]. In patients with hypertension [47] or hypercholesterolemia-associated endothelial dysfunction [48], there will be a reduction in tetrahydrobiopterin and L-arginine due to a perturbation in the electron flow within eNOS. Because of this reduction in the cofactor tetrahydrobiopterin and L-arginine as a substrate for eNOS/iNOS, production of superoxide (O_2^-) increases. The effects of NO can be controversial as NO is involved in cardioprotection but also mediates IR injury by reacting with the superoxide produced to form peroxynitrite ($ONOO^-$) which will dissociate into cytotoxic NO_2 and OH^- [49, 50].

The presence of ROS will lead to lipid peroxidation [32], induction of calcium overloading in the mitochondria [39], oxidative damage to the DNA [51] and opening of the mPTP [52]. In addition to opening the mPTP, ROS also reduces the bioavailability of the intracellular signaling molecule, nitric oxide, which is known to confer cardioprotection effects by inhibition of neutrophil accumulation, inactivation of superoxide radicals, and improvement of coronary blood flow.

1.2.2.2 Calcium Overloading

The calcium overload induced by the Ca^{2+}-induced Ca^{2+} release is a phenomenon that occurs in mitochondria due to the failure of the normal Ca^{2+} regulation system as a result of sarcolemmal-membrane damage, dysfunction of the sarcoplasmic reticulum (SR) and reversal of the Na^{+}-Ca^{+} exchanger, all of which are caused by the increased levels of ROS [53]. Calcium overloading will lead to cardiomyocyte cell death by opening of the mPTP triggered by the restoration of physiological pH following the wash out of lactic acid and hypercontracture, a term to describe the irreversible deformation of cytoskeletal elements in the cardiomyocyte [53]. Experimental studies have shown that using pharmacological agents that inhibit the sarcolemmal Ca^{2+} ion channel, the mitochondrial Ca^{2+} uniporter, or the sodium–hydrogen exchanger decreased myocardial infarct size by up to 50% [54, 55]. Nevertheless, corresponding clinical studies have been found to be inconclusive [56, 57].

1.2.2.3 pH Restoration

The pH paradox is a phenomenon where the restoration of physiological pH occurs upon washout of lactic acid from glycolysis and subsequent activation of the sodium–hydrogen exchanger and the sodium–bicarbonate symporter and this has been identified as a cause of reperfusion injury [58]. Reoxygenation with acidic buffer to maintain a low pH has been shown to protect the neonatal rat cardiomyocytes [59], although clinically, this has been yet to be successful [57, 60].

1.2.2.4 Opening of the Mitochondrial PTP

The mPTP is a nonselective channel in the inner mitochondrial membrane. Opening of the mPTP, which constitutes a cyclophilin D (CypD) component, causes the collapse of the mitochondrial membrane potential and uncoupling of oxidative phosphorylation which causes ATP depletion and cell death, hence placing the mPTP as a critical factor of lethal reperfusion injury [61]. It has been found that the mPTP remains closed during myocardial ischaemia and only opens at the onset of

reperfusion following the introduction of ROS, mitochondrial Ca^{2+} overload, pH increase and depletion of ATP [62, 63]. Further details regarding the mPTP are available in Section 1.7.

1.2.3 Damaging effects of Myocardial Ischaemia-Reperfusion Injury

Lethal myocardial reperfusion injury causes cell death largely by necrosis which is proven by the fact that the central zone of the infarct is mainly made up of a necrotic band which depends on the duration of the ischaemia. Necrosis causes the loss of cellular integrity whereby the outflow of cytosolic contents triggers an inflammatory response [64]. Apoptosis, located in the peri-infarcted area, is highly-regulated and energy dependent and is hampered by the lack of ATP production during ischaemia, but is re-activated during reperfusion [65] (see Figure 1.1).

Death of cardiomyocytes in this setting is the main cause of an increase in infarct size of up to 50% and deaths following a myocardial infarction (MI). Extensive research in animal models have been conducted to reduce infarct size following an MI but these have yet been successfully transferred to clinical settings [66].

The successful application of ischaemic postconditioning (IPost) in which reperfusion therapy is initiated by short-lived episodes of myocardial ischaemia has sparked interest in pursuing the reperfusion phase as a target for cardioprotection, especially following the elucidation of the Reperfusion Injury Salvage Kinase (RISK) pathway (see Section 1.6.2.3) and the mPTP (see Section 1.7) as an end-point for conferring cardioprotection [67, 68]. Formulation of new therapies based on these findings should improve clinical outcomes in acute myocardial infarction and reduce the risk of heart failure following MI.

1.2.3.1 Apoptotic cell death

Apoptosis is a well-organised, highly-regulated, energy-dependent suicidal process whereby a cell commits suicide without damaging the surrounding tissue and is a normal process which occurs during development, tissue turnover, and in the immune system [5]. Apoptosis is characterised by the fact that it is controlled at the

genetic level, and is crucial for cells that are in certain stages of development or senescence [5, 69].

There are two distinctive stages in mitochondrial-related apoptosis: first where the proapoptotic protein Bax translocates from the cytosol to the mitochondria; and second where the mitochondria release cytochrome *c* from the intermembrane space into the cytosol [70]. The Bcl-2 gene, an oncogene that participates in the development of human B cell lymphomas is actively involved in the apoptosis process in mammalians [71]. The Bcl-2 gene encodes for different proteins that are either pro-apoptotic (Bad, Bax, Bid) or anti-apoptotic (Bcl-2, Bcl-x_L). The balance of these proteins determines the cell fate. The mitochondria in eukaryotes are a target of the apoptotic Bcl-2 family proteins such as Bax and Bak. Death signals induce the translocation of the apoptotic protein from the cytosol to the outer membrane of the mitochondria, leading to the release of cytochrome *c*, apoptosis-inducing factor (AIF) and the Smac/Diablo proteins from the intermembrane space. Cytochrome *c* is nuclear-encoded and is translocated to the mitochondrial intermembrane space upon synthesis [72]. A haem group is added to localise the cytochrome *c* in this space. Cytochrome *c* functions to shuttle the electrons from complexes III to IV in the mitochondrial electron transport chain [73]. Only once released can the cytochrome *c* exerts its apoptotic effects [74]. Apoptotic protease activating factor 1 (Apaf-1) can bind to cytochrome *c* upon initial binding of dATP/ATP and subsequent hydrolysis. Once Apaf-1 binds with cytochrome *c*, it undergoes oligomerisation and exposure of the caspase-recruitment domain (CARD). The existing CARD region on procaspase-9 induces binding to the CARD on Apaf-1, thus forming a complex known as apoptosome and subsequent activation of procaspase-9. Activated caspase-9 is then released to activate downstream caspases such as caspase 3, -6 and -7 through proteolytic cleavage to execute cell death action [75]. Smac/Diablo functions to inhibit proteins that inhibit apoptosis (IAP). AIF in the cytosol translocates to the nucleus where it causes chromatin condensation and DNA fragmentation [73].

Two causes underlie the release of proapoptotic proteins from the intermembranous space: the formation of non-specific channels in the outer membrane and the rupture of the outer membrane following swelling of the

mitochondrial matrix in the event of mPTP opening [76]. Besides the release of cytochrome *c* from mitochondria, apoptosis is also initiated by the ligation of membrane-bound death receptors such as the tumour necrosis factor receptor (TNF) family [5, 77].

Apoptosis is linked with two main variations in mitochondria: mPTP opening and mitochondrial fusion/fission, through cristae remodelling the proteins involved in the different processes such as the Bax protein which interacts with the mPTP components and certain fusion/fission proteins such as the Drp1 and Mfn2 [11]. Regulators of apoptosis include inhibitors of caspases e.g., cellular FADD-like inhibitory protein (cFLIP) and the inhibitor of apoptosis (IAP) family, Bcl-2 family of proteins and growth factors [5].

Detection of apoptosis is usually conducted through two assays; Terminal deoxynucleotidyl-transferase-mediated dUTP nick end labelling (TUNEL) assay and *in situ* end labelling (ISEL) [5]. The split DNA is fluorescently labelled in the TUNEL assay showing the occurrence of apoptosis and is used in conjunction with other techniques such as agarose gel electrophoresis for subsequent confirmation [5]. Annexin V is a Ca^{2+} dependent phospholipid binding protein which can be used for measuring apoptosis. During the early stage of apoptosis, phosphatidylserine relocates from the inner plasma membrane to the outer plasma membrane which will then bind to Annexin V [78-80].

Apoptosis can be differentiated from necrosis based on the amount or levels of ATP available. The occurrence of apoptosis relies on the presence of a high amount of ATP whereas necrosis occurs when the ATP is scarce [11]. Another way of determining whether apoptosis or necrosis is predominant is to differentiate the occurence of inner membrane pore opening (iMPT) or outer membrane pore opening (oMPT) [11]. iMPT decreases cellular ATP by blocking the synthesis of ATP while enhancing ATP hydrolysis. oMPT, on the other hand, promotes the release of cytochrome *c* and AIF to trigger the process of apoptosis [11]. Various studies have also used a combination of fluorescein isothiocyanite (FITC) – labelled Annexin V and propidium iodide (PI) to differentiate between apoptosis and necrosis: intact cells ($FITC^-/PI^-$), apoptotic ($FITC^+/PI^-$) and necrotic cells ($FITC^+/PI^+$) [79, 81-83].

1.2.3.2 Necrotic cell death

Necrosis is characterised as the form of cell death that occurs following severe cellular damage [5]. Characteristics of necrosis include uncontrolled disruption of organelles in the cell, severe enlargement of the organelles, membrane rupture, denaturation and coagulation of cytoplasmic proteins and depletion of ATP [69] (see Figure 1.1). Necrosis will induce inflammation in the tissue. In the case of ischaemia-reperfusion, severe or prolonged apoptosis will usually cause necrosis due to the failure of the heart to eliminate apoptotic myocytes [5]. The process of necrosis is swift and irreversible and will usually occur if ischaemia is prolonged [5].

Detection of necrosis is undertaken using propidium iodide (PI), an intercalating agent which is readily taken up by the necrotic cell which has lost its membrane integrity [84, 85]. Upon entering the necrotic cell, PI binds to the DNA by intercalating between the bases with relatively no sequence preference and the fluorescence of the dye is enhanced 20 – 30 fold [84, 85].

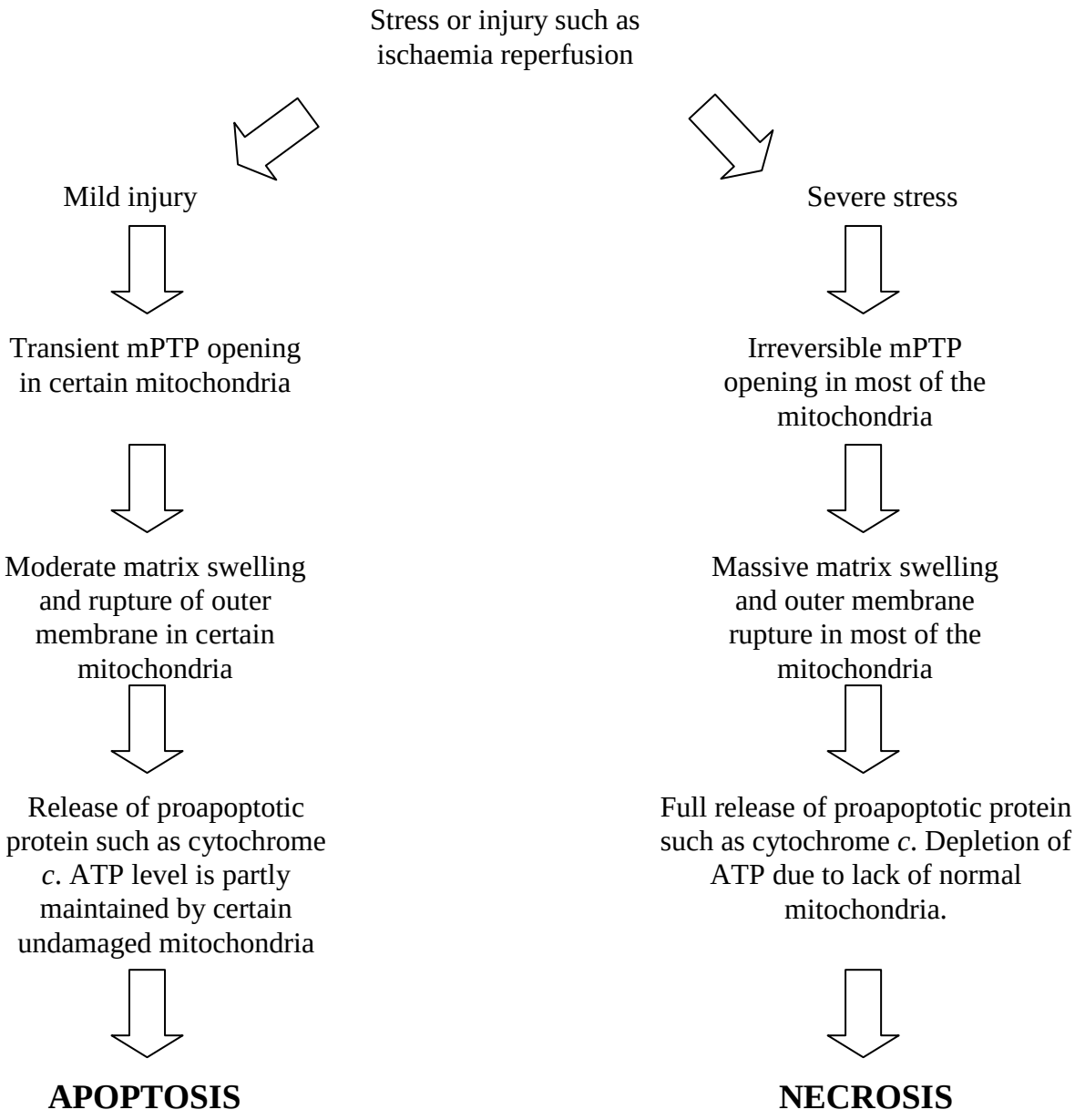

Figure 1.1: Cell death fate as determined by extent of mPTP opening. The extent of injury or stress determines the level of mPTP opening and types of cell death.

1.3 The Mitochondria as Mediators of Cardioprotection

In order to protect the cardiac cells against ischaemia-reperfusion injury, various interventions have been formulated. Many of these interventions, including ours, have placed the mitochondria, a unique organelle in the cell as a central target of action. In the following sections, we will review the characteristics of the mitochondria before further exploring the cardioprotective interventions that target the mitochondria in the myocardium.

1.3.1 The Structure of Mitochondria

Mitochondrial research has a long history but its popularity soared in the 1990's when it was discovered that mitochondria intensify apoptosis by releasing cytochrome *c* and other intermembrane space proteins involved in activating effector caspases [86]. Mitochondria play an important role in the life cycle of eukaryotic cells by governing the different types of cellular metabolic reactions, generating energy in the form of adenosine triphosphate (ATP) to carry out the processes and participating in calcium signalling, apoptosis and the aging process [11, 87, 88]. In reference books, mitochondria are frequently portrayed as kidney bean-shaped organelles found in eukaryotic cells; however due to the advancements in imaging techniques, the mitochondria are found to come in the form of an extended network of tubular threads [89] (see Figure 1.2).

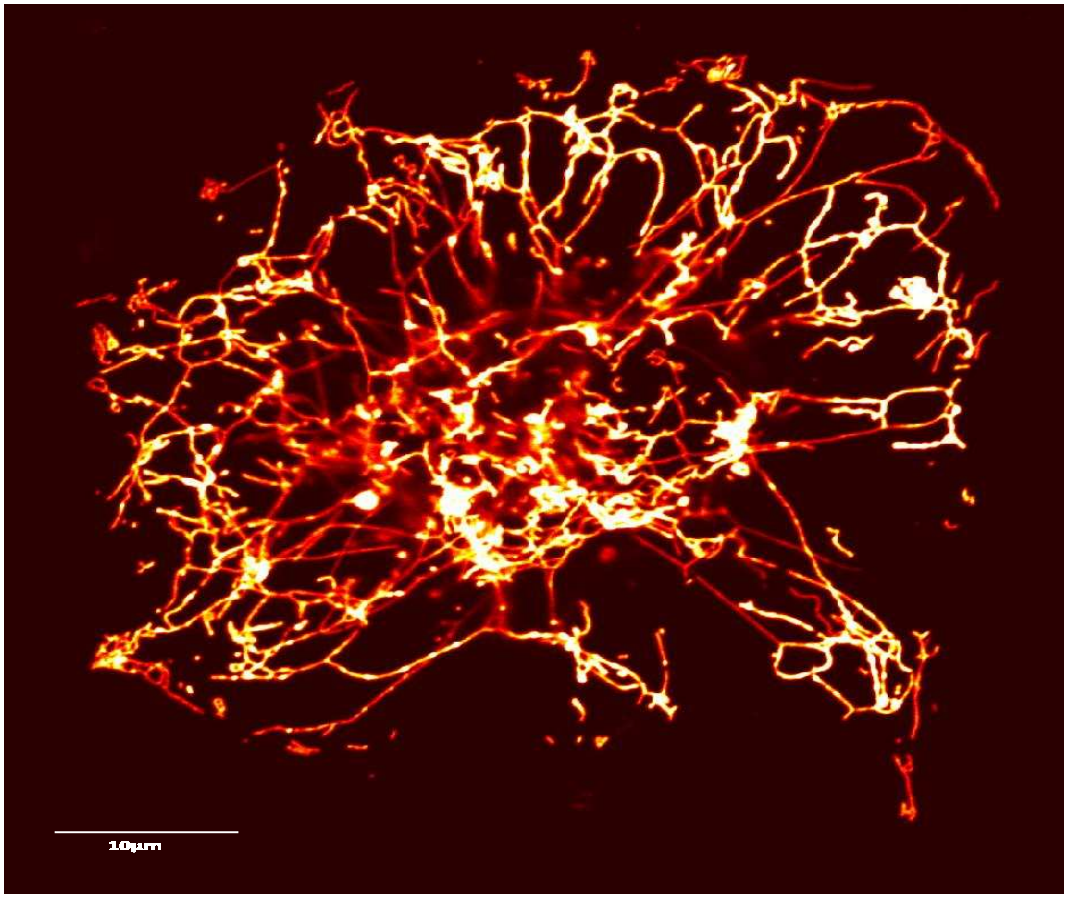

Figure 1.2: Mitochondria in a HL-1 cardiac cell with an overexpression of the mitochondrial-targeted red fluorescent protein (mtRFP) under the confocal microscope.

Studies have shown that mitochondrial morphology is intricate and dynamic. In a typical animal cell, mitochondria come in a mixture of thread-like tubules and spherical globules [90]. But, the shape and size of mitochondria change depending on the variety of cell type and cell's needs [91]. Changes are predominantly in the external shape with the internal structural organisation retaining a highly conserved form [92].

The mitochondria are compartmentalised by two membranes; the inner and outer membrane, the intermembrane space and the matrix [93]. The outer membrane, which encapsulates the whole organelle, acts as a permeability barrier to molecules larger than 1500 Da and separates the intermembrane space from the cell cytosol [94]. The permeability barrier is constituted of integral proteins known as porins or channel formers. Larger proteins, however, can still enter the the matrix of the

mitochondrion provided they contain an N-terminal signalling sequence, which directs the large protein to a translocase of the outer mitochondrial membrane (OMM) to allow the movement of the protein into the mitochondria [93, 95]. The OMM consists of a protein-to-phospholipid ratio of 1:1 by weight, which is very similar to the eukaryotic plasma membrane. The OMM has also been found to associate with the ER membrane via the mitochondria-associated ER-membrane (MAM) where calcium signalling and lipid transfer can take place [96]. When subjected to certain stresses or injury, the OMM will rupture and burst, hence releasing the proteins located in the intermembrane space into the cytosol [97]. Nonetheless, the ionic composition of the intermembrane space is similar to the cytosol due to the fact that the outer membrane is permeable to small ions and solutes. A distinct group of intermembrane protein, the cytochrome *c*, will promote apoptosis or cell death once released into the cytosol.

The inner membrane of the mitochondria (IMM), conversely, is different from the outer membrane in that it consists of regions parallel to the outer membrane as well as regions invaginating the matrix forming unique structures known as cristae, which enhance the ATP production capability by increasing the ratio of surface area to volume [94]. The cristae are where the electron transport chain, transporter proteins and phosphorylation mechanisms can be found, constituting up to 1/5 of the total protein in a mitochondrion [94]. The presence of the ETC creates a membrane potential across the IMM which is crucial to maintain oxidative phosphorylation. Contact sites that are involved in fusion of the inner and outer mitochondrial membranes, protein import and uptake of fatty acids of oxidative metabolism are also located at the cristae. The inner mitochondrial membrane, compared to the outer membrane has a higher protein-to-phospholipid ratio (3:1 by weight) and contains a special phospholipid known as cardiolipin, which confers impermeability to the IMM [98]. Special membrane transporters are required to enable the entry of specific ions and molecules with proteins being transported via the translocase of the inner membrane (TIM) complex or via Oxa1 [95].

Mitochondrial DNA (mtDNA) which is responsible for encoding specific proteins for the electron transport chain can be found in the mitochondrial matrix. In addition to that, ribosomal RNA (rRNA) and transfer RNA (tRNA) for amino acid

synthesis as well as metabolic enzymes involved in the citric acid cycle, oxidation of pyruvate and fatty acids are also located in the mitochondrial matrix [94].

1.3.2 Physical Distribution of the Mitochondria

The distribution of mitochondria depends on various temporal and spatial needs, such as during different developmental stages and specific high-energy regions [99-101]. In addition, the different pathological situations such as cancer and cardiomyopathy also affect mitochondrial morphology and distribution [92]. Mitochondrial content can be reduced by chronic hypoxia, as in mouse diaphragm, with the underlying cause being postulated as increased mitophagy and reduced mitochondrial biogenesis [102]. Mitochondrial subpopulations in skeletal and cardiac muscle (interfibrillar, subsarcolemmal and perinuclear) can also differ in terms of individual mitochondrial number following activity or stress [103, 104].

Mitochondria can move to different parts of the cell depending on energy requirement and utilisation using the microtubule of the cytoskeleton as a migration track [105]. However, fusion of mitochondria does not require the presence of the cytoskeleton. Mitochondria participate in regulation of cell death through several mechanisms such as mitochondrial fragmentation, cristae remodelling and the release of cytochrome *c* [106].

1.3.3 Formation of the Mitochondria

Production of mitochondria by mitosis is based on cellular energy need whereas degradation of mitochondria follows mitochondrial redundancy [107]. The formation of mitochondria or mitochondriogenesis is divided into two distinctive stages with different genetic material involved. First, formation of the mitochondrial outer and inner membrane to facilitate compartmentalisation which is governed by the nuclear genes followed by mitochondrial diffentiation for oxidative phosphorylation which depends on both the mitochondrial and nuclear genes [108]. Mitochondrial synthesis relies on the stimulation of the Peroxisome proliferator-activated receptor- coactivator (PGC-1alpha) - Nuclear respiratory factor 1 (NRF1) - Transcription factor A, mitochondrial (TFAM) pathway with PGC-1alpha being the

first stimulator of mitochondriogenesis and oxidative stress sensor. Upon activation of PGC-1alpha, the downstream intermediate transcription factor NRF1 is produced, which then stimulates expression of TFAM, a duplicator of mitochondrial DNA [109, 110]. As mentioned in *Section 1.3.2*, chronic hypoxia impairs mitochondrial biogenesis. This phenomenon is analogous to performance of competitive sports and exhaustive exercises where mitochondrial content is affected by the presence of damaging levels of ROS. However, during normal daily aerobic training, non-damaging levels of ROS may be required for activation of PGC-1alpha and subsequent muscle adaptation through mitochondriogenesis [107].

1.3.4 Inheritance of the Mitochondria

Mitochondria are unique organelles with their own genomes coupled to a transcription and translation system, which dictates their ability to perform specialized functions such as production of energy for different cellular processes [108, 111]. Due to the fact that the mitochondrial membranes and mtDNA both serve as a crucial template for the proper growth and division of the mitochondria, the 'inheritance' of mitochondria requires the proper transmission of mitochondria to daughter cells before every cell division [108]. The division of mitochondria in eukaryotes is tightly regulated by both cell cycle and the energy needs of the cell. Mitochondrial inheritance in mammalian cells is generally maternal or uniparental-derived. Biparental mitochondrial inheritance however, also exists in certain unicellular organisms such as the yeast [112]. Cellular proliferation requires optimum regulation of DNA replication, organelle segregation and cytosolic contents maintenance through various signalling cascades [113]. Mitochondrial segregation during mitosis is crucial as the mitochondria are also involved in regulation of a viable cell cycle [92, 113, 114]. Using HeLa cells to study the dynamics of the mitochondria during cell cycle, the group of Taguchi found that mitochondria maintain the long tubular network during interphase but fragments in the early mitotic phase. Nevertheless, the filamentous network of mitochondria re-forms in the daughter cells [115]. Fragmentation of the mitochondria during mitosis is regulated by the mitochondrial fragmentation-promoting protein, Dynamin-related protein 1 (Drp1), specifically during the anaphase [115]. In order to fragment the mitochondria

during mitosis, Drp1 has to be phosphorylated at position Ser-585 by the cell cycle-specific kinase Cdk1/cyclin B1 [115]. A recently discovered SUMO protease, SenP5, was also found to be involved in regulation of Drp1 during mitosis [113, 116]. At the G2/M transition prior to breakdown of the nuclear envelope, SenP5 is recruited from the cytosol and nucleolus to the mitochondria where it functions to deSUMOylate Drp1 to fragment the mitochondria and progress into the M phase of the cell cycle [113]. Silencing of SenP5 has been detected to cause cell cycle arrest precisely at the time when the protease is translocated to the mitochondria [113]

1.3.5 Proteins & Compartmentalisation in the Mitochondria

Another distinctive feature of mitochondria is the compartmentalisation of the different proteins and functions present in the matrix and intermembrane space [91]. It has been a long time since mitochondria established themselves as key components affecting the life and death of eukaryotic cells through the presence of various proteins catalysing different biosynthetic (e.g. ATP production via the components of the respiratory chain) and degradative reactions (e.g. cell death via release of cytochrome *c*). The mitochondrial structure, a result of the local synthesis of macromolecules within the mitochondria itself, as well as the import of proteins and lipids from outside the organelle, dictates the optimum performance of the mitochondrial functions with proper localisation of the enzymes in distinct membranes and aqueous compartments [92].

The abundance of different protein molecules in the mitochondria derives from the protein targeting process. Protein targeting to mitochondria is basically defined as the shift of proteins translated from the nuclear genes and synthesised in the cell cytoplasm, into the mitochondria. Ironically, even though this process requires the complementation of different mitochondrial proteins, only a few protein molecules transferred originated from the mitochondrial DNA, synthesised on mitochondrial ribosomes and inserted into the inner membrane from the matrix [93].

Studies have been conducted to shed new light on the mitochondrial protein import pathways and generally it was found that in mammalian cells, preproteins are

directed into the matrix of the mitochondria in a general pathway (via the translocase of the outer membrane) while a series of pathways directing mitochondrial precursor proteins to subsequent sites of functions were defined, with the presequence pathway for proteins to the matrix and inner membrane [117], the carrier protein pathway for the inner membrane [118-120], the redox-regulated import pathway into the intermembrane space [121, 122], and the β-barrel pathway into the outer membrane [93, 123-125].

A recent review by the group of Shirihai categorised the control of mitochondrial proteins to 'local' and 'global'. The 'local' control functions include the micro-environmental changes in the organelle that affect the post-translational modification, oxidation or degradation of the encoded proteins which will affect processes such as energy production, apoptosis and division cycle. Control mechanisms stemming from the cell itself are regarded as 'global' controls. One example is the cell cyle where nuclear transcription factors such as PGC1α, PPARα, NRF1/2, and ERRα control the physical and physiological state of the mitochondria at different stages of the cell cycle [126-128]

Compartmentalisation of the mitochondria is also affected by IMM remodeling which in turn plays a crucial role in regulating ATP production by governing the amount of ADP available to cross the OMM [129, 130]. The cristae in the mitochondria are shown to be tubular and structurally distinct from the inner mitochondrial membrane using advanced tomographic imaging techniques [131, 132]. In addition to that, the cristae were found to be attached to the inner boundary membrane via tubules termed cristae junction, which constitutes a general structural component in all mitochondria [131, 132]. This interconnection between the cristae junction and the inner mitochondrial membrane changes with the respiratory state of the mitochondria [132-134]. According to Hackenbrock and the group of Mannella, using isolated rat liver mitochondria under high-resolution electron microscopy, the number of cristae junction and cristae interconnections decreases during the high-energy state of the mitochondria (state 4: low respiratory rate due to depletion of ADP) while the number increases during the low-energy state of the mitochondria (state 3: maximum respiratory rate in the presence of excess ADP and respiratory substrate) [132, 133]. The increase in cristae junction has been speculated to aid in

reduction of ADP diffusion into the cristae across the IMM and hence ATP production while the low numbers of cristae junction during State 4 of the respiratory state helps ATP production by concentrating the ADP within a smaller intercristal volume [129, 130].

In the matrix, the enzymes of different metabolic pathways are grouped together in entities termed metabolons to facilitate diffusion of solutes from one enzyme to the next enzyme in a pathway. One of the typical metabolon is the pyruvate dehydrogenase complex (PDC).

1.3.6 Role & Function of the Mitochondria

The most prominent function of mitochondria is known to be the generation of ATP by oxidative phosphorylation and electron transport (see Figure 1.3), a process in which electrons from NADH are shifted along a series of complex carrier molecules, generating energy stored in the form of a proton gradient across the mitochondrial membrane which is subsequently utilised by ATP synthase on the inner membrane to produce ATP from ADP and phosphate.

However, mitochondria also contribute to the biosynthesis of different compounds such as pyrimidines, nucleotides, amino acids, heme, and urea [108] as well as regulation of calcium and ROS-mediated processes in cells. The energy metabolism process is coupled to ion homeostasis through dynamic feedback mechanisms between the mitochondria and cell cytoplasm to maintain cell survival [135].

1.3.6.1 Energy conversion

The production of ATP is conducted via cellular respiration through oxidation of glucose, pyruvate and NADH in the presence of oxygen. Aerobic respiration will switch to glycolysis in the absence of oxygen [136].

The pyruvate molecule is transported across the IMM into the matrix where it undergoes oxidization and is combined with coenzyme A to form CO_2, acetyl-CoA, and NADH. The acetyl-CoA then enters the citric acid cycle, also known as the tricarboxylic acid (TCA) cycle or Krebs cycle where it is oxidised to CO_2 and releases reduced cofactors (three molecules of NADH and one molecule of $FADH_2$) that are a source of electrons for the electron transport chain, and a molecule of GTP (that is readily converted to an ATP) [136]

The NADH and $FADH_2$ molecules are transported via the malate-aspartate shuttle system of antiporter proteins or feed into the electron transport chain using a glycerol phosphate shuttle. Components of the ETC include Complex I, II, III, IV and V. Complex I, III and IV perform the transfer of electrons along the ETC and H+ into the intermembrane space. The ETC transfer process is efficient, however, a small percentage of electrons may reduce the oxygen present thus forming ROS which is detrimental to the cell [137].

An electrochemical gradient is established across the IMM following the increase in proton concentration in the intermembrane space. The protons are then pumped back into the matrix through the ATP synthase (Complex V) and the potential energy is used to synthesise ATP from ADP and inorganic phosphate in a process termed chemiosmosis, first described by Peter Mitchell in 1967 [136, 138-140].

1.3.6.2 Heat production

The protons can also re-enter or diffuse into the mitochondrial matrix without leading to ATP synthesis in a process known as proton leak or mitochondrial uncoupling. This can however lead to heat production as a result of unutilised potential energy of the proton electrochemical gradient.

1.3.6.3 Storage of calcium ions

Free calcium exists in the cell for a myriad of reactions and signal transduction processes. Mitochondria act as a cytosolic buffer by transiently taking in calcium from the cytosol or the ER. The ER is a crucial calcium store in the cell and is connected to the mitochondria for calcium uptake into the mitochondria via channels such as the inositol trisphosphate receptor (IP_3R) or ryanodine receptor (RyR) [141-143]. Mitochondrial calcium uptake occurs through a calcium uniporter on the IMM, which passes Ca^{2+} down the electrochemical gradient maintained across the mitochondrial membrane without direct coupling to ATP hydrolysis or transport of other ions [142, 144]. Calcium in the mitochondria can also be released into the cell via a sodium-calcium exchanger or a "calcium-induced-calcium-release" pathway, which can be visualised as calcium spikes or waves that play a role in activation of second messenger systems for signal transduction or changes in mitochondrial membrane potential.

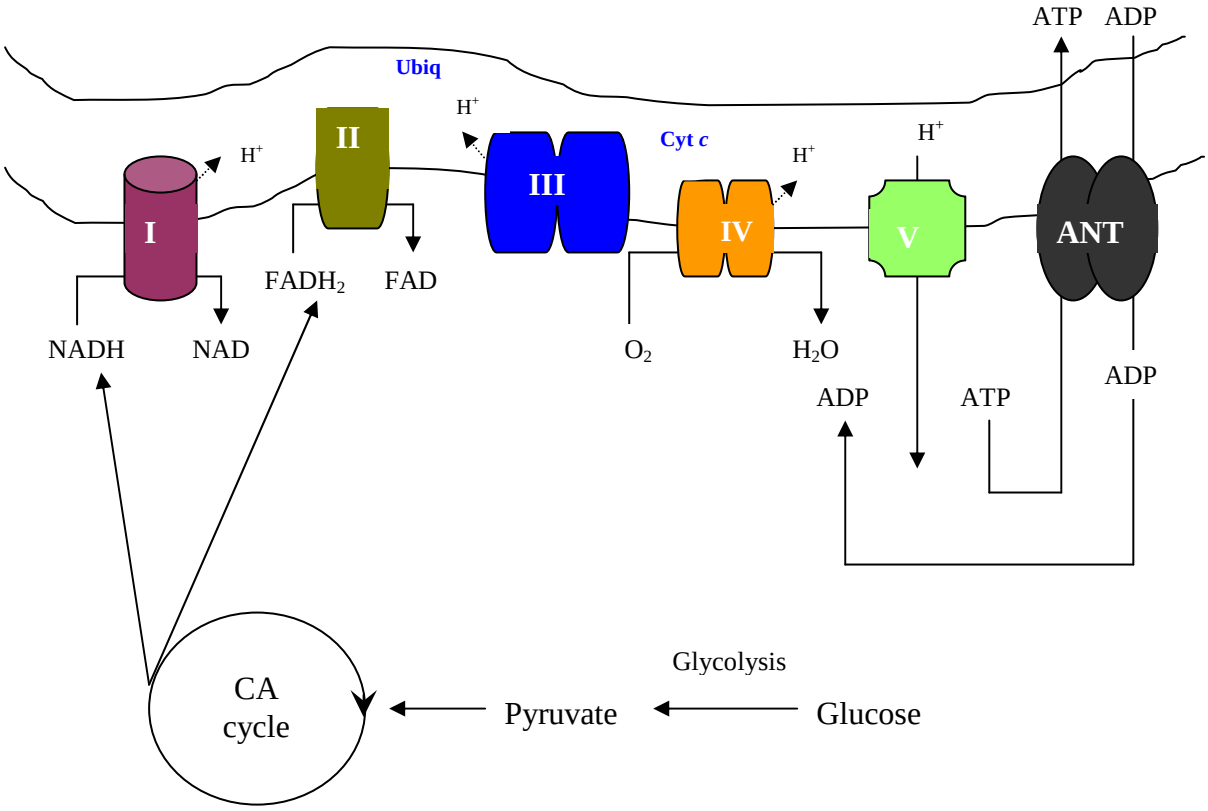

Figure 1.3: Mitochondrial oxidative phosphorylation. Mitochondrial oxidative phosphorylation and electron transport is actively carried out by a chain of multisubunit protein complexes present within the mitochondrial inner membrane. Reducing equivalents are provided within the mitochondrial matrix via metabolism of glucose via glycolysis and the citric acid cycle to complex I (NADH) and complex II ($FADH_2$). Electrons are transferred to complex III via ubiquinol and subsequently to complex IV via cytochrome *c*, with the reduction of O_2 to form H_2O. The movement of electrons through the series of enzyme complexes promotes the pumping of protons (H^+) across the inner membrane at complexes I, III, and IV, creating an electromotive differential across the inner membrane. Complex V (ATP synthase) utilises the potential energy created by this proton gradient to condense a molecule of ADP with P_i to form ATP. ATP is subsequently transported out of the mitochondrial matrix by the adenine nucleotide translocator (ANT), which is also responsible for moving cytoplasmic ADP into the mitochondrial matrix.

As in other cells, mitochondria act as a crucial regulator of the life and death cycle of cardiac myocytes. The key role these mitochondria have in the normal myocytes is in providing ATP through oxidative phosphorylation to meet the high energy requirements of the beating heart cells. The positioning of the mitochondria between the myofibrils and just below the sarcolemma of the myocyte enhances the efficiency of the localised ATP delivery system to support contraction, cell metabolism and ion homeostasis.

Besides maintaining the life of the heart cells, mitochondria also regulate cell death by reacting in response to different stress signals such as damage of inheritable material, oxidative stress, hypoxia and loss of growth factors. Initiation of the death pathway occurs upon the opening of the mPTP in the inner mitochondrial membrane, which subsequently leads to collapse of the membrane potential, mitochondrial swelling, and rupture of the outer membrane followed by release of proapoptotic proteins to stimulate apoptosis or necrosis [145]. The process of apoptosis requires the mitochondria to execute crucial functions such as the release of cytochrome *c* and certain cofactors to trigger the caspases [146]. The particular role of mitochondria in promoting survival or performing apoptosis relies on the interplay between different pro- and anti-apoptotic members of the Bcl-2 protein family [146]. Apoptosis and necrosis are different in the sense that a signaling cascade leading to cell death albeit without an inflammatory response is activated during apoptosis whereas necrosis causes cell swelling and rupture of the plasma membrane, further releasing the cellular content into the extracellular space which causes an inflammatory response which damages the neighboring cells [73]. Both of these processes equally contribute to the loss of myocardial cells in pathologies such as ischaemia-reperfusion injury, cardiomyopathy and congestive heart failure [73]. However, the contribution of apoptosis to cell death predominantly occurs in the reperfusion phase.

1.4 The Morphology of the Mitochondria

The term mitochondria derived from the Greek word *mitochondrion*, a combination of *mitos* (thread) and *chondros* (grain) [147]. In the early days, mitochondria were thought to be isolated cytosolic organelles independent of each other. Upon the advent of bright field microscopy in the 20th century, mitochondria were revealed to be dynamic in nature, and to vary in size and shape depending on the cell-type.

The development of mitochondrial-targeted fluorescent dyes and proteins enabled the characterisation of mitochondrial dynamics involving movement of mitochondria along the cytoskeleton to changes in shapes, ranging from unicellular yeast to the multicellular mammalian cells [90, 148, 149]. The first gene involved in mitochondrial fusion was discovered in *Drosophila melanogaster* in 1997, with subsequent fusion and fission genes being identified in yeast or *Drosophila* models and mammalian cells [92, 150]. The key genes in regulation of mitochondrial fusion and fission have been identified but the mechanisms and effects on metabolism and other physiological effects have yet to be clarified.

The mitochondria consist of two membranes differentiating the intermembrane space and the mitochondrial matrix [106]. Mitochondria in cells come in a variety of shapes, depending on the different physiological stages the cell is in, e.g. the extent of a particular process such as cell cycle and division as well as positioning of cells in different parts of an organ [105]. In addition, the shape and location of the mitochondria in the cell may regulate its respiration and metabolism [106]. Mitochondria can be elongated and fused or fragmented into globules [106]. The fusion and fission events of the mitochondria ensure that exchange of the contents (solutes, metabolites, enzyme, mtDNA) can occur.

The mitochondrial arrangement in the adult cardiac cell differs from that in cardiac cell lines and neonatal cardiomyocytes. Mitochondria in the HL-1 cardiac cell line for example, exist as a mixture of elongated (spaghetti-like form) and fragmented form (see Figure 1.4). In the primary cardiomyocyte however, the

mitochondria are arranged in a very highly organised form, aligned alongside the sarcolemma with the myofibrils in-between, with very little space to move (see Figure 1.5).

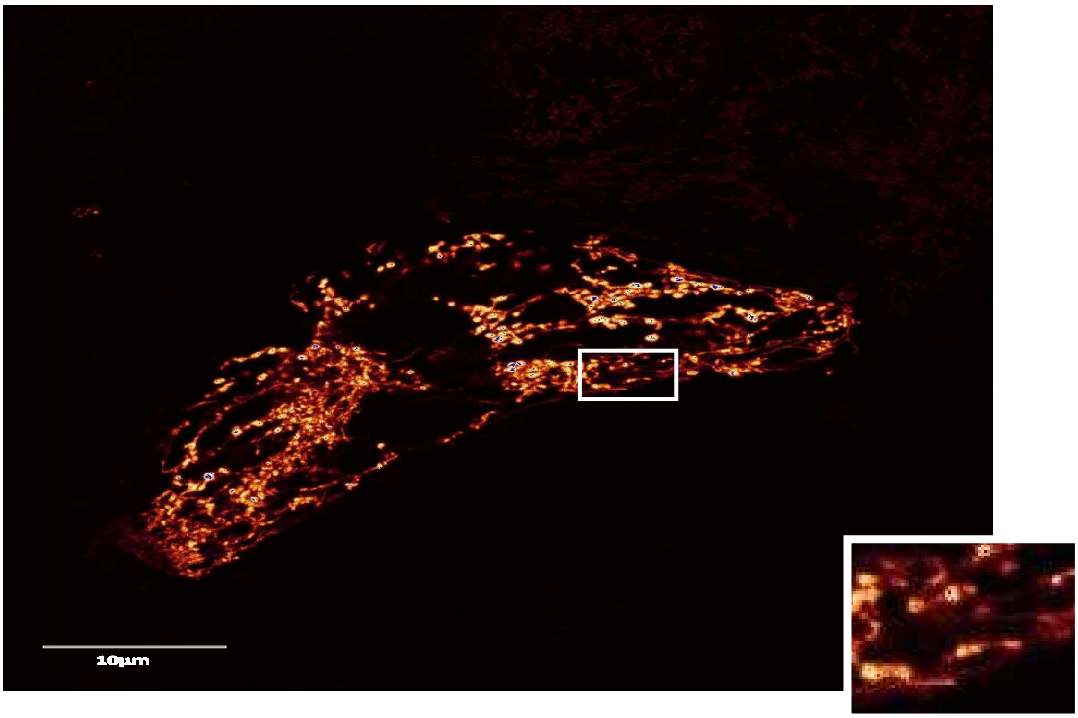

Figure 1.4: Representative image of mitochondria in a HL-1 cardiac cell with an overexpression of the mitochondrial-targeted red fluorescent protein (mtRFP) under the confocal microscope.

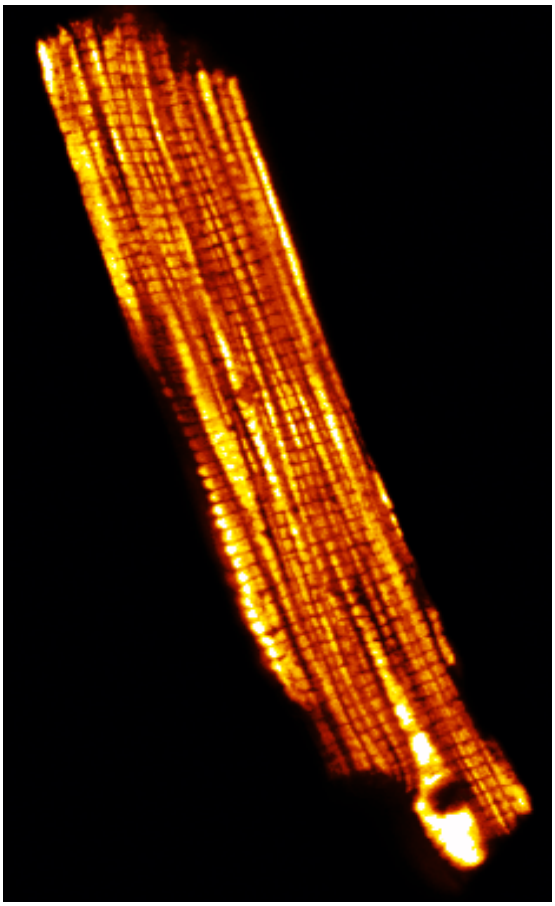

Figure 1.5: Representative image of an adult cardiomyocyte with the mitochondria loaded with Tetramethyl Rhodamine Methyl Ester (TMRM) (bright orange) under the confocal microscope.

Of note, mitochondria in neonatal cardiomyocytes are filamentous in nature showing that the typical longitudinal arrangement of mitochondria in adult cardiomyocytes only arises during cardiac development. The mitochondria in the primary adult cardiomyocytes are generally believed to be static, with very little probability of fusion or fission. Nevertheless, studies carried out by different groups have successfully identified the presence of the mitochondrial-shaping proteins in the adult heart. Santel *et al* in 2003 detected the presence of both Mfn1 and Mfn2 in the heart using Northern and Western blots, and also in the rat and mouse hearts using RT-PCR through the studies of Rojo *et al* and Bach *et al* in 2002 and 2003 respectively [151-154] while Optic Atrophy 1 (OPA1) was detected in adult mouse hearts in 2008 [154, 155]. The mRNA of the fission protein DLP1 was identified in the heart

using Northern Blot analysis in 1998 [154, 156] while hFis1 was found in the isolated mitochondria from the heart in 2004 [157].

1.4.1 Mitochondrial Fusion

Mitochondrial membrane fusion has been shown to be a distinct two-step process which occurs separately for the inner and outer membrane, but in chronology [11]. Both the outer and inner membranes of the mitochondria must fuse properly in order for the matrix contents to mix properly [105].

Specificity of membrane fusion is dictated by the generation of specific protein complexes in *trans* between the donor and acceptor membranes following which fusion is promoted by the formation of specific helical bundles [105].

1.4.2 Fusion Proteins

1.4.2.1 Mitofusins 1 and 2 (Mfn 1 and Mfn2)

Two GTPases of the outer mitochondrial membrane involved in mitochondrial fusion of mammals, Mitofusin (Mfn) 1 and 2, were discovered by Santel & Fuller in 2001 [158]. Mitofusins constitute the mammalian homologues of *Drosophila* Fuzzy onions protein (Fzo1p), a transmembrane GTPase first discovered in 1997, which is responsible for the formation of a giant mitochondria during spermatogenesis [150]. Mitofusins are conserved GTPases localised to the outer membrane of the mitochondria [105]. Structural studies show that mitofusins (Mfn) 1 and 2, are located in the mitochondrial outer membrane and span the membrane twice, exposing an N-terminal GTPase domain and two predicted coiled-coil regions to the cytosol [159] (see Figure 1.6). Both Mfn1 (743 residues) and Mfn2 (757 residues) are made up of a NH_2-terminal region containing the GTP-binding domain, 2 heptad repeats (coiled-coil domain), a transmembrane domain and the COOH-terminal [152] (see Figure 1.6). The GTPase activity is required for both Mfn1- and Mfn2-mediated mitochondrial fusion [158] (see Figure 1.7). The outer membrane of the mitochondria fuses in conditions of low levels of guanosine-5'-triphosphate (GTP) hydrolysis and the presence of a proton gradient across the inner membrane while inner membrane fusion relies on increased levels of GTP hydrolysis [160]. Apart from the identity of fusion-promoting protein, Mfn2 has also been identified in muscle from obese Zucker rats as mitochondrial assembly regulatory factor (MARF) [153]; and in vascular smooth muscle cells as hyperplasia suppressor gene (HSG) [161].

Mfn1 and Mfn2 can substitute each other in terms of function. Overexpression of Mfn2 can replace the loss of function in cells without Mfn1 while overexpression of Mfn1 can replace the loss of function in cells without Mfn2 [105]. Nevertheless, it has been found that Mfn1 has higher GTPase activity and induces fusion more efficiently than Mfn2 [146]. A higher degree of mitochondrial fragmentation has also been observed in Mfn1 -/- mouse embryonic fibroblasts (MEFs) compared to the Mfn2 -/- MEFs indicating the roles of the Mfns do not completely overlap [162]. Mfn1 has been found to be responsible for docking two adjacent mitochondria together for the fusion process while Mfn2 plays a crucial role

in stabilising the interaction between the two mitochondria [162, 163]. In addition to promoting mitochondrial fusion in general, Mfn1 is also important for placental formation during embryonic development [162]. Mfn2 has also pleiotropic effects where it participates in oxidative metabolism of the skeletal muscle and cell division capability of vascular smooth muscle cells [153, 161]. Mfn2 has recently been shown to tether mitochondria to the ER for calcium exchange [164].

Mitochondrial fusion is unaffected by Optic Atrophy 1 (OPA1) (see section 4.1) expression in Mfn1 -/- but not Mfn2 -/- cells, and Mfn2 but not Mfn1 cells promote mitochondrial elongation in cells where OPA1 has been knocked down [165]

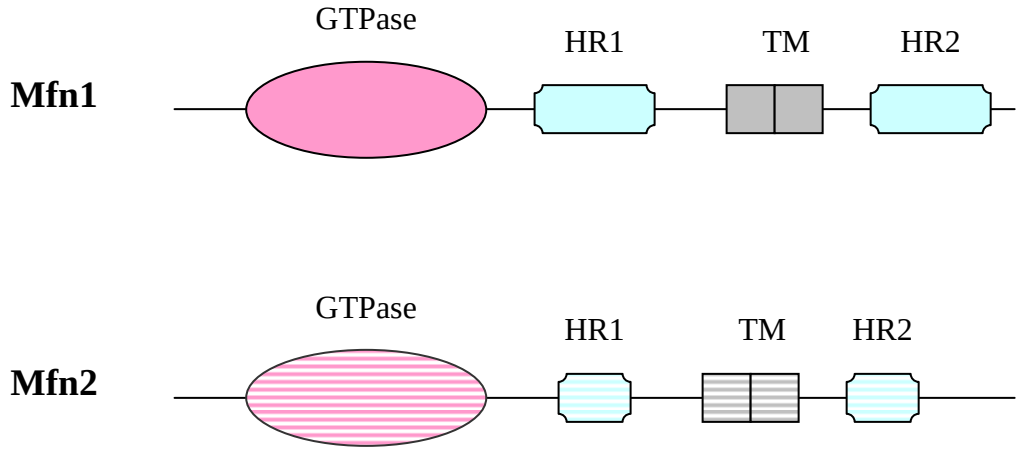

Figure 1.6: Domain structure of the Mitofusin proteins. Both Mfn1 and Mfn2 are similar in that they contain GTPase domains (pink), hydrophobic heptad repeat (HR) regions (light blue) and transmembrane (TM) segments (grey). The transmembrane segments are charged residues and are responsible for the configuration of the protein to face the cytosol by producing a U-turn in the mitochondrial outer membrane.

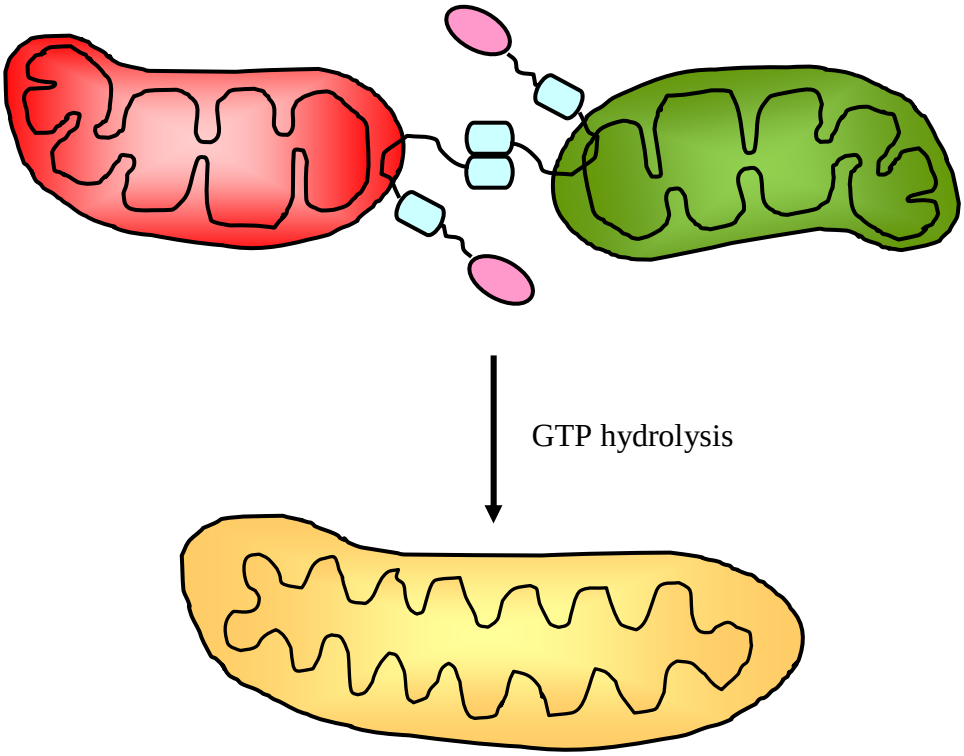

Figure 1.7: The fusion mechanism by fusion proteins. Mfn is a mitochondrial outer membrane protein with a cytosolic GTPase domain (pink) and two hydrophobic heptad repeat (HR) regions (light blue). The C-terminal HR region mediates oligomerisation between Mfn molecules on adjacent mitochodnira. GTP hydrolysis facilitates the fusion process.

4.1 Optic atrophy 1 (OPA1)

The discovery of the Optic Atrophy 1 (OPA1) gene was made from the identification of mutations in the OPA1 gene in 2000 as the cause for the human neurodegenerative condition, autosomal dominant optic atrophy [166]. It is the human homologue of the yeast mitochondrial shaping protein Mgm1, first discovered in yeast in 1992 [167]. OPA1 is a GTPase of the dynamin family, consisting of an N-terminal mitochondrial import sequence (MIS), hydrophobic segments, coiled-coil domain, GTPase domain, a middle domain and a GTPase Effector Domain (GED) at the C-terminus (see Figure 1.8). The MIS is cleaved by the mitochondrial processing peptidase (MPP) upon fulfilling its duty of targeting the OPA1 protein to the mitochondria [168]. The OPA1 is widely known to exert its function at the inner mitochondrial membrane (IMM), although it can also prevent apoptotic cell death with its role in cristae remodelling [169].

OPA1 is expressed throughout the body, but is present in largest quantities in the retina, brain, testis, liver, heart, skeletal muscle, and pancreas [170]. The human OPA1 consists of 8 different isoforms (4 in mice). The function of each isoform is determined by the exon contained. Promotion of mitochondrial fusion and maintenance of mitochondrial membrane potential is dependent on the OPA1 isoform 1 (containing exon 4), whereas alternative isoforms containing exons 4b and 5b may control cytochrome *c* release [170]. OPA1 can also be cleaved by presenilin associated rhomboid-like protease (PARL), a protease into a small soluble form which localises at the intermembrane space and is responsible for preventing apoptosis by 'locking' the cytochrome *c* in the intermembrane space [169, 171]. A recent study by Twig and co-workers has also implicated the OPA1 in 'tagging' of mitochondria for selective removal by autophagy [172].

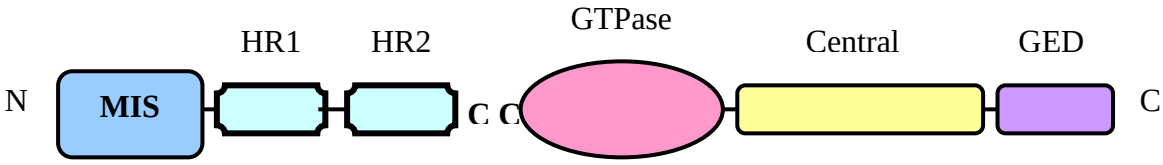

Figure 1.8: Schematic representation of OPA1. The OPA1 protein consists of an N-terminal mitochondrial import sequence (MIS), hydrophobic segments, coiled-coil domain (CC), GTPase domain, a middle domain and a GTPase Effector Domain (GED) at the C-terminus.

1.4.3 Mitochondrial Fission

Mitochondrial fission or fragmentation is signified by generation of small, discrete and globular mitochondria. The fragmentation process is driven by the presence of specific fragmentation-promoting proteins such as the Drp1 and hFis1. During the fission process, mitochondria undergo simultaneous ultrastructural changes involving opening of the narrow tubular cristae junction and fusion of individual cristae [160]. The genome of the mitochondria is organised into distinct structures known as nucleoids and fission occurs to ensure every daughter mitochondria has at least one nucleoid [105].

Fission of mitochondria may be synchronised with other cellular processes. Fission of mitochondria occurs in normal cell during the cell division process, particularly in the late S and M phases, to ensure proper inheritance of the organelle and during apoptosis where the caspase-dependent cell death is initiated by the release of cytochrome *c* from the mitochondria by the fission protein hFis1 [87, 105].

Nevertheless, it should be noted that fission without cytochrome *c* release does not lead to cell death due to the fact that fission also occurs in normal cells where regulation of mitochondrial morphology takes place as mentioned above [173]. In fact, in the case of Ca^{2+}-mediated apoptosis, Drp1-induced mitochondrial fission protected the cell by dispersing the death signal instead of killing it [174].

A similar case would be double-KO cells without the Bcl-2 members Bax and Bak, and cells with a mutated hFis1. In the DKO cells, it was found that only mitochondrial fragmentation occurs in the presence of hFis1 but not apoptosis. Apoptosis or cell death only occurs upon rectification of the endoplasmic reticulum defect, thereby implying the dependency of the effects of hFis1 on the endoplasmic reticulum as well as the fact the hFis1 is also found on the endoplasmic reticulum. Generating a mutant in the intermembrane region of hFis1 caused fission only without progression into cell death [87].

1.4.4 Fission Proteins

1.4.4.1 Dynamin-related protein 1 (Drp1)

One of the proteins involved in mitochondrial fission is Drp1, a GTPase located in the cell cytosol which can translocate and form constrictive rings around the mitochondria for the purpose of fission [106]. Drp1 was first discovered in 1998 as a mammalian homologue to the yeast ortholog Dnm1p [175]. Structurally, Drp1 is made up of a GTPase, the central domain, and the GED or GTPase effector domain [176] (see Figure 1.11).

The translocation of Drp1 involves the generation of a translocation activation signal followed by a vector to transfer the fission protein to the mitochondria in the cell due to the lack of an outer mitochondrial membrane targeting sequence in Drp1 [70, 160]. The GED domain is required for regulation of GTPase activity and for mitochondrial targeting [177]. Drp1 has been proposed to bind to hFis1 which serves as a docking site for Drp1 or it may actually induces mitochondrial fission independently of hFis1 [178]. Alternatively, the presence of adaptor proteins such as Mdv1p and Caf4p (in the yeast system) may mediate the binding of Drp1 to Fis1, such as in the case for Dnm1p, the yeast ortholog for Drp1, although the mammalian homologous proteins have yet to be identified [179, 180]

A small fraction of the Drp1 from the cytosol will be utilised to form punctuate spots on mitochondrial tubules which indicates potential fission locations [177]. Drp1 inhibition by generating a dominant-negative mutant or by RNA interference enhances the length and interconnectivity of the mitochondrial tubules [70, 105, 177]. The GTP-binding defective mutant of Drp1 ($Drp1_{K38A}$) functions as a dominant negative by sequestering endogenous Drp1, thus inhibiting mitochondrial localisation of Drp1 [181].

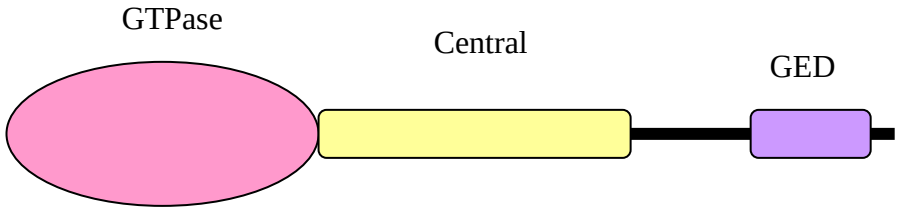

Figure 1.11: Drp1 protein. The Drp1 protein has domains typical of dynamin family GTPases, including a GTPase domain, a central domain and a GTPase effector domain (GED).

Drp1 can be regulated by phosphorylation [182, 183], SUMOylation [113, 116, 184] or ubiquitination [185-188]. Phosphorylation of Drp1 at different sites of different isoforms of the Drp1 produces different effects. The serine residues phosphorylated consist of either Ser616 or Ser637 [182, 189, 190]. Ser616 on human Drp1 splice variant 1 (Ser585 on rat Drp1) is phosphorylated by cyclic dependent kinase 1 (Cdk1/cyclin B) during mitosis in HeLa cells, thereby promoting transient fission of the mitochondria and allowing proper distribution of the mitochondria into daughter cells [115]. Mitochondrial fission induced by nitric oxide has also been demonstrated to involve phosphorylation of the Drp1 at the Ser616 site [191].

In 2008 however, the group of Chang and co-workers showed that Protein Kinase A (PKA) phosphorylates Ser637 on human Drp1 splice variant 1 (Ser656 on rat Drp1 splice variant 1) [182, 190]. The phosphorylation at Ser637 inhibits the fission activity of Drp1 by decreasing the intramolecular interactions that normally drive GTP hydrolysis, albeit this was not observed in phosphorylation of Ser656 [182, 190]. Dephosphorylation by the calcium-sensitive phosphatase, calcineurin, acts in reverse by promoting Drp1 translocation to the mitochondria and causing fission [189, 190].

Phosphorylation at Ser600 of Drp1 isoform 3 (Ser637 on human Drp1 splice variant 1) by the Ca^{2+}/calmodulin dependent protein kinase Iα (CaMKIα) promotes mitochondrial fission [183]. Therefore, it appears that the same serine residue (Ser637 on human Drp1 splice variant 1 and Ser600 on Drp1 isoform 3) resulted in mitochondrial fission if phosphorylated by CaMKIα, but mitochondrial fusion if phosphorylated by PKA.

1.4.4.2 Fis1

Mammalian Fis1 was first identified in 2001 by its homology with Fis1p, the yeast ortholog [178, 192]. Fis1 is a fission protein of 17 kDa and 152 amino acids containing a tetratricopeptide repeat (TPR) motif domain that is located evenly on the outer membrane of the mitochondria via the single C-terminal transmembrane domain (TM) with most of the protein facing the cytosol [105, 193, 194] (see Figure 1.12). The TPR motif is constituted of five α-helices with the first α-helix of rat Fis1 critical for oligomerisation and for its fission activity [195]. The next four α-helices are involved in protein-protein interactions required for fission but are not required for Fis1 oligomerisation [195].

Apoptosis caused by hFis1 relies on the proper interplay between the intracellular calcium concentration, state of the mPTP and endoplasmic reticulum [87]. Inhibition of hFis1protects against apoptotic cell death [70].

Mitochondrial fission caused by overexpression of hFis1 relies on the presence of Drp1 [105] (see Figure 1.13). However, it should also be noted that hFis1 can promote cell death without the influence of Drp1 and can also fragments mitochondria without leading to cell death [87].

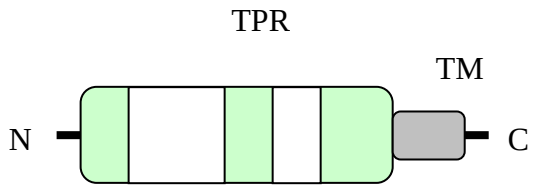

Figure 1.12: hFis1 protein. Fis1 is a small mitochondrial outer membrane protein with the N-terminal facing the cytosol and the cytosolic domain (green and white) forming a six-helix bundle with two central tetratricopeptide repeats (TPR) (white).

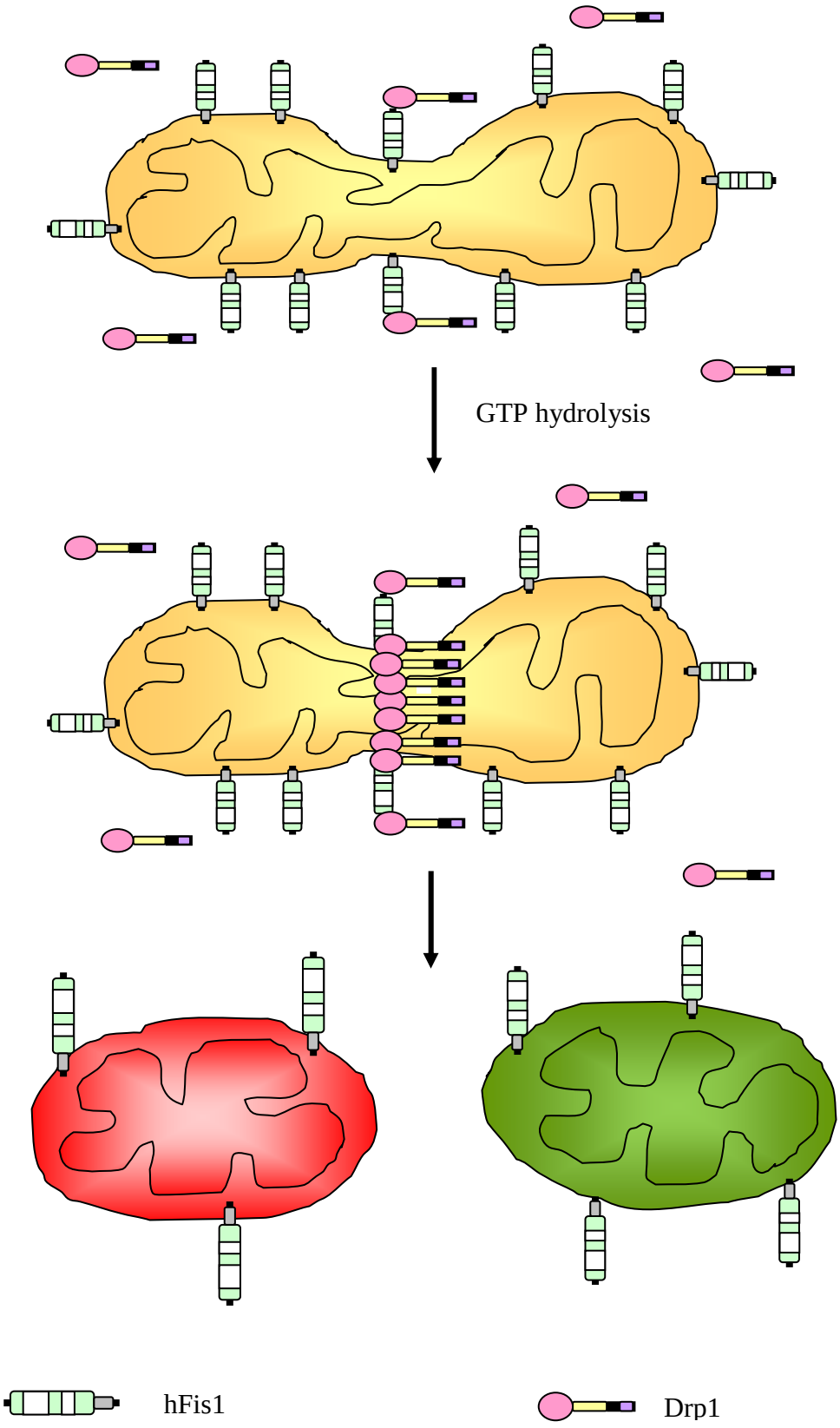

Figure 1.13: The fission mechanism. Fis1 is localised to the mitochondrial outer membrane with most of the protein facing the cytosol while Drp1 is localised to the cytosol and on mitochondria at the punctuate spots. Drp1 will polymerise around the mitochondria to facilitate constriction which in the end will lead to mitochondrial fission.

The two fission proteins hFis1 and Drp1 execute their functions at different steps in the process of apoptosis. Absence of hFis1 (hFis RNAi) in cells inhibits translocation of Bax from cytosol to mitochondria whereas absence of Drp1 inhibits the release of cytochrome *c*, albeit Bax successfully translocates from the cytosol to the mitochondria [70]. It has been found that in the absence of Drp1 (which results in inhibition of cytochrome *c* release), apoptosis still occurs. Absence of hFis1 or the presence of Bcl-2 prevents apoptosis to a larger extent [70]. Indirectly, this shows that Bax translocation may be more potent in inducing apoptosis than cytochrome *c* release [192]. Therefore, it can be concluded that hFis1 and Drp1 exert their effects at different steps of the apoptotic pathway; hFis1 upstream of Bax translocation and Drp1 upstream of cytochrome *c* release [196]. Bax translocation precedes cytochrome *c* release in close time proximity to the extent that cells basically are Bax translocation negative and cytochrome *c* release negative or Bax translocation positive and cytochrome *c* release positive [70].

1.4.5 Other regulators of mitochondrial morphology

Different effectors of mitochondrial morphology have also been identified, such as mitochondrial protein 18kDa (Mtp18) [197], Rab32 [198], Endophilin B1 [199], and the Mitofusin-binding protein (Mib) [200]. A brief summary of the current known mitochondrial shaping proteins is depicted in Table 1.

Table 1

List of some of the known mitochondrial-shaping proteins

Yeast	Drosophila	Human	Location	Function	Notes
Mgm1	OPA1	OPA1	IMM	IMM fusion	Pleiotropic effects include cristae remodelling
Fzo1p	Fzo	Mfn1	OMM	OMM fusion	
Fzo1p	Fzo	Mfn2	OMM	OMM fusion	Pleiotropic effects on metabolism, apoptosis, proliferation, ER tethering
Ugo1	?	?	OMM	OMM fusion	
Dnm1p	Drp1	Drp1 or DNM1L	Cytosol & OMM	OMM fission	
Fis1p	Fis1	Fis1	OMM	OMM fission	
?	?	Mtp18	IMM	IMM fission	Thought to be the IMM equivalent of OPA1
Mdv1p and Caf4p	?	?	OMM	OMM fission	Adaptor proteins which aid Drp1 docking to hFis1
Mdm33	?	?	IMM	IMM fission	

1.4.6. Functions & effects of changes in mitochondrial morphology

Changes in shapes of mitochondria may play a role in reducing the distance between neighbouring organelles, such as the mitochondria and ER, where material exchange is facilitated (e.g. Ca^{2+}) [143, 164, 201], or initiation of certain mechanisms can be performed such as cell death initiation between ER and mitochondria through the unfolded protein response (UPR) pathway [202, 203]. In addition to that, mitochondrial fission is crucial in ensuring proper cellular distribution of the mitochondria to areas of high-energy need such as the neuromuscular junction [204]. With regards to cell death susceptibility there has been intense debate over the role of mitochondrial fragmentation with certain groups showing the influence of mitochondrial fragmentation in apoptosis [192, 205, 206] while others have showed a deviation from the implication of mitochondrial fragmentation in cell death [207, 208]. A study by Yu and co-workers demonstrated that mitochondrial fission was enhanced in the diabetic model while also mediating high glucose-induced cell death through elevated production of reactive oxygen species [209]. Conversely, mitochondrial fusion has yet to be implicated in any major pathological conditions. Elongation of mitochondria was found to protect senescent cells against oxidative stress by reduction of Drp1 and hFis1 [210]. Loss of fusion proteins, particularly OPA1 were found to be detrimental in the settings of heart failure and suggest that OPA1 is needed for maintenance of normal mitochondrial function [211]. A mutation close to the GTPase region of the Mfn2 will lead to Charcot-Marie-Tooth neuropathy type 2A [212]. Studies conducted in cardiomyocytes, skeletal muscle and kidney cells have shown that elongated mitochondria are present in these cells and fusion is needed to maintain integrity of both the mitochondria and the host cell [210, 213-215]. Fragmentation of mitochondria conversely, may imply susceptibility of the cells to the death pathway or subsequent removal by mitophagy [216, 217]. Nevertheless, fragmented mitochondria may also be needed for proper embryonic development, synapse formation and cell division [218].

1.5 Cardioprotection via Ischaemic Preconditioning / Postconditioning

Following a detailed review of the unique functions and characteristics of mitochondria in the previous sections, we now move to explore some of the cardioprotective interventions that target the mitochondria to exert the beneficial effects. In order to prevent IRI, the myocardium has its own endogenous cardioprotective agents, such as production of a cardioprotective nucleoside by the name of adenosine [219, 220], opening of the ATP-sensitive potassium channels (K_{ATP}) to shorten the action potential duration (APD) [221-223] and release of nitric oxide (NO) [224-227] or the activation of the RISK pathway (see Section 1.6.2.3), a cascade of pro-survival kinases. All of these mechanisms confer protection to the myocardium via inhibition of the mitochondrial permeability transition pore (mPTP), a non-specific channel in the inner membrane of the mitochondria [228, 229] (see Section 1.7). Two particularly well-known cardioprotective strategies based on the endogenous system of cardioprotection have been described over the years; ischaemic preconditioning (IPC) (see Section 1.5.1) and ischaemic postconditioning (IPost) (see Section 1.5.2). IPC of myocardium refers to the cardioprotection elicited from periods of brief exposure to ischaemia-reperfusion before the sustained ischaemic event, whereas IPost refers to that elicited by brief episodes of ischaemia-reperfusion at the immediate onset of reperfusion [9]. Recently conducted studies have found that the beneficial effects of both IPC and IPost converge on the mitochondria, particularly inhibition of the mitochondrial permeability transition pore (mPTP) [17, 230].

Different research groups have tried to manipulate or confer cardioprotection by targeting individual mediators of lethal reperfusion injury. Nevertheless there is constant discrepancy in the results generated and transfer to the clinical settings has also proved to be problematic [66]. There have been directives to target more than one mediator at a time, e.g. ischaemic preconditioning and postconditioning where components of the RISK pathway and the mPTP are targeted [61, 67, 229, 231, 232]. A recent 'proof-of-concept' study by Argenta *et al* in 2010 also proposed using mechanical tissue resuscitation (MTR) to remove soluble inflammatory mediators such as TNF-alpha which may assist in enhancing cellular

viability and reduction of tissue oedema [233]. However, it may be more practical and useful if a sole critical factor is identified and targeted for cardioprotection. This statement raises equivocal opinions in which some groups prefer targeting a few different factors in a multifaceted cascade. We believe and postulate that manipulations of the mitochondrial dynamics and function by genetic interventions or drug treatments may serve to prevent IRI. Modulation of mitochondrial morphology may serve as a potential mediator of inhibition of the mPTP and thus can be regarded as a new target for preventing lethal reperfusion injury.

1.5.1 Ischaemic Preconditioning

Ischaemic preconditioning is the term used to describe the intermittent episodes of ischaemia and reperfusion before the prolonged period of ischaemia. The efficacy of IPC was first shown by the group of Murry in 1986 where they significantly reduced the infarct sizes in dog hearts by 75% following 40 minutes of coronary artery occlusion, when the occlusion was preceded by four episodes of 5 minutes ischaemia and 5 minutes of reperfusion [234]. In human subjects, the duration and number of episodes of ischaemia and reperfusion vary between 3 to 5 minutes. Compared to naïve hearts, hearts that have undergone IPC have higher levels of Protein Kinase C (PKC) activation due to activation of the adenosine, bradykinin and opioid receptors. PKC activation can subsequently lead to downstream beneficial effects such as activation of the PI3K kinases, Akt and ERK which are responsible for inhibition of the mPTP [235, 236], and opening of the ATP-sensitive K_{ATP} channel thereby shortening action potential duration and decreasing Ca^{2+} influx into myocytes as well as inhibiting the opening of the mPTP [237, 238]. These results suggest that the mitochondrion is the converging point of the mechanisms evoked by IPC yet the underlying common factor in the mitochondria remains to be elucidated.

1.5.2 Ischaemic Postconditioning

The group of Zhao *et al* demonstrated in 2003 that three intermittent 30-second cycles of myocardial repefusion and ischaemia at the onset of reperfusion following 45 minutes of sustained myocardial ischaemia showed an infarct size reduction from 47% to 11% in a canine model [67]. The term 'ischaemic postconditioning' was thus coined, emphasizing the myocardial reperfusion phase as a target of cardioprotection.

The use of IPost in the clinical settings has been employed on patients with acute myocardial infarction (AMI) who are undergoing primary coronary intervention (PCI) and the results show that myocardial infarct size was reduced by 36% [68] and endothelial and left ventricular (LV) function were improved [239]. In a recent study, the group of Thibault demonstrated a reduction in infarct size at 6 months and preservation of LV function of up to a year following a postconditioning protocol of three to six cycles of inflation and deflation of the angioplasty balloon within the infarct-related coronary artery [240]. The beneficial effects of IPost appear to be related to several important mediators of lethal reperfusion injury such as activation of the RISK pathway [241], reduction of oxidative stress [242], decreasing intracellular Ca^{2+} overload [242], improving endothelial function [67], attenuating apoptotic cardiomyocyte death, reducing neutrophil accumulation [243], delaying the restoration of neutral pH [244, 245] and ultimately inhibition of the mPTP [230, 246]. Postconditioning has been shown to preserve mitochondrial integrity in terms of cristae shapes and mitochondrial membrane structure in isolated rat hearts [247] but there has not been documented evidence of the effects of both preconditioning and postconditioning on mitochondrial morphology.

Another alternative to ischaemia postconditioning is remote ischaemic postconditioning where the same protocol for postconditioning (intermittent ischaemic episodes at the onset of reperfusion) is applied to an organ or tissue but not the heart itself (e.g. the arm or leg) [248-251]. This alternative, while still being subjected to scrutiny in trials involving upper-limb ischaemia in patients with acute MI undergoing PCI, is relatively less invasive compared to direct postconditioning on the heart by manipulating the angioplasty balloon [231, 252, 253].

1.5.3 Targeting the RISK Pathway

The RISK pathway comprises of different pro-survival kinases (explained in Section 1.6) that are activated via pharmacological manipulations such as glucagon-like peptide 1 [254], erythropoietin [255], atorvastatin[256] and atrial natriuretic peptide [257] or mechanical interventions [258] during myocardial reperfusion and are crucial mediators of cardioprotection in the settings of ischaemia-reperfusion. Studies have shown that activation of this RISK pathway can successfully reduce the infarct size by up to 50% and this reduction has been attributed to inhibition of mPTP opening [259], improved uptake of Ca^{2+} in the sarcoplasmic reticulum [260] and the recruitment of anti-apoptotic pathways [228]. A recent clinical study has shown that high-dose atorvastatin given to patients with a non–ST-elevation myocardial infarction at the time of urgent PCI reduces myocardial injury during PCI [261]

1.5.4 Targeting the Mitochondrial PTP

The mPTP is a pore formed in the inner membrane of the mitochondria. Constitutents of the mPTP include CypD and possibly the phosphate carrier [262]. The implication of mPTP in cardioprotection was initiated based on animal studies where pharmacological inhibition of mPTP at the onset of reperfusion by CsA or SfA reduces infarct sizes by up to 50% [232, 232]. Similar results were also obtained in studies involving human atrial trabeculae subjected to sIRI [263]. In addition to that, smaller infarct sizes were also detected in mice lacking CypD (a component of the mPTP) [264]. Inhibition of the mPTP can be categorised into direct or indirect inhibition. Studies are ongoing to determine the feasibility and practicality of the usage of CsA in inhibition of mPTP in the clinical settings, particularly before PCI during an acute MI. Further details are available in Section 1.7.

1.6 Pro-Survival Kinases in Cardioprotection

As mentioned in Section 1.5.3 where kinases play a crucial role in the RISK pathway which is core to both IPC and IPost, we attempt to detail the three kinases which will be used in this study to confer cardioprotection in the following sections.

1.6.1 Protein Kinase A (PKA)

Protein Kinase A (PKA), also known as cyclic AMP-dependent protein kinase, has been investigated since the 1970s when different groups found that PKA phosphorylates troponin, a mediator of contractility in the heart [265] and mediates calcium uptake in the sarcoplasmic reticulum [266]. Since then studies have placed PKA phosphorylation as a crucial mediator of metabolism, contractile activity [267], ion fluxes [268] and gene transcription where pathological conditions ensue in the case of aberration of PKA signalling [269]. PKA is a ubiquitous cellular kinase that phosphorylates serine and threonine residues following activation by cAMP [270]. Structurally, PKA consists of two regulatory subunits, RI and RII, which will release two catalytic subunits, Cα and Cβ upon activation by cAMP [271, 272] (see Figure 1.14).

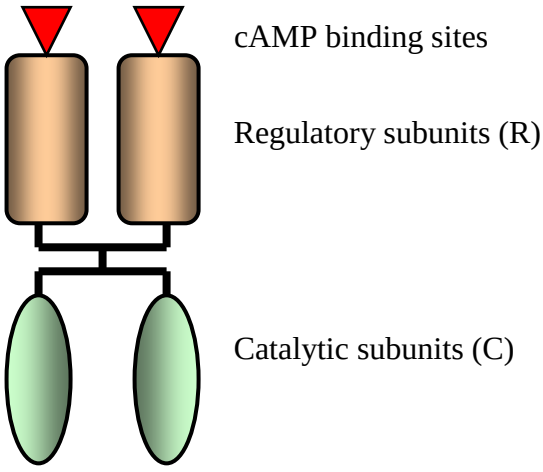

Figure 1.14. Structure of PKA. PKA consists of cAMP binding sites, two regulatory subunits (R) and two catalytic subunits (C).

The expression levels and subcellular localisation of PKA depend on the isoforms of PKA expressed [271]. There are four isoforms of the regulatory subunit (RIα, RIβ, RIIα, RIIβ) and three types of catalytic subunits (Cα, Cβ, Cγ) [271, 273]. PKA activates complex I of the respiratory chain in the inner membrane and the matrix of the mitochondria [76]. Temperature preconditioning has been found to activate PKA prior to PKCε activation as a form of cardioprotection. The activation of PKA in this setting by moderate ROS production and β-adrenergic stimulation causes β-adrenergic desensitisation [274] and attenuation of calpain-mediated degradation pathways [275]. Nevertheless, there have also been claims that PKA confers cardioprotection independent of PKC signalling, in the form of Rho-kinase inhibition which leads to formation of the actin cytoskeleton, chemotactic migration, activation of platelet, and cytokinesis [274, 276-279]. PKA signalling has also been implicated in attenuation of ROS-induced senescence by GLP-1 [280] and reduction of calcium overloading by opening of the mitochondrial Ca^{2+}-activated K^{+} channels in cardiac myocytes [281] Paradoxically, increased PKA phosphorylation of the ryanodine receptor (RyR) has been detected in human heart failure [282]. There has been a study investigating the role of PKA in protection against cerebral ischaemia by suppression of ROS production [283]. Suppression of PKA however, has also been detected to confer cardioprotection by downregulation of the Ca^{2+}/calmodulin-dependent protein kinase II (CaMKII) [284]. PKA has also been demonstrated to phosphorylate and inhibit Drp1, the fission protein at Ser^{637} [182] (see Figure 1.15).

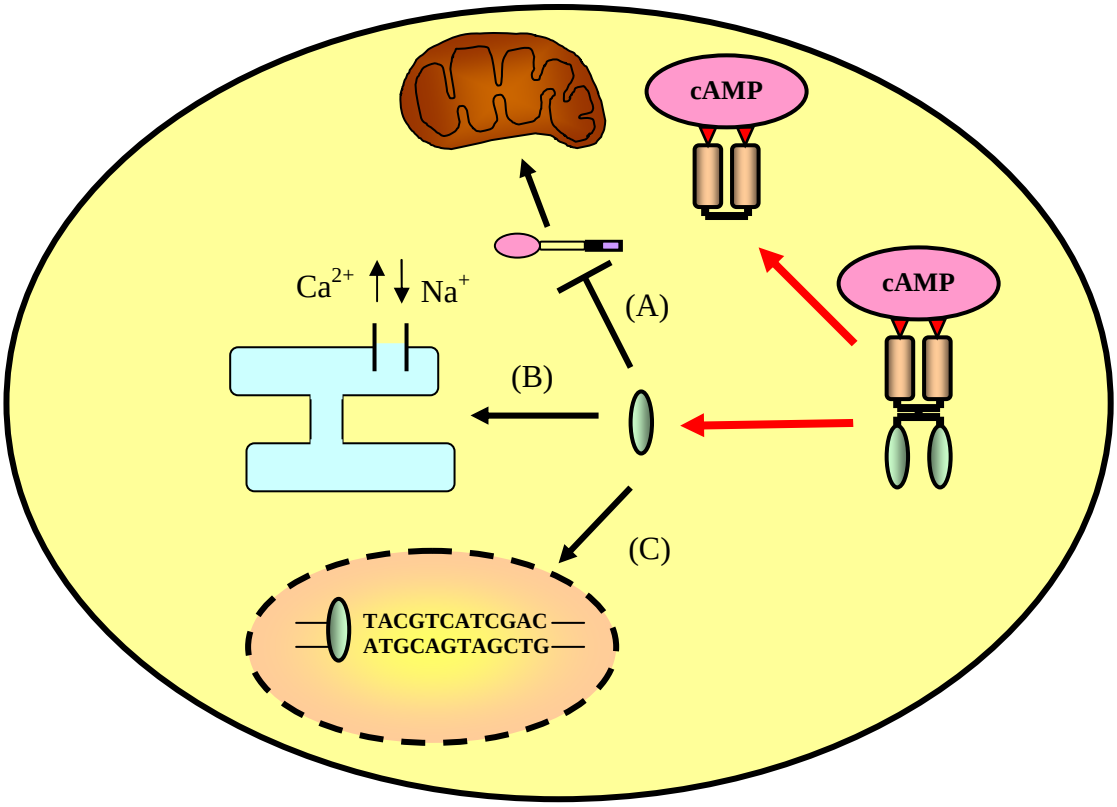

Figure 1.15: Mechanisms of action of PKA in the cell. Activation of PKA (denoted by red arrows) will lead to effects such as (A) inhibition of mitochondrial fission, (B) reduction of calcium overloading by opening of the mitochondrial Ca^{2+}-activated K^+ channels, and (C) expression of growth factors.

1.6.2 Protein Kinase B (PKB)

The PKB/Akt protein consists of three isoforms; PKBα/Akt1, PKBβ/Akt2 and PKBγ/Akt3 with all three comprising of a pleckstrin homology (PH) domain at its amino-terminal end (amino acids 1-106), which makes up the major part of the amino-terminal regulatory domain (residues 1-147), a serine/threonine kinase domain from amino acid 148 to 411, and the carboxy-terminal tail region (amino acids 412 – 480) accounting for the remainder of the protein [285] (see Figure 1.17).

PKB/Akt is involved in phosphorylation of the mitochondrial ATP synthase β subunit and glycogen synthase kinase 3β (Gsk3β), which in turn, inhibits the activity of pyruvate dehydrogenase [76]. Knockouts of the different types of PKB/Akt cause different effects. Akt1 knockout causes retardation of growth [286-288], Akt2 knockout in mice causes insulin resistance and slight retardation of growth depending on the genetic background [286, 289, 290] whereas knockout of Akt3 decreases the neural cell size and cell number hence reducing brain size [286, 291, 292].

Research conducted on transgenic mice has proven that the overexpression of wild-type Akt1 in the nucleus of cardiac myocytes confers cardioprotection from ischaemia-reperfusion [293]. The subcellular distribution affects the respective growth and cardioprotective effects of Akt as detected from the absence of cardiac growth following chronic Akt1 activation [294]. However, overexpression of Akt1 has also been found to exhibit adverse effects. In the case of Akt1 overexpression in endothelial cells, cells undergo apoptosis right from the embryonic stage due to irregular alteration of the vascular tissue up to the adult stage where blood vessel formation deviates from normal physiological state to the pathological state [286, 295, 296].

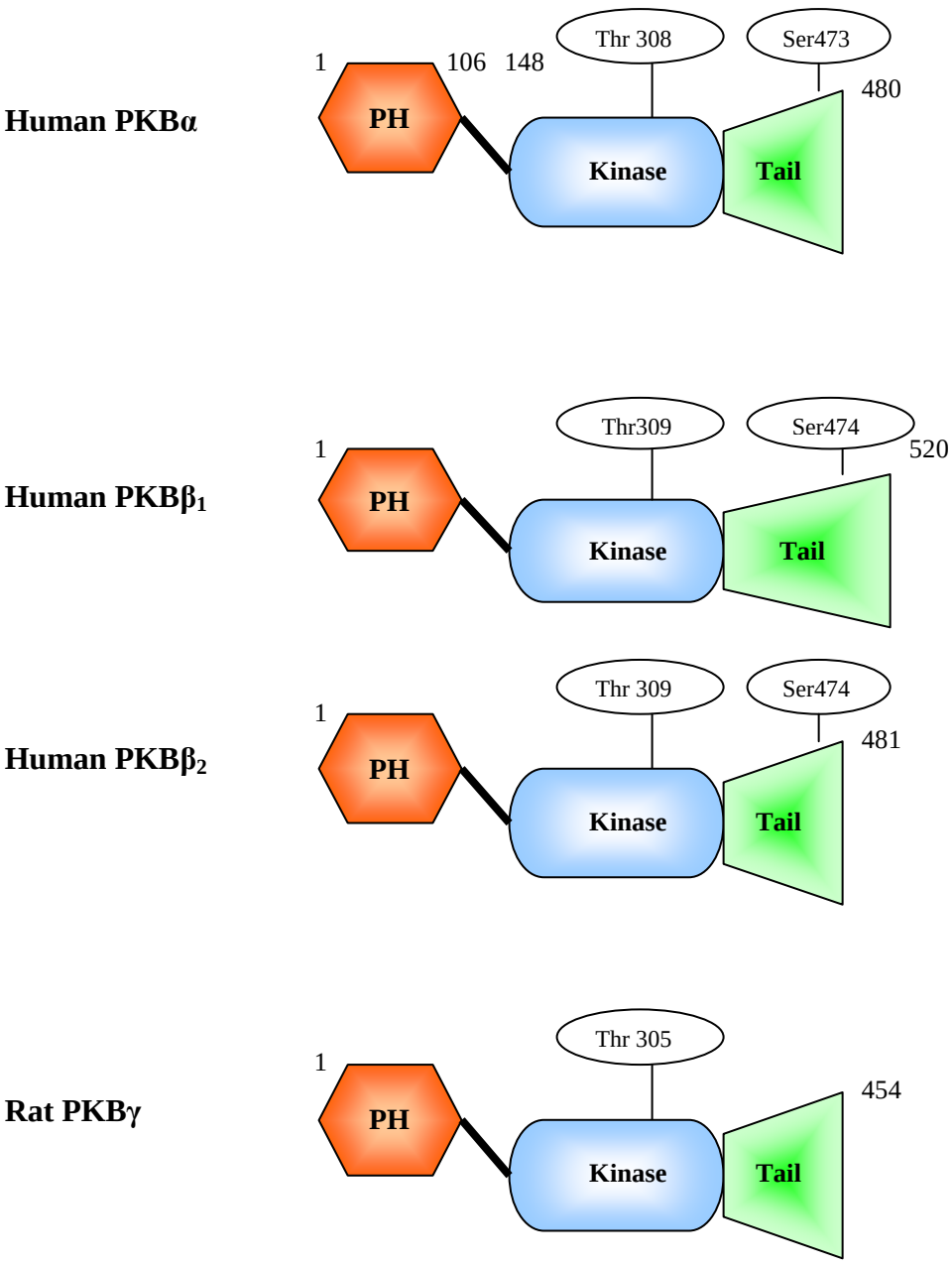

Figure 1.17: The four isoforms of PKB/Akt. PKB and PKB isoforms derived from the same gene but alternatively spliced with different total number of amino acid residues. Phosphorylation sites by insulin-induced kinases are shown. PH: pleckstrin homology domain.

1.6.2.1 Mechanism of action for Akt

Insulin or insulin growth factor-1 (IGF-1) interacts with its respective receptor, phosphatidylinositol 3-kinase (PI3K)

↓

PI3K phosphorylates membrane inositol lipids

↓

The membrane inositol lipids bind to the pleckstrin domain of Akt, inducing its translocation to the plasma membrane.

↓

Akt becomes the substrate of 3β-phosphoinositide-dependent kinase-1 (PDK-1), which activates it through phosphorylation of residue Thr308.

↓

Phosphorylation of Akt results in full activation of Akt kinase activity and the subsequent regulation of multiple cellular processes, including the transmission of growth factor-dependent survival signal

Our study places emphasis on PKB/Akt in view of the documented effects of Akt on cell survival and protection from apoptosis [258, 285, 293, 297-309]. Akt is a member of a kinase family in mammalian cells, but Akt homologs can be found in *Drosophila melanogaster*, *Caenorhabditis elegans* and *Dictyostelium discoideum* [310]. Akt is characterised as a serine/threonine kinase which is regulated by growth factors and consists of a plekstrin homology domain at the amino terminal end, kinase domain as well as the carboxy terminal tail [285]. Akt was identified independently in 1991 by three different groups due to the similarity to both PKA and PKC and as a product of the oncogene v-akt of the acutely transforming retrovirus AKT8 in the rodent T-cell lymphoma [285, 311-313].

.

In general, the activation of the serine-threonine protein kinase Akt in cells exposed to different growth factors such as platelet-derived growth factor (PDGF), epidermal growth factor (EGF), insulin, thrombin and nerve growth factor (NGF) involves sequential steps starting from activation of the PI3K by autophosphorylation of receptor tyrosine kinases and generation of the second messenger PtdIns(3,4,5)P_3 from PtdIns(4,5)P_2 by the PI3K. Following that, Akt is recruited and translocated by PIP_3 through the PH domain to the plasma membrane

followed by its phosphorylation by upstream kinases (PDK1 and PDK2) in a PI3K-dependent signalling system [285, 310, 314-316] (see Figure 1.18). The PH domain is extremely important in the sense that the lipids produced by PIP_3 and $PI(3,4)P_2$ need to bind to the PH domain of Akt with high affinity and specificity in order to activate the Akt and mediates its translocation from the cytosol to the plasma membrane to present to the upstream activating kinases [285]. Phosphorylation of Akt occurs at two sites; Thr308 in the activation loop of the kinase domain and Ser473 in the hydrophobic-motif of the carboxy-terminal tail [317] (see Figure 1.18). Phosphorylation of the two residues occurs independently and is probably mediated by two different kinases, PDK1 for Thr308 and PDK2 for Ser473 [317, 318]. A study by Yang *et al* in 2002 demonstrated that activation of Akt relies on the phosphorylation of Ser473 as it stabilises its active conformation [319]. The activity of PDK1 is stimulated by PIP_3 and $PI(3,4)P_2$, hence suggesting another role for PIP_3 and $PI(3,4)P_2$, the products of PI3-K besides binding to the PH domain of Akt [285]. Nevertheless, the exact identity of PDK2 has yet to be elucidated, with speculations as to the different cellular and physiological context being the main determinants of the exact identity of the PDK2. PDK2 candidates include a myriad of kinases such as PKB itself [320], PDK1 [321], integrin-linked kinase 1 (ILK1) [322], mitogen activated protein kinase activated protein kinase 2 (MAPKAPK2) [317], protein kinase C _II (PKC_II) [323], and the members of the atypical PI 3-kinase related protein kinase (PIKK) family: DNA-dependent protein kinase (DNA-PK) [324], ataxia telangiectasia mutant (ATM) [325] and, more recently, the rapamycin-insensitive mTOR complex TORC2 [326] (see Figure 1.18).

Upon activation at the plasma membrane, phosphorylated Akt then translocates to either the nucleus or cytosol to exert its effects [327]. The downstream substrates of Akt include GSK3, p70 S6K, GLUT4 and the metabolic regulatory enzyme PFK2 [285, 328]. GSK3 is involved in regulation of several intracellular signalling pathways such as the control of certain transcription factors, tumour suppressor gene product APC, and wingless developmental pathway in flies and dorsoventral patterning in frogs [328]. P70 S6K is involved in alteration of the protein synthesis pattern following mitogenic stimulation of cells. GLUT4 translocation from the intracellular environment to the plasma membrane following insulin uptake also relies on the Akt.

In terms of cardiac myocytes, documented effects of Akt include control of metabolism, which is dependent on cytoplasmic phosphorylation, sequestration and consequential inhibition of the FOXO 3 transcription factor, which in turn controls the expression of multiple atrophy-related genes ("atrogenes"), including the ubiquitin ligase atrogin-1 (MAFbx), an enzyme enhancing muscle protein catabolism [329], activation of different mitochondrial proteins which are involved in the inhibition of apoptosis [69], intracellular acidification, mitochondrial hyperpolarisation, and the decline in oxidative phosphorylation that precedes cytochrome *c* release and increases coupling of glucose metabolism to oxidative phosphorylation and regulates mPTP opening via the promotion of hexokinase-VDAC interaction at the outer mitochondrial membrane [5].

The ability of activated Akt, which is dependent on glucose as an interlink between glycolysis and oxidative phosphorylation [330] to prevent apoptosis is mediated by its ability to phosphorylate BAD [310], induce the antiapoptotic protein members of the Bcl-2 family, inhibit the release of cytochrome *c* by maintaining the mitochondrial integrity, activate the mitoK_{ATP} channels, phosphorylate and inactivate the caspase family, as well as inactivate the AMP-activated protein kinase (AMPK) in the heart [69].

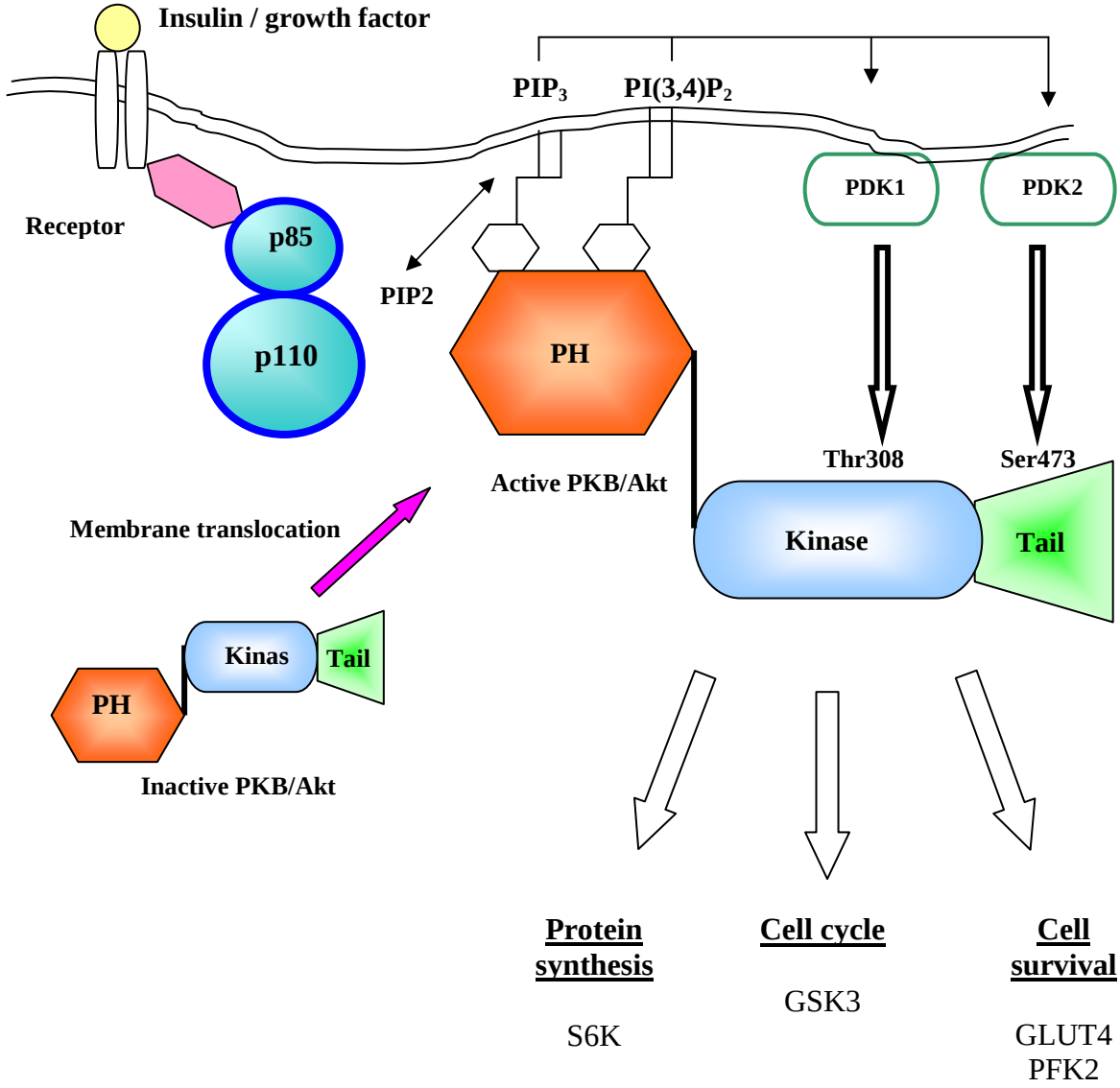

Figure 1.18: The PI3K-Akt signalling pathway. Upon stimulation by insulin or growth factors, PI3K, a heterodimer of p85 regulatory subunit and p110 catalytic subunit is activated, either through Ras molecules or adaptor molecules. The activated PI3K will phosphorylate PIP2 to become PIP3 and PI(3,4)P2. These phosphoinositides recruit the PDK1 and PKB/Akt to the plasma membrane via the N-terminal plekstrin homology (PH) domain. PDK1 subsequently phosphorylates and activates Akt at the Thr308 residue on the kinase domain whereas PDK2 phosphorylates Ser473 on the tail. Activated PKB/Akt translocates to different sites in the cell and phosphorylates other downstream substrates, resulting in a variety of physiological effects such as protein synthesis, cell cycle and survival (Adapted from Downward, 1998; Franke, 1999; Luo *et al*., 2003; Shiojima & Walsh, 2006).

1.6.2.2 Acute vs. Chronic Akt Activation

In human models of advanced-stage heart disease, Akt phosphorylation has been found to be enhanced [331-333]. This implies two possibilities: first is activation of Akt alone is not cardioprotective for long term and second is that chronic or long-term Akt activation may be harmful [334].

Although Akt is known to be a pro-survival protein, chronic Akt activation has been documented to cause several adverse effects. The duration of Akt activation influences cardiac hypertrophy in which activating Akt for a short time induces normal physiological hypertrophy with a reasonable increase in heart size (~80%) while activation for a prolonged period causes 'pathological' hypertrophy with an extreme increase in heart size (2.7-fold) [335].

As an example, chronic Akt activation decreases the GLUT4 expression in insulin-responsive compartments [336]. Besides that, through negative feedback inhibition of IRS-1/PI3K signalling activity, chronic Akt activation has also been found to inhibit cardiac function recovery as well as increasing cardiac injury in an *ex vivo* model of IRI [334]. The negative feedback inhibition relies on proteasome-dependent degradation of insulin receptor substrate–1 (IRS-1) and inhibition of transcription of both IRS-1 and IRS-2 [334, 337]. Chronic Akt activation in the heart also causes an increase in the level of basal glucose uptake and glycogen deposition albeit decreases the sensitivity to insulin [336]. The toxicity of Akt is due to the variance of expression based on the α-myosin heavy chain promoter [338].

Akt can be constitutively activated by artificially targeting Akt to the plasma membrane by attaching a myristoylated/palmitoylated sequence motif fused to the N-terminus of Akt. The Akt gene construct (myr-Akt) has been modified to localise to the sarcolemma in order to be constitutively active [338]. The phosphorylation and activation of Akt can be inhibited by using the PI3K inhibitors such as wortman and LY294002.

Akt/PKB can also be negatively regulated by either the tumor suppressor phosphatase and tensin homology deleted on chromosome ten (PTEN) [302] or the

SH2-domain-containing inositol polyphosphate 5-phosphatase (SHIP) [339], which convert PtdIns(3,4,5)P_3 to PtdIns(4,5)P_2 and PtdIns(3,4)P_2. Protein phosphatase 2A (PP2A) and PH domain leucine-rich repeat protein phosphatase (PHLPP) do so directly by dephosphorylating Ser473 and/or Thr308 on PKB [340, 341].

1.6.2.3 Reperfusion Injury Salvage Kinase (RISK)

Apoptotic cell death following IRI and the ability of the serine/threonine kinase (Akt) and 42- and 44-kDa extracellular signal-regulated kinases (Erk1/2) mitogen-activated protein kinase to promote cell survival through activation of different antiapoptotic mechanisms triggered off the initial investigation of the role of these kinases and cardioprotection [228, 229, 342, 343], leading to the term of RISK pathway being coined by Yellon & colleagues [320].This is the reference that first used the term RISK pathway - The term RISK pathway refers to the group of protein kinases specifically activated during myocardial reperfusion, such as the PI3K-Akt pathway and (Erk1/2) mitogen-activated protein kinase (MAPK) which is responsible for conferring cardioprotection and preventing lethal reperfusion injury [228, 231]. Activation of the RISK pathway can be induced in the presence of growth factors and cytokines, insulin, urocortin and other agents such as atorvastatin and bradykinin [256, 344, 345].

The cardioprotective function of the RISK components has been demonstrated in 2000 by Fujio *et al* and Miao *et al* where gene constructs encoding for constitutively active Akt transfected in mural or rat hearts protect against IRI [304, 346]. In the presence of IPC stimulus using the isolated perfused rat heart, the protection effects can be traced as far as the reperfusion period where the opening of the mPTP is inhibited following phosphorylation of Akt as well as ERK 1 and ERK 2 (referred to as ERK 1/2) [17, 235, 307]. Tong *et al* in 2000 demonstrated the phosphorylation of both Akt and its downstream target, GSK3β by a standard IPC stimulus on the same model. The phosphorylation of ERK and its potential signalling role is debatable, with some studies showing phosphorylation of ERK by a standard IPC stimulus [347] and some studies reporting no changes in phosphorylation status of ERK [348]. However, the study by Hausenloy *et al* in 2005 demonstrated that the IPC stimulus actually phosphorylates both the Akt and ERK at the time of reperfusion,

thereby showing two phases of phosphorylation, one before the index ischaemia and one at the onset of reperfusion [235]. These findings were verified by the use of the PI3K inhibitor, wortmannin, where application of wortmannin at the onset of reperfusion completely abrogates the IPC-induced protection [235, 349]. IPost, comprising six 10-seconds episodes of alternating myocardial ischaemia and reperfusion, applied onto the isolated perfused rat heart also showed simultaneous activation of the RISK pathway through phosphorylation of Akt and ERK1/2 at reperfusion occurring in line with mPTP inhibition [241]. Pharmacologically inhibiting the phosphorylation of Akt and ERK again blocks the protective effect of IPost [241, 350, 351]. In a nutshell, irrespective of Akt or ERK, IPC and IPost converge on a common signaling pathway – the RISK pathway to mediate cardioprotection at the onset of reperfusion [235, 308, 352] (see Figure 1.19). The activation mechanism of the RISK pathway by IPC or IPost remains unclear but has received various speculations. In the settings of IPC, the biphasic phosphorylation response may serve to activate the Akt and ERK before ischaemia so as to potentiate full phosphorylation at the onset of reperfusion [258]. An alternative hypothesis is IPC induces the release or activation of an intermediary factor, such as adenosine, ROS or PKC to activate the RISK pathway at reperfusion [258]. The activation of the RISK pathway by IPost is much more defined by the results of studies by Kin *et al*., and Philipp *et al*., where G-protein-coupled receptor (GPCR) activation by adenosine receptors occupancy as a result of PKC activation from IPost has been proposed to activate the RISK pathway [353, 354]. Downstream effectors of the upregulation of the RISK pathway include inhibition of mitochondrial PTP opening [259], improved uptake of Ca^{2+} in the sarcoplasmic reticulum [260] and the recruitment of antiapoptotic pathways [231].

The mPTP is believed to be the central target of the RISK pathway because both IPC and IPost have been shown to confer cardioprotection by inhibiting the mPTP opening as an endpoint [258]. Downstream effects of the RISK pathway itself involves closing the mPTP as shown by the phosphorylation of various downstream effectors such as the p70S6K [305], activation of endothelial NO synthase (eNOS) to inhibit mPTP opening through its release of NO [256, 344, 355], inactivation of Bcl-2-associated death promoter (BAD) which exerts its apoptotic actions via the opening

of the mPTP [305] and activation of GSK3β which has been demonstrated to mediate inhibition of mPTP opening [356, 357]. These effectors are the main players in inhibiting the opening of the mPTP during the onset of reperfusion in response to mitochondrial calcium overload, oxidative stress, and ATP depletion [61]. The interplay between cardioprotection of IPC and IPost, activation of RISK pathway and inhibition of mPTP opening was further proven by pharmacologically inhibiting the IPC- or IPost-induced phosphorylation of these kinases, leading to the failure in limitation of infarct size [241, 258]

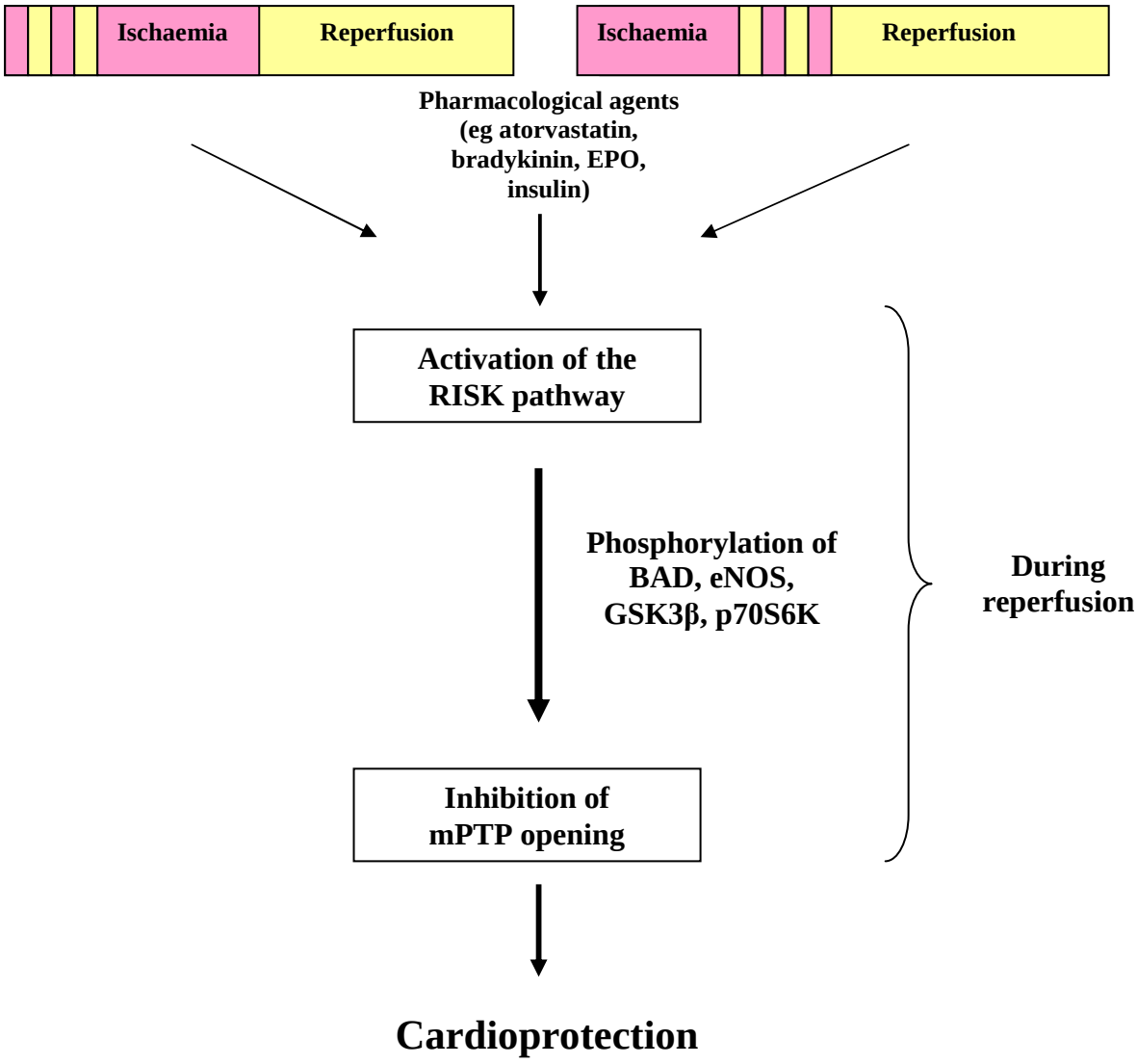

Figure 1.19: Scheme demonstrating the role of IPC and IPost in conferring cardioprotection through activation of the RISK pathway and subsequent inhibition of the mPTP opening (Adapted from Hausenloy *et al*., 2005).

1.6.3 Protein Kinase C (PKC)

PKC in the mitochondria exist in a variety of different isoforms with different function. PKCε confers cardioprotection by phosphorylating the VDAC component of the mPTP and hence prevents its opening [10, 76]. The combination of both PKCε and PKCδ plays a crucial role in regulating mitochondrial KATP channel during the ischaemic preconditioning phase [7, 76, 358]. PKC has also been found to phosphorylate the BH3-only protein Bad which increases the availability of Bcl-2 for antioxidant and anti-apoptotic functions [359, 360]. The activation of PKCε by PKA during temperature preconditioning underlies the cardioprotection elicited through mechanisms such as myocardial glycogen breakdown prior to ischaemia which will reduce the amount of calcium overloading during ischaemia, reduction of ROS and inhibition of mPTP opening [361, 362].

1.7 The Mitochondrial Permeability Transition Pore (mPTP)

In the previous sections, we have reviewed the myocardial IRI (Section 1.2), the mitochondria as a crucial organelle for cardioprotection (Sections 1.3 & 1.4), the cardioprotective interventions that targets the mitochondria (Section 1.5) and the survival kinases that play a role in the cardioprotective interventions (Section 1.6). In this section, we will be reviewing the discovery, characteristics and components of the mPTP in the mitochondria, which is a central mediator of cell death following ischaemia-reperfusion and an important target for successful cardioprotective interventions.

1.7.1 Origins of the mPTP

The mPTP was first recognised in the 1960s when studies discovered that mitochondria swell upon exposure to high levels of calcium and this swelling decreases light scattering in the spectrophotometer [363, 364]. Using calcium chelators, the light scattering effect returned to normal [363, 364]. This effect was originally attributed to the non-specific permeabilisation of the IMM by the build up of fatty acids and lysophospholipids from the activation of Ca^{2+}-sensitive phospholipases [142]. It was not until the late 1970s that two different groups: Haworth and Hunter [365, 366] and the group of Crompton [367] identified the opening of a non-specific channel in the IMM as the cause of the increase in permeability.

1.7.2 Characterisation of the mPTP

Intra- or extracellular stress causes cellular malfunctioning which usually congregates on mitochondria, triggering an increase in the permeability of the inner mitochondrial membrane, a phenomenon known as mitochondrial permeability transition [135]. This mitochondrial permeability transition is actually caused by the opening of permeability transition pore (PTP) in the inner mitochondrial membrane with ensuing loss of ionic homeostasis, matrix swelling as well as outer membrane rupture [135]. The mPTP was traditionally thought to be made up of a complex of inner [adenine nucleotide translocase (ANT)] and outer [voltage-dependent anion channel

(VDAC) or porin] membrane proteins as well as the ciclosporin A (CsA)-binding protein, cyclophilin D (CypD) in the matrix [76, 368] (see Figure 1.20). However, following subsequent studies by Baines and colleagues in 2005, Nakagawa and colleagues in 2005, found that only the CypD remains as a regulatory component of the mPTP, while the mitochondrial permeability transition was still detected in cells lacking ANT or VDAC [369-371]. Recent studies have also implicated the mitochondrial phosphate carrier as a key component of the mPTP [262, 370, 372] (see Figure 1.21). Cardiac cell death by apoptosis or necrosis during ischaemia-reperfusion is associated with mPTP opening of the mitochondria, of which opening is induced by certain conditions in the heart, particularly post-ischaemia and during reperfusion, such as the generation of reactive oxygen species (ROS), calcium overload, low levels of adenine nucleotides and a normalised intracellular pH (pH_i) [31, 373, 374]. Once opened, external solutes <1500Da enter the mitochondria causing swelling of mitochondria, rupture of the mitochondrial outer membrane and the subsequent release of pro-apoptotic proteins such as cytochrome *c* and second mitochondria-derived activator of caspases/direct IAP-binding protein with a low isoelectric point (Smac/DIABLO) in line with depolarisation of the inner membrane potential and inhibition of ATP synthesis [10]. Failure to inhibit pore opening will therefore causes apoptosis and ensuing necrosis if prolonged.

1.7.2.1 ANT

The ANT was implicated as a component for the mPTP based on findings that ATP and ADP both inhibit mPTP. However, complexes formed with other compounds such as Mg, AMP, GDP or GRP failed to inhibit the mPTP [365]. The notion was further solidified when studies found that inhibition of the binding of ATP and ADP to the ANT by depletion of adenine nucleotides or modification of thiol groups on the ANT leads to mPTP opening [375]. CypD when bound to ANT with the 'c' conformation under high levels of Ca^{2+} will undergo a conformational change to facilitate pore formation [375-377]. The role of ANT as a core component of the mPTP remained widely accepted until the group of Kokoszka in 2004 showed that genetic ablation of ANT1 and ANT2 did not prevent mPTP activation in mouse liver mitochondria [371]. Nevertheless, the Ca^{2+} threshold needed to induce mPTP opening

in these mitochondria was increased compared to wild-type mitochondria while efficiency of the ANT ligands such as ADP and CAT was decreased [371]. The availability of the isoform ANT4 however, is probably the factor that determines the normal functions of the liver [378, 379]. The ANT therefore, will possibly play a regulatory role in the opening of the mPTP [380].

1.7.2.2 VDAC

VDAC was originally proposed to be a constituent of the mPTP based on the fact that it was found to co-purify with the ANT in a complex under certain conditions. Re-constitution of this complex can lead to formation of a calcium-activated pore that can be inhibited by CsA [381]. Nevertheless, it was later demonstrated that mitochondria lacking all three isoforms of VDAC can still have normal mPTP opening hence eradicating the role of VDAC as an essential constituent of the mPTP [369].

1.7.2.3 CypD

CypD was initially identified as a component of the mPTP based on the fact that the opening of the mPTP is inhibited by CsA [382]. The mechanism for this inhibition lies in the inhibition of a matrix peptidyl-prolyl cis–trans isomerase (PPIase) which was subsequently purified and identified as CypD [376, 383, 384]. CyPD is a matrix protein of about 18 kDa and is encoded by the nuclear gene PPIF [385]. CypD is different from the cytosolic cyclophilin A (CypA) where a combination of CypA and CsA will lead to immunosuppressive reactions and inhibition of calcineurin, a calcium-sensitive phosphatase [386]. The role of CypD in mPTP was confirmed by studies using mitochondria from livers of CypD knockout mice in which calcium-induced mPTP opening was not significantly detected, in line with studies using mitochondria from wild-type mice treated with CsA [264, 387, 388]. Nevertheless, it is noteworthy to point out that loss of CypD does not signify loss of mPTP opening. The loss of CypD only raises the threshold levels of calcium needed for mPTP

opening as the main role of CypD is to provide conformational changes to the membrane protein through its PPIase activity [388, 389].

1.7.2.4 Mitochondrial phosphate carrier (PiC)

The studies carried out in the laboratory of Halestrap demonstrated that the PiC may be involved as a component of the mPTP [262]. According to the study carried out, ANT binding to the phenylarsine oxide (PAO) affinity column was prevented by carboxyatractylate (CAT). Yet induction of mPTP opening by PAO was not prevented by CAT [262]. Based on this data, an additional activating site apart from the ANT was speculated and the PiC was identified from the component IMM proteins isolated from CAT-treated beef heart mitochondria [262]. Inhibitors of the mPTP can prevent both the binding of the PiC and the activation of the mPTP by PAO in isolated mitochondria, in line with the mode of action on PiC [262]. PiC binding with CypD has also been shown in the same study where co-immunoprecipitation and GST-CyP-D pull-down experiments were carried out [262].

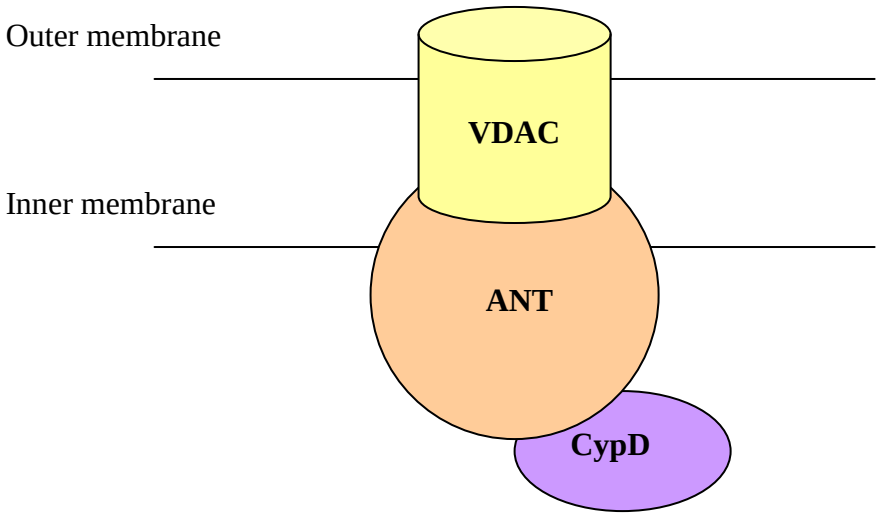

Figure 1.20: Original proposed structure of mPTP: a complex of voltage-dependent anion channel (VDAC) on the outer membrane, adenine nucleotide translocase (ANT) on the inner membrane and cyclophilin D (CypD) from the matrix.

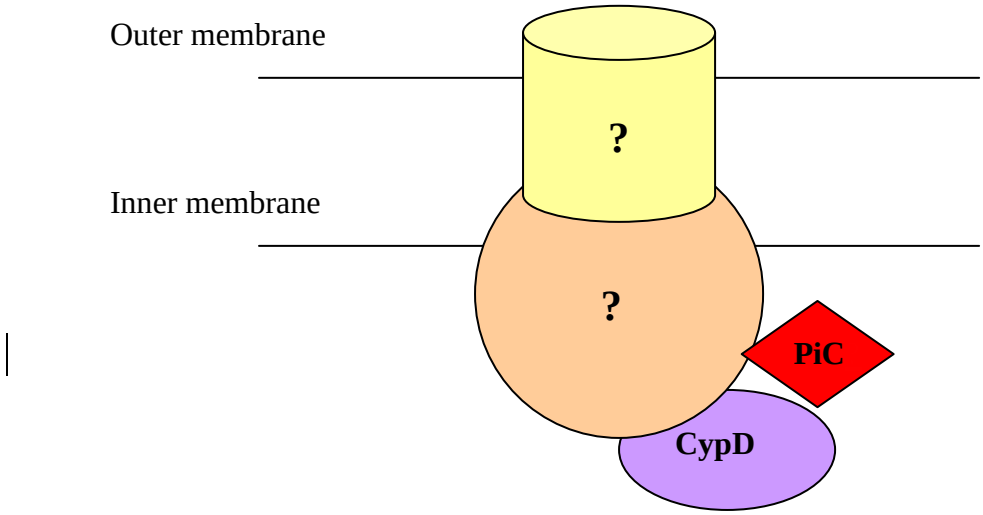

Figure 1.21: Current structure of mPTP. The mPTP complex is currently thought to be composed of the CypD component with the phosphate carrier (PiC) bound to it.

1.7.3 Triggers of mPTP opening

mPTP opening is induced by calcium overloading in the mitochondria, increased ROS, changes in membrane potential, matrix pH, divalent cation concentrations, reduced/oxidised thiol balance and reduced pyridine nucleotide pools, all of which occurs during myocardial ischaemia and reperfusion [11, 35, 368, 390-393] (see Figure 1.22).

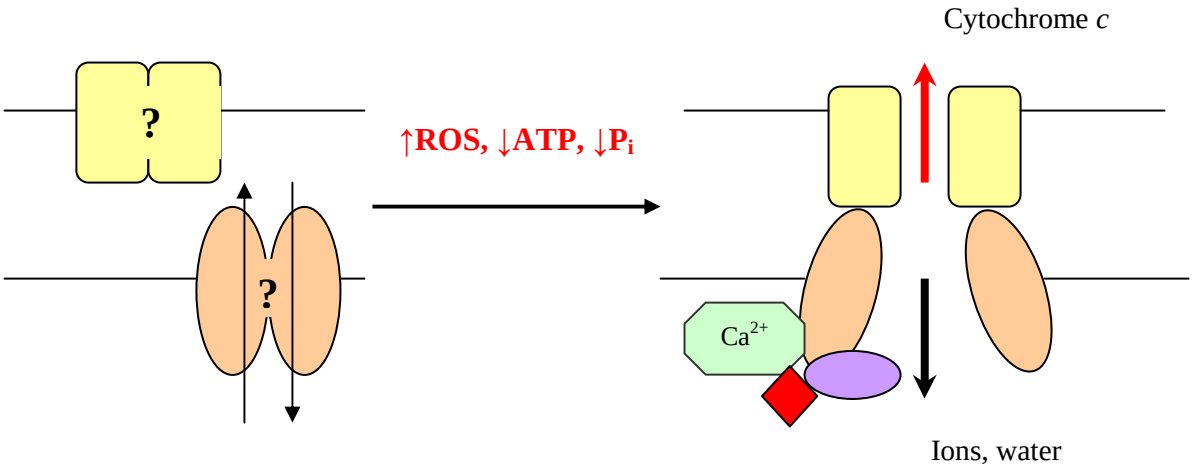

Figure 1.22: mPTP formation. The current core components of the mPTP consist of only Cyclophilin D (purple) with the phosphate carrier (PiC) (red) as a regulator. Under normal aerobic conditions, the mitochondrial membrane is impermeable to most solutes hence providing an optimum environment for oxidative phosphorylation and ATP synthesis. In the presence of external stress such as ischaemia-reperfusion with the increase of reactive oxygen species (ROS), mitochondrial calcium overload and ATP depletion, the permeability of the membrane changes leading to mPTP formation. Mitochondria will depolarise due to influx of water and ions from the cytosol and cytochrome *c* will be released by rupture of the outer membrane.

During ischaemia-reperfusion, ROS originates from two sources: xanthine oxidase and the mitochondrial respiratory chain [394]. Xanthine oxidase, an enzyme formed from xanthine dehydrogenase by the oxidation of enzyme thiols and Ca^{2+} activated proteases during ischaemia and reperfusion, oxidises xanthine into oxygen free radicals. Xanthine itself is produced from adenosine monophosphate (AMP) which originates from the ATP hydrolysis during ischaemia [373]. The second source is the mitochondrial electron transport chain where ubiquinone, a component of the Complex III, is partially reduced to ubisemiquinone during the lack of oxygen in ischaemia, which then reacts with oxygen during reperfusion to produce oxygen free radicals [373]. Oxidative stress produced by chemicals sensitises the mPTP to Ca^{2+} by thiol modification as can be seen in the usage of PAO and diamide where ADP binding to the ANT is impaired by the cross-linking of Cys_{160} to Cys_{257} on two matrix-facing loops of the ANT [395-397]. This particular effect will causes the mPTP to open even at negative MMP potential as the adenine nucleotides can no longer bind to the ANT [398, 399].

The positioning of mitochondria itself near calcium-release sites in the endoplasmic reticulum (ER) can promote uptake of calcium released from the ER [73]. Mitochondrial calcium overload occurs when the mitochondria becomes unable to cope with the increasing calcium influx. The calcium concentration in the matrix is controlled by a calcium uniporter channel for influx and a Na^{+}/Ca^{2+} exchanger (NCX) for efflux [141]. When the calcium concentration in the matrix increases beyond a certain threshold, the NCX becomes saturated whereas the uniporter which acts as a channel is unaffected [141]. Therefore, calcium overload occurs, hence promoting mPTP opening by binding to the cyclophilin D component. In the case of ischaemia, there is a drop in both ATP and intracellular pH levels, caused by a build-up of lactic acid produced from the glycolysis used to synthesis ATP in the absence of oxygen. In order to increase the pH_i, the cell utilises the sodium-hydrogen exchanger 1 (NHE-1) to extrude the H^{+} while pumping in Na^{+}. Due to the lack of ATP levels, the Na^{+} cannot be pumped out by the NCX. Similarly, malfunctioning of the NCX will promote loading of Ca^{2+} which it normally extrudes. Either situation will lead to increased Ca^{2+} in the cytoplasm and subsequent increase in the mitochondria [135].

A low pH particularly during ischaemia will also inhibit the opening of the mPTP. This may be due to the presence of high levels of protons that will inhibit binding of Ca^{2+} at its trigger site [366, 400, 401]. Conversely, during reperfusion the pH levels return to normal and the pore will open as there are fewer protons available to compete with Ca^{2+}.

A hyperpolarised (more negative) mitochondrial membrane potential will also inhibit the opening of the mPTP [402, 403]. The impairment of the respiratory chain by the presence of ROS at the onset of reperfusion will lead to uncoupling of the mitochondria, MMP depolarisation and subsequent mPTP opening.

There are a few explanations for the role of phosphates in triggering the mPTP. Enhancement of calcium uptake in the mitochondria is the primary role of phosphate in inducing the mPTP [363, 396]. In addition to that, there are also other roles of phosphate such as the chelation of free Mg^{2+} cations which are responsible for the inhibition of mPTP and prevention of matrix acidification [402, 404]. The phosphate carrier (PiC) also serves as an additional binding site for PAO in the activation of the mPTP [262].

Free adenine nucleotides have been known to inhibit the mPTP by inducing the ‘m’ conformation of the ANT [405]. Bongkrekic acid (BKA) desensitises the mPTP to Ca^{2+} while CAT sensitises the pore to Ca^{2+} [365, 405]. The mode of action of both of these chemicals converges on the ANT. The sensitivity of the mPTP is reduced in the presence of both ATP and ADP but not by the complexes of ATP with cations such as Mg^{2+} or by other nucleotides that are not transported by the ANT such as AMP, GDP or GTP [365, 376, 405]

1.7.4 Types of pore opening

Membrane pore opening can be divided into inner membrane pore opening and outer membrane pore opening. Inner membrane pore opening can cause membrane depolarisation, release of low molecular weight compounds, cristae reorganisation and swelling of the mitochondrial matrix. A number of factors can cause iMPT, including increasing intracellular calcium concentration, reactive oxygen species, and the process of ischaemia-reperfusion [11]. In the absence of inner membrane cristae remodelling, outer membrane pore opening is responsible for the partial release of apoptotic proteins while the presence of cristae remodelling will allow the complete release of apoptotic proteins [11].

The function of the mitochondrial pore complex is based on two operating modes; a high conductance mode and a low conductance mode. The high conductance mode renders permeability to solutes with the MW of less than 1500 Da which then causes iMPT leading to loss of membrane potential that will inhibit mitochondrial fusion, release of Ca^{2+} and interruption of oxidative phosphorylation. The low conductance mode allows solutes with MW of less than 343 Da responsible for signal transduction to enter the mitochondria [11].

The number of mitochondria involved in iMPT dictates the different cellular response pathways occurring. In the case of few mitochondria with iMPT, the organelles become encapsulated in autophagosomes for subsequent lysosomal digestion which removes the damaged and probably lethal mitochondria. If MPT becomes more prevalent and ATP depletion occurs, then the glycine-sensitive organic anion channel will be opened leading to the initiation of a metastable state with subsequent rupture of the plasma membrane and necrosis [11].

1.8 Summary and Main Objectives of the Thesis

We hypothesise that one potential way to keep the mPTP closed is to promote mitochondrial fusion. Mammalian mitochondria exist in a typical network of branched reticular tubules originating from the nucleus [146, 406]. Nonetheless, mitochondrial shape is not constant, with interchanges between the fused state and the fragmented state [87, 91]. Different proteins (e.g. Mfn1, Mfn2, Drp1 and hFis1) which govern the morphology of the mitochondria have been subsequently identified in the yeast and the mammalian system [151, 158, 176, 407].

The myriad of functions performed by the mitochondria is complemented by its dynamics, which appear to be linked to cellular development, cell cycle and death [77, 84, 99, 114, 128, 149, 150, 297, 368, 408, 408, 409]. Recent studies conducted have seen an advance in the understanding of the molecular basis of mitochondrial dynamics where the morphology, allocation and activity of mitochondria are regulated by the fusion and fission cycles [106, 126, 196, 215, 410-415]. The balance between fusion and fission is vital for several important cellular processes and the changes in the shape rely on the extracellular signals received and intracellular requirements, the particular cell type and organism [87, 159, 416].

On the basis that changes in mitochondrial morphology appear to impact on many factors known to be relevant to the cellular response to ischaemia-reperfusion injury; we were keen to examine this phenomenon in the context of cardioprotection. It has been demonstrated that mitochondrial fragmentation precedes cellular apoptosis and fragmentation is caused by an increase in oxidative stress from reactive oxygen species (ROS) with the endpoint to this fragmentation being the opening of the mPTP [409, 417]. Therefore, we hypothesised that promoting mitochondrial fusion or inhibiting mitochondrial fragmentation in the HL-1 cardiac cell line, endothelial cells and adult cardiomyocytes protects against simulated ischaemia-reperfusion injury by inhibiting mPTP opening. In addition, we also proposed that the application of drugs modulating mitochondrial morphology *in vitro* such as the mitochondrial division inhibitor-1 (*mdivi-1*) and the cAMP-dependent protein kinase (PKA) activator, Sp-5,6-dichloro-1-f-D-ribofuranosylbenzimidazole-

3',5' monophosphorothioate (Sp-5,6-DCl-cBiMPS) may actually enhance myocardial protection in the face of ischaemia-reperfusion injury by inhibiting the opening of the mPTP. *Mdivi-1* was chosen because it was shown by Cassidy-Stone and colleagues in 2008 to be a specific small molecule inhibitor of Drp1 in various different cell types [418]. Similarly, PKA activation was used in our study due to the findings of Chang and Blackstone in 2007 where they found that PKA can phosphorylate the fission protein, Drp1 at Ser^{637} and inhibit its mitochondrial fragmentation capability by inhibiting its GTPase activity [182]. cBiMPS was chosen because it has been tested to be a potent and specific PKA activator [419]. We are also interested to determine whether erythropoietin (EPO), a known cardioprotective agent can actually protect cardiomyocytes by promoting mitochondrial fusion and inhibiting mPTP opening. It has been shown that EPO protects the heart by activating the PI3K pathway and subsequently protein kinase B (Akt) which inhibits the mPTP opening [420-422]. However, we were keen to investigate whether EPO can actually promote mitochondrial fusion through the activation of Akt and hence inhibit the mPTP opening.

Chapter Two: HYPOTHESES

2.1 HYPOTHESIS ONE

Modulating mitochondrial morphology protects cardiac cells against ischaemia-reperfusion injury by inhibiting mPTP opening.

This first major hypothesis was divided into 3 parts:

2.1.1 Mitochondrial morphology in cardiac cells can be manipulated using either genetic or pharmacological manipulations

2.1.2 ***Modulating mitochondrial morphology*** by genetic or pharmacological manipulations protects the cardiac cells against ischaemia-reperfusion injury

2.1.3 ***Modulating mitochondrial morphology*** by genetic or pharmacological manipulations inhibits the opening of the mPTP in cardiac cells

In the introduction, the unique role of mitochondrial morphology in pathological conditions was described. We hypothesised that modulation of mitochondrial morphology by increasing fusion may protect heart cells against ischaemia reperfusion by inhibition of mPTP opening. The first objective of the study (2.1.1) was to demonstrate that mitochondrial fusion can be promoted via genetic or pharmacological means. The next objective (2.1.2) was to determine whether increasing the presence of elongated mitochodnria in cardiac cells protect aginst IR. We also attempted to inhibit mPTP opening in cardiac cells by promoting mitochondrial fusion in the last objective of hypothesis one (2.1.3)

2.2 HYPOTHESIS TWO

The known cardioprotective effect of kinases such as Protein Kinase A and B is mediated via mitochondrial morphology

Pro-survival kinases inhibits mPTP opening in cardiac cells via modulating mitochondrial fusion

In the introduction, the cardioprotective roles of the kinases were described. We attempted to investigate whether these kinases may modulate mitochondrial morphology and hence confer cardioprotection via inhibition of mPTP opening.

Chapter Three: GENERAL METHODS

3.1 List of chemicals

3.1.1 Pre-coating flasks for HL-1 cell culture

Name **Fibronectin, 0.1% solution from bovine plasma**
Company **Sigma®**
Catalogue No. **F1141-5mg**

Name **Gelatin from bovine skin, Type B**
Company **Sigma®**
Catalogue No. **G9391-100g**

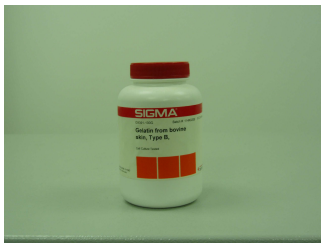

3.1.2 Components for HL-1 cell culture

Name **Claycomb w/o Glutamine**
Company **SAFC BiosciencesTM**
Catalogue No. **51800C**

Name **Foetal Bovine Serum**
Company **SAFC Biosciences™**
Catalogue No. **12103C-500ml**

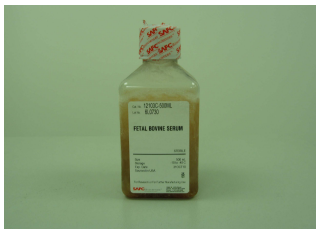

Name **L-Glutamine**
Company **Sigma®**
Catalogue No. **G7513**
[Stock] **200 mM**

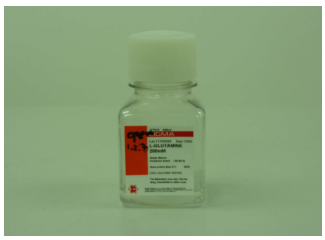

Name **Norepinephrine**
Company **Sigma®**
Catalogue No. **A0937-1g**

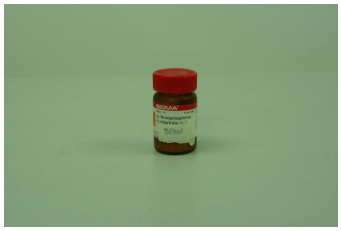

Name **Penicillin-streptomycin (5000 U penicillin with 5 mg streptomycin/ml)**
Company **Sigma®**
Catalogue No. **P4458-100ml**

3.1.3 Components for endothelial cell culture

Name **Endothelial Basal Medium without L-glutamine**
Company **PAA Laboratories GmbH**
Catalogue No. **U15-011**

Name **Endothelial Medium without L-glutamine**
Company **PAA Laboratories GmbH**
Catalogue No. **U15-002**

3.1.4 Components adult cardiomyocytes culture

Name **Earle's Medium 199 (1x) without L-glutamine – 500 ml**
Company **PAA Laboratories GmbH**
Catalogue No. **E15-033**

Name **Albumin fraction V – 100 g**
Company **Merck**
Catalogue No. **1.12018.0100**

Name **Creatine hydrate min 99% - 100 g**
Company **Sigma**
Catalogue No **C-3630**

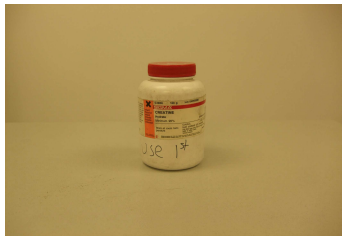

Name **Taurine – 1 kg**
Company **Sigma**
Catalogue No. **T8691**

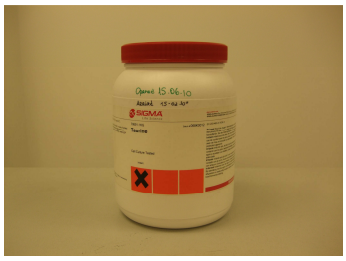

Name **(±) – Carnitine – hydrochloride**
Company **Sigma**
Catalogue No. **C9500 – 25 g**

Name **Penicillin-streptomycin (5000 U penicillin with 5 mg streptomycin/ml)**
Company **Sigma®**
Catalogue No. **P4458-100ml**

3.1.5 Chemicals for experimental use

Name **(+)-Sodium L-ascorbate (Ascorbic acid)**
Company **Sigma®**
Catalogue No. **A7631 – 25g**
Purpose: Component of norepinephrine

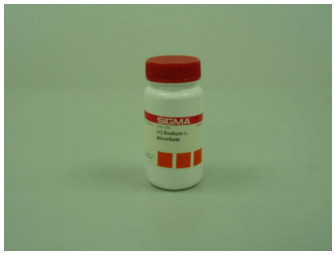

Name **Dimethyl sulfoxide (DMSO)**
Company **Sigma®**
Catalogue No. **D8418 – 50 ml**
Purpose: Solvent and component for cell culture

Name **25% Trypsin – EDTA 1×**
Company **Gibco**
Catalogue No. **25200**
Purpose: For cell passaging (HL-1 and endothelial)

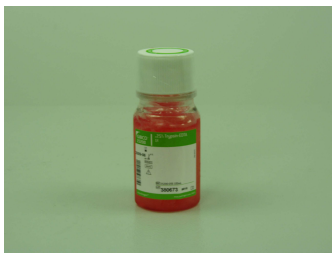

Name **FuGENE® 6 Transfection Reagent**
Company **Roche**
Catalogue No. **11814443001-1 ml**
Purpose: For transfection (HL-1 and endothelials)

Name **MEM 1x (+Earle's, + L-Glutamine)**
Company **Gibco**
Catalogue No. **31095-500ml**
Purpose: Serum starvation for endothelials

Name **Propidium iodide (minimum 95% HPLC)**
Company **Sigma®**
Catalogue No. **P4170-100mg**
Purpose: Cell death marker

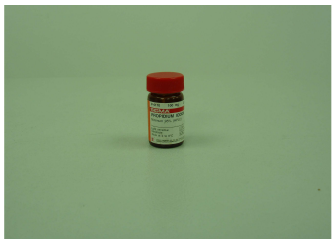

Name **Ciclosporin A *Tolypocladium inflatum***
Company **Calbiochem®**
Catalogue No. **239835-100mg**
[Stock] **0.2 M**
[Working] **0.2 µM**
Purpose: Positive control for mPTP inhibition

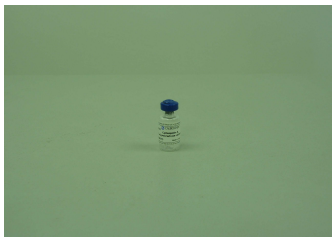

Name **Tetramethylrhodamine methyl ester perchlorate, minimum 98% (TMRM)**
Company **Sigma-Aldrich®**
Catalogue No. **T5428 – 25 mg**
Purpose: ROS source for mPTP assay

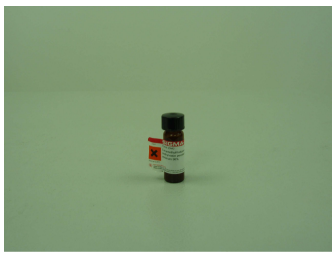

3.1.6 Drugs for modulating mitochondrial morphology

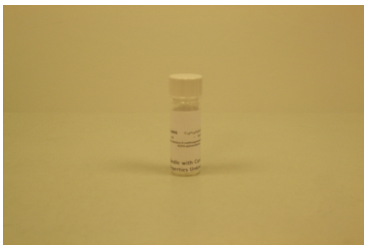

Name ***mdivi-1***
Company **Key Organics Ltd. UK**
Catalogue No.

Function: Inhibitor of Drp1

Name **Sp-5,6-Dichloro-cBIMPS**
Company **Biomol International**
Catalogue No. **BML-CN120-0001**

Function: Inhibitor of Drp1

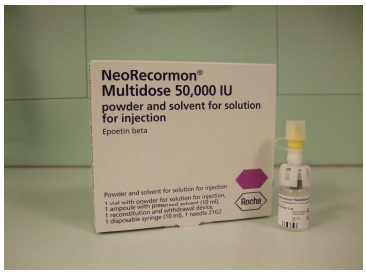

Name **Erythropoietin beta (EPO)**
Company **Roche**
Catalogue No.

Function: Red blood cell producer

3.2 Molecular formulas and structures of drugs and indicator dyes used

Ciclosporin A

Molecular Formula: $\mathbf{C_{62}H_{111}N_{11}O_{12}}$
Molecular Weight: **1202.6**
Molecular structure:

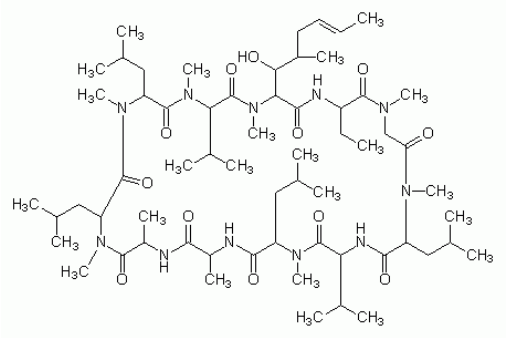

** Molecular structure obtained from the website of Merck Chemicals UK [423].*

Propidium iodide (PI)

Molecular Formula: $\mathbf{C_{27}H_{34}I_2N_4}$
Molecular Weight: **668.40**
Molecular structure:

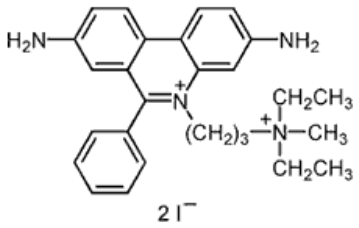

** Molecular structure obtained from the website of Sigma-Aldrich UK [424].*

Tetramethylrhodamine methyl ester (TMRM)

Molecular Formula: **$C_{25}H_{25}ClN_2O_7$**
Molecular Weight: **500.93**
Molecular structure:

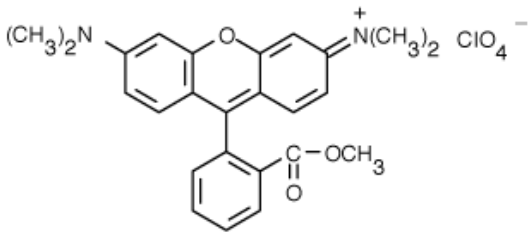

** Molecular structure obtained from the website of Sigma-Aldrich UK* [425]

Sp-5,6-Dichloro-cBIMPS

Molecular Formula: **$C_{12}H_{10}N_2O_2SCl_2$. Na**
Molecular Weight: **419.2**
Molecular structure:

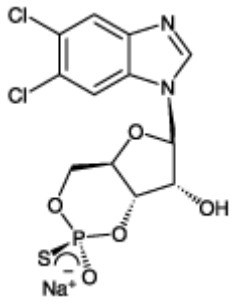

**Molecular structure obtained from the website of Enzo Life Sciences UK* [426]

mdivi-1

Molecular Formula: **$C_{15}H_{10}Cl_2N_2O_2S$**
Molecular Weight: **353.2**
Molecular structure:

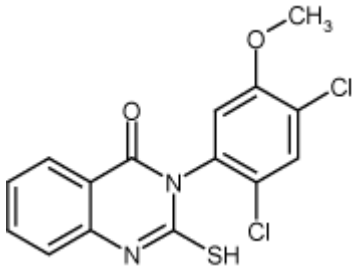

** Molecular structure obtained from the website of Sigma-Aldrich UK* [427]

Erythropoietin (EPO)

Molecular Formula: **$C_{134}H_{226}N_{38}O_{41}$**
Molecular Weight: **3025.49**

Vector:

RcCMV

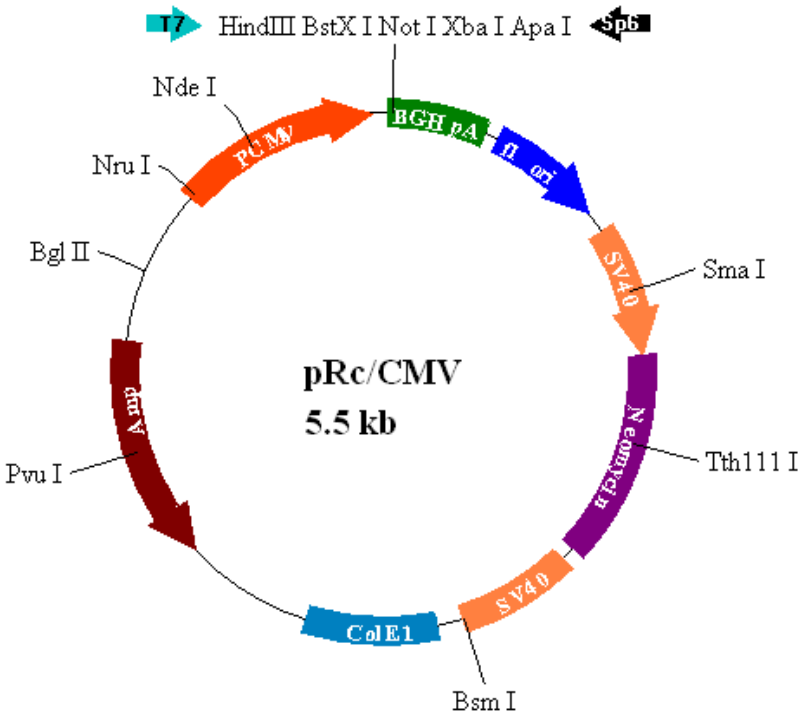

* There is an ATG upstream of the XbaI site. The vector map was obtained from the website of Invitrogen [428].

3.3 Cell Culture

3.3.1 HL-1 cardiac cell line

Cardiovascular studies carried out in most laboratories utilise isolated embryonic as well as neonatal rat primary cardiomyocytes as the standard cellular models. However, the use of these cells is limited because of the lack of many typical adult cardiomyocytes characteristics such as the expression of certain genes and receptors, presence of sarcomeres for contraction as well as the ability of depolarisation and generation of action potentials [429]. Additionally, overgrowth of nonmyocytes in culture, termination of cell division after the neonatal stage and difficulty in genetic manipulation further increases the challenges of using these cells [429-431].

At present, HL-1 is the only cardiac cell line available that is able to divide continuously in culture and contract while maintaining a differentiated cardiac phenotype [429]. HL-1 cells are derived from the AT-1 mouse atrial cardiomyocytes tumour lineage which was originally muscle cells from the atria of transgenic mice which exhibits unilateral right atrial tumorigenesis by having the atrial natriuretic factor (ANF) promoter to control the expression of the SV40 large T antigen [432, 433]. Useful characteristics of HL-1 cells include the ability to be passaged indefinitely in culture while retaining a differentiated cardiomyocyte phenotype as well as the ability to be thawed and recovered from frozen stock [432]. The morphology of HL-1 is irregular with most of them containing a nucleus surrounded by contracting myofibrils [432].

Furthermore, the structural characteristics of HL-1 such as cytoplasmic organisation and myofibrillogenesis (myofibril formation) have been found to be similar to that of the mitotic cardiomycytes of the developing heart, whereas ultrastructural studies reveal them to be similar to primary cultures of adult atrial cardiac myocytes and AT-1 cells [432-434]. This explains why HL-1 in general represent a hybrid between an embryonic and an adult myocyte. Ongoing cellular division underlies the reason why they are less differentiated and less organised compared to the adult myocyte while the existence of atrial granules do not classify them as a mitotic embryonic myocyte [432].

In order to ensure that HL-1 cells maintain the contractile cardiac phenotype during the passages, a fibronectin: 0.02% gelatin substrate (1:200) and a specially formulated growth medium – Claycomb medium (SAFC Biosciences), are needed [429, 432]. The medium should be changed approximately every 24 hours. HL-1 cells are grown at 37°C in an atmosphere with 5% CO_2 and 95% oxygen at a relative humidity of approximately 95%. Upon reaching adequate confluency, which is judged from the proportion of cells reaching contractile state, the cells can be split 1 to 3 and this can be designated a passage [432]. The confluency and frequency of passaging should be taken into account when performing the experiments. In order to maintain reproducibility, the same density of HL-1 cells cultured for every experiment has to be achieved [429].

HL-1 cells can be serially passaged in culture indefinitely. However, the natural phenotype and characteristics have to be examined with caution. Under selective culture conditions, HL-1 cells are able to maintain contractility through at least 240 passages [432].

3.3.1.1 Thawing frozen stocks of HL-1

Frozen glycerol stocks of HL-1 were thawed in a water bath at 37°C and the contents transferred to a sterile 15-ml Falcon tube using a sterile Pasteur pipette (VWR International). 5 ml of Claycomb medium (SAFC Biosciences) was slowly added to equilibrate the DMSO (Sigma) from the cells. The tube containing the cells was then centrifuged at 1000 rpm for 3 minutes and the supernatant was discarded directly. The remaining pellet was dispersed and 7 ml of Claycomb medium was added in slowly. The cell suspension was then pipetted out slowly into a fibronectin pre-coated culture flask.

3.3.1.2 Culturing and passaging of HL-1

Once the HL-1 cells reach confluency, clusters of cells will start ‘beating’ in culture. The presence of huge ‘beating’ clusters signifies adequate confluency to perform cell passaging. New culture flasks or plates were coated with fibronectin two to three hours prior to passaging,. The flask with confluent cells was washed and coated with 2 ml pre-warmed Trypsin-EDTA (PAA Laboratories) and returned to the 37°C incubator for 10 minutes. After 10 minutes, the flask was then ‘tapped’ at the side to dislodge the cells. Pre-warmed Claycomb medium (8 ml) was then added and the solution transferred to a sterile 15-ml Falcon tube. Fifteen microlitres of this cell suspension was then used for cell-number determination on a haemacytometer and the required volume pipetted into the flasks and plates.

3.3.1.3 Preparation of frozen stocks of HL-1

To prepare frozen stocks of HL-1 cells, the remaining cell suspension in the 15-ml Falcon tube was centrifuged at 1000 rpm for 3 minutes. The supernatant was discarded and the flask was tapped to dislodge the pellet. A pre-mixed concoction of 1.8 ml FBS and 200 µl DMSO was then slowly added to the tube and the solution pipetted out using a sterile Pasteur pipette into sterile tubes for storage at -80°C.

3.3.2 Rat coronary endothelial cells

Rat coronary endothelial cells were isolated by Dr. Sean Davidson, Senior Research Fellow in our laboratory. Cell culture dishes were coated with 50 µl laminin from Engelbreth-Holm-Swarm murine sarcoma basement membrane (Sigma UK) in the centre and left to dry. The isolation rig was also warmed up with circulating water at 37°C.

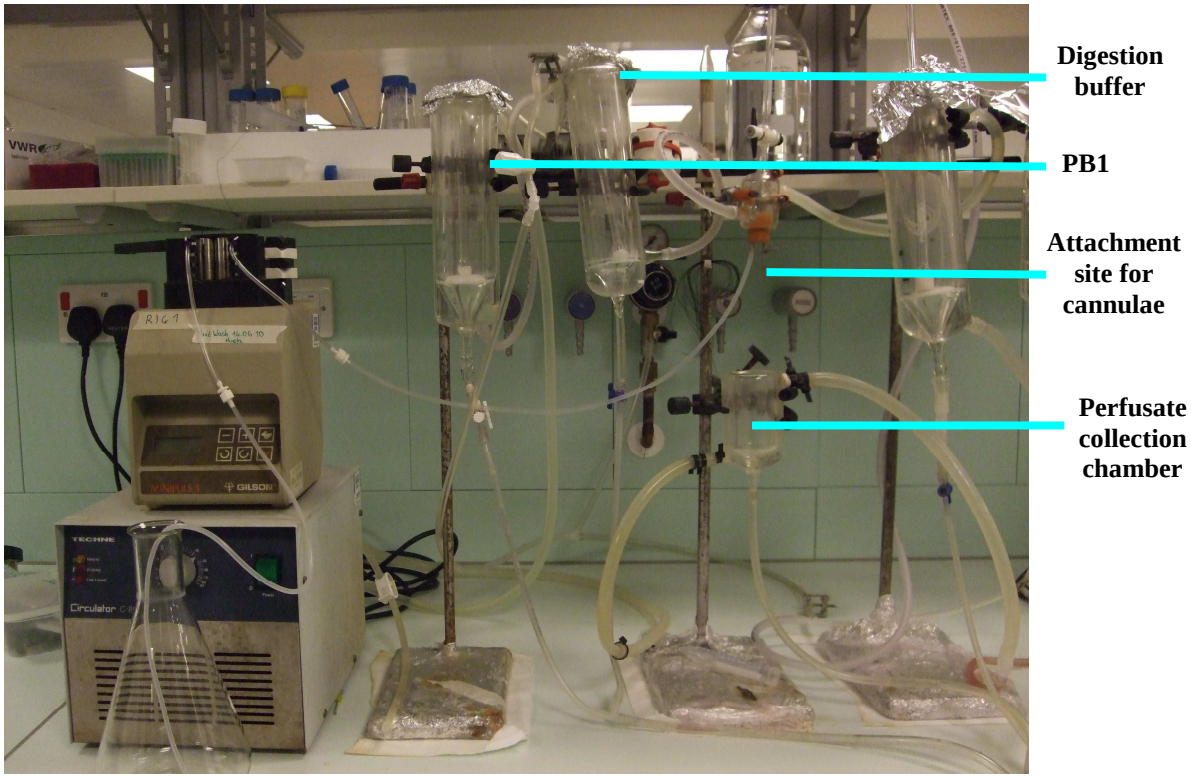

Figure 3.1: Isolation rig for endothelial cells and murine cardiomyocytes.

The specific chambers on an isolation rig (see Figure 3.1) were filled up with calcium-free perfusion buffer (PB1) containing (in mM): $NaHCO_3$ 25.0, NaCl 116.0, KCl 5.4, $MgSO_4.7H_2O$ 0.4, KH_2PO_4 1.2, glucose 10.0, taurine 20.0, Na pyruvate 5.0 and digestion buffer, which is CaCl2 (44.0 µM) and collagenase (1 mg/ml) dissolved in 50 ml of PB1, respectively and oxygenated. Tubings were pre-filled with PB1 and the bubble-trap was also filled half-full with PB1. The flow rate of the isolation rig

was set at 3 ml/min. the heart of the mouse was excised and placed in cold PB1 in a weighing boat and immediately perfused with PB1 for 4 minutes and subsequently changed to digestion buffer until the 14th minute. At the 13th minute, a weighing boat was placed under the heart to collect the drops of digestion buffer. The heart was removed from the rig at the 14th minute and the tissue was gently teased apart with forceps in the weighing boat containing the drops of digestion buffer. The tissue suspension was then placed in a 50 ml tube and transferred to a 37°C shaking incubator at 177 rpm with flow of 100% oxygen for 10 minutes. The solution was discarded leaving tissue in the tube. Before discarding, the solution should be checked under the microscope where there should be mainly red cells and debris, but also some live myocytes. Fresh digestion buffer (15 ml) was added to the tissue and transferred to a 37°C shaking incubator at 177 rpm with flow of 100% oxygen for 20 minutes. After allowing the cell debris to settle, the supernatant is re-centrifuged at 1000 rpm for 5 minutes. The resulting pellet was then resuspended endothelial growth medium (Lonza). Cells were stained with LDL-Alexa488 to confirm their identity as endothelial cells (the endothelial cells take up the labelled LDL thus emitting fluorescence).

3.3.3 Adult Mouse Cardiomyocytes

Isolation of adult mouse cardiomyocytes was performed with the assistance of Dr. Shiang Yong Lim (Postdoctoral Research Fellow from our laboratory). Cell culture dishes were coated with 50 µl laminin from Engelbreth-Holm-Swarm murine sarcoma basement membrane (Sigma UK) in the centre of the coverslips and left to dry. The isolation rig was also warmed up with circulating water at 37°C. The chambers were filled with calcium-free perfusion buffer (PB1) containing (in mM): NaCl 113.0, KCl 4.7, KH_2PO_4 0.6, Na_2HPO_4, $MgSO_4.7H_2O$ 1.2, $NaHCO_3$ 12.0, $KHCO_3$ 10.0, Taurine 30.0, HEPES 10.0, glucose 11.0, and 2,3-butanedione monoxime (BDM) 10.0 and digestion buffer, which is CaCl2 (12.5 µM), collagenase (0.045 g) and hyaluronidase (6.25 mg) dissolved in 50 ml of PB1, respectively and oxygenated. Tubings were pre-filled with PB1 and the bubble-trap was also filled half-full with PB1. The flow rate of the isolation rig was set at 3 ml/min. the heart

was excised from the anaesthetised mouse and placed in cold PB1 in a weighing boat and immediately perfused with PB1 for 4 minutes and subsequently changed to digestion buffer until the 14th minute. At the 13th minute, a weighing boat was placed under the heart to collect the drops of digestion buffer. The heart was cut off from the rig at the 14th minute and the tissue was gently teased apart with forceps in the weighing boat containing the drops of digestion buffer. The tissue suspension was then placed in a 50 ml tube and transferred to a 37°C shaking incubator at 177 rpm with flow of 100% oxygen for 5 minutes. Following that, the tissue suspension was resuspended using a Pasteur pipette and a small drop was placed on a glass slip to check for the presence of cells (see Figure 3.2)

Figure 3.2: Cardiomyocytes under a fluorescent microscope.

The supernatant was collected in a separate 15-ml tube and 250 µl cold FCS was added to it. The tube was inverted gently a couple of times. Fresh digestion buffer (5 ml) was added into the remaining pellet in the 50-ml tube and shaken in the incubator for another 10 minutes. Resuspension was performed and the presence of cells determined again. The resulting supernatant was transferred to the previous 15-

ml tube and the tube was centrifuged at 600 rpm for 3 minutes. Using a Pasteur pipette, the supernatant was discarded and 10 ml of low calcium perfusion buffer (PB2) containing $CaCl_2$ (12.5 µM) was added to resuspend the cells. Calcium was re-introduced in a step-wise manner with the tube horizontal at all times; starting at 10 µl of 0.1 M calcium chloride for 4 minutes, 10 µl of 0.1 M calcium chloride for 4 minutes, 20 µl of 0.1 M calcium chloride for 4 minutes, and two addition of 30 µl of 0.1 M calcium chloride for 4 minutes respectively. The solution was then centrifuged at 600 rpm for 3 minutes. The supernatant was discarded using Pasteur pipette and 2 ml of cardiomyocytes growth medium (M199 buffer: BSA 2 mg/ml, creatine 5 mM, taurine 5 mM, carnitine hydrochloride 1.6 mM, Pencillin-Streptomycin 1%) with 25 µM blebbistatin was added into the tube. The tube was tapped vigorously until pellet is dissolved. The cell suspension was pipetted onto the laminin-coated dishes and sent into the 37°C incubator for 1 hour. After 1 hour, the dish was washed gently with 1 ml culture medium without blebbistatin and 1 ml of fresh M199 with 25 µM blebbistatin was added into each well.

3.4 Animals

C57BL/6 adult male mice (9 – 12 weeks old) were used in this study. All animals were obtained from Charles River UK Limited, (Margate, UK) and received humane care in accordance with the Guidance on the Operation of the Animals (Scientific Procedures) Act 1986 (The Stationery Office, London, UK). Animals were allowed to acclimatise or a minimum of 4-5 days prior to use. They were kept in cages of four and had free access to fresh water and standard pellet chow (RM1) diet and were subjected to a 12 hour light-dark cycle, and maintained at 19°C-22°C, and 55+-10% humidity.

3.5 Nonviral Gene Transfers

Viral vectors have been used to generate stable cell lines for expression of various proteins [435-438]. Nevertheless, generation of viral vectors are time consuming and require appropriate expertise, besides the fact that the vector itself can be cytotoxic, immunogenic as in the case of adenovirus and can only carry a limited size of insert gene as in the case of adeno-associated virus. Use of retroviruses too, can cause random integration into the host genome, risks of inducing tumorigenic mutations and generating active viral particles through the process of recombination [439].

The use of nonviral vectors has gained immense popularity because there are not many safety issues concerned based on the fact that the non-viral vectors are non-replicative, and have low immunogenicity. Besides that, the ease of production as well as ability for repeated administration further justify the increasing tendency to use nonviral vectors [440]

There are many types of cationic lipid-based nonviral vectors available in the market. These may consist of liposomal or nonliposomal vectors which are different in terms of size and zeta potential, *in vitro* transfection activity, resistance to the presence of serum, effect of lipid/DNA charge (+/-) or volume/weight (v/w) ratio, protective effect against nuclease degradation and stability under different storage conditions, incubation time, and degree of cell confluency needed before transfection [441].

To ensure efficiency and efficacy of transfection, the entire pathway of binding of the transfection reagent/DNA-complexes to the cell surface, entry into the cells, dissociation of the complexes, and finally, their transport through the cytosol and the uptake of the DNA into the nucleus, plays an indispensable role [442].

3.5.1 Lipofection

Different types of lipofection reagents have different methods to deliver the DNA into the cytoplasm of the cell. These lipofection reagents are user-friendly, non-immunogenic and can accommodate gene constructs of various sizes [443].

One of the methods of lipofection involves a mixture of the cationic lipids with the plasmid DNA. The lipid-DNA complex will fuse with the plasma membrane of the cell and enter the cell via endocytosis to promote the uptake of plasmid DNA by the target cell. The term 'cationic liposome' derives from the structure of the anionic DNA coated by the cationic layer of lipid micelles [441], producing a residual net positive charge which can interact easily with the negatively charged plasma membrane of the target cell. Fusion of this complex with the cell will enable uptake of DNA into the cell nucleus where it will remain as an extrachromosomal DNA with transient expression for approximately 7-10 days. This process of gene delivery is influenced by the size of the gene construct, the condition of the cells and the stability of the DNA.

The ideal vector should be small in size to facilitate larger gene construct while maintaining the integrity of the DNA, promote specific targeting to cells and achieve optimum gene expression levels without triggering immune responses from the host cell as well as reproducible in large scale processes [439].

3.5.1.1 Fugene 6 Transfection Reagent

FuGENE 6 Transfection Reagent (Roche Molecular Biochemicals) is a lipid-based transfection reagent made up of different components that complex with and transport DNA into the cell during transfection [444].

The advantages of using FuGENE 6 include very high transfection efficiency in many common cell types, the absence of cytotoxicity, robust and functionable in

both the presence and absence of serum as well as minimal optimisation requirement [444].

Due to the fact that FuGENE 6 is non-toxic and able to transfect cells even in the presence of serum, the transfection complex can be added into cell culture containing serum without the washing step.

For experiments using 35 mm culture dish with a monolayer of cells reaching a confluency of 50-80%, transfection can be performed using a ratio of FuGENE 6 (µl): DNA (µg) of 3:2, 3:1, and 6:1 [445]. Initially, the Fugene 6 is mixed together with the DNA or plasmid to be transfected (an empty plasmid expression vector (RcCMV); one expressing mitofusin 1 (pCB6-MYC-Mfn1); one expressing mitofusin 2 (pCB6-MYC-Mfn2); one containing $Drp1_{K38A}$ (pcDNA3.1-HA-$_{K38A}$-DRP1), the dominant negative mutant form of the mitochondrial fission protein Drp1; and one containing hFis1) in serum free medium. The cells to be transfected have to be plated one day before the transfection experiment. The growth rate and condition of the cells determine the suitable plating density. A crucial point is that the cells have to reach a confluency of around 50-80% on the day of the transfection [445].

For the simulated ischaemia-reperfusion injury and mPTP experiments, a 1:2 ratio of pEGFP expression plasmid (Clontech): plasmid of interest was included in order to identify those cells which had been successfully transfected. After transfection for 24 hours, the buffer was replaced with fresh culture medium and the cells were left in an incubator overnight.

3.5.2 Plasmids midiprep

3.5.2.1 Transformation of bacteria with plasmid

Eppendorf tubes (1.5ml) were prepared and left on ice, including one for the positive control (known plasmid) and one for the negative control (no DNA). The competent cells (HB101, Promega or JM109, Promega) were thawed on ice, flicked gently to mix and then pipetted 50 µl into each tube. 50 ng of plasmid DNA was then added into each tube and left on ice for 10 minutes. The competent cells were then heat-shocked into taking up the plasmids by placing the tubes in a 42°C water bath for 45 seconds without shaking. The tubes were then returned to ice for 2 minutes. 900 µl of sterile Luria-Bertani (LB) broth (10g tryptone, 5g yeast extract, 10g NaCl, pH 7.5) was then added into each tube and incubated for 60 minutes in the shaking incubator at 37°C. A hundred microlitres of this mixture was then plated onto LB-agar (15 g agar in 1L LB broth) plates with the appropriate antibiotics and incubated at 37°C overnight.

3.5.2.2 Growth of transfected bacteria

A single colony was transferred from the LB-agar plate onto sterile 15 ml Falcon tubes containing 4 ml of LB + antibiotics (4 µl of 50 mg/ml ampicillin or 4 µl of 40 mg/ml kanamycin). The tube was then incubated in shaking 37°C incubator for approximately 8 hours before transferring the solution into a conical flask containing 70 ml LB + antibiotics (4 µl of 50 mg/ml ampicillin or 4 µl of 40 mg/ml kanamycin) for overnight culture in shaking 37°C incubator to achieve maximum growth density.

3.5.2.3 Preparing cell lysate

Midiprep for purification of high-quality plasmid DNA from the transfected bacteria was performed according to manufacturer's instructions using the PureLink™ HiPure Plasmid DNA Midiprep Kit (Invitrogen) (see Figure 3.3).

Figure 3.3: The components in the PureLink™ HiPure Plasmid DNA Midiprep Kit from Invitrogen.

3.5.2.4 Measuring the DNA concentration

The Jenway 6405 UV/Vis spectrophotometer was blanked using 500 µl sterile distilled water. To measure the concentration of the DNA, 1 µl of DNA was mixed with 500 µl of distilled water and measured in the cuvette.

3.5.3 Plasmids Transfection

Upon reaching 50-80% confluency, the cells were transfected with plasmids according to a standardised protocol (see Figure 3.4). A variety of gene constructs encoding for different proteins validated through DNA sequencing were used throughout this study: caAkt, Mfn1, Mfn2, $Drp1_{K38A}$ and hFis1. These gene constructs were inserted into the CMV backbone vector provided by Dr. Luca Scorrano, Venetian Institute of Molecular Medicine, Italy. Sterile Eppendorf tubes were prepared based on the number of plasmid types used. 1 µg of plasmid encoding the fluorescent protein (mtRFP for morphology studies or EGFP for hypoxia-reoxygenation and mPTP studies) per well was pipetted into each of the Eppendorf tubes. Following that, 2 µg of plasmids per well encoding the different fusion/fission proteins was added into the tubes. 100 µl of Gibco® serum-free medium MEM 1× (SFM) per well was added into each of the tubes for dilution. In a separate Eppendorf tube, 100 µl of SFM per well and 9 µl of Roche® Fugene 6 Transfection Reagent per well was added in consecutive order. A hundred microlitres per well of this mix was then added into each of the 6 tubes and left at room temperature in the laminar air flow for 15 minutes. The plates containing the HL1 cell culture were taken out from the incubator into the laminar air flow and the medium inside the wells was replaced with 2 ml of fresh Claycomb medium per well. After 15 minutes, 200 µl of the solution from each of the tubes was pipetted into the corresponding wells in a circular motion. The plates were then sent back into the 37°C incubator. Medium in the plates and flasks were discarded and replaced with fresh medium every day. 48 hours after transfection, the cells can be used for subsequent morphology, hypoxia-reoxygenation and mPTP experiments.

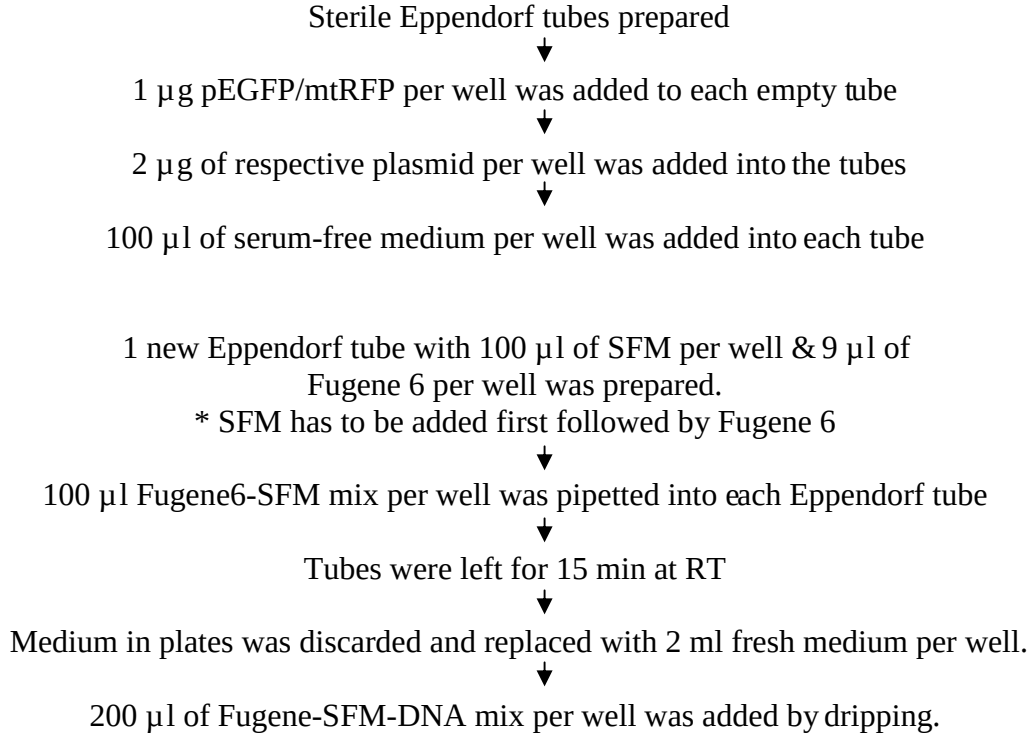

Figure 3.4: Schematic flow of transfection protocol for HL-1 cells and endothelial cells.

In the following section (Section 3.6), the process of transcription and translation of plasmid DNA into protein will be detailed as a natural process occurring in cells.

3.6 From plasmids to proteins

3.6.1 Transcription and Translation

The plasmid DNA in the eukaryotic cells is transcripted into a single-stranded messenger RNA (mRNA) and subsequently translated into a polypeptide chain. The enzyme that encodes mRNA from the DNA template is called the RNA polymerase and is recognised for its ability to incorporate nucleotides one at a time to produce the RNA which is complementary to one of the DNA strands (see Figure 3.5) [136].

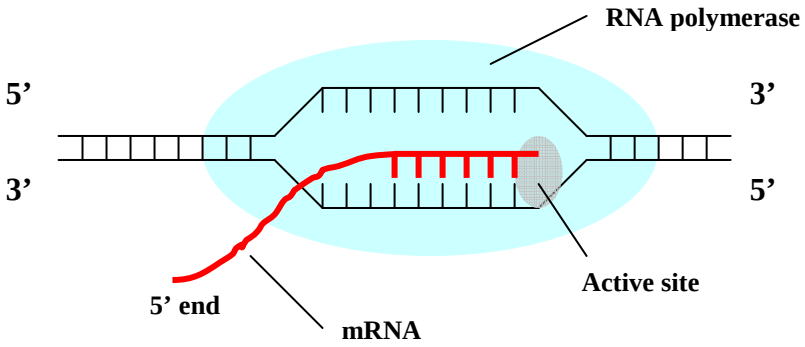

Figure 3.5. Schematic model of the formation of an mRNA strand. The RNA polymerase moves along the DNA template strand in the 3’ – 5’ direction while synthesising the mRNA strand in the 5’ – 3’ direction. The RNA polymerase will span across approximately 35 base pairs of DNA and the DNA-RNA hybrid consists of around 8 base pairs.

Prior to the start of transcription, the RNA polymerase has to bind to the correct and specific position on the DNA template known as the promoter region with the assistance of specific transcription factors. The critical promoter region for eukaryotic cells is located between 24 and 32 bases upstream from the initiation site. This region is known as the TATA box – the site of the assembly of a preinitiation complex containing the general transcription factors (GTFs) and the RNA polymerase. The assembly of the preinitiation complex is started off by binding of a protein called TATA-binding protein (TBP) that specifically recognises the TATA box of eukaryotic promoters. TBP is present as a subunit of a transcription factor for polymerase II, fraction D (TFIID). Binding of TFIID allows the subsequent binding of TFIIA and TFIIB and the interaction between these three GTFs allow the binding of the huge multisubunit polymerase with its attached TFIIF. Once this is completed, another pair of GTFs (TFIIE and TFIIH) will join this complex and transform the polymerase into an active transcribing machine. TFIIH is the only GTF which has enzymatic activities with two of the subunits of TFIIH functioning as helicases to unwind and separate the DNA double strands while another subunit functions to phosphorylate the RNA polymerase. After binding, the RNA polymerase moves along the template DNA in a 3' – 5' direction, thus generating the mRNA in the 5' – 3' direction by incorporating single nucleotides complementary to the template DNA strand. The DNA will be temporarily unwound as the polymerase progresses and rewind after the polymerase moved past. The mRNA transcript that is initially produced is only a primary transcript. This transcript will then be processed in the nucleus by specific processes such as addition of 5' caps, poly(A) tails and RNA splicing involving removal of introns to produce a mature mRNA which will then be transported into the cytoplasm (see Figure 3.6) [136].

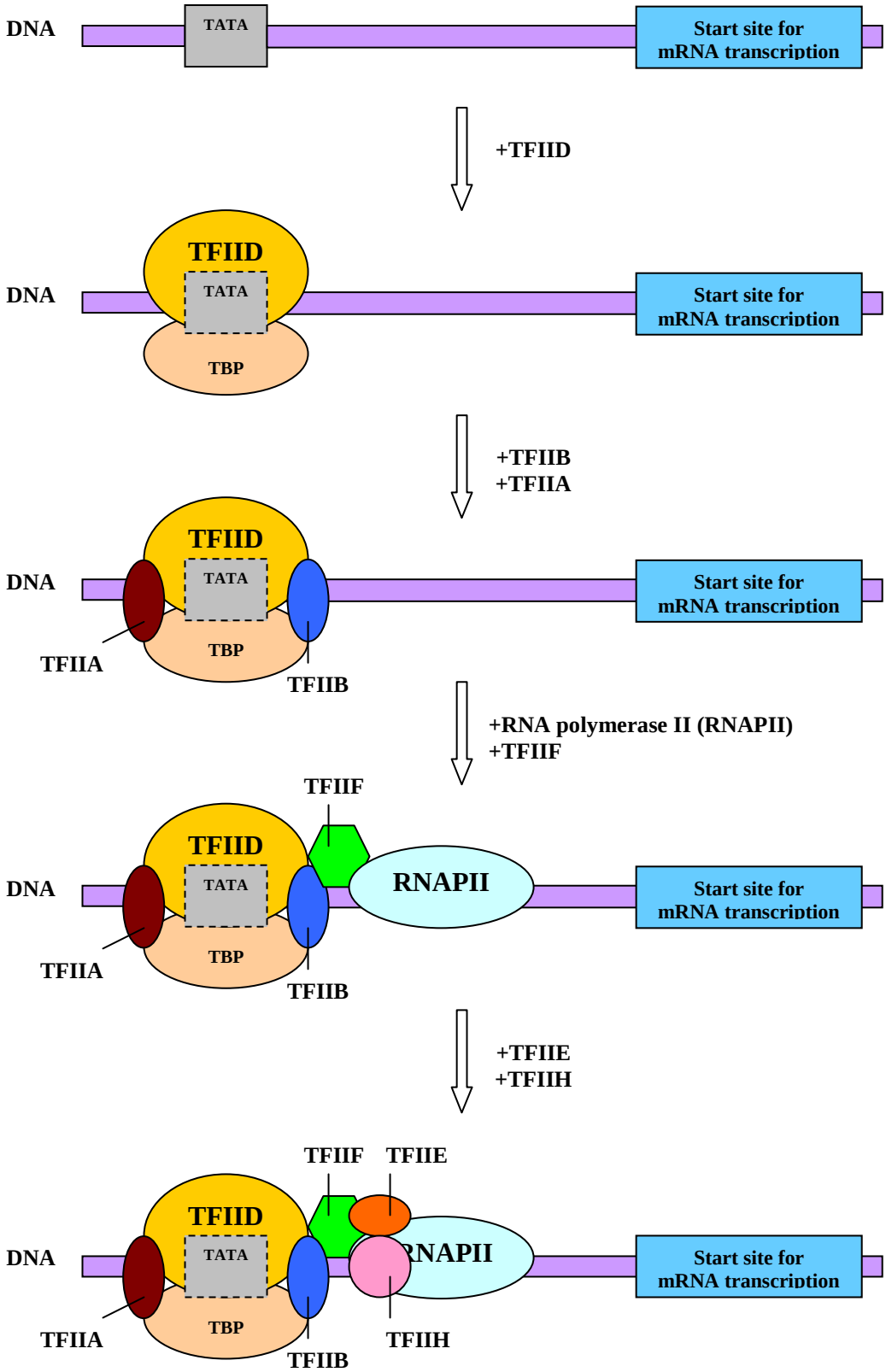

Figure 3.6: Model of initiation complex for RNA polymerase II at the TATA box of a eukaryotic promoter. The general transcription factors (GTFs) associate with the DNA strand and the RNA polymerase II to form the preinitiation complex for eukaryotic mRNA transcription.

Upon reaching the cytoplasm, the mRNA will be translated by the ribosome and transfer RNA (tRNAs) into a polypeptide chain. The ribosome that attaches to the mRNA will move along the mRNA in sets of three nucleotides (from one codon to the other) starting from the initiation codon with the nucleotides AUG so that the proper reading frame can be adhered to and the entire message can be read. Each ribosome consists of three sites, E, P and A specifically to accommodate every tRNA that comes in during each of the elongation cycle.

The translation process can be divided into three stages: initiation, elongation and termination. Initiation in eukaryotic cells involves at least 10 initiation factors consisting of a minimum of 25 polypeptide chains (see Figure 3.7). A number of these initiation factors such as eIF1, eIF1A and eIF3 will initially bind to the 40S subunit as a preparation for subsequent binding to the mRNA together with the initiator tRNAiMet which is associated with another separate initiation factor, eIF2-GTP. The small ribosome subunit together with all these initiation factors and initiator tRNA forms the 43S preinitiation complex which will locate the 5'end of the mRNA bearing the methylguanosine cap. On the mRNA itself, a subset of different initiation factors exert different functions to facilitate the binding of the 43S preinitiation complex. eIF4E will bind to the 5' cap of the mRNA to facilitate recognition by the preinitaition complex while eIF4A will move along the 5' end of the mRNA to remove any double-stranded regions which will restrict the movement of the 43S complex. Another initiation factor, eIF4G links the 5' cap of the mRNA with the 3' polyadenylated end of the mRNA, thus turning the linear form of the mRNA into a circular form. The 43S complex will bind to the 5' end of the mRNA and move along the strand until reaching the initiator codon AUG which will leads to release of the bound initiator factors and subsequent binding of the large 60S subunit to complete the initiation process.

.

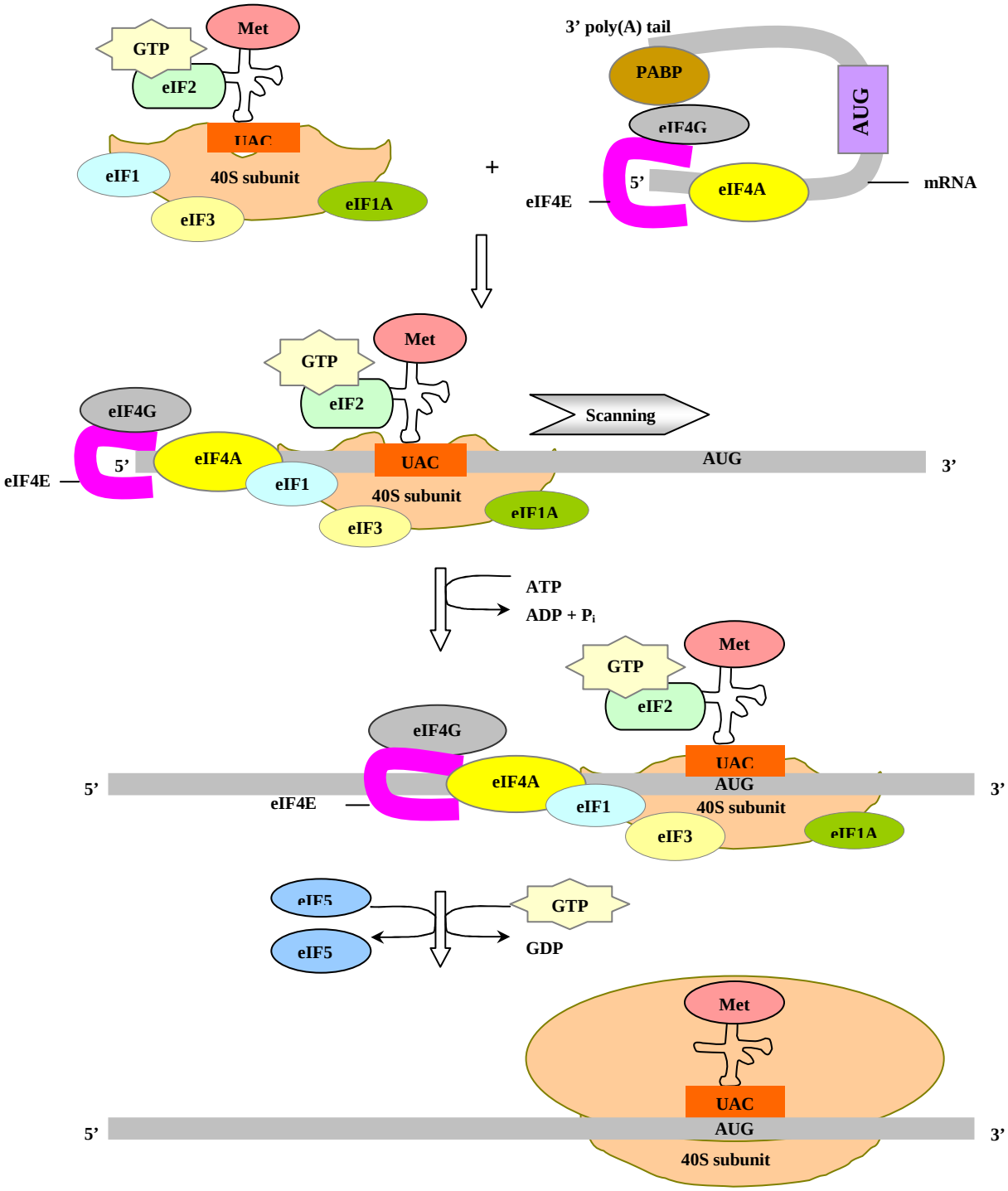

Figure 3.7: Initiation of translation in a eukaryotic cell. Translation of the mRNA is initiated by the formation of two complexes, the 43S complex containing the 40S ribosome subunit bound to several initiation factors (eIF1, eIF1A and eIF3) and the initiator methionine tRNA as well as the mRNA associated with eIF4E at the 5' cap, eIF4G which binds to both the poly(A) binding protein and eIF4E, and the eIF4A which moves long the 5' end of the mRNA to remove any double-stranded regions that would interfere with the movement of the 43S complex. These two complexes then join together to scan along the mRNA to identify the first AUG initiation codon, coupled with ATP hydrolysis. Once the initiator AUG is identified by the complexes, eIF5 facilitates the hydrolysis of GTP bound to eIF2, all the initiation factors are released and the large 60S subunit joins the complex to complete initiation of the translation process.

The first step of elongation begins with the entry of a charged initiator tRNA in the P site followed by an aminoacyl-tRNA into the vacant A site (see Figure 3.8). However, the aminoacyl-tRNA has to bind to a protein elongation factor (eEF1α in eukaryotes) linked to GTP beforehand so that it can bind properly to the mRNA in the A site. Upon binding, the GTP is hydrolysed and the Tu-GDP complex released, leaving the aa-tRNA bound in the ribosome A site. The two amino acids attached to their tRNAs respectively can interact to form a peptide bond between the amino group of the aa-tRNA in the A site and the carbonyl group of the aa-tRNA in the P site with the peptidyl transferase as a catalyst, thereby causing the tRNA in the A site to have a dipeptide while the tRNA in the P site is deacylated and devoid of any amino acid.

Translocation then follows, with the ribosome moving three nucleotides (one codon) again along the mRNA in the 5; - 3’ direction, hence transferring the dipeptide-tRNA from the A site to the P site of the ribosome and the deacylated tRNA from the P site to the E site. This process is promoted by another GTP-bound elongation factor, known as eEF2 in eukaryotes. The deacylated tRNA in the E site then exits the ribosome leaving the E site empty while the A site is used to accommodate a new aminoacyl-tRNA whose anticodon is complementary to the corresponding codon of the mRNA. The dipeptide of the tRNA in the P site is then displaced by formation of a second peptide bond with the new amino acid on the tRNA in the A site followed by translocation again to remove the deacyulated tRNA to the P site and allow the entrance of a new aa-tRNA into the A site.

Upon reaching one of the stop codons: UAA, UAG and UGA, elongation will stop in the presence of release factors such as eRF1 and eRF3 in eukaryotes and the polypeptide will be released [136].

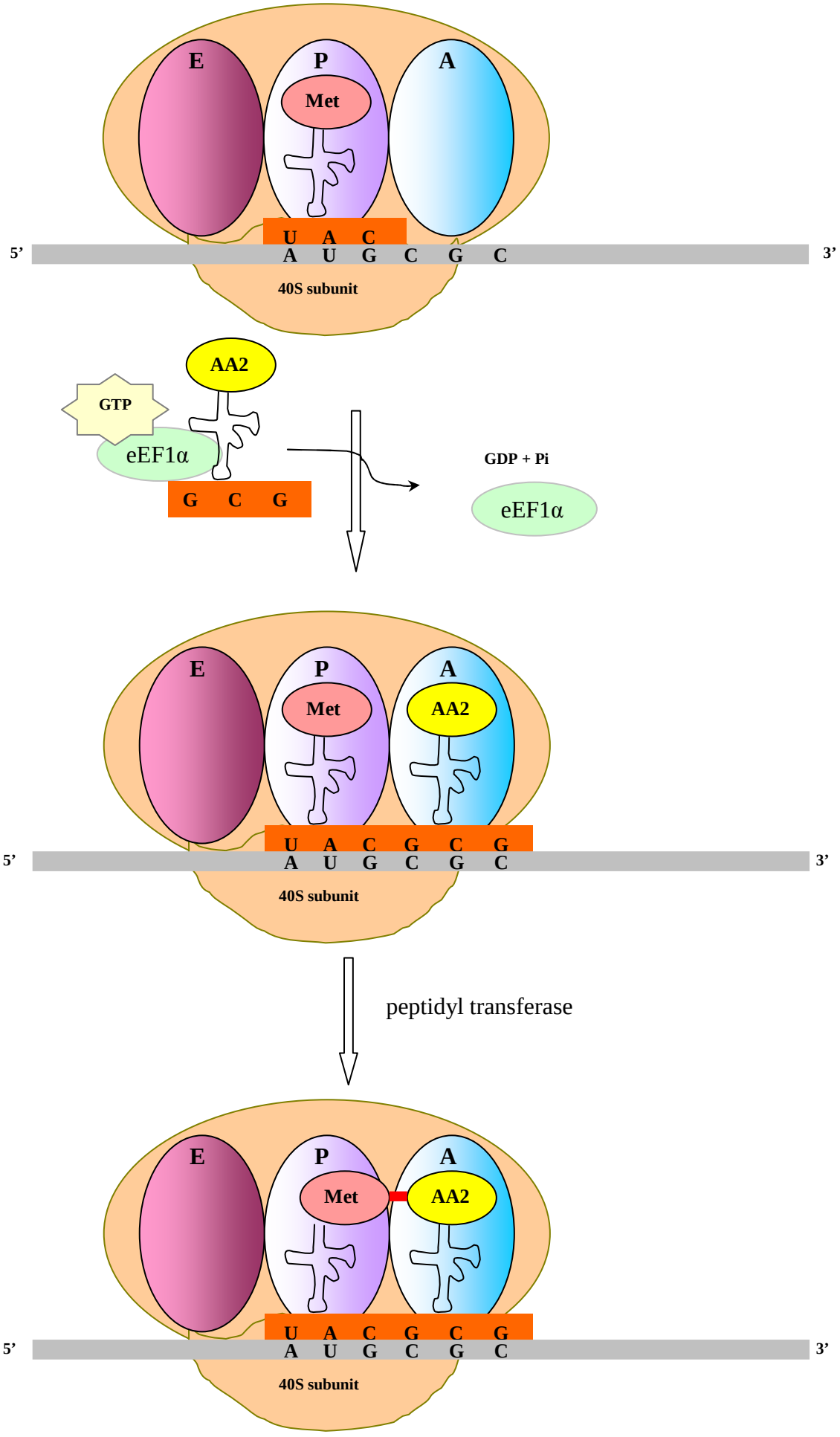
E
P
A
Met
U A C
A U G C G C
5'
3'
40S subunit
AA2
GTP
eEF1α
G C G
GDP + Pi
eEF1α
E
P
A
Met
AA2
U A C G C G
A U G C G C
5'
3'
40S subunit
peptidyl transferase
E
P
A
Met
AA2
U A C G C G
A U G C G C
5'
3'
40S subunit

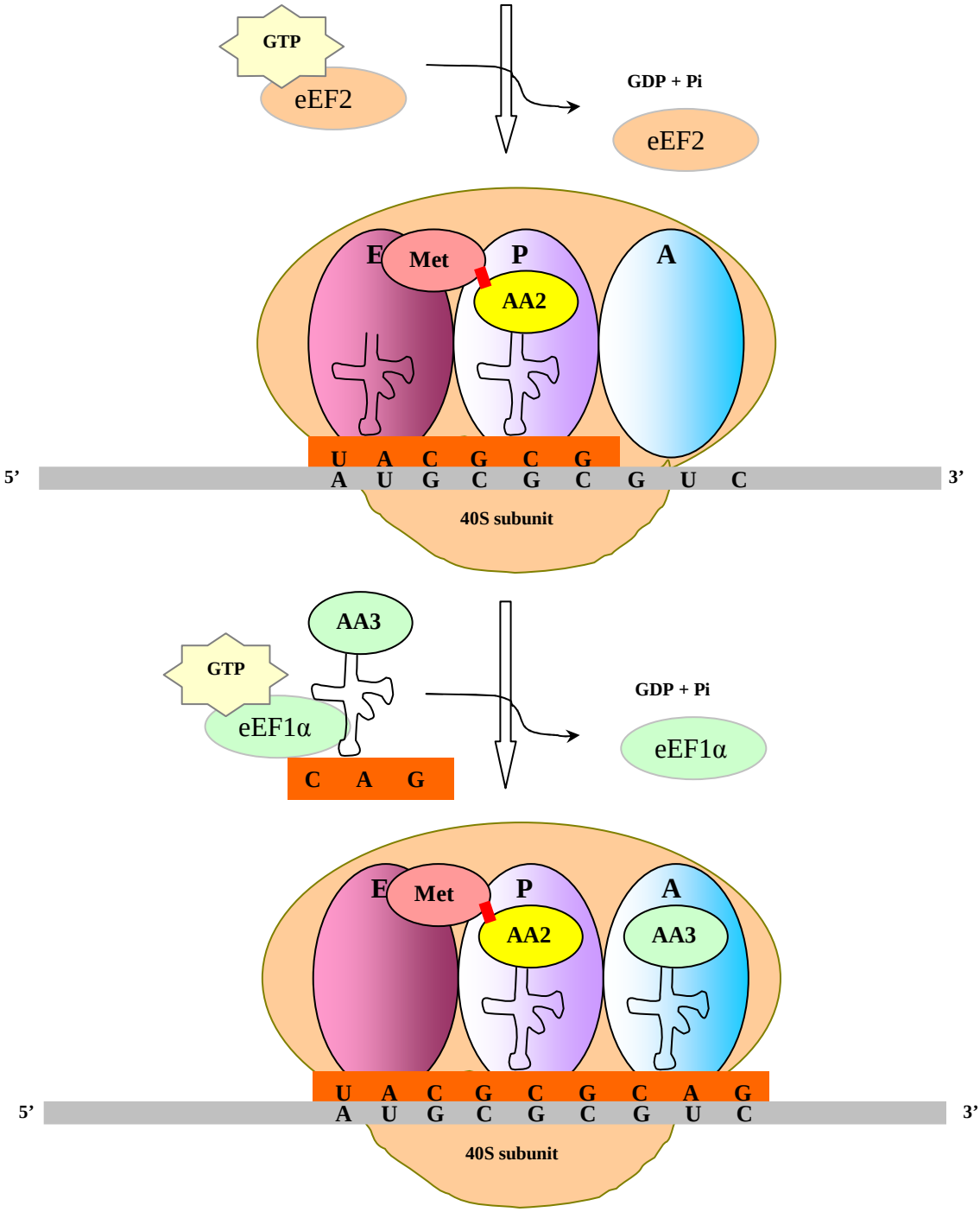

Figure 3.8: Formation and elongation of the polypeptide during translation in the eukaryotic cell. The ribosome contains three tRNA-binding sites, E (exit), P (peptidyl) and A (aminoacyl). The initiator methionyl tRNA is located in the P site while another aminoacyl-tRNA with a complementary anticodon to the codon of the mRNA will enter the empty A site with EF1α and GTP hydrolysis. A peptide bond will be formed between the methionine and the new amino acid, generating a peptidyl-tRNA in the A site and a deacylated tRNA in the P site. Translocation then ensues with the ribosome moving three nucleotides along the mRNA mediated by eEF2 coupled with GTP hydrolysis. The deacylated tRNA will now occupy the E site while the peptidyl-tRNA will be in the P site. The deacylated tRNA will then exit the ribosome and a new aminoacyl-tRNA will enter the A site.

3.7 Construction of mitochondrial matrix targeted PA-GFP adenoviral vectors

To visualise the mitochondria in the adult rat cardiomyocytes, an adenoviral vector has to be generated as lipofection only transfect primary cells at a very low efficiency. Adult rat cardiomyocytes was used as rat cardiomyocytes are more robust than mouse cardiomyocytes and the period of adenoviral transfection (72 hours) necessitate robust cells. This section was performed by Dr. Sapna Subrayan, a postdoctoral research fellow in our laboratory in collaboration with Dr. Sean Davidson, a Senior Research Fellow also from our laboratory. The AdEasy XL Adenoviral Vector System (Stratagene) was used to generate the adenoviral vectors carrying the mtPA-GFP expression cassette. The plasmid encoding the mtPA-GFP was a kind gift from Dr. Luca Scorrano. A KpnI restriction site was introduced upstream of the COX VIII encoding sequence by PCR using mutagenic oligonucleotide primer pair (Left primer 5'-GCTGGTTTAGGGTACCGTCAG-3'; Right primer 5'-GGAGGTGTGGGGAGGTTTT-3'). Using the restriction sites KpnI and NotI, the PCR product was cloned into the multiple cloning site of shuttle vector pShuttle-CMV provided in the kit. The modified shuttle vector was then used to prepare the adenovirus vector as per the instructions. An adenovirus stock solution of 3-3.5 x 10^6 pfu/ml was used for the experiments. The multiplicity of infection used for the adenovirus was 1000.

3.8 Confocal Microscopy

The advent of confocal microscopy has brought cell imaging and physiology studies to greater heights than ever before. Using the confocal microscope, we are now able to study the single cell originating from thick specimens, generating 3D to 4D images in real-time without having to resort to physical shearing of the tissue [446]. The power of the confocal microscope lies in its ability to eliminate out-of-focus light and in turn produce high-contrast sharper images compared to conventional fluorescent microscopes [446].

The underlying principle in confocal microscopy can be simplified by using two sets of light from two different points focused by a pair of lenses causing images to be formed at two different locations (see Figure 3.9). Confocal microscopy is used to visualise only the image at a certain point and excluding the other image. This is done by using a screen with a pinhole to focus the light source at the in-focus or desired point and another pinhole to allow only the light from the desired point to pass through. The term 'confocal' derives from the conjugate position of the pinhole (image position) to the focal point of the lens (sample position) [447].

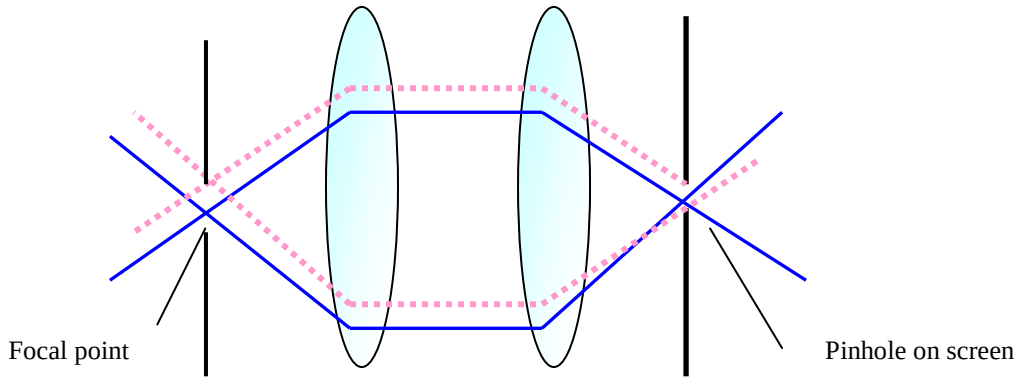

Figure 3.9: Principle of confocal microscopy. Light from the focal point is allowed through the pinhole of the screen. Light away from the focal point is rejected

Image acquisition of the confocal microscope is based on point-by-point illumination of the specimen and exclusion of out-of-focus light. There is however, a

drawback with the point-by-point illumination system of the confocal microscope – fewer emitted photons to collect. The solution is to illuminate each point for a sufficient length of time so that enough light can be collected and a higher signal-to-noise ratio can be obtained. One method is to use a laser light source which has high intensity as well as a variety of wavelengths [447].

The 488 nm laser generates the high intensity blue excitation light which reflects off a dichroic mirror to vertically and horizontally-assembled scanning mirrors that scan the laser across the specimen. This causes excitation of the dye or fluophore in the specimen and the emitted fluorescent (green) light is then descanned by the same set of mirrors to pass though the dichroic mirror which then focuses it onto a pinhole. Only the light going through the pinhole is measured by a detector (see Figure 3.10) [447].

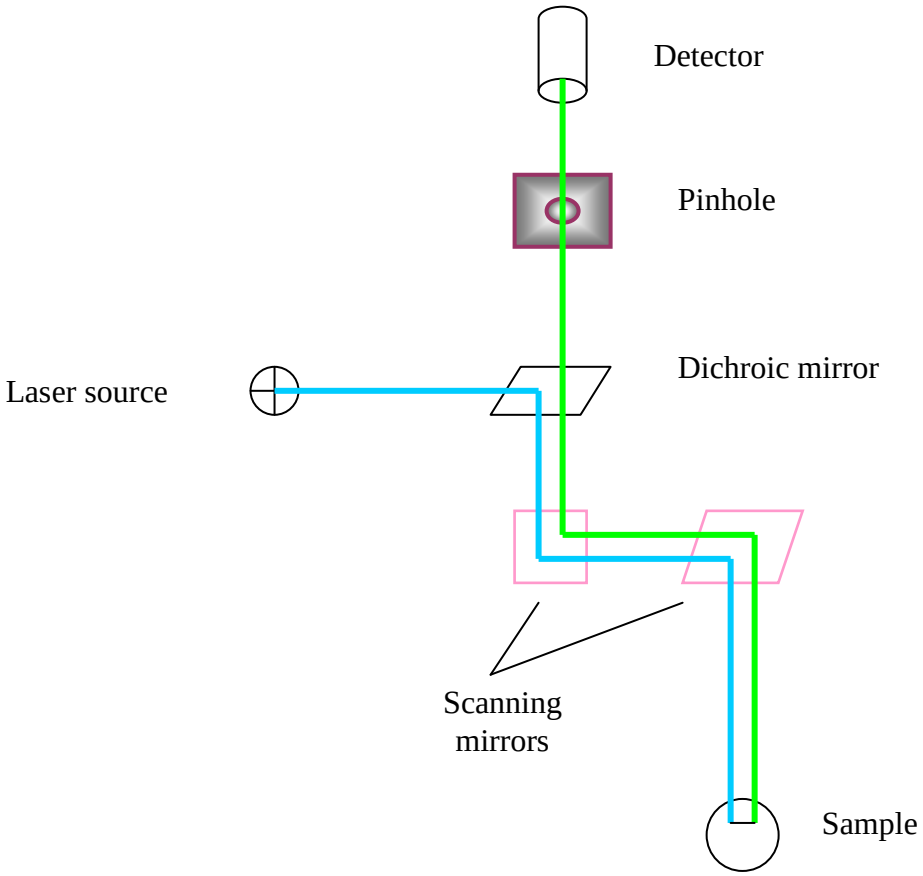

Figure 3.10: Schematic diagram showing the operation principles of the confocal microscope. The blue line shows the excitation light. Green line shows the emission light. Excitation light from the laser source passes through the dichroic mirror and scanning mirrors and scans the fluorescent dye labelled-sample. Emitted light then goes through the pinhole for focusing onto the detector.

The principle of fluorescence is based on differences in energy states of an excited molecule (see Figure 3.11). A particle or molecule at the lowest energy state or ground state will absorb incident light thus entering into a higher energy level and then spontaneously emit light of a different colour from the absorbed light when the molecule return to the ground state [447].

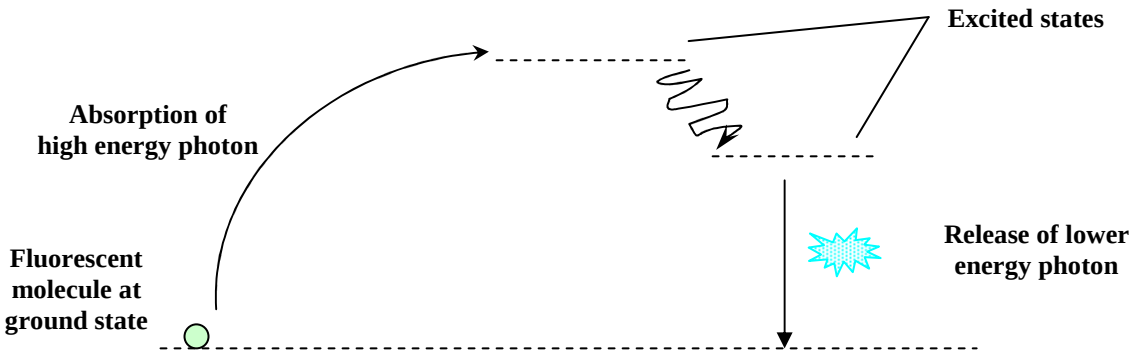

Figure 3.11: Principle of fluorescence. The fluorescent molecule is raised to an excited state by absorption of a high energy photon followed by dissipation of energy to other molecules and finally reverts back to the ground state by releasing light of a lower energy.

There is never a complete image of the specimen because only one point is visualised at any one time. Hence, to get an image of the whole specimen, the detector is linked to a computer which generates the image of the whole specimen one pixel at a time resulting in a thin optical section of the specimen [447].

Recent advancements have seen an addition of an enhanced light source consisting of air-cooled krypton argon ion laser for multiple wavelength lasers. This

laser can produce wavelengths at 488 nm, 568 nm and 647 nm, corresponding to the most common fluorophores: fluorescein, rhodamine and cyanine 5, consecutively [448]. The light path in the microscope has been modified to enable proper filtering of the emitted signal from the three fluorophores to three different PMTs [448]. Another modification would be to use three separate lasers: the 488 nm line of an argon laser for the fluorescein channel, a green helium neon laser (543 nm) for the rhodamine channel and a red diode laser (635 nm) for the cyanine 5 channel [448]. Certain microscopes are also equipped with the 405 nm UV laser.

3.8.1 Limitations of the confocal microscope

3.8.1.1 Resolution

In confocal microscopy, the point of light focused on the specimen actually produces an airy disk in the focal plane and the size of this airy disk is dependent on the wavelength of the laser and the numerical aperture of the objective lens. The resolution of the microscope is limited by the airy disk to about 200 nm [447].

3.8.1.2 Pinhole Size

The pinhole is used to reject out-of-focus light emitted from the specimen and theoretically, making the pinhole as small as possible would be desired. However, the decrease in pinhole size will also decrease the number of photons from the specimen detected by the detector and therefore cause a reduced signal-to-noise ratio. Increasing the fluorescence emitted from the specimen by increasing the excitation light intensity can compensate for this phenomenon but high intensities of lasers can cause damage to the specimen and degrade the fluorophore. Therefore, adjusting the pinhole to about the size of an airy disk is the optimum solution [447].

3.8.1.3 Fluorophores

The fluorophore chosen should be able to attach to the correct part or interior of the specimen and be sensitive enough to the corresponding excitation wavelength. Besides that, usage of fluorophore for imaging under the high intensities of lasers

should not interfere with the normal physiological characteristics of the specimen and vice versa. The time needed for imaging and data collection should be carefully determined so that the adverse effects of photodamage and ROS generation can be minimised [447].

3.8.1.4 Intensity of Incident Light

The amount of fluorescence is dependent on the concentration of fluorophores and light intensity, both of which are factors to be taken into account when attempting to increase the fluorescence intensity. A compromise has to be reached when using either of these factors to increase fluorescence. Quenching occurs under high fluorophores concentrations and can reduce the fluorescence amount deep inside the specimen. The light source is absorbed by the nearest fluorophores, causing a lack of light reaching the other parts of the specimen. Increasing the intensity of the excitation light however, will induce higher amount of fluorophores into the excited states and eventually saturation. When the excitation rate becomes similar to the decay rate, a phenomenon known as ground state depopulation is formed leading to inhibition of fluorescence increase [447].

3.8.1.5 Multicolor Fluorescence

One of the advantages of using the confocal microscope is that different fluorophores can be used simultaneously to differentiate between different proteins or organelles within a cell. The fluorophores to be used can be determined by either selecting fluorophores sensitive to a multiwavelength laser or a fluorophore that emits different wavelengths following excitation by a single wavelength laser. The emitted light is then separated by suitable filters which are linked to different detectors. Nonetheless, there may be some overlap between the emission spectra of certain fluorophores causing complete channel separation to be difficult. To overcome this, the level of overlapping emission spectra has to be predetermined and then deducted out using computer statistical applications [447].

3.9 Electron Microscopy

The transmission electron microscope generates images by using electrons to transmit through the specimen that is partly transparent and partly impermeable where the electrons are scattered (see Figure 3.12). The electron source is a tungsten filament cathode in a device known as ‘electron gun’ where an anode functions to accelerate the electrons through the specimen. The electron beam that passes through the specimen is magnified through the objective lens of the microscope and projected onto a fluorescent screen coated with phosphor to enable direct visualisation. The image can also be recorded using a camera connection to the computer. The advantage of using electron microscopy over confocal microscopy is that the use of electrons significantly increases the resolution power for fine specimens. However, the process of preparing specimens to very fine slices for transmission of electrons is tedious and time-consuming. Processing of the specimens may also causes a certain level of damage to the specimen. Another drawback to using electron microscopy is only a very small area can be analysed at a time, therefore impairing the judgement of the characteristic of the whole sample.

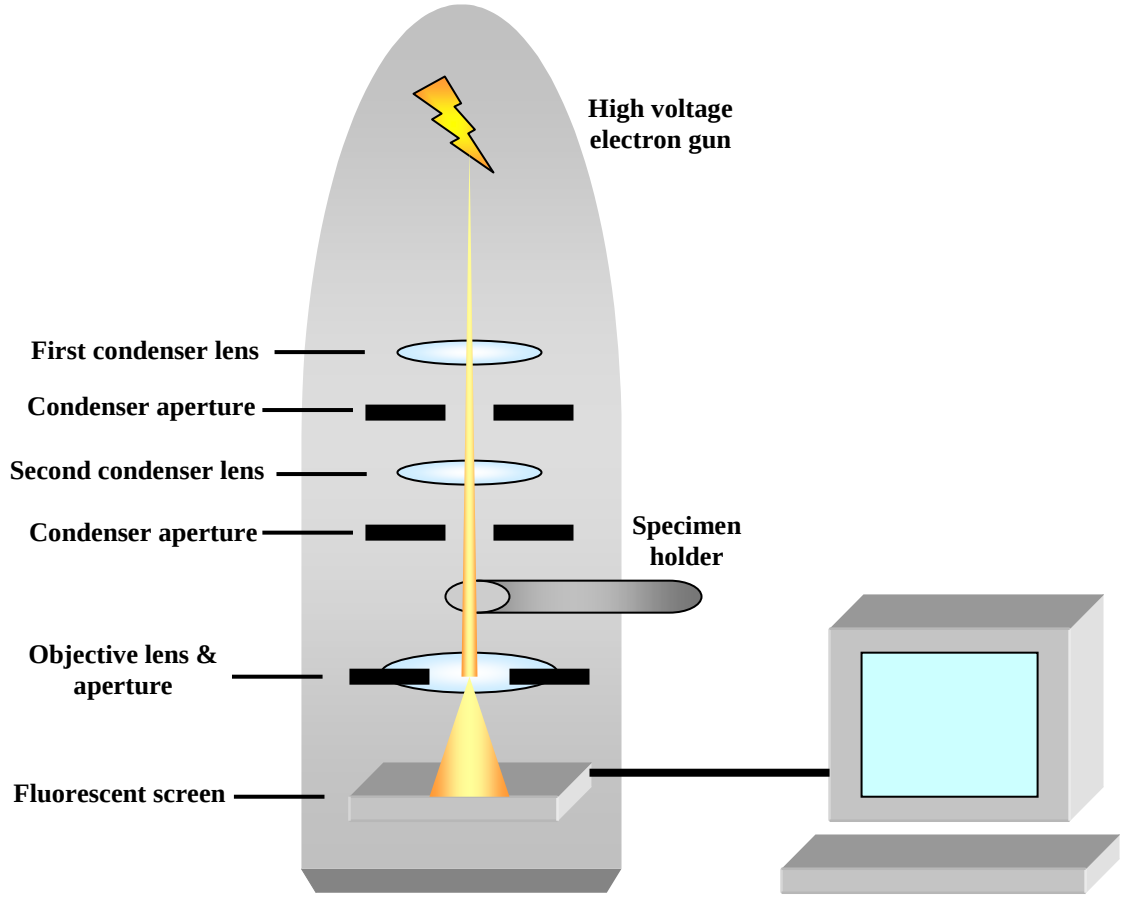

Figure 3.12: Diagram of the operating components of the electron microscope.

3.10 Mitochondrial Morphology Determination

3.10.1 HL-1 and endothelial cells

The shapes of the mitochondria in HL-1 and endothelial cells transfected with mtRFP were determined using a Zeiss 510 CLSM confocal microscope equipped with 63x oil immersion, quartz objective lens (Plan Apochromat, NA 1.3). The cells were illuminated using the 543-nm emission line of a HeNe laser and the fluorescence of mtRFP collected using a 560-nm long pass filter. Images were analysed using the Zeiss software (LSM Image Browser v3.5 or 4.0). After the stage where the Hatter Institute acquired our own confocal microscope, we started doing mitochondrial morphology imaging work on the Leica TCS SP5 Confocal Laser Scanning Microscope (CLSM) equipped with HCX PL APO lambda blue 63x / 1.40 oil objective lens (see Figure 3.13).

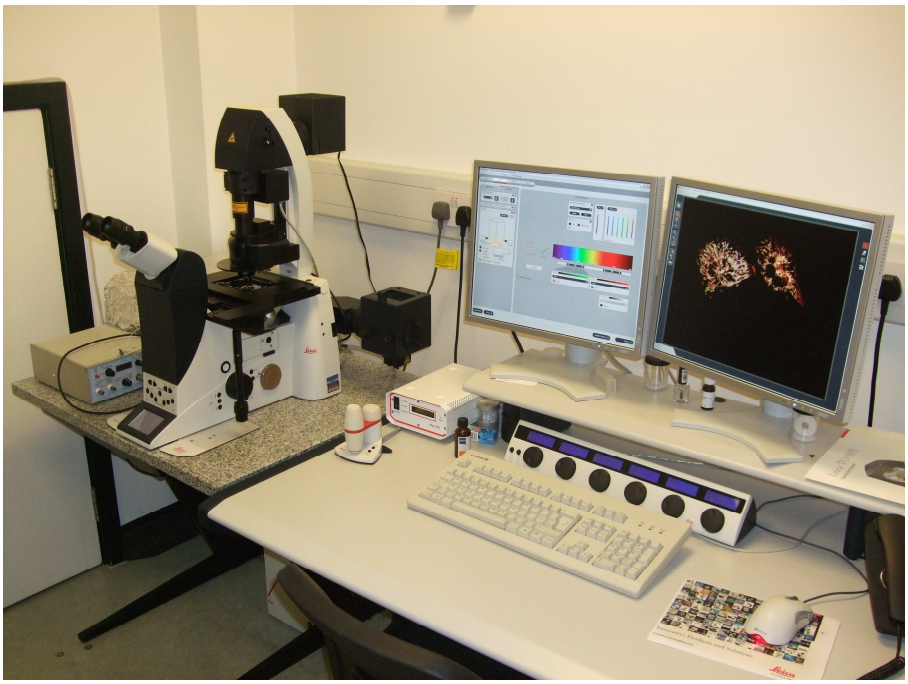

Figure 3.13: Picture of the Leica TCS SP5 Confocal Laser Scanning Microscope (CLSM).

The cells were illuminated using the 543-nm emission line of a HeNe laser. The fluorescence of mtRFP was collected at 555-700 nm. Images were analysed using the LAS AF Version 2.0.0 Build 1934 software programme. Krebs buffer comprising (in mM): NaCl 118.0, $NaHCO_3$ 25.0, d-Glucose 11.0, KCl 4.7, $MgSO_4.7H_2O$ 1.2, KH_2PO_4 1.2, $CaCl_2.2H_2O$ 1.8, and HEPES 10.0 (pH 7.4) was used as imaging buffer. Images of twenty randomly chosen cells were taken and this was repeated for each group in at least four independent transfection experiments giving a total number of approximately 80 cells per treatment group. Three investigators, blinded to the initial treatment, independently assigned the cells as displaying either predominantly (>50%) elongated or (>50%) fragmented mitochondria, indicating that either mitochondrial fusion or fission, respectively, was the predominant process in that cell at that particular time, a method which has been adapted from previously published studies.

3.10.2 Real-time changes in mitochondrial morphology during ischaemia and reperfusion

In order to determine the effect of simulated ischaemia-reperfusion injury on changes in mitochondrial morphology, HL-1 cells were imaged in real-time using an air-tight hypoxic chamber mounted on the confocal microscope. HL-1 cells transfected with mtRFP and either RcCMV or $Drp1_{K38A}$ were seeded onto coverslips, and placed into a Warner PM-2 heated perfusion chamber (Harvard Apparatus, USA) (see Figure 3.14).

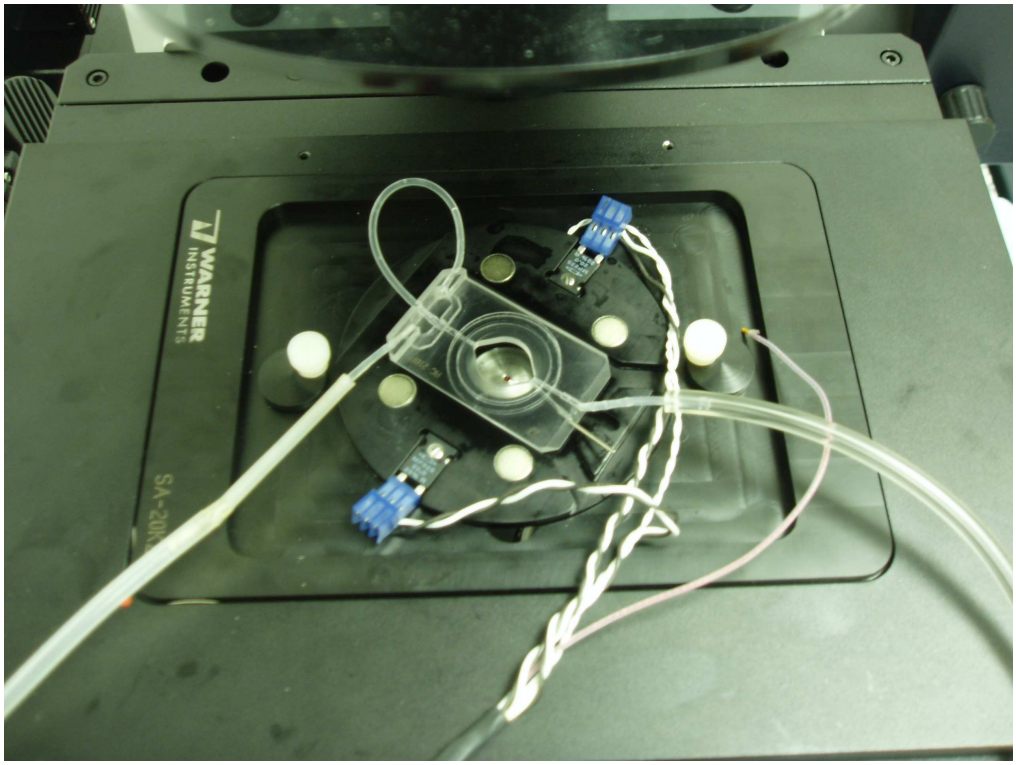

Figure 3.14: Picture of the Warner PM-2 heated perfusion chamber (Harvard Apparatus, USA).

Initially, the HL-1 cells were perfused with normoxic buffer specific for the real-time imaging experiments (in mM: NaCl 110, KCl 4.7, KH_2PO_4 1.2, $MgSO_4$ 1.25, $CaCl_2$ 1.2, $NaHCO_3$ 25.0, glucose 15.0, HEPES 20.0, pH 7.4) equilibrated with 95% O_2-5% CO_2. HL-1 cells with predominantly (>50%) elongated mitochondria were then located and imaged using the 63x objective lens. The cells were then perfused with hypoxic ischaemic buffer specific for the real-time imaging experiments (in mM: NaCl 125, KCl 8, KH_2PO_4 1.2, $MgSO_4$ 1.25, $CaCl_2$ 1.2, $NaHCO_3$ 6.25, Na-lactate 5.0, HEPES 20.0, 2-deoxyglucose 2.5, pH 6.6) equilibrated with 95% N_2–5% CO_2, at a rate of 1 ml/min, for 120 minutes to simulate ischaemia. After this, to simulate reperfusion, the HL-1 cells were reoxygenated with normoxic buffer. Images of the same HL-1 cells were acquired prior to simulated ischaemia, after 120 minutes simulated ischaemia, at the immediate onset of simulated reperfusion and after 30 minutes of simulated reperfusion. For each treatment group 7-10 cells were counted. This experiment was repeated on three independent occasions giving a total of 21-30 cells per treatment group.

3.10.3 Pharmacological inhibition of Drp1 to induce mitochondrial fusion

The recently described pharmacological inhibitor of Drp1, called *mdivi-1* (mitochondrial division inhibitor-1) (Key Organics Ltd, UK), was used in my PhD research to investigate the effects of pharmacologically inducing mitochondrial fusion on cardioprotection. Using the HL-1 cardiac cells we determined the optimum time required for *mdivi-1* treatment in order to induce maximal mitochondrial fusion. HL-1 cells were transfected with mtRFP and were treated with *mdivi-1* dissolved in Krebs imaging buffer at two different concentrations: at 50 µM, the dose shown previously to induce maximum mitochondrial fusion, and at 10 µM. HL-1 cells with predominantly fragmented mitochondria were identified and the subsequent changes in mitochondrial morphology monitored over a period of 40 minutes. Twelve HL-1 cardiac cells from each treatment group were imaged for mitochondrial morphological analysis and this was repeated for each group in at least four independent experiments giving a total number of approximately 50 cells per treatment group. To further validate the results in a population of cells, a separate group of HL-1 cardiac cells were incubated in *mdivi-1* at 50 µM or 10 µM dissolved in Krebs imaging buffer for forty minutes, and mitochondrial morphology determined. Twenty cells from each treatment group were imaged for subsequent mitochondrial morphological analysis and this was repeated for each group in at least four independent experiments giving a total number of 80 cells per treatment group.

3.10.4 Adenovirus-mediated transduction of mtPA-GFP in adult rat cardiomyocytes

All animal experiments were carried out in accordance with the United Kingdom Home Office Guide on the Operation of Animal (Scientific Procedures) Act of 1986. After 1 hour of incubation in the cardiomyocytes growth medium (M199 buffer: BSA 2 mg/ml, creatine 5 mM, taurine 5 mM, carnitine hydrochloride 1.6 mM, Pencillin-Streptomycin 1%), the cells were incubated with plating medium containing an appropriate titre of virus for 4 hours, after which the medium was replaced by fresh virus-free plating medium. The cells were imaged using confocal microscopy for the expression of mtPA-GFP after 72 hours. After excitation of the

cells with the ultraviolet laser to activate mtPA-GFP, images were collected to determine the length of the mitochondria as confirmed by co-localisation of TMRM, a cell-permeable red-fluorescent dye that is sequestered by mitochondria according to the mitochondrial membrane potential. A background image of the cardiomyocyte was obtained initially using the 488nm laser to avoid auto-fluorescence signal. Next PA-GFP within a specified Region of Interest (ROI) was photo-activated by scanning with the 405 nm wavelength ultraviolet laser. The cell was immediately re-imaged at 488nm and the difference in the intensity of green fluorescence between the two images – prior to and after photo-activation, was determined using Image J software (NIH, US). If all mitochondria are fragmented and disconnected, the photo-activated GFP should remain within the boundaries of the ROI. However, the fact that photo-activated GFP was able to spread outside the ROI would imply that it has diffused throughout an elongated mitochondria or alternatively fusion had occurred between neighbouring mitochondria hence enabling the exchange of matricial contents (see Figure 3.15).

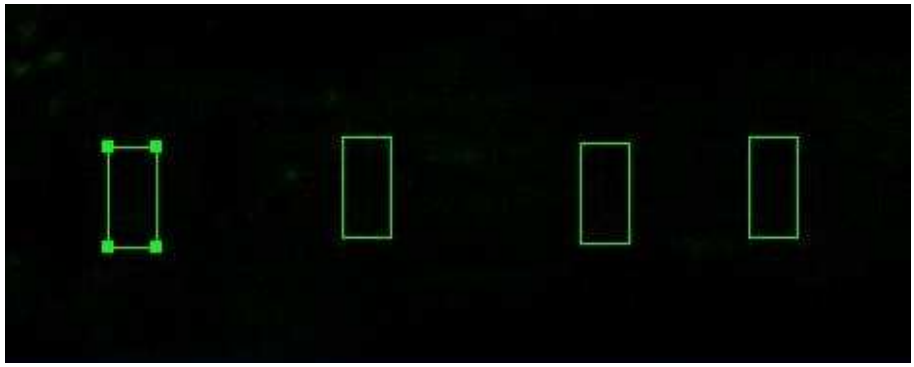

(A)

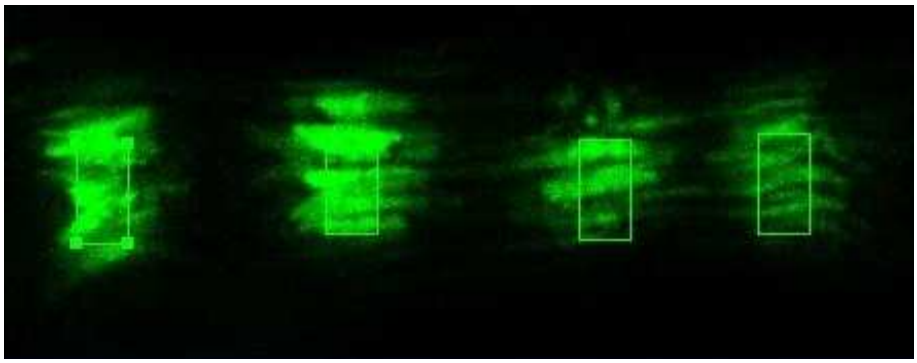

(B)

Figure 3.15: Tracking of mitochondrial-targeted photoactivatable green fluorescent protein (mtPA-GFP) in an adult cardiomyocyte. (A) prior to irradiation with UV laser and (B) following irradiation with UV laser.

The spread of GFP beyond the ROI was expressed as a fold increase relative to the intensity within the ROI, to account for different efficiency of activation in different transfectants. Results were obtained from 30 randomly chosen cells isolated from 3 rats (N=3 experiments with 30 cells). The imaging parameters were identical the same for all the experiments.

3.10.5 Detecting mitochondrial fusion in adult cardiomyocytes using electron microscopy

C57BL/6 male mice treated with either the vehicle control or *mdivi-1*, were anesthetised and the hearts rapidly excised and perfused with a fixative containing fresh paraformaldyhyde 1%, glutaraldehyde 1%, $CaCl_2$ 0.5 mM), glucose 0.031% in phosphate buffer 0.1 M (pH 7.3), and left in fixative overnight before sampling. A 2 mm transverse slice through the whole heart, 3 mm from the apex, was obtained from each heart. These heart slices were then post-fixed in OsO_4 (1%) in phosphate buffer (0.1 M) pH 7.3 at 3.0ºC for 1.5 hrs. They were then washed in phosphate buffer (0.1 M) pH 7.4 and Enbloc stained with 0.5% uranyl acetate in distilled water at 3.0ºC for 30 minutes. After rinsing with distilled water, the specimens were dehydrated in a graded ehthanol-water series and infiltrated with Agar-100 resin overnight (Agar Scientific, UK). Semi-thin sections were cut at 1µm, and mounted on glass slides and stained with toluidine blue (1%) in distilled water for light microscopy. Ultra-thin sections were then cut at 70-80 nm using a diamond knife on a Reichert Ultracut E microtome (Reichert Microscope Services, USA). Sections were collected on 200 mesh copper grids, stained with uranyl acetate and lead citrate. The heart specimens were then viewed and recorded with a Jeol 1010 transition electron microscope (Jeol Ltd, UK).

The assessment of mitochondrial morphology was accomplished by randomly selecting 4 random electron micrographs of longitudinally-arranged cardiomyocytes from each adult heart (N=4 hearts). The arrangement and morphology of the interfibrillar mitochondria were noted and the number of mitochondria whose length was greater than 2 µm (the length of a single sarcomere) was determined.

3.11 Cell survival Assay

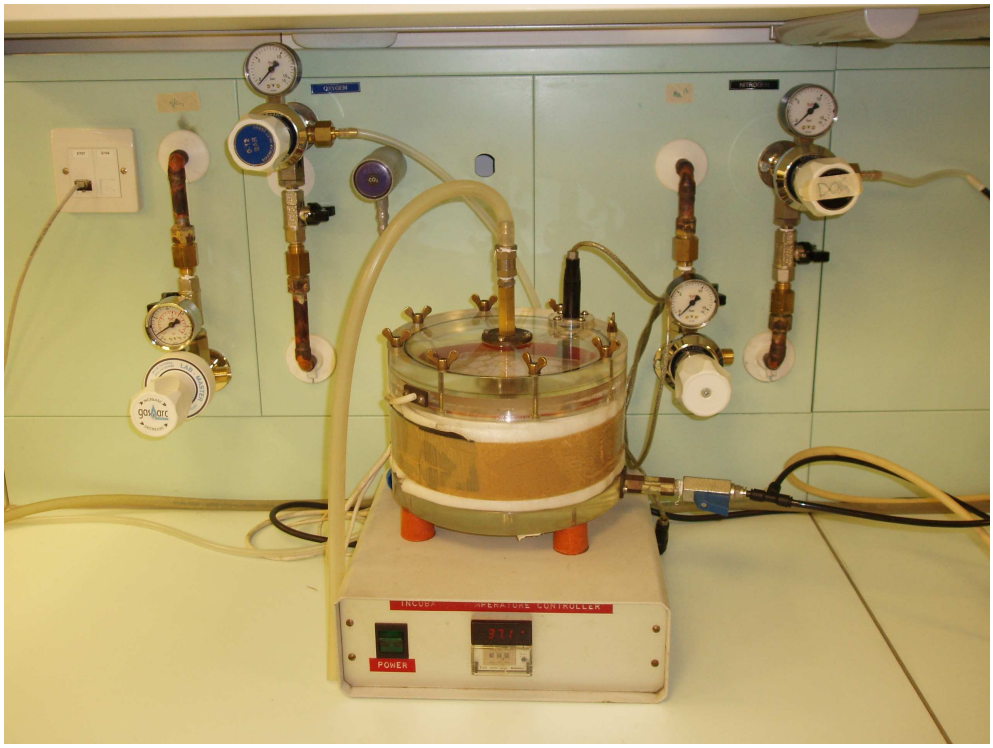

Figure 3.16: Hypoxia-reoxygenation chamber.

3.11.1 HL-1 cell death following simulated ischaemia-reperfusion injury

In order to determine the effect of inducing mitochondrial fusion on the susceptibility to simulated ischaemia-reperfusion injury, HL-1 cells were subjected to a lethal episode of simulated ischaemia and reperfusion. The culture medium was removed and replaced by hypoxic ischaemic buffer specific for the cell-death experiments (comprising in mM: KH_2PO_4 1.0, $NaHCO_3$ 10.0, $MgCl_2.6H_2O$ 1.2, NaHEPES 25.0, NaCl 74.0, KCl 16, $CaCl_2$ 1.2 and NaLactate 20 at pH 6.2, bubbled with 100% nitrogen) and then placed in an airtight custom-built hypoxic chamber (see Figure 3.16) kept at 37ºC for 12 hours to simulate ischaemia. Following the period of simulated ischaemia, the cells were removed from the hypoxic chamber and placed in normoxic Claycomb medium (containing 3 µM propidium iodide) and returned to a tissue culture incubator, to simulate reperfusion. After 1 hour of simulated reperfusion at 37ºC, the percentage of GFP-transfected cells stained with propidium iodide was determined using a Nikon Eclipse TE200 fluorescent

microscope (see Figure 3.17) in order to calculate the percentage cell death in each treatment group.

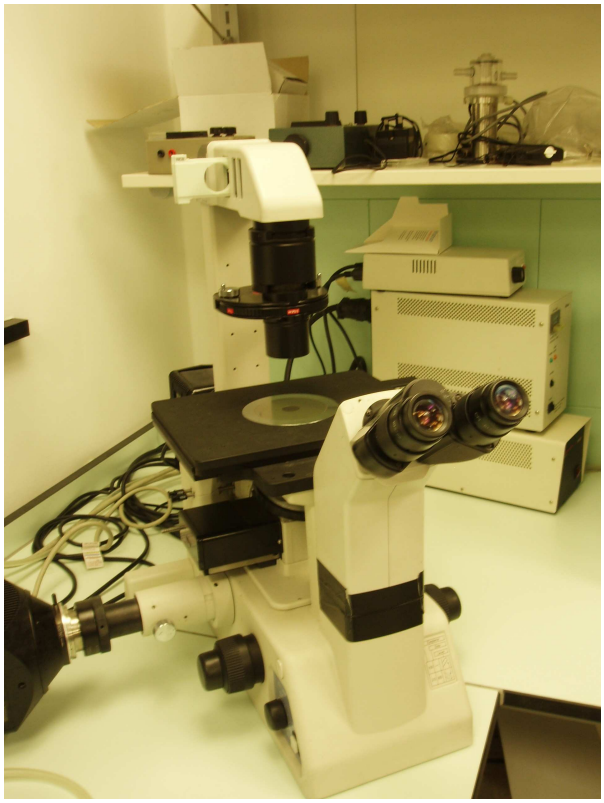

Figure 3.17: Picture of the Nikon Eclipse TE200 fluorescent microscope used for cell death counting.

For each treatment group 80 cells were counted, taken from four randomly-selected fields of view. This experiment was repeated on at least four separate occasions giving a total of 320 cells per treatment group. For a time-matched normoxic control group, HL-1 cells were placed in normoxic buffer specific for cell-survival experiments (comprising in mM: KH_2PO_4 1.0, $NaHCO_3$ 10.0, $MgCl_2.6H_2O$ 1.2, NaHEPES 25.0, NaCl 98.0, KCl 3, $CaCl_2$ 1.2, d-glucose 10.0, Na pyruvate 2.0 at pH 7.4, bubbled with 5% CO_2/95% O_2) for the total 13 hours duration of the experiment and the percentage cell death was determined.

3.11.2 Pharmacological inhibition of Drp1 to induce mitochondrial fusion and delay mPTP opening in HL-1 cells

In order to examine the effects of pharmacological inhibition of Drp1 on cell survival following a period of simulated ischaemia-reperfusion injury, HL-1 cells were incubated with 0.01% DMSO (vehicle control), 10 µM *mdivi-1* or 50 µM *mdivi-1* for 40 minutes and were then subjected to 12 hours of simulated ischaemia followed by 1 hour of simulated reperfusion in the presence of the *mdivi-1*. For each treatment group 80 cells were counted, taken from four randomly-selected fields of view. This experiment was repeated in at least four independent experiments giving a total of 320 cells per treatment group.

3.11.3 Cell survival assay in adult myocytes

All cells were subjected to 45 minutes of simulated ischaemia then 30 minutes of simulated reperfusion to simulate ischaemia-reperfusion injury, a model which we have previously established in our laboratory Simulated ischaemia was induced in a custom-made airtight hypoxic chamber, using a hypoxic ischaemic buffer specific for cell survival experiments (in mM: KH_2PO_4 1, $NaHCO_3$ 10, $MgCl_2.6H_2O$ 1.2, NaHEPES 25, NaCl 74, KCl 16.0, $CaCl_2$ 1.2 and Na lactate 20.0, pH 6.2), bubbled with 100% nitrogen. Simulated reperfusion was achieved by replacing the buffer with M199 culture medium. Cells were seeded onto laminin-coated cover-slips and randomized to the following treatment groups: (1) vehicle control, and (2) *mdivi-1* treatment at either 10 µM or 50 µM (N>250 cells per experiment for 4 experiments). At the end of the simulated reperfusion, 5 µl of propidium iodide (PI, 1 µg/ml) was added to the cells for 5 minutes. The percentage of dead cells (as indicated by red fluorescence, PI positive) was calculated by fluroscence microscopy and was expressed as a percentage of the total number of cardiomyocytes (PI positive and PI negative)

3.12 *In vivo* murine model of acute myocardial infarction

We used an *in vivo* murine model of myocardial infarction to determine the effect of inducing mitochondrial fusion on the susceptibility of the heart to myocardial infarction. C57BL/6 male mice (8-12 weeks of age and weighing 25-30g) were anesthetised by intraperitoneal injection with a combination of ketamine, xylazine and atropine (0.01 ml/g, final concentration of ketamine, xylazine and atropine were 10 mg/ml, 2 mg/ml and 0.06 mg/ml respectively) and body temperature was maintained at 37°C. The external jugular vein and carotid artery were isolated and cannulated for drug administration and mean arterial blood pressure (MABP) measurement, respectively. A tracheotomy was performed for artificial respiration at 120 strokes/min and 200 μl stroke volume using a rodent Minivent (type 845, Harvard Apparatus, Kent, UK) and supplemental oxygen was supplied. A limb lead I electrocardiogram (ECG) was recorded. A left anterior thoracotomy and a chest retractor were used to expose the heart. Ligation of the left anterior descending (LAD) coronary artery was performed ~2 mm below the tip of the left atrium using a 8/0 prolene monofilament polypropylene suture. Successful LAD coronary artery occlusion was confirmed by the presence of ST-segment elevation and a reduction in arterial blood pressure. At the end of reperfusion, the heart was isolated and the aortic root was cannulated and used to inject TTC (5 ml of 1%) in order to demarcate the infarcted tissue. The LAD coronary artery was then re-ligated and Evans blue dye (2 ml of 0.5%) was perfused to delineate the area at risk (AAR). The heart was frozen and sectioned perpendicularly to the long axis (1-2 mm thick). The slices were then transferred to 10 % neutral buffer formalin for 2 hours at room temperature to stabilise the staining. AAR and infarct size were determined by computerised planimetry using the NIH software Image. AAR was expressed as a percentage of the left ventricle and infarct size was expressed as a percentage of the AAR.

C57BL/6 male mice were randomly assigned to one of three treatment groups: (1) Vehicle control (n=6): an intravenous bolus of DMSO (0.1ml of 0.1%) was given 15 minutes prior to the index myocardial ischaemic episode, (2) *mdivi-1* (n=6): an intravenous bolus of *mdivi-1* (0.24 mg/kg) was given 15 minutes prior to the index myocardial ischaemic episode, and (3) *mdivi-1* (n=6): an intravenous bolus of *mdivi-*

1 (1.2 mg/kg) was given 15 minutes prior to the index myocardial ischaemic episode. These *mdivi-1* concentrations were estimated from the *ex vivo* concentrations of 10 µM and 50 µM used in the isolated adult murine cardiomyocytes experiments. Hearts were subjected to 30 min of ischaemia followed by 120 min of reperfusion at the end of which infarct size was determined by triphenyl-tetrazolium staining.

3.13 mPTP assay

Detection of the mPTP

Opening of the mPTP at the onset of reperfusion was first demonstrated by the groups of Crompton and Halestrap in 1993 [63, 449]. The opening of the mPTP can be inhibited by ciclosporin A which prevents binding of CypD to the ANT or silencing of the Ppif gene which encodes for CypD, hence reducing infarct size [263, 264, 387, 450]. There are several limitations in the study of mPTP. First of all, certain mPTP inhibitors are consistently present in normal myocytes during IR and we have to assume that mPTP is conferred by the presence of other pro-mPTP factors such as the production of reactive oxygen species, pH increase, free fatty acid accumulation [451].

It has been relatively easier for the study and identification of the mPTP using isolated mitochondria in electrophysiology and isolated cells with specific dyes in confocal microscopy compared to the *in vivo* model where MPTP is only indirectly studied using either genetic ablation of the constituent proteins or the pharmacological inhibitors such as CsA.

Opening of the mPTP will lead to depolarisation of the inner membrane potential, swelling of the matrix and subsequent rupture of the OMM leading to release of cytochrome *c* which is responsible for caspases-dependent cell death.

mPTP inhibition was first postulated to be the effector of IPC by the group of Yellon and co-workers [17] and IPost by the group of Ovize through studies using CsA [230] as well as the non-immunosupressive derivatives and the analysis of changes in the calcium retention capacity of isolated mitochondria.

3.13.1 Techniques for measuring the mPTP in isolated mitochondria

The most direct method in measuring mPTP in isolated mitochondria is the sucrose-entrapment technique by Crompton and co-workers where 14C sucrose is used to permeabilise through the pore and the rate is monitored hence allowing the characterisation of the kinetics and specifics of the pore [452]. Nevertheless, this technique is extremely laborious and continuous monitoring of this process is not easy. The most commonly used method however, is the light scattering method where the degree of light scattering in a spectrophotometer depends on the swelling magnitude of the mitochondria. [376] Upon mPTP opening, small molecular mass solutes equilibrate through while higher molecular mass solutes promote entrance of water into the matrix by providing the required osmotic force.

Quantification of mPTP opening can be performed by using either the TMRE or calcium rention capacity in isolated mitochondria. The calcium retention method was originally developed in liver mitochondria where the release of calcium into the extramitochondrial environment was monitored [453]. Nevertheless, the respiratory capability of the mitochondria has to be ascertained by measurement of complex I activity as Complex I plays a crucial role in maintaining the sensitivity of mPTP opening to ensure the viability of the mitochondria [454] Proper controls should be determined when studying the function and viability of the mitochondria such as the use of FCCP or dinitrophenol and stimulation of respiration with ADP [455].

3.13.2 ROS generation by lasers induce mPTP opening as visualised by the increase of TMRM fluorescent intensity

TMRM, a cationic fluorescent dye has been reported to be used as a photoactivable dye to generate oxidative stress upon illumination and consequently for studying MMP with depolarisation signifying mPTP opening. TMRM loaded into cells accumulate in the mitochondria due to the negative charge located in the mitochondria matrix and the solubility of the TMRM in both the inner mitochondrial membrane and matrix space [232, 456]. Once accumulated in the mitochondria, TMRM exhibit a red shift in both the absorption and fluorescence emission spectra [456]. The relatively high concentration of TMRM localised in the mitochondria will induce

auto-quenching of fluorescence, which will reduce the red fluorescent intensity of the TMRM [232].

The lasers of the confocal microscope are able to break down TMRM to its chemical derivatives in the mitochondria, thus generating ROS which induces mPTP opening. This model has been widely used and accepted as a form of reoxygenation-induced cell injury synonymous with generation of oxidative stress and radical species from mitochondria at the onset of reperfusion [31, 232, 457, 458]. The red fluorescent intensity of TMRM will increase once the mPTP is opened, showing depolarisation of the mitochondrial membrane potential and leakage of the TMRM from the mitochondria into the cytosol [232].

TMRM has several advantages over other indicators of MMP such as lowest binding affinity to mitochondria and other organelles, accumulation in mitochondria only occurs in response to membrane potentials, nontoxic to cells, and is not a substrate for other ionic channels [459]. The ratio of red fluorescent intensity in the mitochondria to that of the cytosol allows the MMP to be assessed reliably regardless of the efficiency of dye loading [459].

3.13.3 Use of ciclosporin A to inhibit the mPTP

Ciclosporin A, a cyclic undecapeptide isolated originally from the fungus *Tolypocladium inflatum* inhibits the mPTP by binding to the cyclophilin D component of the mPTP. The cyclophilin D acts as a mitochondrial enzyme, peptidylprolyl cis-trans isomerase (PPIase) which is involved in changing the shape of proteins by altering the conformation of the peptide bond around proline residues. This provides the impetus for the deduction of the mPTP where a membrane protein can be converted into a channel by action of the PPIase. Many groups speculated that this might be the ANT protein which functions to transport the ATP out of and ADP into the mitochondria. Under conditions favouring the mPTP opening such as presence of ROS, low ATP and high pHi, cyclophilin D binds to the ANT, changing this specific transporter into a non-specific pore. The use of ciclosporin A to inhibit mPTP opening is limited to a narrow concentration range of 0.2 µM due to the fact

that ciclosporin A inhibits calcineurin, a Ca^{2+}-dependent protein phosphotase through Ca^{2+}-calmodulin-dependent inhibition [373] by binding with the cytosolic cyclophilin (CyP-A) to form a complex with a high affinity to the catalytic subunit of calcineurin and hence preventing dephosphorylation of NFAT and its translocation to the cell nucleus.

3.13.4 Induction and detection of mPTP opening

In order to determine the effect of inducing mitochondrial fusion on the susceptibility to mPTP opening, we used a well-characterised and validated model of oxidative stress to induce and detect mPTP opening. The culture medium was removed and replaced with Krebs imaging buffer. The HL-1 cells were then loaded with the fluorescent dye tetramethylrhodamine methyl ester (TMRM, 3 µM) for 15 min at 37ºC and then washed with Krebs imaging buffer. Confocal laser-stimulation of TMRM generates reactive oxygen species (ROS) within the mitochondria, thereby simulating mitochondrial ROS production during reperfusion, which induces mPTP opening. The opening of the mPTP is visualised as mitochondria membrane depolarisation and the dequenching of TMRM fluorescence as it moves into the cytoplasm (see Figure 3.18).

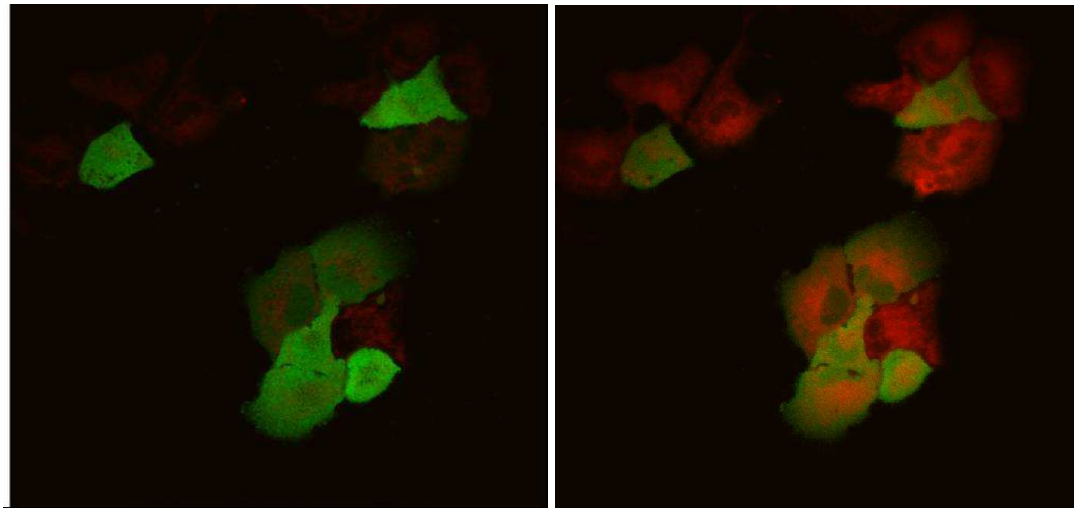

Figure 3.18: Representative confocal images of HL-1 cells transfected with GFP and loaded with TMRM at baseline (left) and demonstrating subsequent mPTP opening as indicated by mitochondrial membrane depolarisation (an increase in TMRM fluorescence resulting from dequenching) after oxidative stress from confocal laser breakdown of TMRM (right).

The time taken to induce mitochondrial membrane depolarisation is recorded as a measure of susceptibility to mPTP opening. This was defined as the time taken to reach half the maximum TMRM fluorescence intensity. Twenty transfected cells were randomly selected for the induction and detection of mPTP opening from each treatment group, and this was repeated in at least four independent experiments giving a total of 80 cells per treatment group. As a positive control and in order to confirm that mitochondrial membrane depolarisation was indicative of mPTP opening following TMRM loading, a group of cells were pre-treated for 10 minutes with the mPTP inhibitor, ciclosporin A (0.2 µM). In order to confirm that this model was actually measuring mPTP opening, we pre-treated cells for 10 minutes with Sanglifehrin A (SfA, 1.0 µM), which does not inhibit calcineurin. In a previous study, we have also confirmed that the mitochondrial membrane depolarisation induced by oxidative stress in this experimental model reflects mPTP opening as evidenced by the redistribution of mitochondrial-loaded calcein.

To confirm the efficacy of the experimental protocol used for inducing and detecting mPTP opening, we also examined the effect of laser-induced mitochondrial oxidative stress on the redistribution of the fluorescent dye, calcein, from the mitochondrial matrix. We used an established method for detecting mPTP opening in the intact cell. HL-1 cells were loaded for 10 minutes at room temperature with 1µM calcein-AM + 1 mM $CoCl_2$. In this model, calcein-AM, which is membrane permeable, enters the cytosol and mitochondria, where on de-esterification the calcein becomes entrapped within the cytosol and the mitochondria. The $CoCl_2$ quenches the calcein signal within the cytosol only, leaving calcein fluorescence selectively visible within the mitochondria. Because of its relatively large size (620 Da), the only way calcein can exit the mitochondria is if the mPTP opens. Therefore, the extent of mPTP opening can be measured by the loss of mitochondrial calcein fluorescence.

HL-1 cells were visualised using a Zeiss 510 CLSM confocal microscope equipped with 40x oil immersion, quartz objective lens (Plan-Neofluar, NA 5 1.3) using the 488-nm of an Argon laser and the 543-nm emission line of a HeNe laser. Time scans were recorded with simultaneous excitation at 488 nm (for GFP and calcein) and 543 nm (for TMRM), collecting fluorescence emission at 505–530 nm

and >560 nm, respectively. For these mPTP experiments, all conditions of the confocal imaging system (laser power, confocal pinhole - set to give an optical slice of 1 micron - pixel dwell time, and detector sensitivity) were identical to ensure comparability between experiments. Images were analysed using the Zeiss software (LSM Image Browser v3.5 or 4.0).

3.13.5 Pharmacological inhibition of Drp1 to induce mitochondrial fusion and delay mPTP opening in HL-1 cells

In order to examine the effects of pharmacological inhibition of Drp1 on the susceptibility to mPTP opening in response to oxidative stress, HL-1 cells were treated with either 0.01% DMSO (vehicle control), 10 µM *mdivi-1* or 50 µM *mdivi-1* for 40 minutes. The HL-1 cells were then loaded with TMRM; 3 µM with either 0.01% DMSO, 10 µM 10 µM *mdivi-1* or 50 µM *mdivi-1* for 15 min at 37ºC and then washed with either Krebs imaging buffer containing 0.01% DMSO, 10 µM *mdivi-1* or 50 µM *mdivi-1*. Twenty cells were randomly selected for the induction and detection of mPTP opening from each treatment group, and this was repeated in at least four independent experiments giving a total of 80 cells per treatment group.

3.13.6 mPTP assay in adult myocytes

In adult cardiomyocytes a different model of mPTP opening was used because we found that it was difficult to measure changes in red fluorescent intensity in adult myocytes treated with *mdivi-1* using the confocal laser-stress induced ROS model. For the adult myocytes, we opted to use the simulated ischaemia-reperfusion model for mPTP assay which we have previously established in our laboratory. The cells were subjected to 45 minutes of simulated ischaemia then 30 minutes of simulated reperfusion. Simulated ischaemia was induced in a custom-made airtight hypoxic chamber, using a hypoxic ischaemic buffer specific for cell-survival experiments (5) (in mM: KH_2PO_4 1, $NaHCO_3$ 10, $MgCl_2.6H_20$ 1.2, NaHEPES 25,

NaCl 74, KCl 16.0, $CaCl_2$ 1.2 and Na lactate 20.0, pH 6.2), bubbled with 100% nitrogen. Simulated reperfusion was achieved by replacing the buffer with M199 culture medium containing 100 nM TMRM, or a combination of M199 containing 100 nM TMRM with either 50µM *mdivi-1* or 1 µM Sanglifehrin A. At the end of the simulated reperfusion, the M199 reperfusion medium was replaced with fresh M199 medium alone and images of the cells were obtained to determine differences in fluorescent intensities. Therefore, in this model of the resultant TMRM flurescence at reperfusion provides a measure of mPTP sensitivity.

3.14 Statistical Analysis

All values are expressed as mean ± standard error of the mean (SEM). Data were analysed by 1-way analysis of variance (ANOVA) followed by a Tukey multiple-comparison post hoc test. Differences were considered significant at values of $P<0.05$.

Chapter Four:

MODULATION OF MITOCHONDRIAL MORPHOLOGY IN CARDIAC CELLS

4.1 Introduction

Mitochondria have been demonstrated to exist in a dynamic equilibrium state, with two opposing morphologies: a fused or fragmented state which is maintained by different proteins: Mfn1, Mfn2 and OPA1 for promotion of mitochondrial fusion and Drp1, hFis1 for promoting the fragmented state of mitochondria [149, 158, 175, 176, 192, 460]. The morphology of the mitochondria varies depending on cell type and condition of the cells [90]. Neonatal cells, endothelial cells and certain types of cell lines such as the HL-1 have similar mitochondrial arrangements in the form of 'spaghetti (fused) and meatball (fragmented)' like-shapes [213]. Cells which are unhealthy and subjected to stress or injury will also have mitochondria that are either swollen or fragmented.

Previous studies have shown that the fused state of mitochondria may be beneficial in terms of viability, e.g. in neurons while the fragmented states play a role in cell death [87, 160, 162, 205, 207, 418, 461]. A study by the group of David Chan in 2010 showed that the fused state of mitochondria prevents the deleterious effects of the loss and mutated DNA [214]. Excessive fragmentation of the mitochondria however, is linked to depolarisation of the MMP, uncoupling of the respiratory chain, loss of ATP and release of the pro-apoptotic cytochrome *c* [70, 173, 209, 462].

Manipulation of mitochondrial morphology has been performed before in different cell types; neurons, yeast and mammalian cell lines [152, 159, 169, 412, 460]. However, there is still a lack of information pertaining to manipulation of mitochondrial morphology in cardiac cells, especially in which the mitochondria is arranged in tightly regulated rows along the myofibrils. The consensus at the time when this study was carried out was that mitochondria in the adult cardiomyocytes move only at a very minute range and therefore, general dynamics such as fusion and fission are virtually immeasurable [154]. mito-PAGFP has been used in several studies to monitor mitochondrial dynamics but are limited to cells such as beta-cells [463], HeLa cells [206], primary hippocampal neurons [206] or zebrafish embryo [464]. Karbowski and co-workers used mito-PAGFP to visualise mitochondrial fusion in human myocytes but the mitochondria arrangement in the human myocyte depicted differs from the mitochondrial arrangement in a cardiomyocyte [206]. Interestingly, giant

swollen mitochondria were observed in adult myocytes using electron microscopy but proper quantification was not performed [148, 465].

A number of different substances have been reported to modulate mitochondrial morphology such as the kinase PKA [182] and the drug *mdivi-1* [418]. PKA has been documented to inhibit mitochondrial fission by phosphorylating the fission protein Drp1 at Ser^{637} [182]. Similarly, the drug, mitochondrial division inhibitor-1 (*mdivi-1*) was formulated after a yeast screening assay. The *mdivi-1* drug works by phosphorylating the Drp1 at an allosteric site not exclusive to the GTPase domain and has been shown to increase the percentage of cells with elongated mitochondria in yeast, mammalian COS and HeLa cells [418].

In this section of the study, I aim to determine whether mitochondrial fusion can be promoted in a cardiac cell line using genetic manipulations such as the overexpression of fusion-promoting proteins such as Mfn1, Mfn2 as well as pharmacological manipulations such as using the drug *mdivi-1* in the hope that manipulation of mitochondrial morphology may serve as a potential mediator of cardioprotection against ischaemia-reperfusion injury in the heart. Following the cell line, I shall proceed on to using endothelial cells and primary cardiomyocytes to determine whether mitochondria elongation can be increased.

4.2 Hypothesis & Objectives

Mitochondrial morphology can be modulated in cardiac cells

The first part of the study was to determine whether mitochondrial morphology in the HL-1 cardiac cell line can be manipulated or changed. Fusion (Mfn1, Mfn2) or fission (hFis1) promoting proteins were used in this study were plasmids containing genes encoding for these proteins were transfected together with plasmids encoding for mitochondrial-targeted fluorescent proteins into these cells to promote overexpression of these proteins in the cells. Following transfection, mitochondrial morphology in the cells was determined using confocal microscopy.

In the second part of the study, we investigated whether the drug *mdivi-1*, also increased the proportion of elongated mitochondria in HL-1 cardiac cells. The *mdivi-1* drug has been shown to successfully increase the proportion of elongated mitochondria in yeast, HeLa and COS cells [418]. Due to the fact that this is the first time that *mdivi-1* has been used on the HL-1 cells, we conducted a time and dose response.

In the third part of the study, we investigated whether mitochondrial morphology in the endothelial cells can be similarly manipulated as in the HL-1 cardiac cells. The endothelial cells were isolated directly from the blood vessels and may function as an intermediate cell type between HL-1 and adult cardiomyocytes..

The presence of elongated mitochondria in adult myocytes was determined subsequently using confocal microscopy and electron microscopy. Any mitochondria longer than the standard length of a sarcomere (2 μm) will be considered as elongated mitochondria.

The effect of *mdivi-1* in promoting mitochondrial elongation in primary cardiomyocytes was also determined. A single intraperitoneal dose of *mdivi-1* was injected into C57BL/6 mice and the hearts were examined under electron microscopy for determination of mitochondrial length.

4.3 Aim (1)

To determine whether mitochondrial morphology can be modulated in the HL-1 cardiac cell line using genetic manipulation.

In this section, we wanted to confirm whether mitochondrial morphology in HL-1 cardiac cells can be manipulated using genetic overexpression of fusion-promoting proteins (Mfn1, Mfn2), fission-promoting protein (hFis1) or the dominant negative form of the fission protein, $Drp1_{K38A}$.

4.3.1 Materials

Plasmids: an empty plasmid expression vector (RcCMV); one expressing mitofusin 1(pCB6-MYC-Mfn1); one expressing mitofusin 2 (pCB6-MYC-Mfn2) [165]; one containing $Drp1_{K38A}$ (pcDNA3.1-HA-$_{K38A}$-DRP1), the dominant negative mutant form of the mitochondrial fission protein Drp1 [205]; and one containing hFis1. $Drp1_{K38A}$ has a mutation in the GTPase domain that results in replacement of lysine 38 with alanine (designated as $Drp1_{K38A}$), disabling its ability to induce mitochondrial fission by sequestering endogenous Drp1 [181, 205]. For the mitochondrial morphology studies a ratio of 1:2 mitochondria-targeted red fluorescent protein (mtRFP: Mitochondria-targeted dsRED) expression plasmid: plasmid of interest was included in order to permit visual assessment of mitochondrial morphology. All plasmids were a generous gift of Dr Luca Scorrano (Padova, Italy). Krebs buffer comprising (in mM): NaCl 118.0, $NaHCO_3$ 25.0, d-Glucose 11.0, KCl 4.7, $MgSO_4.7H_2O$ 1.2, KH_2PO4 1.2, $CaCl_2.2H_2O$ 1.8, and HEPES 10.0 (pH 7.4) was used as imaging buffer for confocal microscopy studies.

4.3.2 Experimental protocol for mitochondrial morphology determination

Upon reaching confluency of around 50 – 60% (~24 hours after seeding), the cells were transfected with one of the following plasmids:

1. RcCMV – empty vector (Vector Control)
2. $Drp1_{K38A}$ – the dominant negative form of the fission protein
3. Mfn1 – fusion-promoting protein
4. Mfn2 – fusion-promoting protein
5. hFis1 - fission-promoting protein

mtRFP was always co-transfected to visualise the mitochondria as well as to indicate uptake and expression of the plasmids. As this was the first time that these proteins were overexpressed in a HL-1 cardiac cell line, we had to determine the optimum duration of plasmids expression to induce significant changes in mitochondrial morphology. Images of twenty randomly chosen cells for both experiments with either 24 hours expression duration or 48 hours of expression duration were obtained and this was repeated for each group in at least four independent transfection experiments giving a total number of approximately 80 cells per treatment group. Three investigators, blinded to the initial treatment, independently assigned the cells as displaying either predominantly (>50%) elongated or (>50%) fragmented mitochondria, indicating that either mitochondrial fusion or fission, respectively, was the predominant process in that cell at that particular time, a method which has been adapted from a previously published study [165].

4.3.3 Results

The first objective was to ensure that the mitochondrial fusion/fission proteins were performing their respective functions in the HL-1 cardiac cell line. The mitochondria in the HL-1 cells were illuminated red in colour due to the expression of the mtRFP. HL-1 cells were determined as either containing predominantly fragmented (globular and dot-like) (see Figure 4.1 (A & E) for an example) or predominantly fused mitochondria (thin and elongated) (see Figure 4.1 (B – D) for an example).

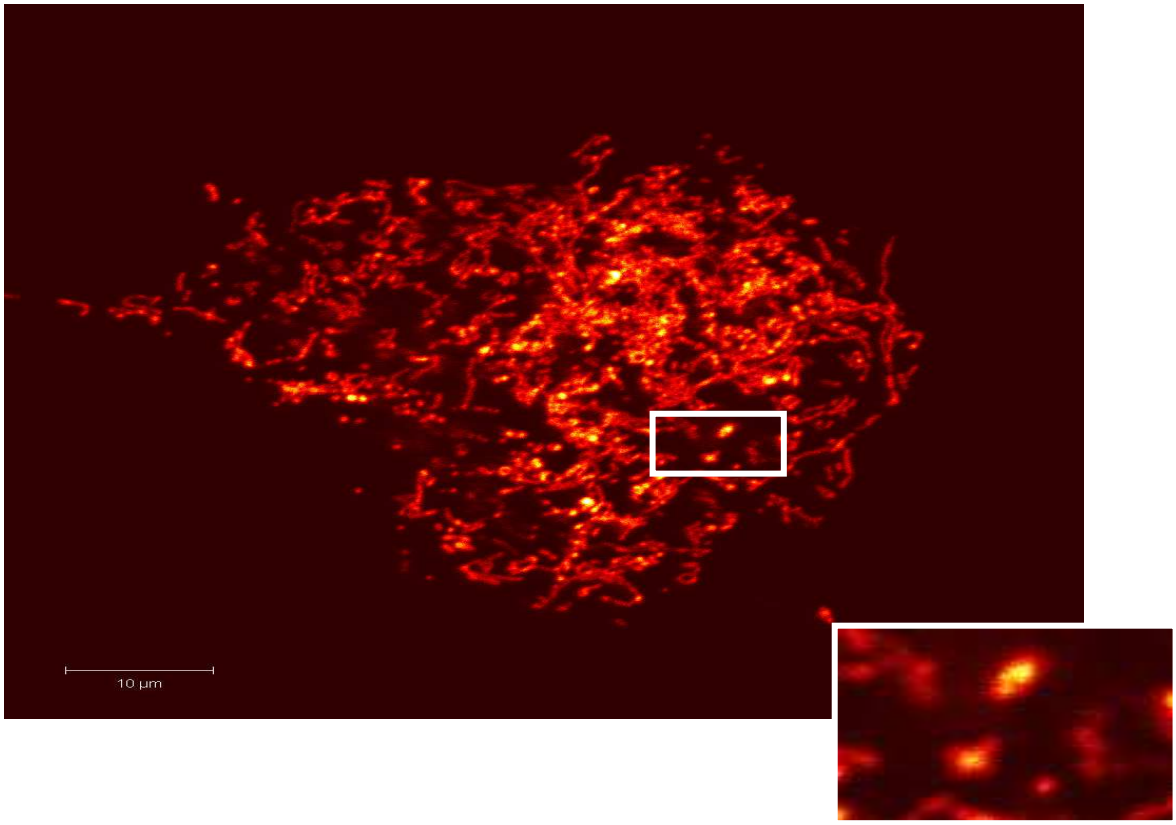

(A)

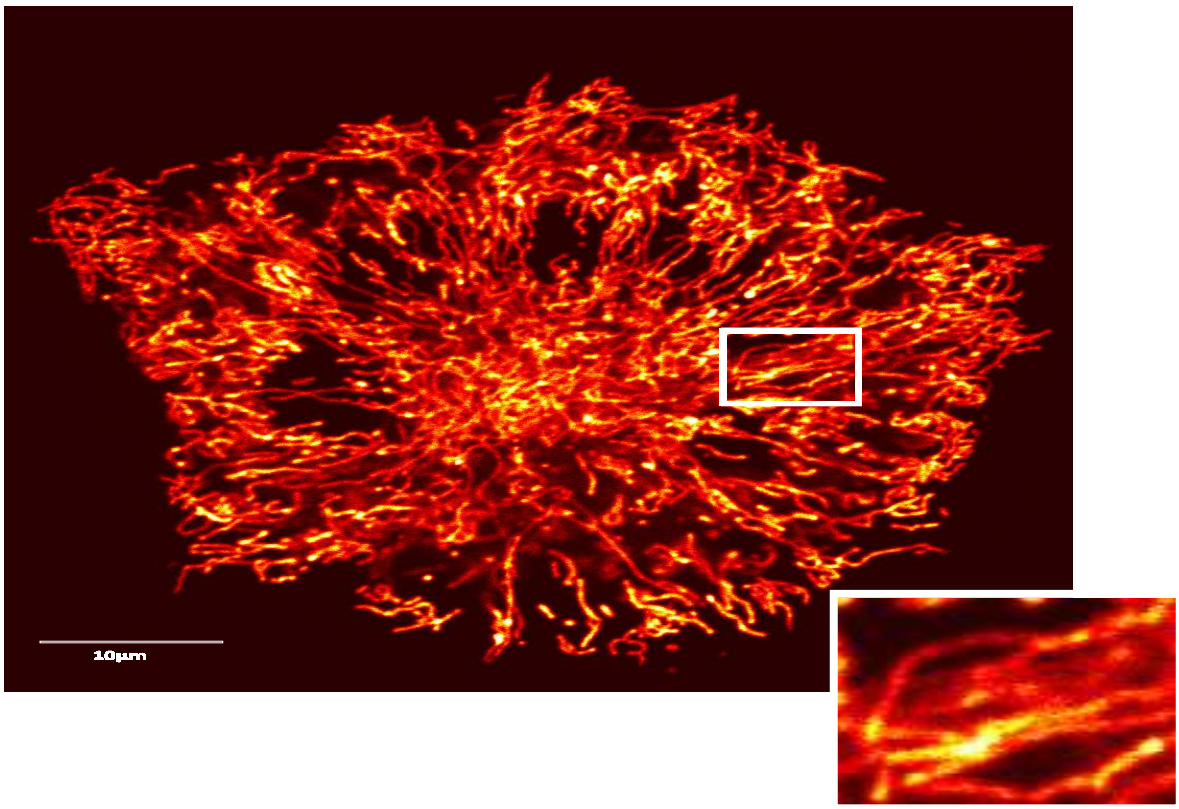

(B)

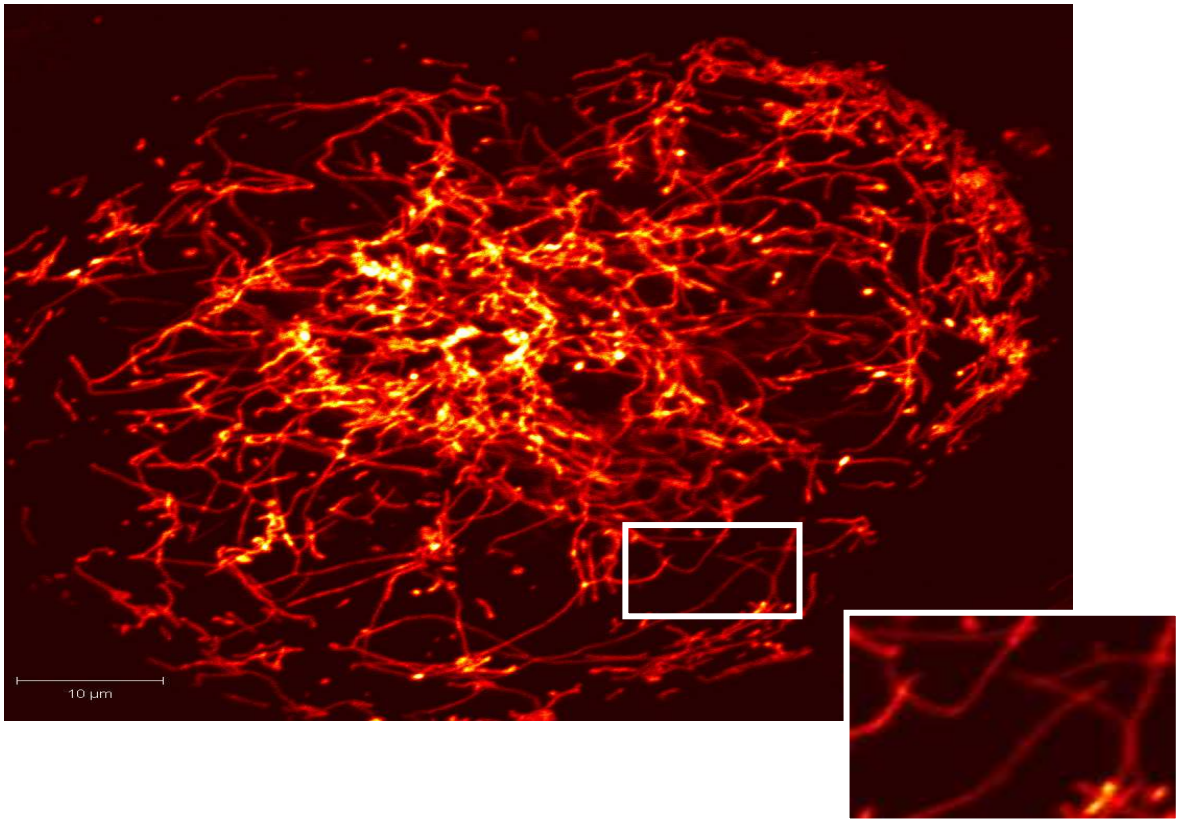

(C)

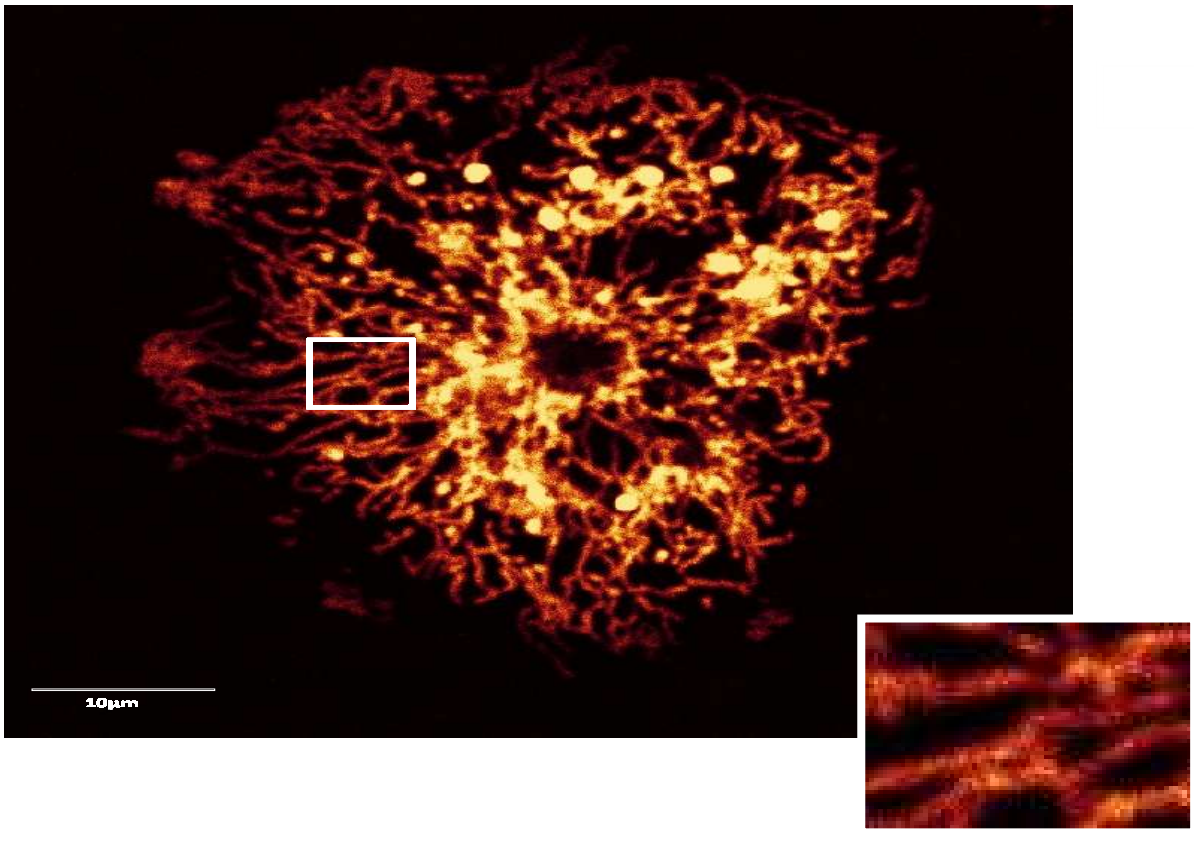

(D)

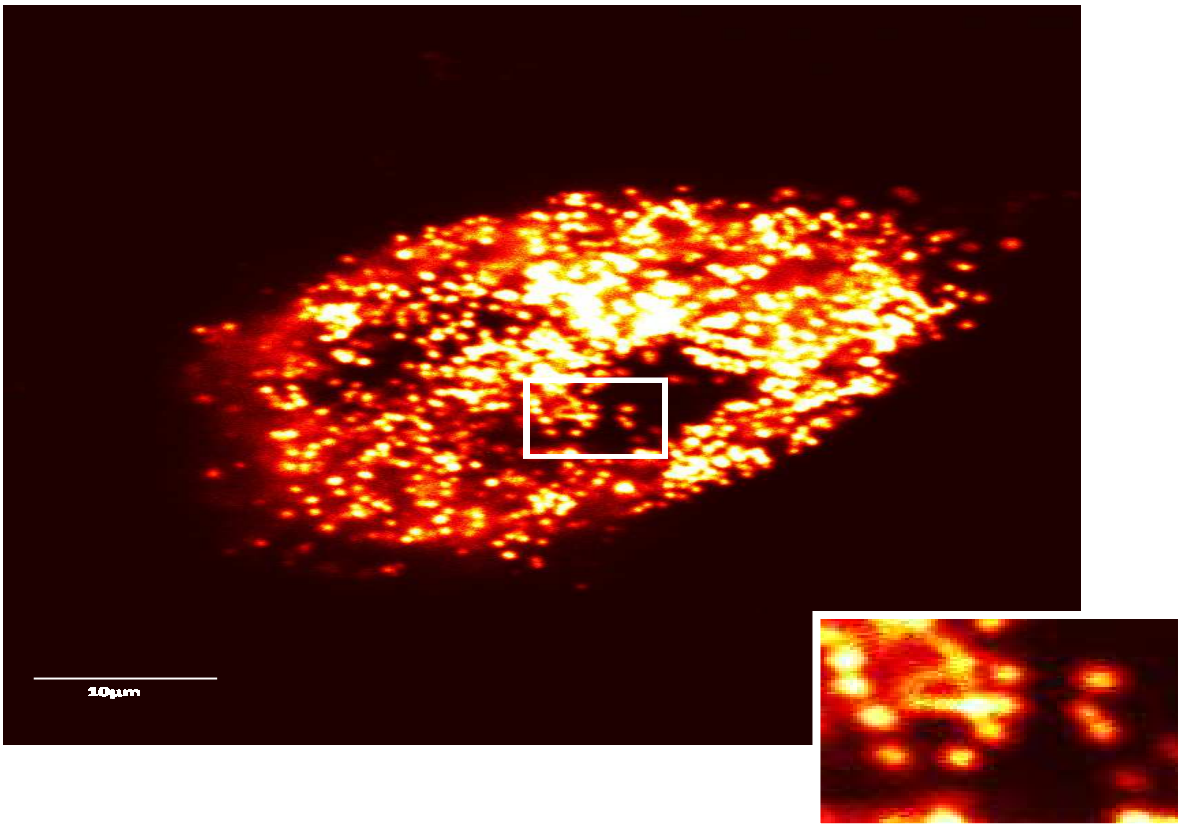

(E)

Figure 4.1: Representative confocal images of HL-1 cells transfected with red fluorescent protein targeted to the mitochondrial matrix in addition to (A) empty vector control, (B) Mfn1, (C) Mfn2, (D) $Drp1_{K38A}$ (all demonstrating predominantly [>50%] elongated mitochondria in B-D), and hFis1 (E) (demonstrating predominantly fragmented mitochondria).

Cells with has an overexpression of Mfn2 show a marked increase in elongated mitochondria after 24 hours (68.0 ± 4.4%) compared to cells with the empty vector, RcCMV (43.0 ± 6.9%), (n=4; *P<0.05). The overexpression of the dominant negative form of the fission protein, $Drp1_{K38A}$, showed a trend of increasing the cells with elongated mitochondria but was not significant (64.8 ± 6.1%). Fragmentation of the mitochondria by the overexpression of hFis1 was also not significant (26.1 ± 5.9%) compared to the vector control (see Figure 4.2).

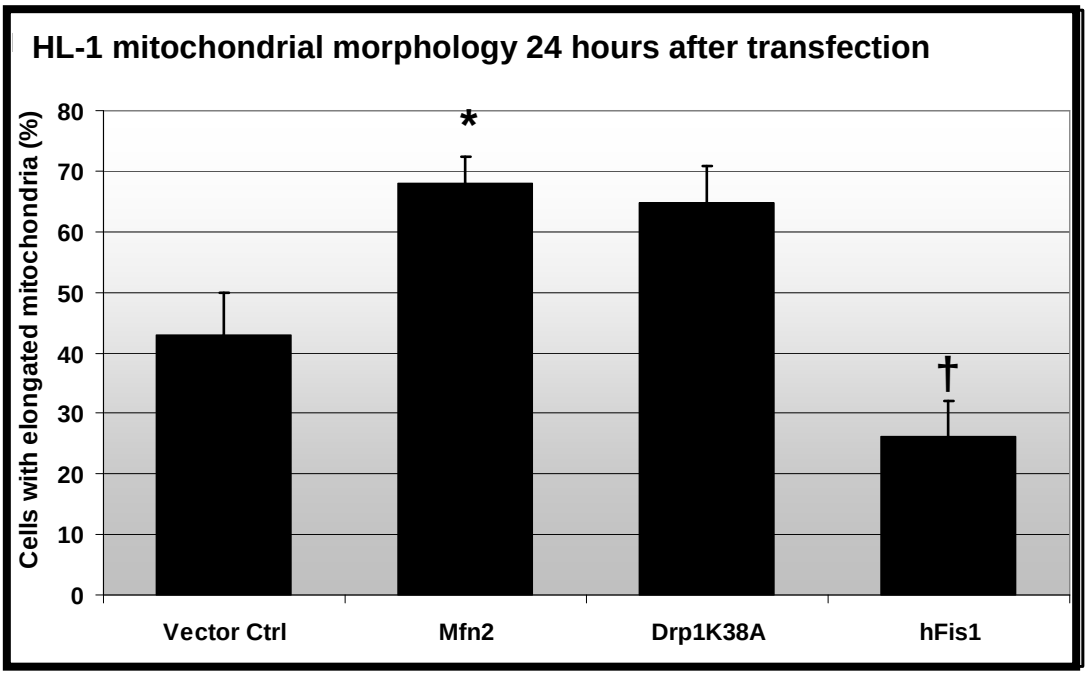

Figure 4.2: Effect of overexpression of different proteins to the morphology of mitochondria in HL-1 cells over a period of 24 hours. A trend of increasing cells with elongated mitochondria was seen for cells with an overexpression of Mfn2 and $Drp1_{K38A}$ with only the Mfn2 achieving significance. Overexpression of the hFis1 at 24 hours did not fragment the mitochondria significantly (N=4 experiments with 80 cells per group; *p<0.05 compared to vector control; †p<0.05 compared to Mfn2 and $Drp1_{K38A}$).

Compared to the cells which were transfected with the empty vector for 48 hours, cells which were transfected with plasmids encoding for Mfn1, Mfn2 and $Drp1_{K38A}$ demonstrated a significant increase in numbers of fused mitochondria (65.3 ± 4.1%, 69.1 ± 4.9% and 62.8 ± 6.3% vs.. 45.7 ± 5.6% with RcCMV, n = 4; *p < 0.05) (see Figure 4.4). We used a mutated form of Drp1 (a known fission protein), $Drp1_{K38A}$ to demonstrate that the potential effects of fused mitochondria were indeed caused by the overexpression of the proteins and not other factors present in the cell. Cells with overexpression of hFis1 as a negative control has markedly reduced number of cells with fused mitochondria (19.0 ± 8.5% vs. 45.7 ± 5.6% with RcCMV, n = 4; *p < 0.05) (see Figure 4.3).

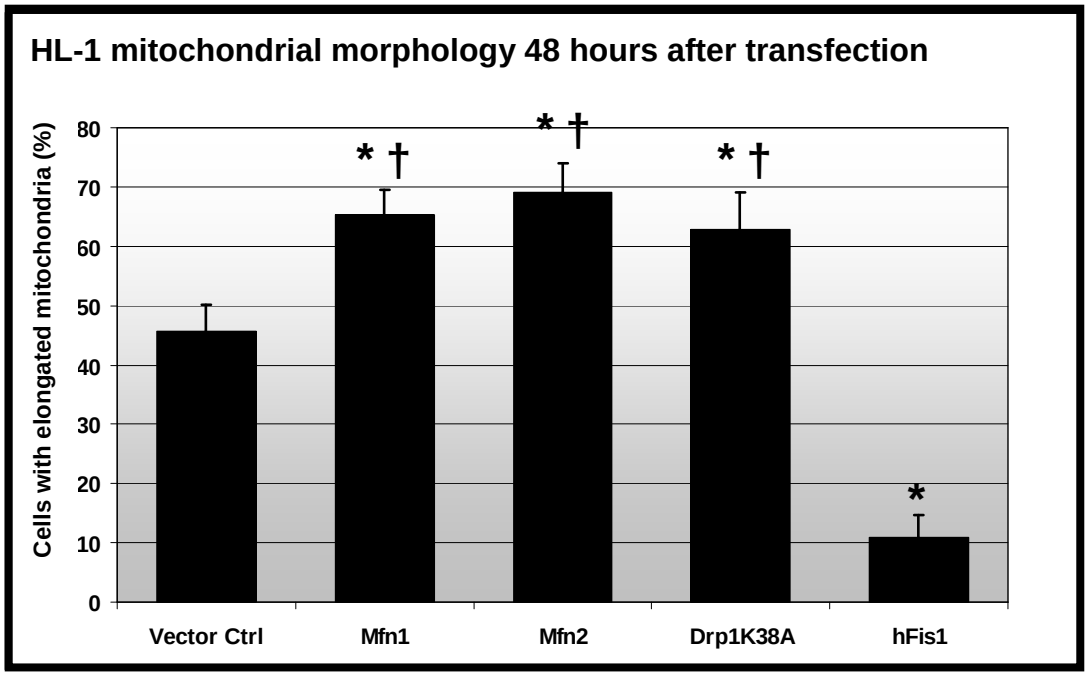

Figure 4.3: Effects of overexpression of different proteins to the morphology of mitochondria in HL-1 cells over a period of 48 hours. Mitochondrial elongation was significantly increased in cells with an overexpression of Mfn1, Mfn2 and $Drp1_{K38A}$. Mitochondrial fragmentation was significantly induced in cells with an overexpression of hFis1. N=4 experiments with 80 cells per group; *p < 0.05 compared to Vector Control; †p<0.05 compared to hFis1.

4.4 Aim (2)

To determine whether mitochondrial morphology can be modulated in the HL-1 cardiac cell line using pharmacological manipulation.

In this section, we investigated the use of a small molecule inhibitor of the Drp1 fission protein, *mdivi-1* as a pharmacological agent in modulating mitochondrial morphology in HL-1 cells.

4.4.1 Materials

To monitor the changes in mitochondrial morphology, 1 ug per well of mitochondria-targeted red fluorescent protein (mtRFP: Mitochondria-targeted dsRED) expression plasmid was transfected to enable viewing of mitochondria using the confocal microscope. *Mdivi-1* drug was purchased from Key Organics Ltd., UK. The drug was dissolved in DMSO (Sigma UK) to achieve a working concentration of 10 mM and 50 mM and subsequently in Krebs buffer comprising (in mM): NaCl 118.0, $NaHCO_3$ 25.0, d-Glucose 11.0, KCl 4.7, $MgSO_4.7H_2O$ 1.2, KH_2PO_4 1.2, $CaCl_2.2H_2O$ 1.8, and HEPES 10.0 (pH 7.4) to achieve a final concentration of 10 µM and 50 µM.

4.4.2 Experimental protocol

HL-1 cardiac cells were transfected with plasmids encoding for mitochondrial-targeted red fluorescent protein (mtRFP). Cells with predominantly fragmented mitochondria were selected using confocal microscopy and monitored over time for the changes in mitochondrial morphology following treatment with either one of the following three treatments:

- Vehicle control (<0.01% DMSO in Krebs)
- 10 uM *mdivi-1*
- 50 uM *mdivi-1*

Following the determination of the optimum duration of incubation with the optimum concentration of *mdivi-1*, a separate batch of cells were imaged using

confocal microscopy to determine number of cells with elongated mitochondria prior to incubation with *mdivi-1* and repeated after incubation with *mdivi-1*.

4.4.3 Results

In order to determine the optimum concentration of *mdivi-1* drug to be used for enhancing proportion of cells with elongated mitochondria as well as the optimum duration of treatment, a time and dose response was carried out. Three different doses were initially tested for this study. However, there was a problem of solubility for 100 µM of the drug where crystal-like particles was still visible under the microscope. A point worth mentioning here is that *mdivi-1* has to be vortexed and sonicated prior to use. A population of cells with pre-dominantly fragmented mitochondria was selected for monitoring throughout the whole duration of 1 hour with 3 different concentrations of *mdivi-1*. Percentage of cells with elongated mitochondria increased to (8 ± 8.4% for 10 µM *mdivi-1*) and (17 ± 7.1% for 50 µM *mdivi-1*) after 20 minutes. Interestingly, the percentage of cells with elongated mitochondria treated with 0.1% DMSO also increased to (19 ± 10.8%) within the same time duration. Nevertheless there was no significance between these values. Forty minutes of incubation with 50 µM *mdivi-1* increased the cells with elongated mitochondria to (60.0 ± 7.5%) compared to (19.0 ± 2.8% for 10 µM *mdivi-1*) and (13.0 ± 10.8% for vehicle control) (n = 4; *$p<0.05$ compared to vehicle control and 10 µM; † $p<0.05$ compared to time 0') (see Figure 4.4). After 60 minutes, number of cells with elongated mitochondria decreased to (16.0 ± 9.7% for 50 µM) while the number of cells with elongated mitochondria remained approximately the same for 10 µM (19.0 ± 2.8%). The number for vector control however, reduced to 0% after 1 hour. These results suggest that *mdivi-1* at a concentration of 50 µM seem to increases the number of cells with elongated mitochondria following a treatment duration of 40 minutes (see Figure 4.5).

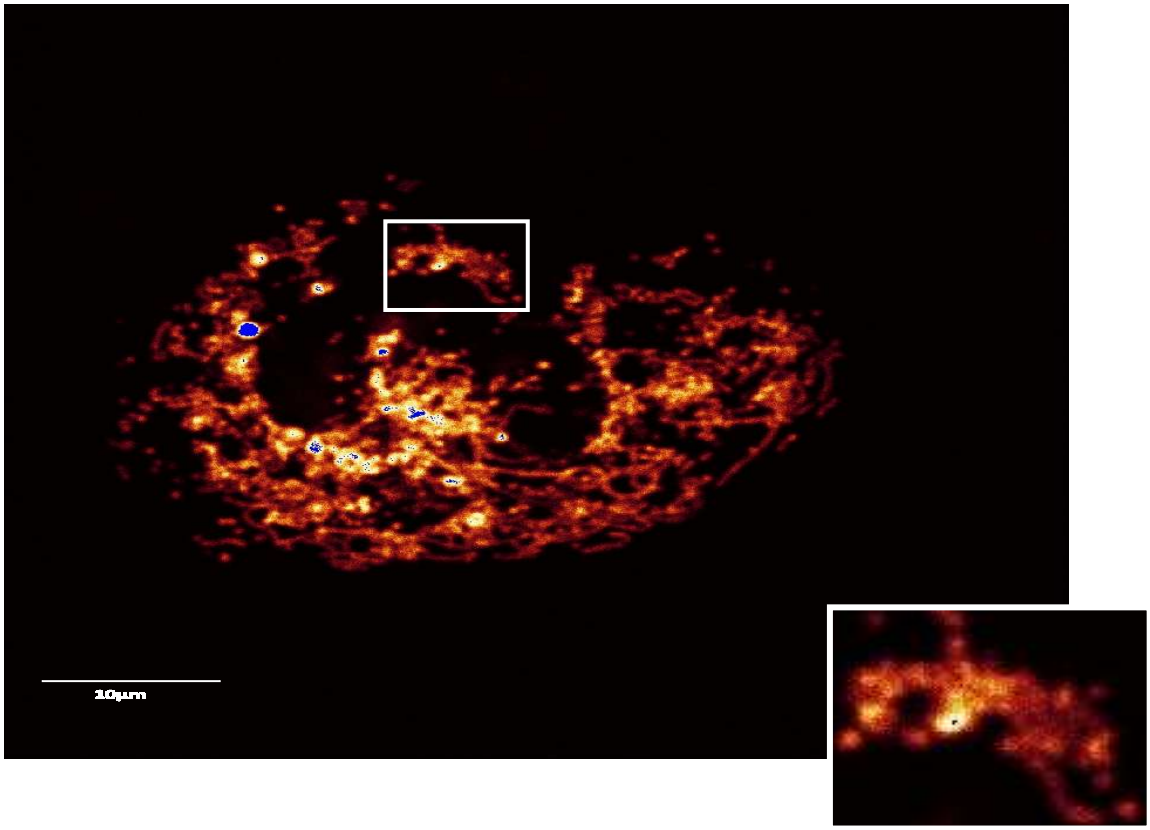

(A)

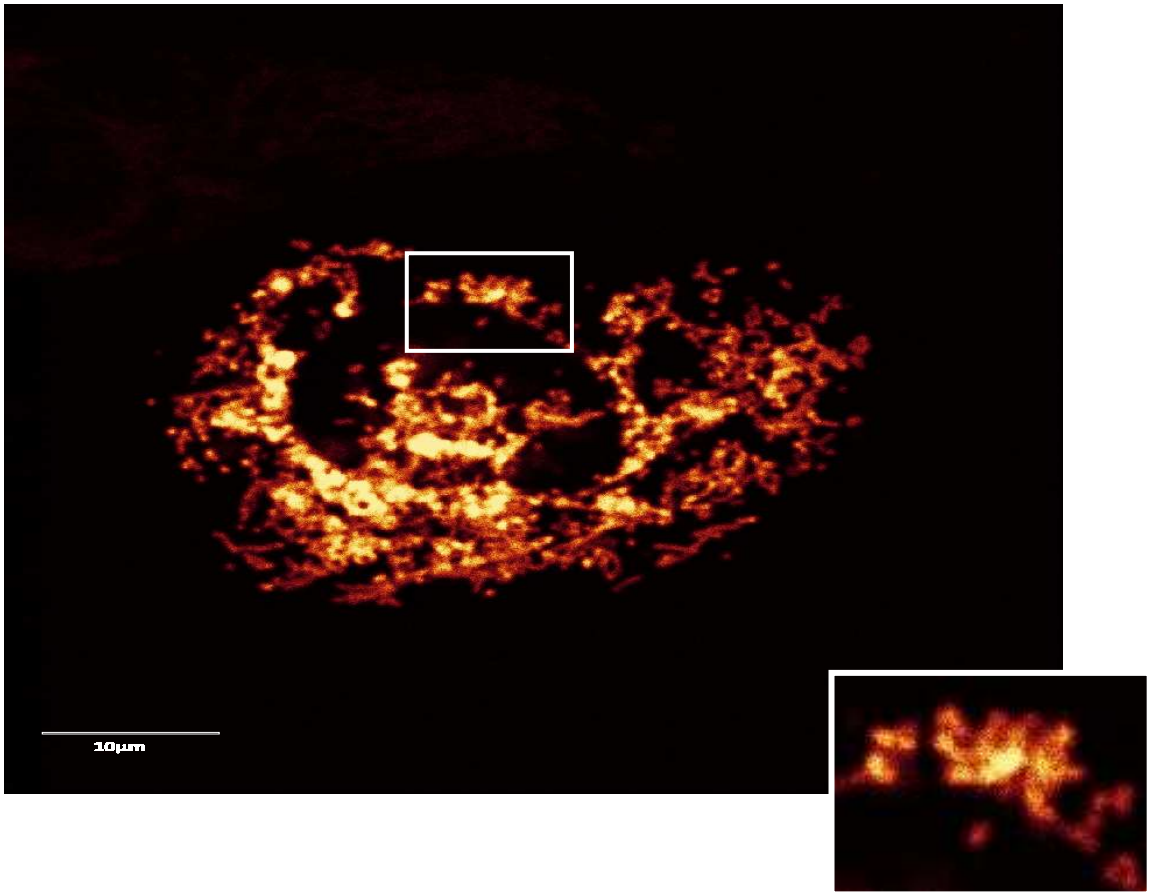

(B)

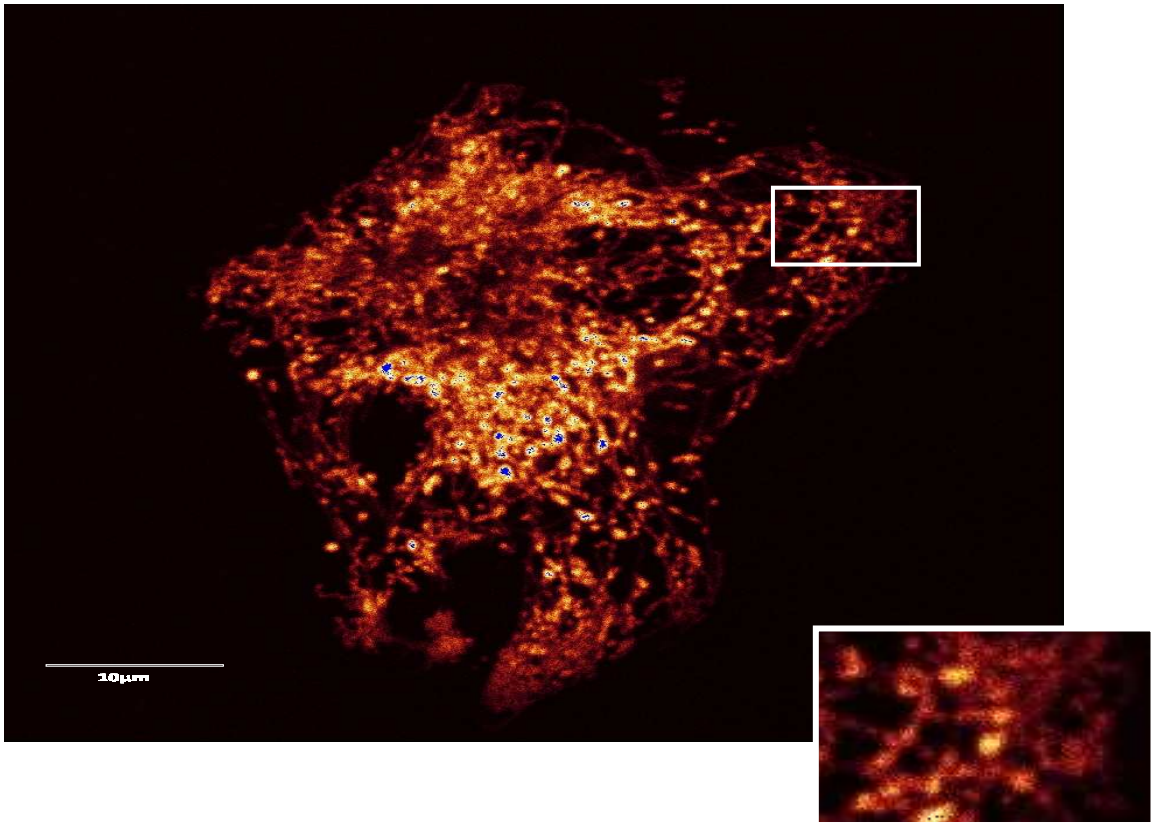

(C)

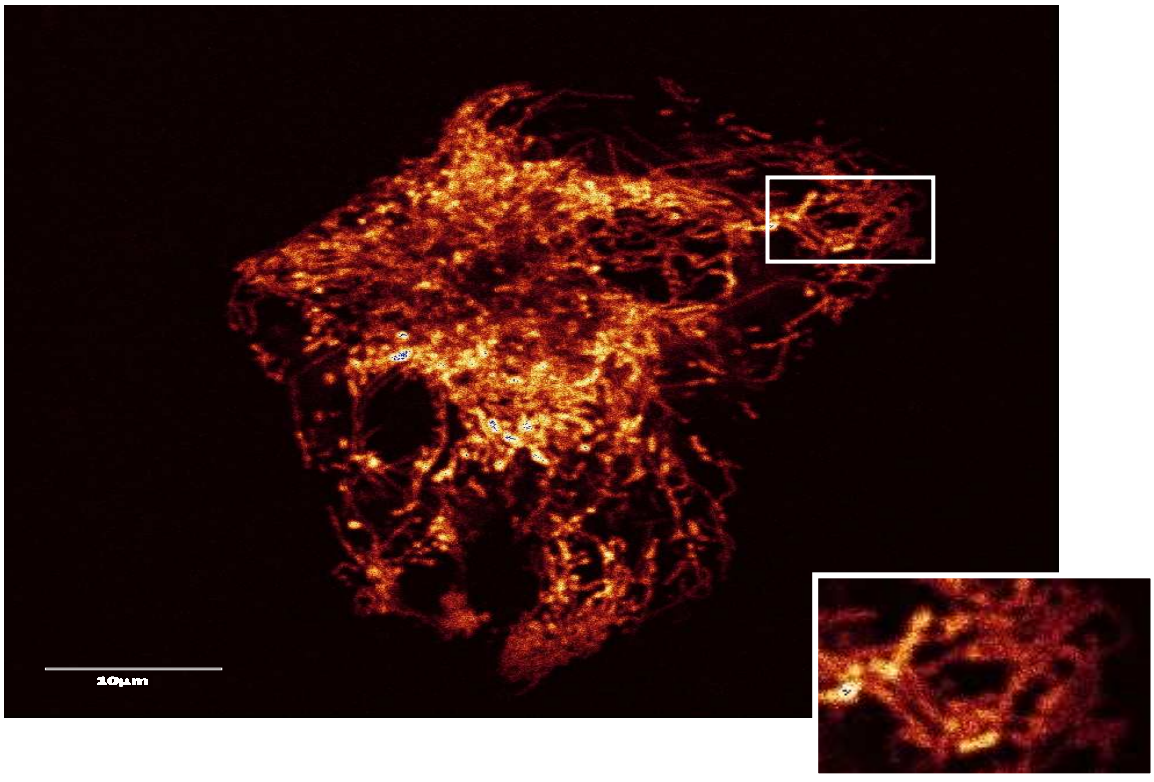

(D)

Figure 4.4: Representative images of mitochondria in HL-1 cells treated with vehicle control at (A) time 0’ and (B) 40’ or 50 µM *mdivi-1* at (C) time 0’ and (D) 40’.

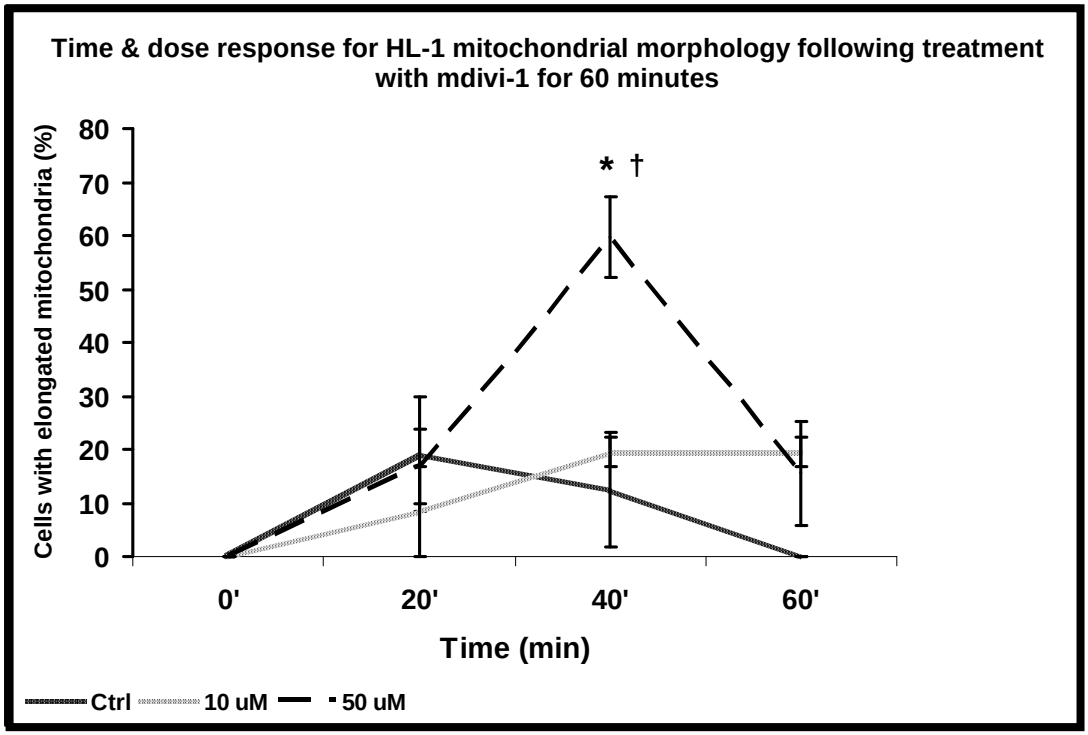

Figure 4.5: Time & dose response changes in HL-1 mitochondrial morphology for 60 minutes. In HL-1 cells identified as containing predominantly fragmented mitochondria at the beginning of the experiment, treatment with *mdivi-1* at 50 µM but not at 10 µM for 40 minutes significantly increased the proportion of cells displaying elongated mitochondria. N=4 experiments with 30 cells per treatment group. *P<0.05.

To verify the dosage and duration that we obtained, a separate set of HL-1 cells was incubated in either 0.1% DMSO as vehicle control or 50 µM *mdivi-1* for a period of 40 minutes and the percentage of cells with elongated mitochondria determined. Number of cells with elongated mitochondria at time 0' was (24.2 ± 8.5% for vehicle control) and (25.9 ± 6.9% for 50 µM *mdivi-1*). After 40 minutes of 37°C incubation, the percentage increased to (67.3 ± 3.8% for 50 µM *mdivi-1* vs. 29.0 ± 8.1% for vehicle control; n=4; *p<0.05 compared to vehicle control at 40 minutes) (see Figure 4.6).

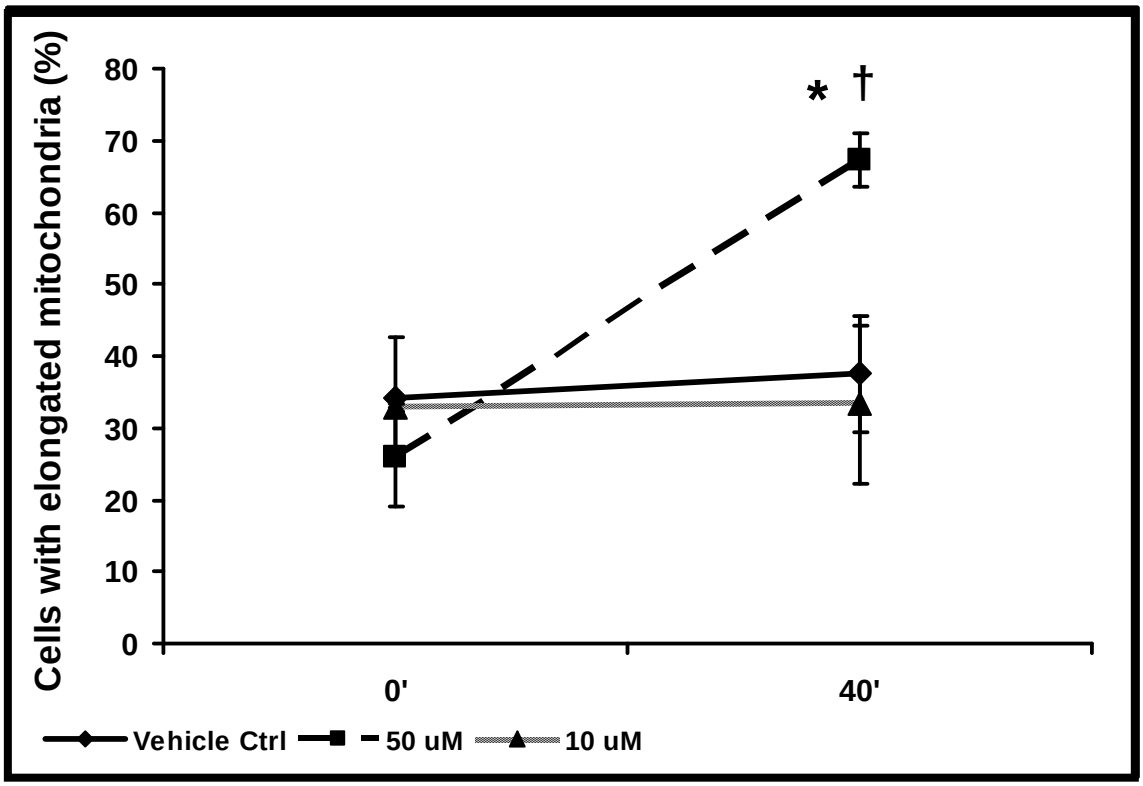

Figure 4.6: Effects of 40 minutes *mdivi-1* treatment to the morphology of mitochondria in HL-1 cells. In HL-1 cells containing either fragmented or elongated mitochondria under basal conditions, treatment with *mdivi-1* at 50 µM but not at 10 µM for 40 minutes also significantly increased the proportion of cells displaying elongated mitochondria. n┐ 5 experiments with 80 cells per treatment group. *P<0.05 vs. time 0; †P<0.05 vs. control at 40 minutes.

4.5 Aim (3)

To determine whether mitochondrial morphology can be modulated in endothelial cells using genetic manipulation

In this part of the study, we aimed to investigate whether mitochondrial morphology can be manipulated in endothelial cells using the same mitochondrial-shaping proteins used for the HL-1 cells.

4.5.1 Materials

Plasmids included in the study of mitochondrial morphology of endothelial cells are similar to the study in HL-1 cells: an empty plasmid expression vector (RcCMV); one expressing mitofusin 1(pCB6-MYC-Mfn1); one expressing mitofusin 2 (pCB6-MYC-Mfn2) [165]; one containing $Drp1_{K38A}$ (pcDNA3.1-HA-$_{K38A}$-DRP1), the dominant negative mutant form of the mitochondrial fission protein Drp1 [205]; and one containing hFis1. $Drp1_{K38A}$ has a mutation in the GTPase domain that results in replacement of lysine 38 with alanine (designated as $Drp1_{K38A}$), disabling its ability to induce mitochondrial fission by sequestering endogenous Drp1 [181, 205]. For the mitochondrial morphology studies a ratio of 1:2 mitochondria-targeted red fluorescent protein (mtRFP: Mitochondria-targeted dsRED) expression plasmid: plasmid of interest was included in order to permit visual assessment of mitochondrial morphology. All plasmids were a generous gift of Dr Luca Scorrano (Padova, Italy). Krebs buffer comprising (in mM): NaCl 118.0, $NaHCO_3$ 25.0, d-Glucose 11.0, KCl 4.7, $MgSO_4.7H_2O$ 1.2, KH_2PO_4 1.2, $CaCl_2.2H_2O$ 1.8, and HEPES 10.0 (pH 7.4) was used as imaging buffer for confocal microscopy studies.

4.5.2 Experimental protocol for mitochondrial morphology determination

Upon reaching confluency of around 50 – 60% (~24 hours after seeding), the cells were transfected with one of the following plasmids:

1. RcCMV – empty vector (Vector Control)
2. $Drp1_{K38A}$ – the dominant negative form of the fission protein
3. Mfn1 – fusion-promoting protein
4. Mfn2 – fusion-promoting protein
5. hFis1 – fission-promoting protein

mtRFP was always co-transfected to visualise the mitochondria as well as to indicate uptake and expression of the plasmids. Similar to the HL-1 study, this was the first time these proteins were overexpressed in endothelial cells. Therefore, we had to determine the optimum duration of plasmids expression to induce significant changes in mitochondrial morphology. Images of twenty randomly chosen cells were taken after 24 hours for one set of experiments and 48 hours for another set of cells and this was repeated for each group in at least four independent transfection experiments giving a total number of approximately 80 cells per treatment group. Three investigators, blinded to the initial treatment, independently assigned the cells as displaying either predominantly (>50%) elongated or (>50%) fragmented mitochondria, indicating that either mitochondrial fusion or fission, respectively, was the predominant process in that cell at that particular time, a method which has been adapted from a previously published study [165].

4.5.3 Results

Endothelial cells have a similar mitochondrial arrangement to the HL-1 cardiac cell line where the mitochondria resemble a network of elongated tubules (see Figure 4.7).

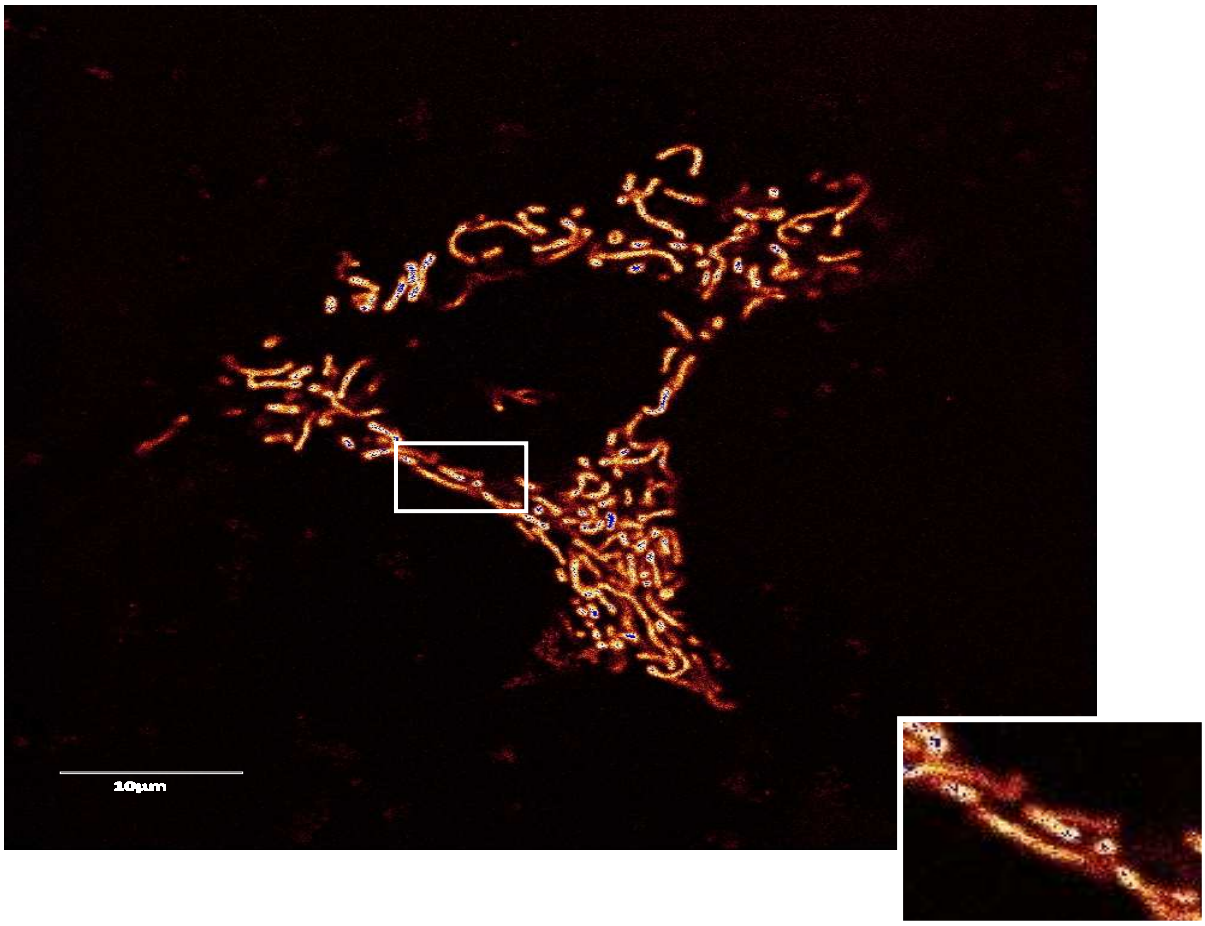

Figure 4.7: Representative image of mitochondria in an endothelial cell with an overexpression of mtRFP under the confocal microscope.

Nevertheless, endothelial cells are smaller and rounded hence the mitochondria are also much more tubular and elongated. It is precisely due to this fact that the percentage of cells with elongated mitochondria in cells with the vector control, RcCMV alone is considerably higher (65.3 ± 1.2%) than that of the HL-1 cells (45.7 ± 5.6%). Endothelial cells with elongated mitochondria which have an overexpression of Mfn1, Mfn2 or $Drp1_{K38A}$ were scored at 66.7 ± 5.7%, 67.5 ± 4.7% and 80.1 ± 1.3% respectively after 48 hours, none of which are significant compared to vector control. The overexpression of the fission protein, hFis1 however, significantly reduced the number of cells with elongated mitochondria to (17.7 ± 7.5%; n=4; *$p<0.05$ compared to vector control; †$p<0.05$ compared to hFis1) (see Figure 4.8).

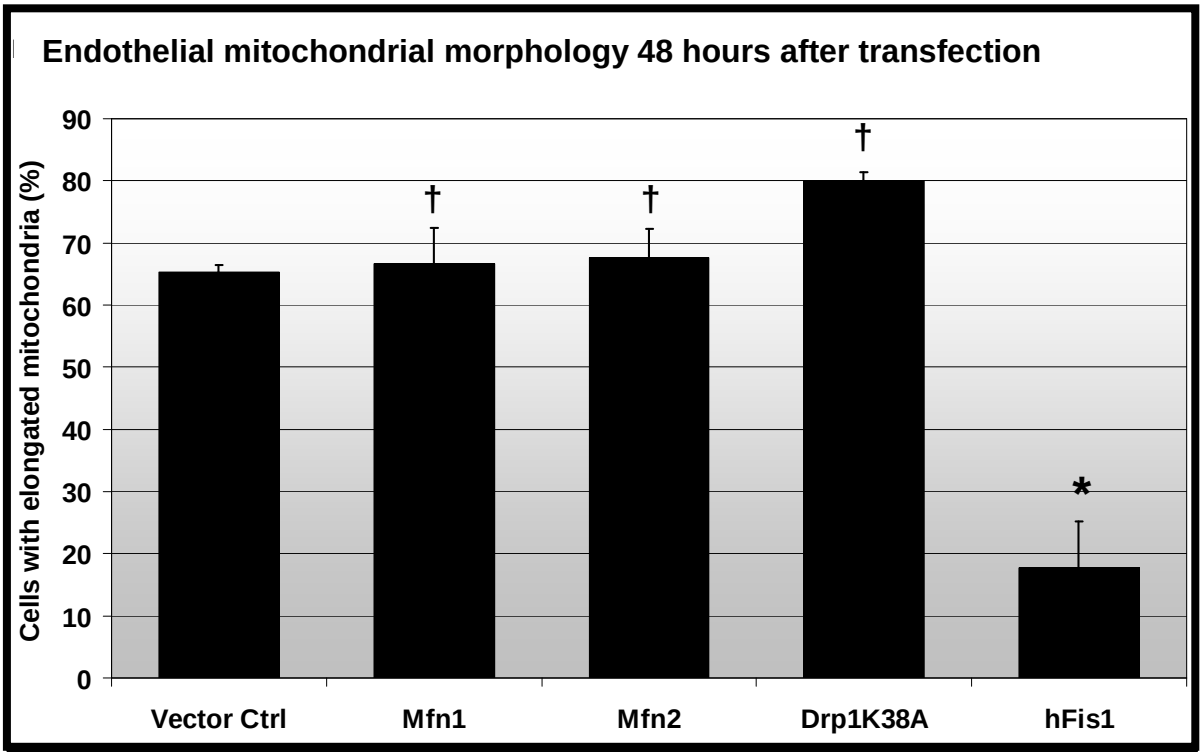

Figure 4.8: Effects of overexpression of different proteins to the morphology of mitochondria in endothelial cells over a period of 48 hours A trend of increasing cells with elongated mitochondria was seen for cells with an overexpression of $Drp1_{K38A}$. Overexpression of the hFis1 at 48 hours fragments the mitochondria significantly N=4 experiments with 80 cells per group; *$p < 0.05$ compared to Vector Control; †$p<0.05$ compared to hFis1.

4.6 Aim (4)

To determine whether elongated mitochondria can be detected in the adult cardiomyocytes

Due to the difference in spatial arrangement of the mitochondria in adult cardiomyocytes, we aimed to investigate whether elongated mitochondria (> 2 µm) exists in adult cardiomyocytes using both confocal and electron microscopy in this section.

4.6.1 Materials

Mdivi-1 drug was purchased from Key Organics Ltd., UK. The drug was dissolved in DMSO to achieve a working concentration of 1 M in 100% DMSO and subsequently in saline to achieve a final concentration of 1 mM of *mdivi-1* in 0.1% DMSO (~ 50 µM *mdivi-1* in plasma).

4.6.2 Experimental protocol

For confocal microscopy studies on adult cardiomyocytes, ventricular cardiomyocytes were isolated from adult Sprague-Dawley rats by perfusion and digestion of ventricles with collagenase according to a previously described method. The cells were incubated with plating medium containing an appropriate titer of virus for 4 hours and were imaged 72 hours later. mtPA-GFP within a prespecified region of interest (ROI) was photoactivated by scanning adult rat cardiomyocytes with the 405-nm wavelength ultraviolet laser. The cell was immediately reimaged at 488 nm, and the difference in the intensity of green fluorescence between the 2 images before and after photoactivation was determined with Image J software (National Institutes of Health, Bethesda, Md). The spread of GFP beyond the ROI was expressed as a fold increase relative to the intensity within the ROI. Results were obtained from 30 randomly chosen cells isolated from 3 rats.

For electron microscopy studies on adult cardiomyocytes, hearts were excised from C57BL/6 male mice after an intravenous injection of either vehicle control (0.1 mL of 0.1% dimethyl sulfoxide) or *mdivi-1* (0.24 mg/kg) after 15 minutes of stabilization (n=4 mice). The excised hearts were perfused with a fixative overnight, following which a 2-mm transverse slice, 3 mm from the apex, was obtained from each heart. Ultrathin sections were viewed with a Jeol 1010 transition electron microscope (Jeol Ltd, Warwickshire, UK). In 6 randomly selected electron micrographs of longitudinally arranged cardiomyocytes, the proportions of interfibrillar mitochondria with lengths that were <2, 2, or >2 µm (the length of a single sarcomere) were determined (see Figure 4.9). For each heart, the lengths of >500 to 600 interfibrillar mitochondria were assessed.

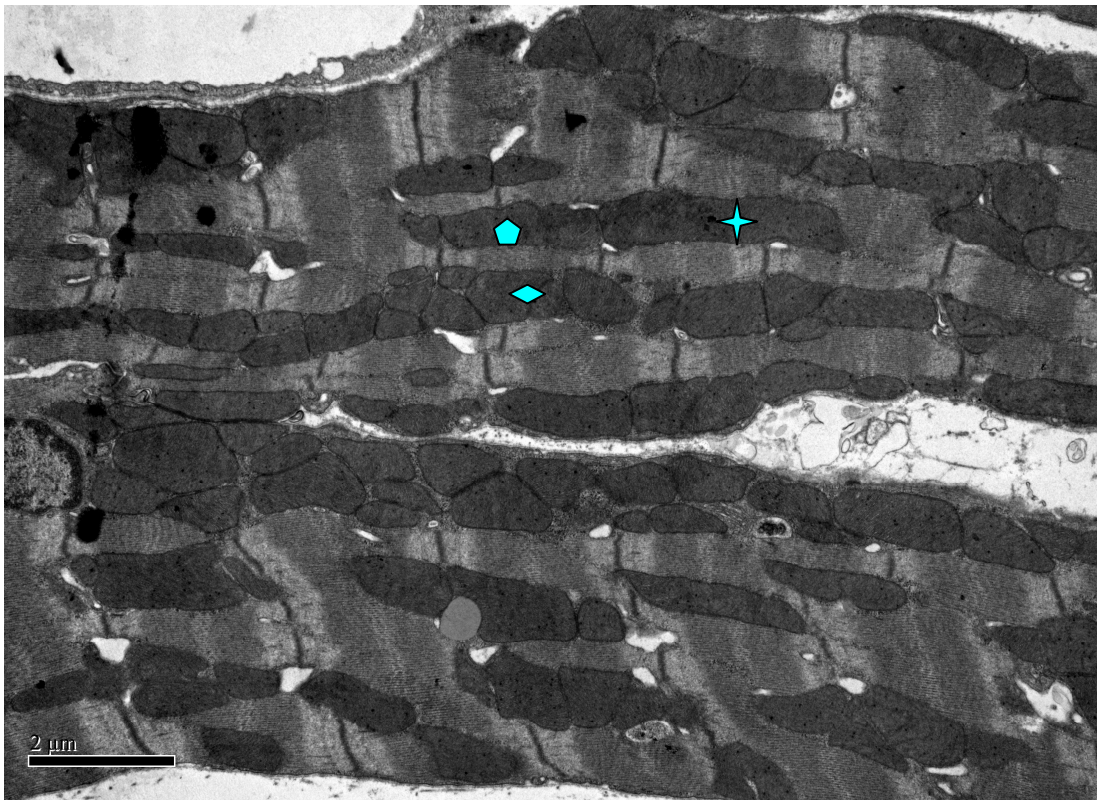

(A)

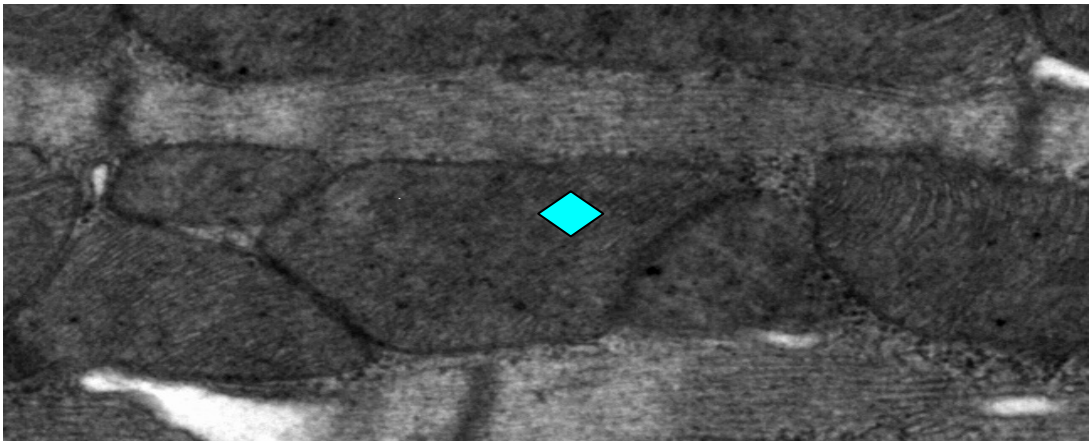

(B)

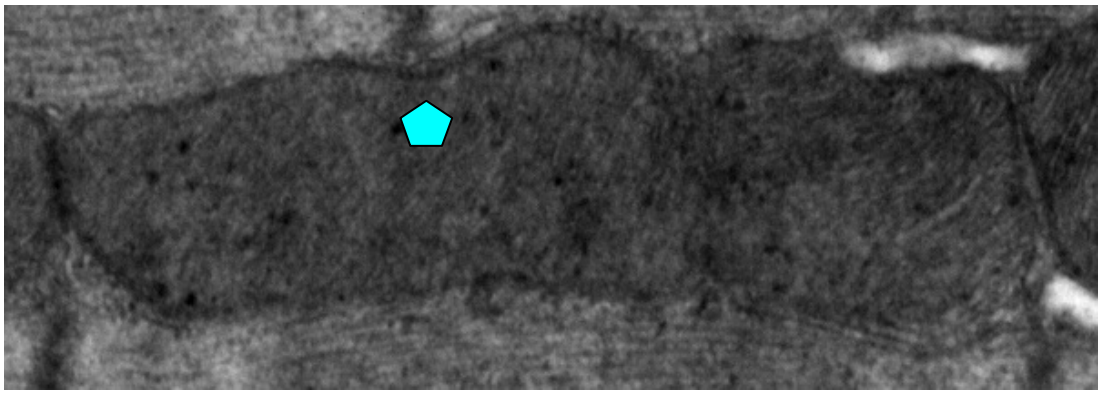

(C)

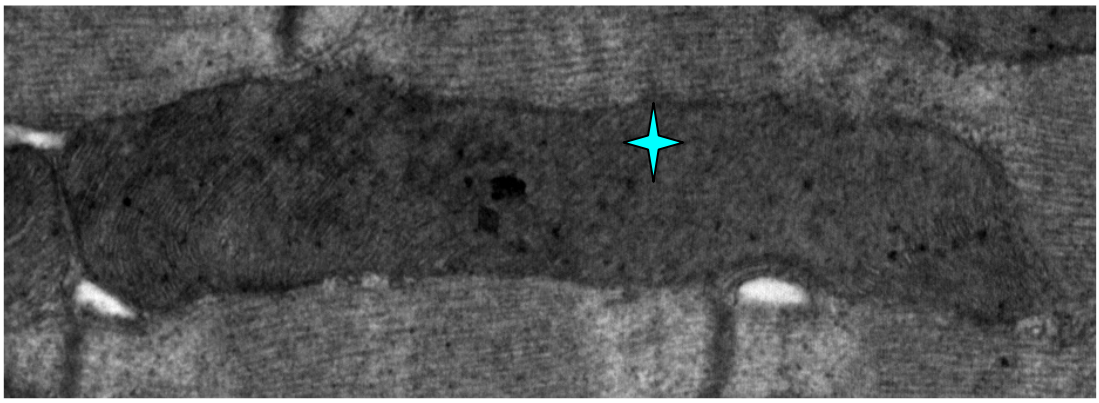

(D)

Figure 4.9: (A) Representative electron micrograph depicting interfibrillar mitochondria with lengths that are <2, 2, or >2 µm (the length of a single sarcomere) in an adult cardiomyocyte. (B) Enlarged micrograph of a mitochondria < 2 µm in length. (C) Enlarged micrograph of a mitochondria 2 µm in length. (D) Enlarged micrograph of a mitochondria > 2 µm in length.

4.6.3 Results

Using confocal microscopy, we were able to visualise mitochondrial morphology in adult rat cardiomyocytes infected with adenoviral vector harbouring plasmids encoding for mitochondrial-targeted photo-activatable green fluorescent protein (mtPA-GFP) which is non-fluorescent but can be activated in a highly localised manner by scanning with the ultraviolet confocal laser line 405 nm. The photo-activated GFP diffuses rapidly within the mitochondrial matrix to the full extent of the inner mitochondrial membrane and can therefore be used to "tag" individual mitochondria. Using this experimental approach, we were able identify elongated, interfibrillar mitochondria in primary adult cardiomyocytes. The length of these elongated mitochondria ranged from 2 to 6 µm (corresponding to 1 to 3 sarcomeres). In addition, we observed the spread of photo-activated mitochondrial GFP outside the initial area of photo-activation (2.17 ± 0.06-fold increase in the area of GFP; Figure 4.10). This finding was confirmed by observing the changes in mitochondrial membrane potential taking place in individual mitochondria in response to low levels of oxidative stress generated by laser scanning of TMRM. This results in "flickering" of individual mitochondria as they depolarise and repolarise, with coincident loss and re-accumulation of TMRM dye. Both mitochondrial membrane depolarisation and re-polarisation were found to occur in a synchronous fashion along the entire length of the elongated mitochondria.

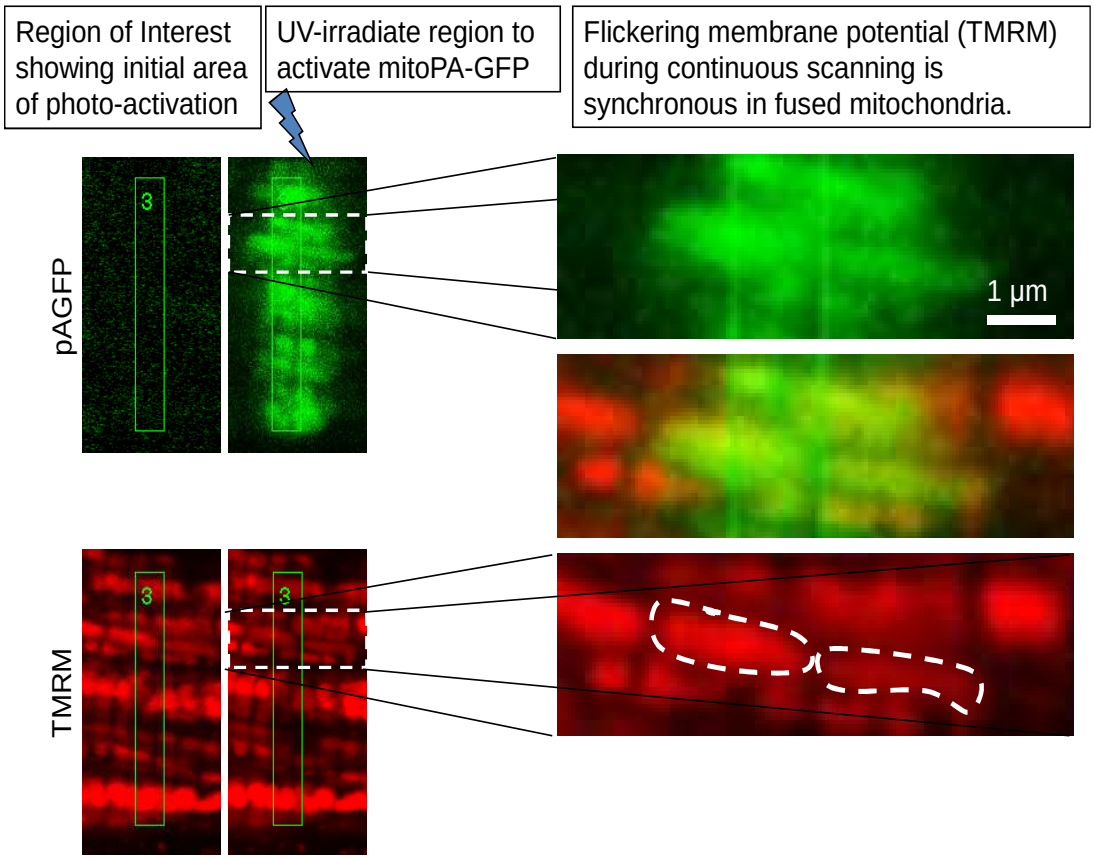

Figure 4.10: Representative example of an adult rat ventricular cardiomyocyte expressing mitochondrial matrix targeted photo-activatable green fluorescent protein (mtPA-GFP). Photo-activation of mtPA-GFP within a Region of Interest (ROI) resulted in an increase in GFP fluorescence within the ROI. Interestingly, immediately following photo-activation, the GFP was found to spread beyond the boundaries of the ROI, demonstrating that individual mitochondria extend up to 5 µm beyond the edge of the ROI. This indicates transfer of the GFP along the full length of elongated mitochondria which overlap the boundaries of the ROI, suggesting the presence of elongated mitochondria (extending 2-3 sarcomeres in length), which display exactly synchronous depolarisation and repolarisation in mitochondrial membrane potential in response to minimal oxidative stress

In the vehicle control-treated hearts, percentage of interfibrillar mitochondria with a longitudinal length less than 1 sarcomere (<2 µm), 1 sarcomere (=2 µm) and more than 1 sarcomere (>2 µm) is 82.0 ± 1.9%, 10.5 ± 1.8% and 7.3 ± 0.5% respectively. For the *mdivi-1* treated hearts, percentage of interfibrillar mitochondria with a longitudinal length less than 1 sarcomere (<2 µm), 1 sarcomere (=2 µm) and more than 1 sarcomere (>2 µm) is 86.3 ± 2.7%, 8.0 ± 1.7% and 6.0 ± 1.7% respectively (see Figure 4.11).

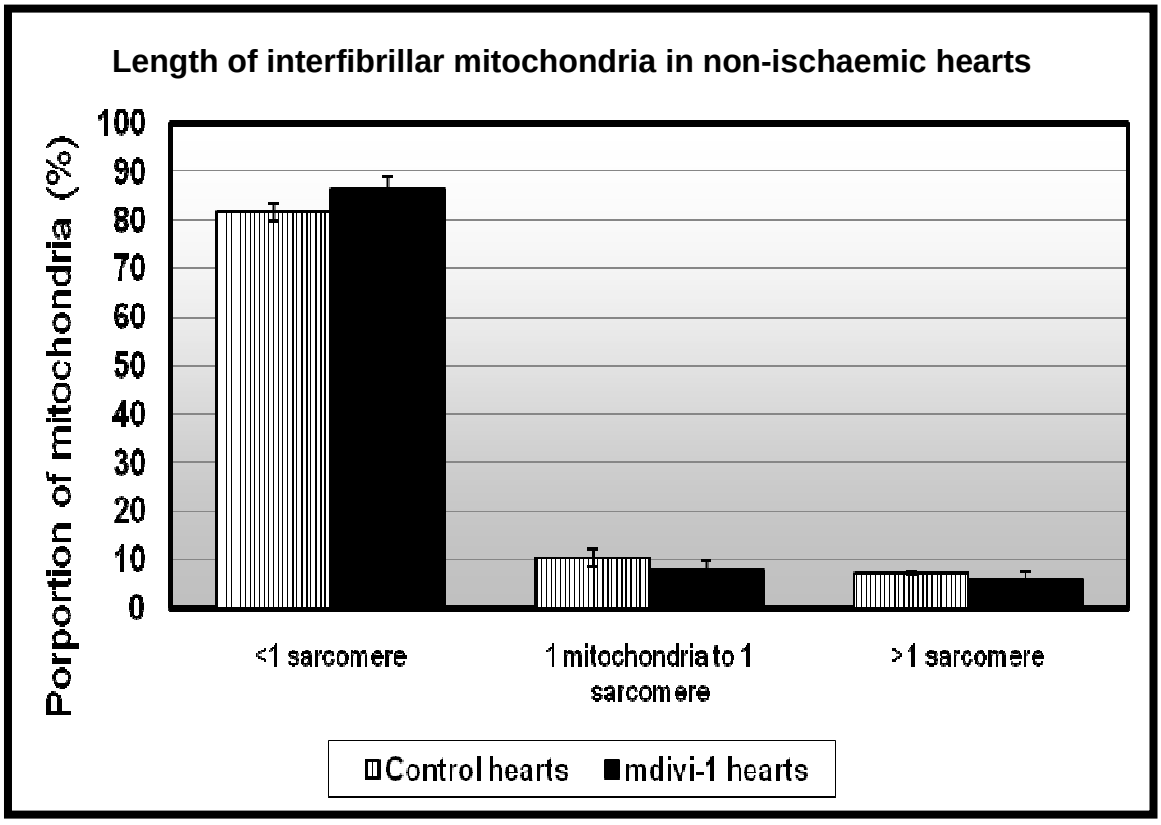

Figure 4.11: Proportion of varying lengths of interfibrillar mitochondria in non-ischaemic hearts. The percentages of mitochondria of lengths < 1 sarcomere, equal to 1 sarcomere (1:1), or >1 sarcomere were determined by electron microscopy in hearts treated with placebo and *mdivi-1 in vivo* before ischaemia

4.7 Aim (5)

To determine whether the presence of elongated mitochondria can be increased in the adult cardiomyocytes using pharmacological manipulation

In this section, we aimed to determine whether the use of the small molecule inhibitor of Drp1 fission protein, *mdivi-1* as a pharmacological agent inhibits mitochondrial fission in the adult cardiomyocytes.

4.7.1 Materials

Mdivi-1 drug was purchased from Key Organics Ltd., UK. The drug was dissolved in DMSO to achieve a working concentration of 1 M in 100% DMSO and subsequently in saline to achieve a final concentration of 1 mM of *mdivi-1* in 0.1% DMSO (~ 50 µM *mdivi-1* in plasma).

4.7.2 Experimental protocol

Hearts were excised from C57BL/6 male mice, following an intravenous injection of either vehicle control (0.1ml of 0.1% DMSO) or *mdivi-1* (0.24 mg/kg), after 15 minutes stabilization followed by 20 minutes regional ischaemia (N=4 mice). The excised hearts were perfused with a fixative overnight, following which a 2mm transverse slice, 3mm from the apex, was obtained from each heart. Ultra-thin sections were viewed with a Jeol 1010 transition electron microscope (Jeol Ltd, UK). In six randomly selected electron micrographs of longitudinally-arranged cardiomyocytes, the proportion of interfibrillar mitochondria whose lengths were less than, equal to or greater than 2µm (the length of a single sarcomere) were determined. For each heart, the lengths of over 500-600 interfibrillar mitochondria were assessed.

4.7.3 Results

The interfibrillar mitochondria for this section of the study derived from the outer layer of the tissue, where the ischaemic insult was less severe as the mitochondria in the inner section of the tissue was too severely disrupted for further analysis (see Figure 4.12).

Figure 4.12: Representative electron micrographs depicting severely disrupted mitochondria and sarcomeres in the inner layer of the tissue.

In vehicle control-treated hearts subjected to ischaemia, proportion of mitochondria less than 1 sarcomere was 85.6 ± 2.4% whereas the proportion was 67.5 ± 5.4% in *mdivi-1* treated hearts subjected to ischaemia. The proportion of mitochondria equivalent to a sarcomere's length was 10.9 ± 2.1% in vehicle control-treated hearts and 18.0 ± 2.7% in *mdivi-1* treated hearts. The proportion of mitochondria longer than 1 sarcomere was 3.6 ± 0.5% in vehicle control-treated hearts whereas this

proportion increased significantly to 14.5 ± 2.8% in *mdivi-1* treated hearts following ischaemia; n=4 animals per treatment group, *P<0.05 (see Figure 4.13 - 4.15).

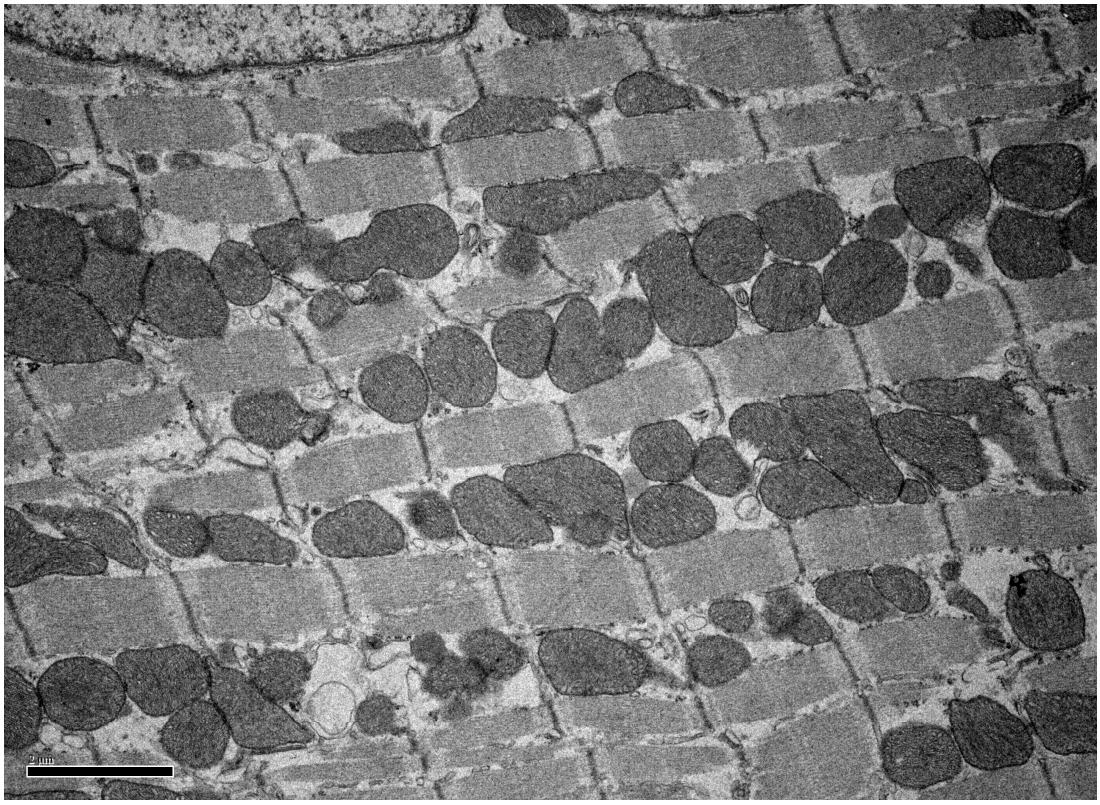

Figure 4.13: Representative electron micrographs depicting relatively fragmented mitochondria in a placebo-treated ischaemic adult murine heart.

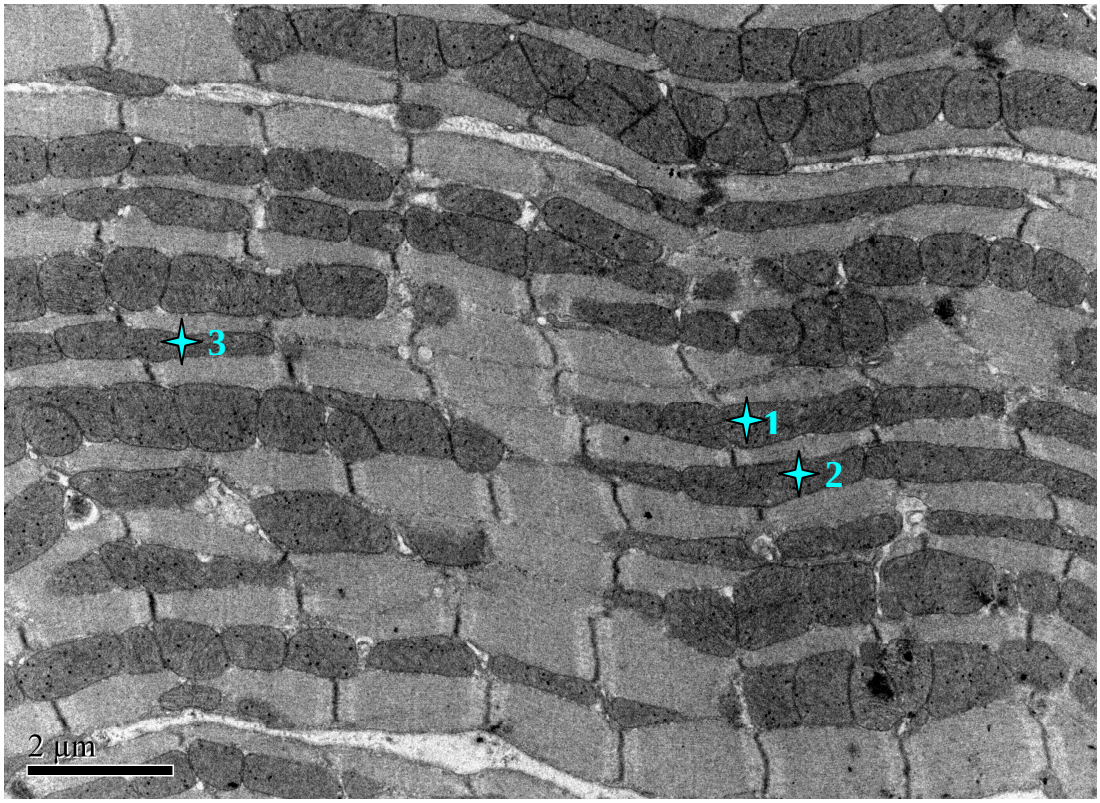

(A)

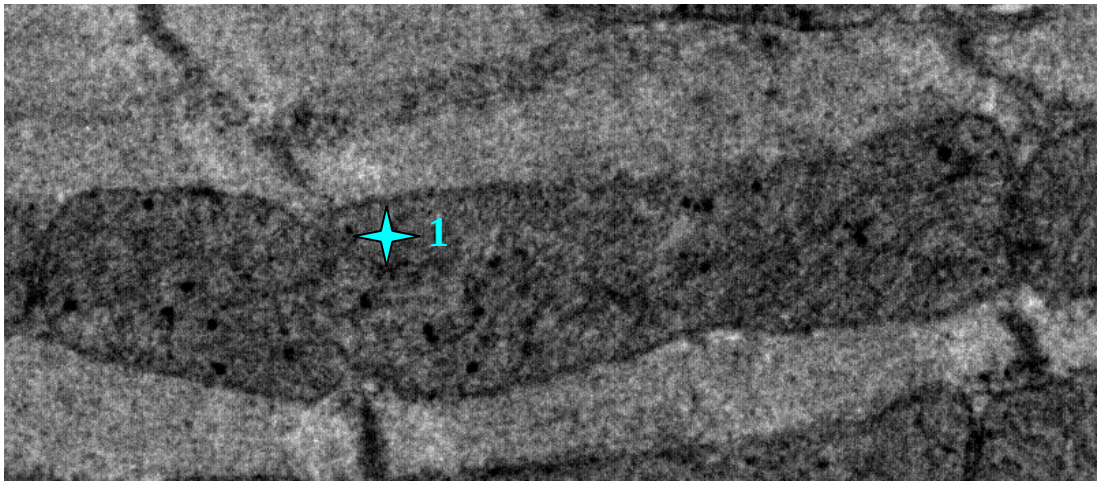

(B)

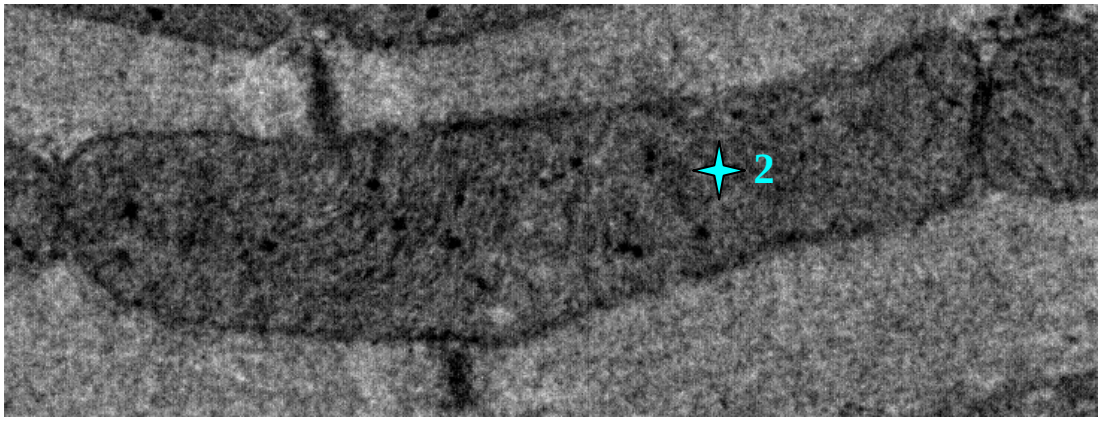

(C)

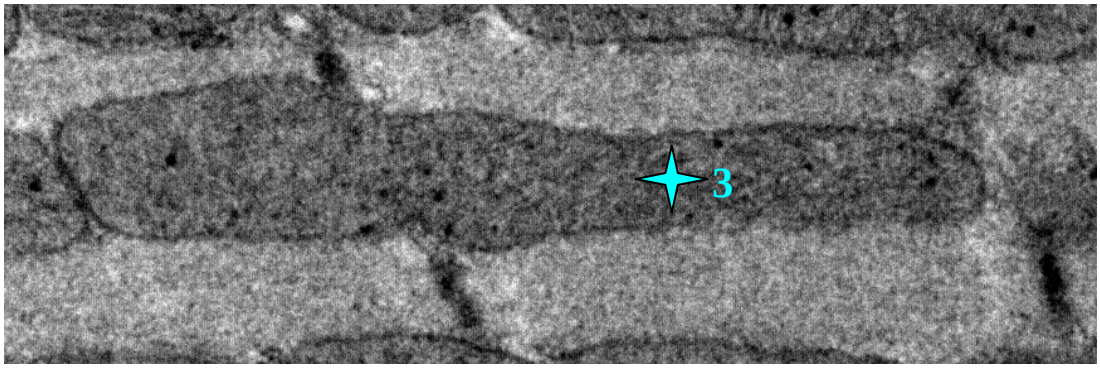

(D)

Figure 4.14: (A) Representative electron micrographs depicting elongated mitochondria (marked with ✦) in an *mdivi-1*–treated ischaemic adult murine heart. (B – D) Enlarged micrographs of elongated mitochondria (> 2 µm)

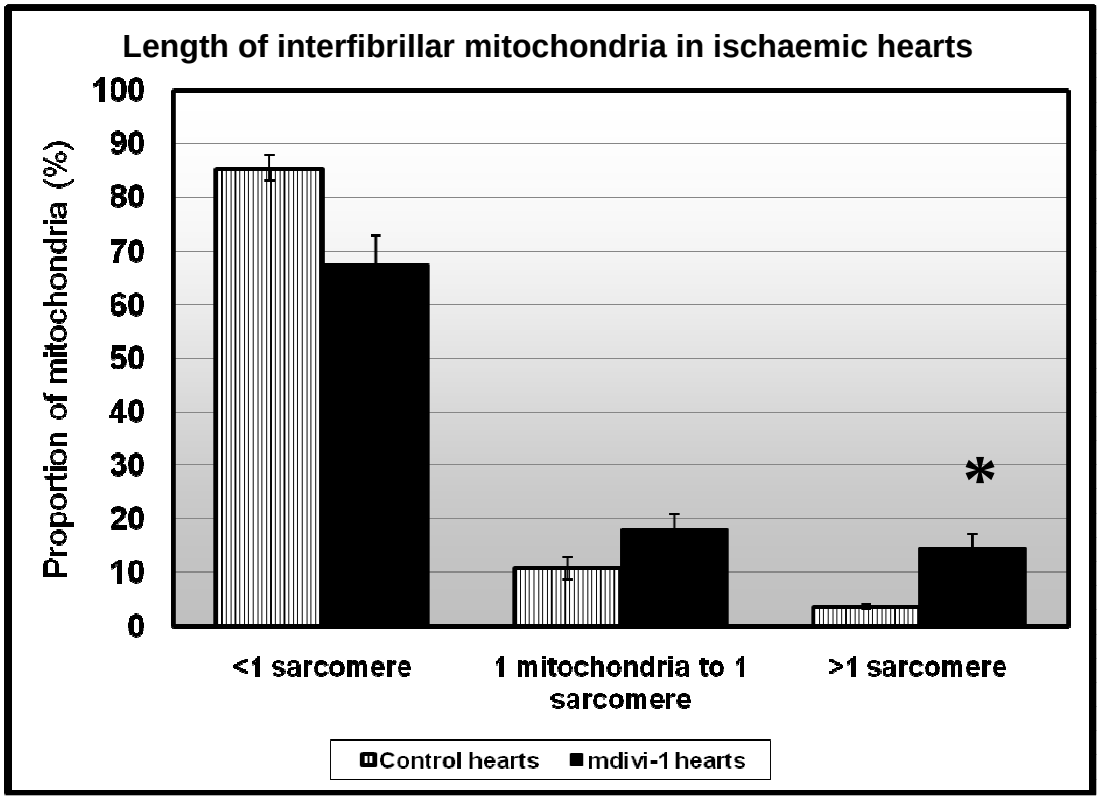

Figure 4.15: Proportion of varying lengths of interfibrillar mitochondria in ischaemic hearts. The percentages of mitochondria of lengths <1 sarcomere, equal to 1 sarcomere (1:1), or >1 sarcomere were determined by electron microscopy in hearts treated with placebo and *mdivi-1 in vivo* after ischaemia. After ischaemia, *mdivi-1* pre-treatment increased the percentage of mitochondria >1 sarcomere compared with placebo. N=4 animals per treatment group. *P<0.05.

4.8 Discussion

Modulation of mitochondrial morphology in HL-1 cells by genetic manipulation

In this section of the study, we showed that overexpression of the fusion proteins Mfn1, Mfn2 and the mutant form of the fission protein, $Drp1_{K38A}$ over a duration of 48 hours promotes mitochondrial elongation in the HL-1 cardiac cells. Conversely, hFis1 overexpression fragments the mitochondria.

Different transfection periods were tested before significant mitochondrial elongation in the cells could be observed. Overexpression for 24 hours failed to achieve significance in mitochondrial elongation, apart from Mfn2 (fusion) and hFis1 (fragmentation), compared to the significant mitochondrial elongation effects following 48 hours of overexpression. The use of mtRFP as a marker of successful transfection and overexpression of the respective plasmids in addition to illuminating the mitochondria has also been applied and verified by numerous different studies [87, 164, 165, 169, 171, 466-469] In our study, only the cells with the brightest mitochondria were selected to ensure impartiality and successful overexpression of the plasmids.

This study employed three blinded operators to determine the condition of the mitochondria in the cells in each image and categorise them as either predominantly elongated or fragmented. We initially thought of adding in another category of 'balanced state of elongation and fragmentation' but refrained from doing so because the extra category would further complicate the analysis where there will be a natural tendency to group cells into this particular category. Furthermore, this analysis method of blinded operators was previously verified by the group of Luca Scorrano in Padova, Italy where they demonstrated that this technique produces similar results to a 3D computer re-modelling of the mitochondrial structure from z-stacks.

Studies in various cell types using the mitochondrial-shaping proteins showed varying durations of overexpression to achieve significant changes in the morphology of the mitochondria. Most of the studies conducted previously showed that the cells only require approximately 24 hours to show fusion / fragmentation

under the confocal microscope [165, 169, 171, 467]. As an example, significant elongation of mitochondria was achieved after 24 hours of overexpression of OPA1 in MEFs [165]. Fragmentation of the mitochondria in MEFs by overexpression of hFis1 was also observed after 24 hours [467]. Nevertheless, the original morphology of the mitochondria plays a significant role in determining the results of manipulation where Cipolat *et al* claimed that the overexpression of OPA1, a known fusion-promoter protein may actually fragment mitochondria in HeLa cells where the mitochondria are already in an interconnected network [165]. Our study showed that 48 hours is needed for adequate expression to achieve significant mitochondrial elongation. This is possibly due to the fact that the mitochondria in HL-1 cardiac cells are quite elongated to begin with. Therefore, more time is needed until a significant change can be detected in the morphology of the mitochondria of HL-1 cells. The mitochondria in HL-1 cardiac cell line move constantly in a huge range thus increasing the time needed for neighbouring mitochondria to connect to each other to become elongated or 'spaghetti-like' or for longer mitochondria to sufficiently fragment to achieve an easily-recognisable fragmented state. Another factor will probably be the dependency of transfection and expression of plasmids on the variability in cell types. One point worth mentioning here is that expression of the vector control, RcCMV alone seem to promote mitochondrial elongation to a certain extent, though not significantly compared to cell with mtRFP alone (data not shown). In the initial set of data for 24 hours of overexpression, Mfn1 was not used as the plasmid was only prepared at a later stage in my PhD. hFis1 fragmented the mitochondria but not significantly when compared to the vector control, RcCMV. The trend led us to believe that a longer duration of overexpression was much more feasible. Having successfully shown that mitochondrial morphology in the HL-1 cardiac cell line can be manipulated using the mitochondrial-shaping proteins, we were interested to determine whether the morphology of mitochondria can also be manipulated using the pharmacological agent, *mdivi-1* which supposes prevents fragmentation of mitochondria.

Modulation of mitochondrial morphology in HL-1 cells by pharmacological manipulation

In order to effectively promote mitochondrial fusion or inhibit mitochondrial fission in adult cardiomyocytes or in an *in vivo* model, we have to employ the use of a drug because transfection of cardiomyocytes is not easily performed and viruses have to be used. Furthermore, the overexpression of a certain protein in a whole mouse is not easily achieved. We were fortunate in the sense that a new drug that inhibits mitochondrial fission, *mdivi-1* was discovered at the time this study was carried out in 2008. The *mdivi-1* drug was discovered following a screening of the yeast library by Cassidy-Stone *et al* in 2008 [418]. The mode of action for this drug was by inhibition of the fission protein Drp1. Previous studies of Cassidy-Stone *et al*., Brooks *et al.,* and Cui *et al* have shown that the drug promotes mitochondrial fusion in mammalian COS [418], rat proximal tubular cells (RPTC) [215] and neuronal cell lines [470]. However, this was not shown before in a cardiac cell line. A time and dose response was performed and we found that the dosage of 10 µM did not promote mitochondrial fusion compared to the 50 µM concentration. We also tried 100 µM accordingly but we had a problem in dissolving the drug at 100 µM. We were still able to detect crystal-like structures under the microscope using 100 µM of the drug. The 50 µM concentration correlates with the dosage used in the study of Cassidy-Stone and co-workers [418]. The study of Brooks *et al.* used 50 mg/kg *mdivi-1* in C57BL/6 mice to prevent mitochondrial fragmentation and reduce damage in renal tissue [215]. Cui *et al*., gave a treatment of 10 µM *mdivi-1* in a neuronal cell line for up to 24 hours to rescue the adverse effects of mitochondrial fragmentation [470]. The time response study carried out in this section showed an optimum duration of 40 minutes of incubation prior to confocal imaging. The different cell types used may underlie the difference in treatment durations of the various studies. We have tried extending the duration of drug incubation to 1 hour but we found that the mitochondria of the cells start to fragment, possibly due to the cold temperature in the confocal room as the experiment was carried out with the cover slips on the metal rings. A better alternative will be to conduct the experiments using the heated perfusion chamber that we have for this particular time response study.

To further verify our results, we determined the number of cells with predominantly elongated mitochondria before and after drug treatment for the stipulated duration of 40 minutes and we found that the proportion of cells with elongated mitochondria following treatment with 50 µM *mdivi-1* increased significantly compared to using the vector control alone or with 10 µM *mdivi-1*. Nevertheless, we discovered that compared to genetic interventions such as overexpression of mitochondrial fusion-promoting proteins, the mitochondrial elongation effect of the *mdivi-1* drug is slightly weaker. This is not surprising as the drug treatment is considered an *ex vivo* effect whereas the plasmids transfection goes directly into the nucleus where the proteins are expressed and acts directly on the mitochondria. Furthermore, the duration of plasmid transfection (48 hours) is longer than the drug treatment protocol (40 minutes). The concentration of the drug (50 µM) and cell type variability are also important factors to explain this phenomenon.

Modulation of mitochondrial morphology in endothelial cells by genetic manipulation

Endothelial cells were used because it serves as an alternative to adult cardiomyocytes and easier to isolate. The mitochondria in endothelial cells come in a relatively uniform network of tubular threads. The arrangement of the mitochondria in endothelial cells is similar to the HL-1 cells with the significant difference being that the cells are smaller and rounder in shape compared to the HL-1 cells.

As mentioned in the previous section, due to the highly tubular arrangement of the endothelial mitochondria, which is even more than the HL-1 cells (~70% in endothelial cells compared to ~50% in the HL-1 cells), it has proved to be quite difficult to enhance further elongation of the endothelial mitochondria by genetic manipulation. We did not detect any significant mitochondrial elongation following 48 hours of overexpression. Nevertheless, we managed to fragment the mitochondria significantly with an overexpression of the hFis1 plasmid. Compared to the mitofusins, inhibiting fragmentation with the mutant form of the fission protein, $Drp1_{K38A}$ appear to slightly increase the number of cells with elongated mitochondria, albeit not significant.

To rectify the issue of not detecting significant mitochondrial fusion in the endothelial cells, we might need to subject the endothelial cells to a brief period of simulated ischaemia to induce some mitochondrial fragmentation before determining the effects of different fusion proteins in maintaining the fused state of the mitochondria. However, this aspect will need further investigation as to the optimum duration of simulated ischaemia and the requirement of DOG.

Detecting the presence of elongated mitochondria in adult cardiomyocytes

Following the demonstration that mitochondrial elongation can be promoted in the HL-1 cardiac cell line, we aimed to investigate whether elongated mitochondria exist in the adult cardiomyocyte where the spatial arrangement of the mitochondria is totally different from a cardiac cell line. According to the studies of Shimada *et al* in 1984, the interfibrillar mitochondria are positioned along the myofibril, with the length of each mitochondria less than or approximately the length of a sarcomere (~2 µm) [471]. Nevertheless, there were also studies by Sun *et al* as early as 1969 [465] and Bakeeva *et al* in 1983 [472] where they detected mitochondria with lengths spanning to 7 sarcomeres in myocytes. Certain injury or stress such as hypoxia also causes the formation of giant mitochondria, the underlying mechanisms or function of which are unknown [473, 474]. Using electron microscopy, we detected mitochondria longer than 2 µm in the interfibrillar area, albeit we did not detect an increase in the number of interfibrillar mitochondria longer than a sarcomere in the *mdivi-1* treated hearts. The groups of Hom *et al* and Beraud *et al* have maintained the claim that mitochondria in the adult cardiomyocytes are very limited in movement and hence do not experience fusion and fission [154, 414]. Yet, the presence of mitochondrial-shaping proteins were successfully detected using Western Blots leading us to believe that fusion and fission will still occur, albeit to a lesser extent compared to a cell line [154]. The discrepancy in opinions regarding fusion and fission in myocytes lies in the fact that mathematical simulations were used in certain studies to projectile the possible outcomes of fusion and fission compared to conventional imaging techniques combined with fluorescence proteins to determine mitochondria size or length.

Investigating the effects of *mdivi-1* on mitochondria morphology in adult cardiomyocytes following ischaemia

In this section of the study, we investigated whether the *mdivi-1* drug will produce the same elongation effect as can be detected in the HL-1 cardiac cell line. We injected C57BL mice with the *mdivi-1* drug and harvested the hearts for electron microscopy. Based on the previous section, the proportion of elongated mitochondria was not significantly different from the control non-treated hearts, even with different methods of quantification. Therefore, we decided to test the same protocol, but with the presence of stress in the form of a short period of simulated ischaemia to determine the possibility that the drug may be more potent under stress. We found for the first time that the proportion of elongated interfibrillar mitochondria longer than 2 µm was significantly increased following treatment of the *mdivi-1* drug before 20 minutes of simulated ischaemia in the murine heart. This may be due to several reasons:

1) The arrangement of the mitochondria in adult myocytes is different from the cardiac cell line. Percentage of elongated mitochondria in the adult myocyte is very low and it might prove to be difficult to increase the percentage to a significant level in basal non-ischaemic hearts.
2) In the settings of adult myocytes, the mode of action of the *mdivi-1* drug may be more obvious following stress to induce mitochondrial fragmentation. We chose ischaemia as it is directly linked to IRI and ischaemia has been proven to induce mitochondrial fragmentation. With non-excessive, moderate fragmentation and disruption to the mitochondria, we were then able to detect a difference in number of elongated interfibrillar mitochondria against total interfibrillar mitochondria.
3) The combined duration of drug treatment following ischaemia (15 minutes stabilisation + 20 minutes ischaemia) is longer than the basal non-treated hearts (15 minutes stabilisation only), hence allowing more time for the drug to act.

It should be noted that even following ischaemia, the mitochondria in the inner area of the heart when ischaemia is the most severe, are too disrupted to be taken into

account in this study. We therefore, included only the mitochondria in the outer layer of the heart slices in this study. This area can be identified by the higher proportion of longitudinal mitochondria available. It would also be interesting to determine the effects of this drug on the number of elongated mitochondria in basal non-treated hearts for the whole duration of 35 minutes without ischaemia. In the settings of renal ischaemia reperfusion, Brooks *et al* showed the use of *mdivi-1* reduced IR damage to renal tissues and cellular apoptosis, albeit in a different drug treatment and IR protocol in which *mdivi-1* was administered to the C57BL/6 mice 1 hour prior to 30 minutes of ischaemia followed by 48 hours of reperfusion [215]. The proportion of mitochondria equivalent to a single sarcomere (2 µm) was increased in *mdivi-1* treated hearts following ischaemia compared to the vehicle control-treated hearts while the proportion of mitochondria less than a sarcomere was reduced in *mdivi-1* treated hearts. These two observations may provide a notion of the effects of *mdivi-1* in inhibition of fragmentation of mitochondria but the values are not significant compared to the vehicle control-treated hearts.

4.9 Conclusion

In this chapter of the thesis, we have demonstrated that mitochondrial morphology can be modulated in cardiac cells including adult cardiomyocytes, albeit to varying degrees. The arrangement of the mitochondria in the different cell types may influence the manipulation used, e.g. methodology, duration and degree of manipulation. In the next chapter, we will be exploring whether modulation of mitochondrial morphology protects the cardiac cells against simulated ischaemia-reperfusion.

Chapter Five

PROTECTING THE HEART AGAINST ISCHAEMIA-REPERFUSION INJURY BY MODULATING MITOCHONDRIAL MORPHOLOGY

5.1 Introduction

Myocardial reperfusion has long been known to generate a paradoxical situation in which early coronary artery reperfusion by thrombolysis or primary percutaneous coronary intervention (PCI) is mandatory for limiting infarct size but at the same time constitutes a detrimental stage at which most cardiac cells die [12, 16, 23-25, 49, 231, 342, 475]. The cause of reperfusion injury as an effect arising from the prolonged ischaemic period or the stimulus of reperfusion itself has been under debate [22, 342]. The state of mitochondria has been shown to impact on cell fate following IR. Multiple parameters such as levels of intramitochondrial calcium, ROS, ATP and hydrogen ions at the onset of reperfusion determine subsequent condition of the mitochondria and the host cell [31, 145, 380, 391, 400, 401, 452]. Previous studies have shown that mitochondrial fragmentation predisposes the cells to cell death, either by apoptosis or necrosis [190, 207, 209, 211, 215, 412, 476]. Fragmentation of the mitochondria can be caused by calcium overload, particularly during ischaemia when excessive calcium is transferred from the ER to the mitochondria and the calcium-sensitive phosphatase, calcineurin is activated hence promoting Drp1 translocation to the mitochondria and subsequent fragmentation of the mitochondria [189]. The site of translocation of Drp1 on the mitochondria has been identified as hFis1 [178]. Nevertheless, there have been studies demonstrating the actions of Drp1 and hFis1 to be independent of each other. Release of cytochrome *c* from the intermembrane space of the mitochondria causes cell death. In the settings of IR, the opening of the mPTP is a crucial mediator of cell death. Opening of the mPTP in the mitochondria will lead to uncoupling of oxidative phosphorylation, reversal of ATP synthase, mitochondrial swelling and release of the pro-apoptotic cytochrome *c* [35, 52, 61, 63, 88, 232, 368, 377, 409, 452, 477-479]. Therapeutic interventions aimed at reducing cell death following IR have focused on activation of the endogenous cardioprotective strategies such as the RISK pathway. Indeed, the drugs formulated such as erythropoietin (EPO) [480, 481], insulin [260, 305, 337, 482, 483] and statins [256, 261, 484, 485] have been shown to activate the RISK pathway. This cascade of pro-survival kinases (including Akt and ERK 1/2) functions to phosphorylate different downstream effectors which will culminate in the inhibition of the opening of the mPTP and prevention of release of cytochrome *c* [229, 258, 308, 482, 486]. Along the same train of thought, we aim to investigate whether promoting mitochondrial fusion or inhibiting

mitochondrial fragmentation using genetic or pharmacological manipulations can lead to enhanced cell survival in the settings of IR.

5.2 Hypothesis & Objectives

Modulation of mitochondrial morphology protects the heart against ischaemia-reperfusion injury

In the first part of the study, we investigated whether the promotion of mitochondrial fusion in the HL-1 cardiac cell line by genetic or pharmacological manipulation can protect the cells against sIR. A time response was carried out in which the HL-1 cells with an overexpression of fusion proteins or treated with the *mdivi-1* drug were subjected to different durations of simulated ischaemia and reoxygenation to determine the optimum percentage of cell death in cells over-expressing the vector control.

In the second part of the study, we tried to investigate the response of the endothelial cells over-expressing the fusion proteins towards sIR. A time response was also carried out.

We also aimed to investigate the effects of inhibiting mitochondrial fragmentation on the survival response of primary cardiomyocytes toward sIR. A previously established model of sIR in primary mouse myocytes was used for this study where *mdivi-1* as an inhibitor of the Drp1 fission protein was used to treat the cells for the whole duration of sIR.

Similarly, *mdivi-1* drug was used in the settings of sIR in an *in vivo* mouse model where the effects of inhibiting mitochondrial fragmentation was correlated with infarct size reduction as an endpoint.

5.3 Aim (1)

To determine the changes in mitochondrial morphology in HL-1 cardiac cells following sIR

Prior to determining the impact of changes in mitochondrial morphology to cell survival, we need to determine the resulting changes in mitochondrial morphology in cells subjected to simulated ischaemia-reperfusion. Using HL-1 cells as a basic model in this section, we aimed to investigate the differences in mitochondrial morphology in HL-1 cells transfected with either the empty vector control or the dominant negative form of the Drp1 fission protein, $Drp1_{K38A}$ following simulated ischaemia-reperfusion.

5.3.1 Materials

Plasmids: an empty plasmid expression vector (RcCMV); and one containing $Drp1_{K38A}$ (pcDNA3.1-HA-$_{K38A}$-DRP1), the dominant negative mutant form of the mitochondrial fission protein Drp1 [205]. $Drp1_{K38A}$ has a mutation in the GTPase domain that results in replacement of lysine 38 with alanine (designated as $Drp1_{K38A}$), disabling its ability to induce mitochondrial fission [205]. For mitochondrial morphology, a ratio of 1:2 mitochondria-targeted red fluorescent protein (mtRFP: Mitochondria-targeted dsRED) expression plasmid: plasmid of interest was included in order to permit visual assessment of mitochondrial morphology. All plasmids were from Dr Luca Scorrano (Padova, Italy). To simulate ischaemia, the cells were perfused with hypoxic ischaemic buffer specific for real-time imaging experiments (in mM: NaCl 125, KCl 8, KH_2PO_4 1.2, $MgSO_4$ 1.25, $CaCl_2$ 1.2, $NaHCO_3$ 6.25, Na-lactate 5.0, HEPES 20.0, 2-deoxyglucose 2.5, pH 6.6) equilibrated with 95% N_2–5% CO_2. Normoxic buffer specific for real-time imaging experiment (in mM: NaCl 110, KCl 4.7, KH_2PO_4 1.2, $MgSO_4$ 1.25, $CaCl_2$ 1.2, $NaHCO_3$ 25.0, glucose 15.0, HEPES 20.0, pH 7.4) equilibrated with 95% O_2-5% CO_2. 2-deoxyglucose (2-DOG) was dissolved in water to achieve a working concentration of 5 M.

5.3.2 Experimental Protocol

HL-1 cells containing predominantly (>50%) elongated mitochondria under basal conditions were identified and subjected to 120 minutes of simulated ischaemia and 30 minutes of simulated reperfusion (SIRI) with a Warner PM-2 heated perfusion chamber (Harvard Apparatus, Holliston, Mass) mounted on the confocal microscope. The real-time effects of SIRI on changes in mitochondrial morphology were determined in HL-1 cells over-expressing red fluorescent protein targeted to the mitochondrial matrix and either empty vector or $Drp1_{K38A}$. Over 3 independent experiments, 10 cells for each treatment group were analysed.

5.3.3 Results

By the end of the simulated ischaemia period, the percentage of cells displaying elongated mitochondria had fallen from 100% to 11.0 ± 11.0% in control cells and to 91.0 ± 5.6% in the $Drp1_{K38A}$-transfected cells (N=3 experiments with 7 to 10 cells per treatment group; *$P<0.05$), a difference that persisted into simulated reperfusion (see Figure 5.1 & 5.2).

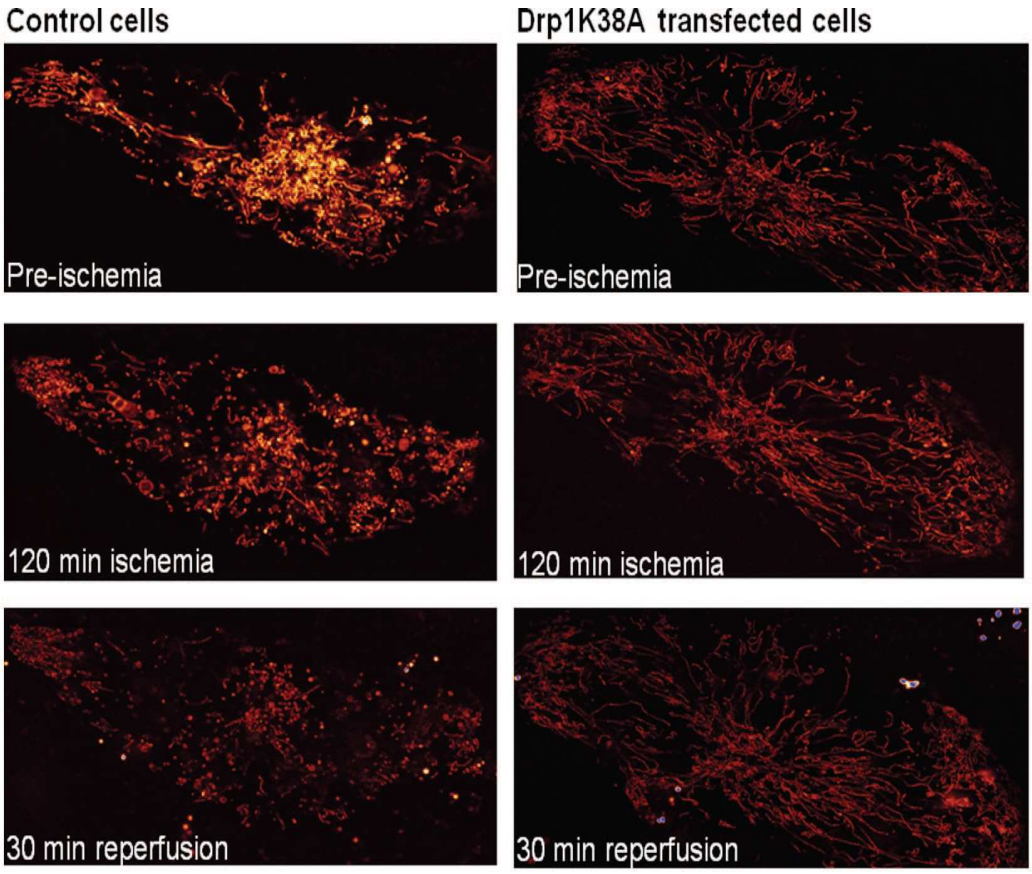

Figure 5.1: Representative confocal microscope images depicting HL-1 cells subjected to SIRI. The mitochondria in the control cell undergo fission; the mitochondria in the cell transfected with $Drp1_{K38A}$ are maintained in an elongated formation.

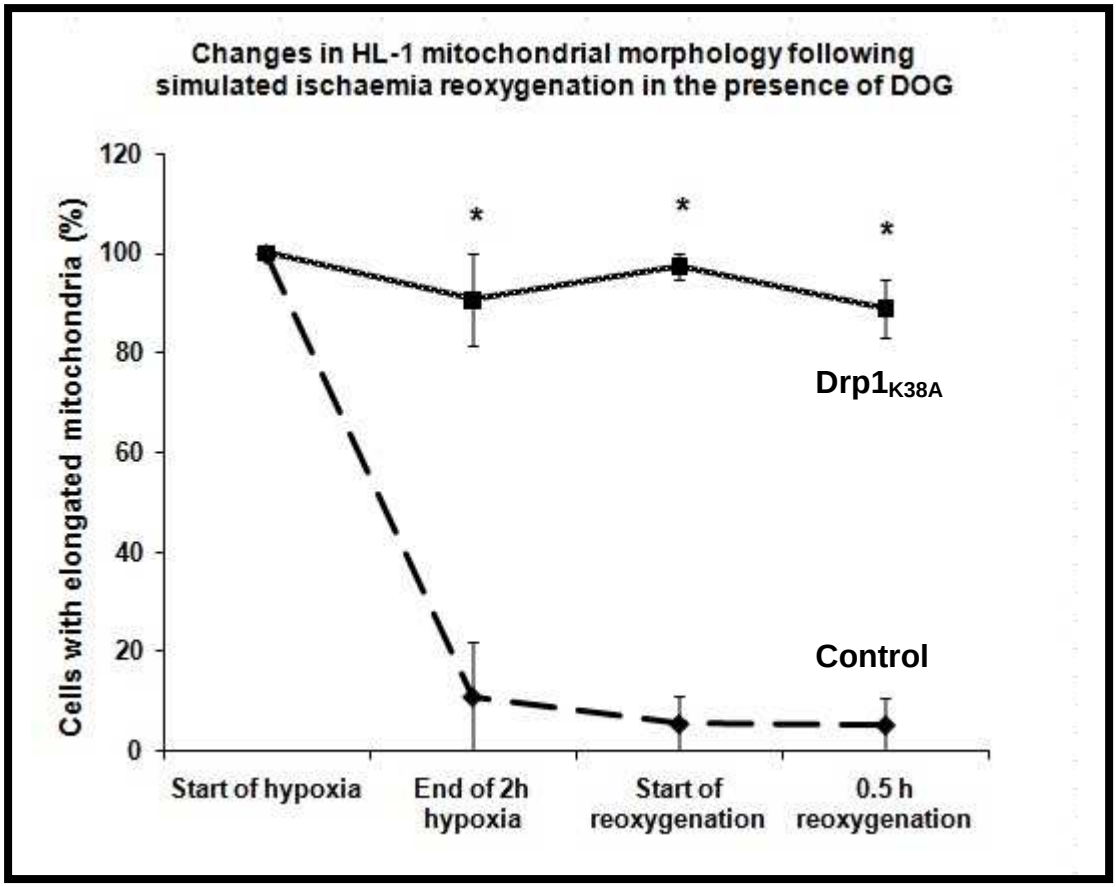

Figure 5.2: Changes in HL-1 mitochondrial morphology following sIR in the presence of 2-deoxyglucose (2-DOG). HL-1 cells containing predominantly (>50%) elongated mitochondria under basal conditions were identified and subjected to SIRI. By 2 hours of simulated ischaemia, the majority of control cells displayed fragmented mitochondria, whereas in those cells transfected with $Drp1_{K38A}$, mitochondrial fission induced by simulated ischaemia was largely prevented. N=3 experiments with 7 to 10 cells per treatment group. *P<0.05.

5.4 Aim (2)

To determine whether modulating mitochondrial morphology by genetic manipulation protects the HL-1 cells against sIR

In this section of the study, we aimed to determine whether manipulation of mitochondrial morphology in HL-1 cells protects against simulated ischaemia-reperfusion.

5.4.1 Materials

Plasmids: an empty plasmid expression vector (RcCMV); one expressing mitofusin 1(pCB6-MYC-Mfn1); one expressing mitofusin 2 (pCB6-MYC-Mfn2) [165]; one containing $Drp1_{K38A}$ (pcDNA3.1-HA-$_{K38A}$-DRP1), the dominant negative mutant form of the mitochondrial fission protein Drp1 [205]; and one containing hFis1. $Drp1_{K38A}$ has a mutation in the GTPase domain that results in replacement of lysine 38 with alanine (designated as $Drp1_{K38A}$), disabling its ability to induce mitochondrial fission [205]. For the survival assay, a ratio of 1:2 plasmid enhanced green fluorescent protein (pEGFP) (Clontech) expression plasmid: plasmid of interest was included in order to permit detection of cells with plasmids of interest. All plasmids were a generous gift of Dr Luca Scorrano (Padova, Italy). Simulated ischaemia was performed in hypoxic ischaemic buffer comprising (in mM): KH_2PO_4 1.0, $NaHCO_3$ 10.0, $MgCl_2.6H_2O$ 1.2, NaHEPES 25.0, NaCl 74.0, KCl 16, $CaCl_2$ 1.2 and NaLactate 20 at pH 6.2, bubbled with 100% nitrogen. Reoxygenationwas performed using Claycomb medium. Propidium iodide (Sigma UK) was dissolved in distilled water and added to the Claycomb medium such that the final concentration was 3 uM.

5.4.2 Experimental protocol

Next, we investigated the role of the fusion proteins in protecting the HL-1 cardiomyocytes against simulated ischaemia-reperfusion injury. My first objective

was to characterise a suitable model of simulated ischaemia-reperfusion injury given that our laboratory had not previously established such a model in HL-1 cells.

The HL-1 cells transfected with plasmids encoding for the different proteins were initially subjected to 24 hours of hypoxia followed by 1 hour reoxygenation:

1. RcCMV – empty vector (Vector Control)
2. $Drp1_{K38A}$ – the dominant negative form of the fission protein
3. Mfn1 – fusion-promoting protein
4. Mfn2 – fusion-promoting protein
5. hFis1` - fission-promoting protein

However, it was found that the hypoxia was too severe and the percentage of total cell death as determined by PI staining was too high (>90%) hence rendering the effects of the overexpressed proteins insignificant. Therefore, the hypoxia period was reduced from 24 hours to 16 hours and 12 hours followed by 1 hour reoxygenation. A cell count was performed to determine the number of dead transfected cells against live transfected cells. Dead cells transfected with the desired proteins were represented as green cells with a red spot in the nucleus while live transfected cells were green cells without any red spot (see Figure 5.3). Cell death was reduced to approximately 40% for 12 hours hypoxia followed by 1 hour reoxygenation.

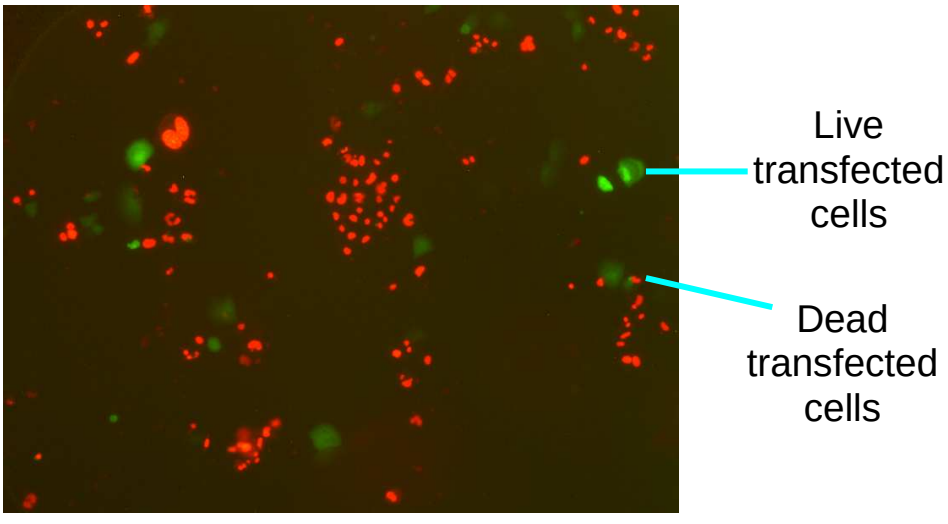

Figure 5.3: Image of cells stained using 3 µM PI under the fluorescent microscope. Following 12 hours of hypoxia and 1 hour of reoxygenation, cells were stained with PI to determine number of dead transfected cells (green + red) against live transfected cells (green).

5.4.3 Results

In cells with an overexpression of fusion proteins, 24 hours of simulated ischaemia followed by 1 hour of reoxygenation in the presence of 3 µM PI saw a cell death of 48.6 ± 3.1% in vector control, 33.8 ± 2.5% in Mfn1, 40.2 ± 2.1% in Mfn2, 42.8 ± 2.8% in $Drp1_{K38A}$ and 45.7 ± 7.2% in hFis1. In this model, Mfn1 overexpression reduced cell death significantly compared to the vector control. N=4 experiments with 80 cells per treatment group. *P<0.05 vs. control (see Figure 5.4).

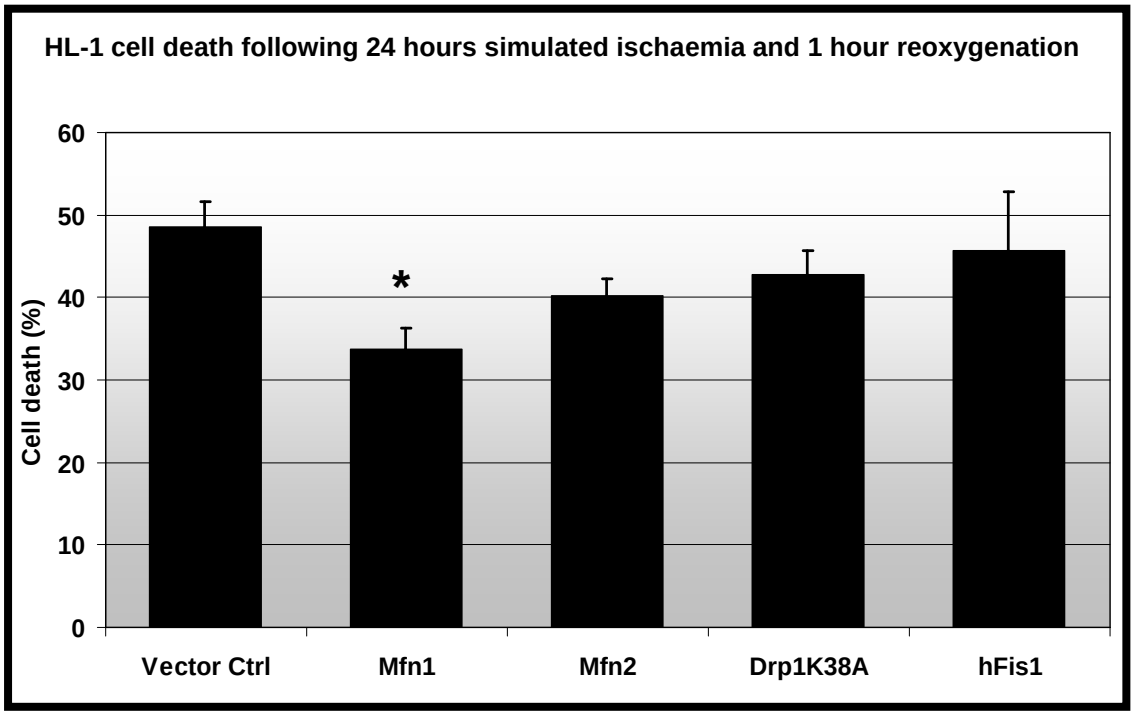

Figure 5.4: Percentage of HL-1 cell death following 24 hours simulated ischaemia and 1 hour reoxygenation. Only the overexpression of Mfn1 protects the HL-1 cells in this model. N=4 experiments with 80 cells per treatment group. *P<0.05 vs. control

Overexpression of the fusion proteins enhanced the resistance of HL-1 cells to 12 hours of simulated ischaemia followed by 1 hour reoxygenation with a reduction in cell death; Mfn1, 11.6 ± 3.0 %, Mfn2, 16.2 ± 3.9% and $Drp1_{K38A}$ 12.1 ± 2.9% vs.. 41.8 ± 4.1% for vector control, N=4 experiments with 80 cells per treatment group. *P<0.05 vs. control; †p<0.05 compared to hFis1. Overexpression of the hFis1 increases the cell death significantly to 65.5 ± 2.1% vs. 41.8 ± 4.1% for vector control; N=4 experiments with 80 cells per treatment group. *P<0.05 vs. control (see Figure 5.5).

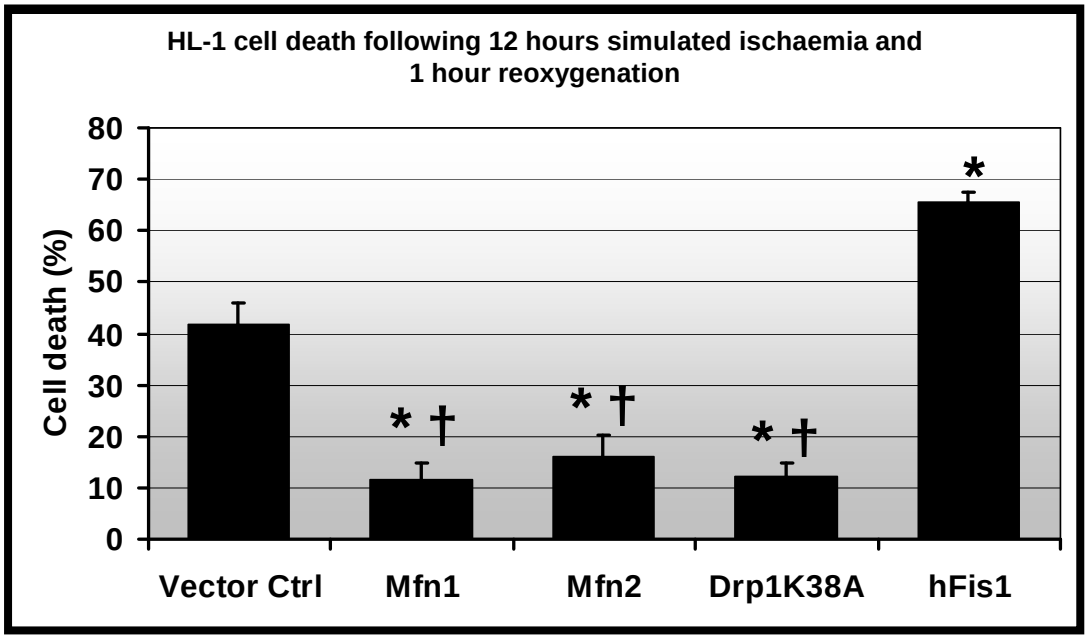

Figure 5.5: Cell death in HL-1 cells transfected with plasmids encoding for different proteins promoting mitochondrial fusion against empty vector, RcCMV following 12 hours hypoxia and 1 hour reoxygenation. Overexpression of HL-1 cells with Mfn1, Mfn2, or $Drp1_{K38A}$ decreased cell death after a period of SIRI, whereas overexpression with hFis1 increased cell death compared with control; n = 4; *p < 0.05 compared to vector control; †p<0.05 compared to hFis1.

In order to test a longer period of reoxygenation to mimic the clinical settings, cell death following 24 hours of reoxygenation was also investigated. Cell death for the vector control was lower (29.6 ± 4.2%) than the data set for 1 hour reoxygenation (41.8 ± 4.1%). Only cells with an overexpression of Mfn1 has a significant reduction of cell death (14.0 ± 2.2%; n=4; *p<0.05 compared to vector control; †p<0.05 compared to hFis1) while Mfn2 has a percentage of cell death at (19.9 ± 3.1%), $Drp1_{K38A}$ at (14.0 ± 2.8%; n=4; †p<0.05 compared to hFis1) and hFis1 at (36.0 ± 4.6%) (see Figure 5.6).

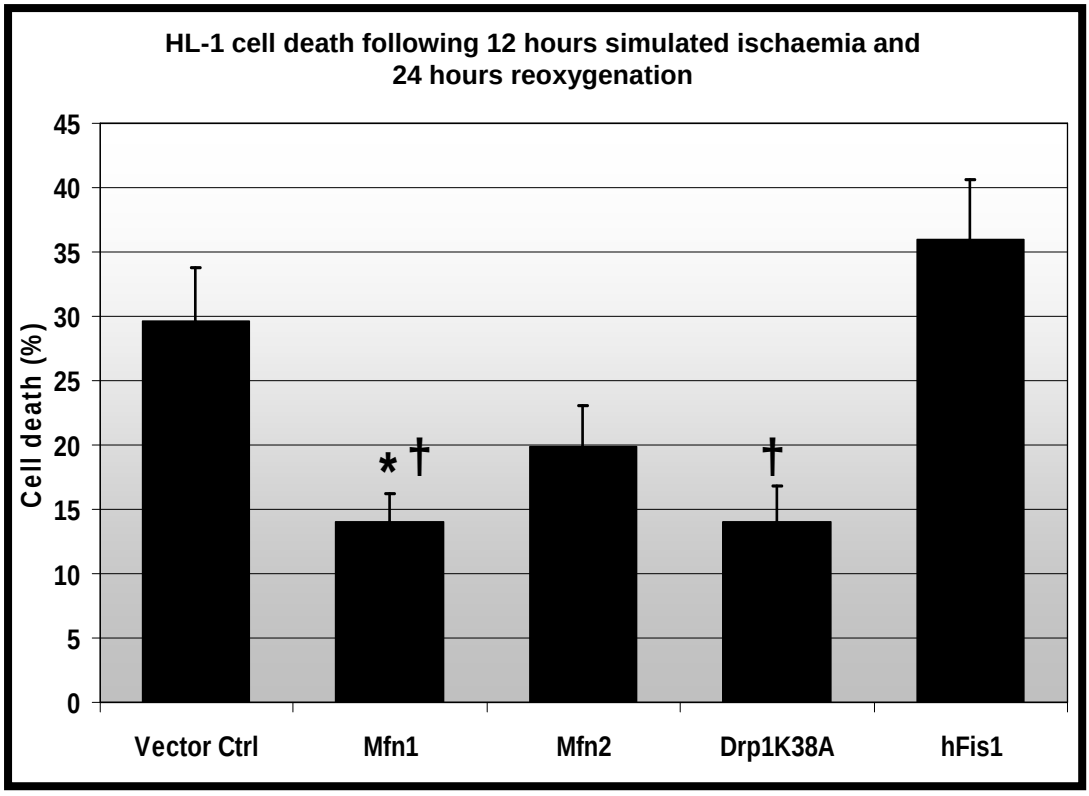

Figure 5.6: Cell death in HL-1 cells transfected with plasmids encoding for different proteins promoting mitochondrial fusion against empty vector, RcCMV following 12 hours hypoxia and 24 hour reoxygenation. Overexpression of HL-1 cells with Mfn1 decreased cell death after a period of SIRI; n = 4; *p < 0.05 compared to vector control; †p<0.05 compared to hFis1

.

5.5 Aim (3)

To determine whether modulating mitochondrial morphology by pharmacological manipulation protects the HL-1 cells against sIR

Using the small molecule inhibitor of Drp1, *mdivi-1* as a pharmacological agent to inhibit mitochondrial fission, we investigated the effects of inhibiting mitochondrial fission in HL-1 cells in protecting against simulated ischaemia-reperfusion.

5.5.1 Materials

Mdivi-1 drug was purchased from Key Organics Ltd., UK. The drug was dissolved in DMSO to achieve a working concentration of 10 mM and 50 mM and subsequently in hypoxic ischaemic buffer comprising (in mM): KH_2PO_4 1.0, $NaHCO_3$ 10.0, $MgCl_2.6H_2O$ 1.2, NaHEPES 25.0, NaCl 74.0, KCl 16, $CaCl_2$ 1.2 and NaLactate 20 at pH 6.2, bubbled with 100% nitrogen and Claycomb medium to achieve a final concentration of 10 µM and 50 µM.

5.5.2 Experimental protocol

HL-1 cells were pre-treated with either one of the following treatments: 1) vehicle control; 2) 10 µM *mdivi-1* or 3) 50 µM *mdivi-1* for 40 minutes in the 37C incubator and subjected to simulated ischaemia for 12 hours in the presence of hypoxic buffer followed by 1 hour reoxygenation with Claycomb medium. The hypoxic buffer and Claycomb medium used for reoxygenation will contain whichever treatment used prior to simulated ischaemia.

5.5.3 Results

HL-1 cells that were incubated for 40 minutes in the presence of 50 µM of *mdivi-1* followed by 12 hour hypoxia and 1 hour reoxygenation in the presence of 50 µM of *mdivi-1* have a reduced cell death (20.5 ± 3.4% vs.. 36.8 ± 5.8% for RcCMV, n = 4; $p<0.05$) (see Figure 5.7). Cells that were treated with 10 U/ml EPO for the same period of time also showed a significant reduction in cell death (17.0 ± 2.7% vs.. 43.1 ± 2.7% for cells with normal Krebs) (see Figure 5.7).

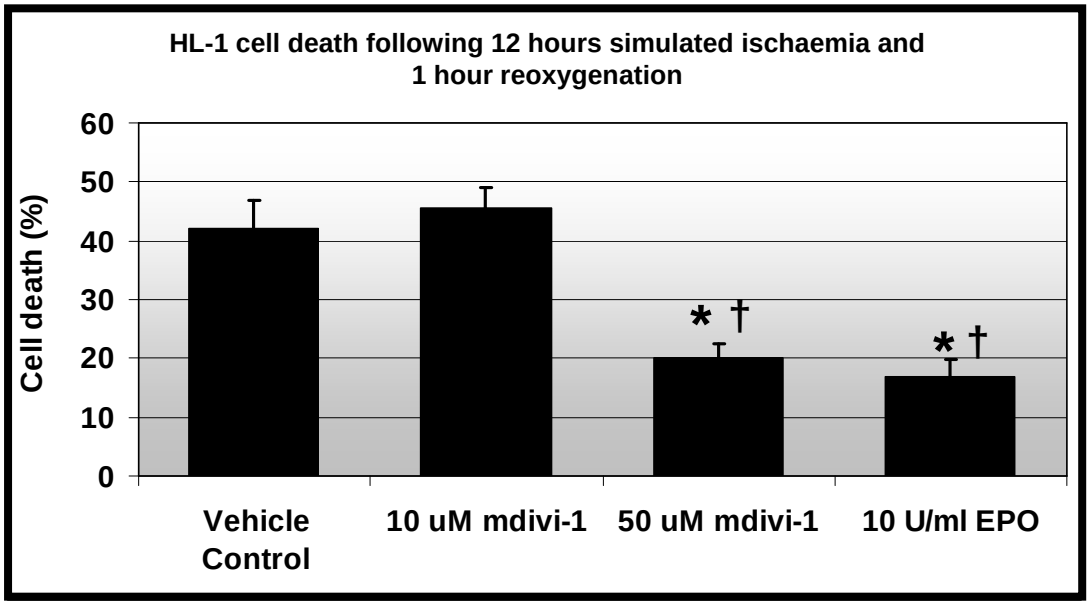

Figure 5.7: Cell death in HL-1 cells treated with different drugs following 12 hours hypoxia and 1 hour reoxygenation. Treatment with *mdivi-1* at 50 but not 10 µM for 40 minutes resulted in less cell death after SIRI. N=4 experiments with 80 cells per treatment group. *P<0.05 compared to vehicle control; †p<0.05 compared to hFis1.

5.6 Aim (4)

To determine whether modulating mitochondrial morphology by genetic manipulation protects the endothelial cells against sIR

In this section, we investigated whether manipulation of mitochondrial morphology in endothelial cells using the mitochondrial-shaping proteins protects against sIR.

5.6.1 Materials

Plasmids: an empty plasmid expression vector (RcCMV); one expressing mitofusin 1(pCB6-MYC-Mfn1); one expressing mitofusin 2 (pCB6-MYC-Mfn2) [165]; one containing $Drp1_{K38A}$ (pcDNA3.1-HA-$_{K38A}$-DRP1), the dominant negative mutant form of the mitochondrial fission protein Drp1 [205]; and one containing hFis1. $Drp1_{K38A}$ has a mutation in the GTPase domain that results in replacement of lysine 38 with alanine (designated as $Drp1_{K38A}$), disabling its ability to induce mitochondrial fission [205]. For the survival assay, a ratio of 1:2 plasmid enhanced green fluorescent protein (pEGFP) (Clontech) expression plasmid: plasmid of interest was included in order to permit detection of cells with plasmids of interest. All plasmids were a generous gift of Dr Luca Scorrano (Padova, Italy). Simulated ischaemia was performed in hypoxic ischaemic buffer comprising (in mM): KH_2PO_4 1.0, $NaHCO_3$ 10.0, $MgCl_2.6H_2O$ 1.2, NaHEPES 25.0, NaCl 74.0, KCl 16, $CaCl_2$ 1.2 and NaLactate 20 at pH 6.2, bubbled with 100% nitrogen. Reoxygenationwas performed using Claycomb medium. Propidium iodide (Sigma UK) was dissolved in distilled water and added to the Claycomb medium such that the final concentration was 3 uM. 2-deoxyglucose (2-DOG) was dissolved in water to achieve a working concentration of 5 M.

5.6.2 Experimental protocol

Next, we investigated the role of the fusion proteins in protecting the endothelial cells against simulated ischaemia-reperfusion injury. My first objective was to characterise a suitable model of simulated ischaemia-reperfusion injury given that our laboratory had not previously established such a model in endothelial cells.

The endothelial cells transfected with plasmids encoding for the different proteins were initially subjected to 24 hours of hypoxia followed by 1 hour reoxygenation:

1. RcCMV – empty vector (Vector Control)
2. $Drp1_{K38A}$ – the dominant negative form of the fission protein
3. Mfn1 – fusion-promoting protein
4. Mfn2 – fusion-promoting protein
5. hFis1 – fission-promoting protein

Following 48 hours after transfection, the cells were subjected to either one of the following IR protocols:

1. 12 hours of simulated ischaemia: 1 hour reoxygenation
2. Overnight serum starvation: 12 hours of simulated ischaemia: 1 hour reoxygenation
3. 24 hours serum starvation: 12 hours of simulated ischaemia: 1 hour reoxygenation
4. 24 hours serum starvation: 12 hours of simulated ischaemia with 2.5 mM DOG: 1 hour reoxygenation
5. 24 hours serum starvation: 12 hours of simulated ischaemia with 2.5 mM DOG: 24 hour reoxygenation

5.6.3 Results

In the model of 24 hours of serum starvation followed by 12 hours of simulated ischaemia in the presence of 2.5 mM 2-DOG and 1 hour reoxygenation, over-expression of the fusion proteins in endothelial cells reduced cell death significantly in cells with Mfn1 and Mfn2 (29.5 ± 4.2% & 28.3 ± 4.5% respectively vs. 48.5 ± 2.9% for vector control); n = 4; *p < 0.05 compared to vector control. Overexpression of hFis1did not kills the cells significantly (51.5 ± 7.4%) (see Figure 5.8).

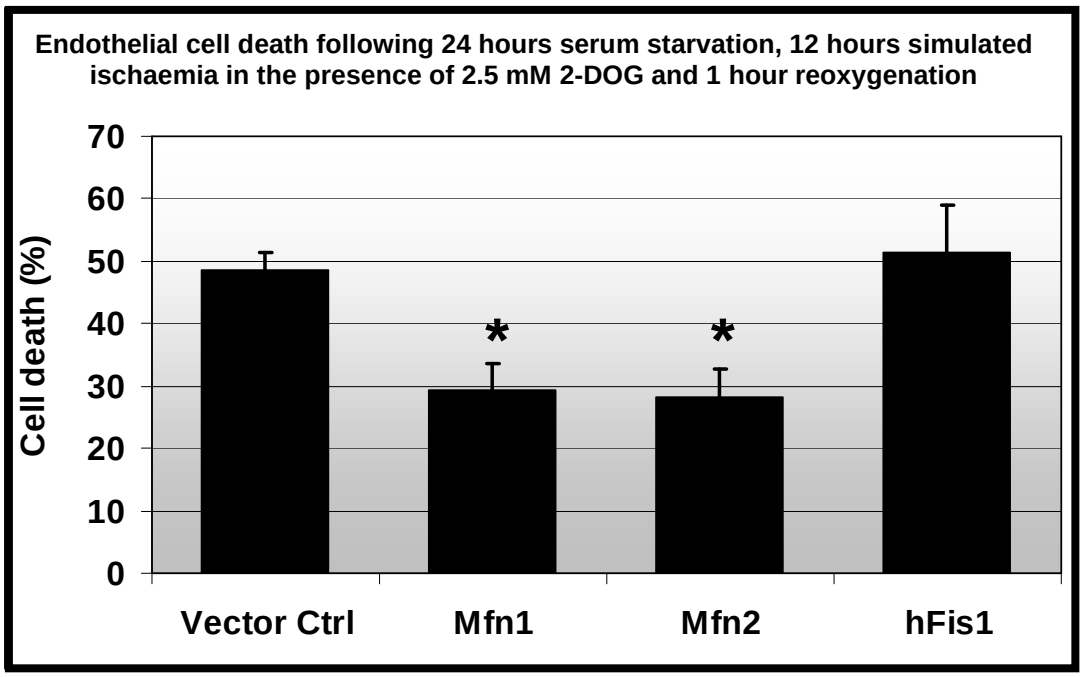

Figure 5.8: Cell death in endothelial cells transfected with plasmids encoding for different proteins promoting mitochondrial fusion against empty vector, RcCMV following 24 hours serum starvation, 12 hours simulated ischaemia in the presence of 2.5 mM 2-DOG and 1 hour reoxygenation. Overexpression of Mfn1 and Mfn2 decreased cell death after a period of SIRI; n = 4; *p < 0.05 compared to vector control.

Using a model of 24 hours of serum starvation followed by 12 hours of simulated ischaemia in the presence of 2.5 mM 2-DOG and 24 hours reoxygenation, overexpression of Mfn1 lost its cardioprotective effect (24.3 ± 2.6%) compared to vector control (34.8 ± 5.4%). Overexpression of Mfn2 still protects significantly (18.4 ± 1.8% vs. 34.8 ± 5.4% for control; n = 4; *p < 0.05) compared to vector control while cells with an overexpression of hFis1 showed a percentage of cell death at 44.4 ± 5.0% (see Figure 5.9).

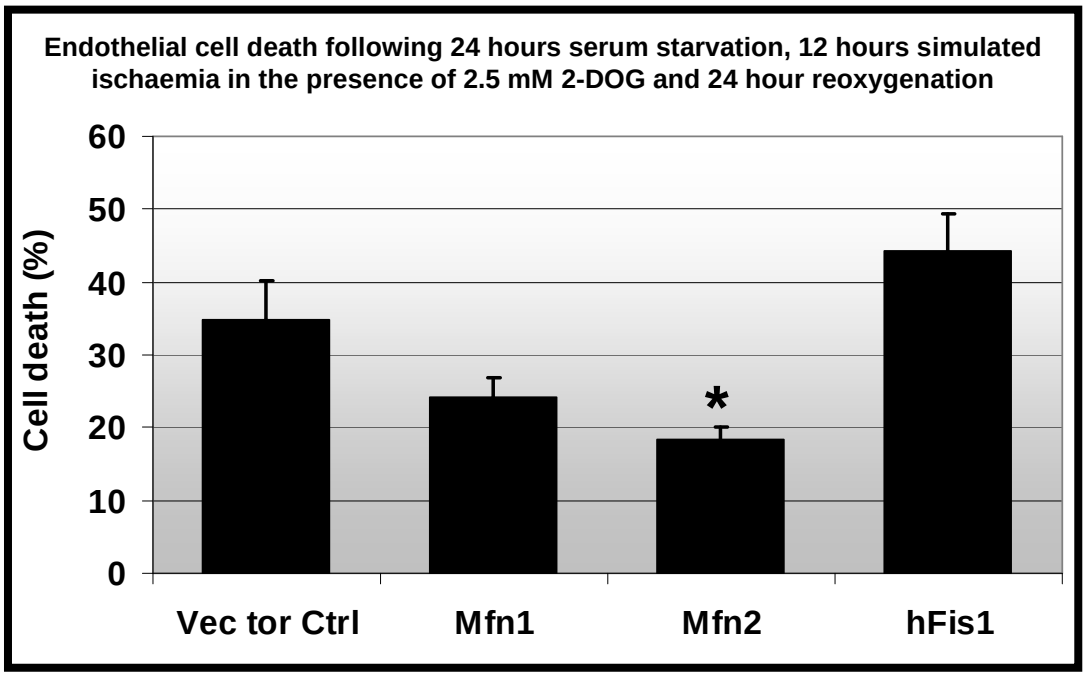

Figure 5.9: Cell death in endothelial cells transfected with plasmids encoding for different proteins promoting mitochondrial fusion against empty vector, RcCMV following 24 hours serum starvation, 12 hours simulated ischaemia in the presence of 2.5 mM 2-DOG and 24 hour reoxygenation. Overexpression of Mfn2 decreased cell death after a period of SIRI; n = 4; *p < 0.05 compared to vector control.

5.7 Aim (5)

To determine whether modulating mitochondrial morphology by pharmacological manipulation protects adult cardiomyocytes against sIR

In this section, we investigated whether inhibiting mitochondrial fission in adult cardiomyocytes, using *mdivi-1* as a pharmacological Drp1 inhibitor, protects adult cardiomyocytes against sIR.

5.7.1 Materials

Mdivi-1 drug was purchased from Key Organics Ltd., UK. The drug was dissolved in DMSO to achieve a working concentration of 10 mM and 50 mM and subsequently in hypoxic ischaemic buffer comprising (in mM): KH_2PO_4 1.0, $NaHCO_3$ 10.0, $MgCl_2.6H_2O$ 1.2, NaHEPES 25.0, NaCl 74.0, KCl 16, $CaCl_2$ 1.2 and NaLactate 20 at pH 6.2, bubbled with 100% nitrogen and cardiomyocyte growth medium (M199 buffer: BSA 2 mg/ml, creatine 5 mM, taurine 5 mM, carnitine hydrochloride 1.6 mM, Pencillin-Streptomycin 1%) to achieve a final concentration of 10 µM and 50 µM.

5.7.2 Experimental protocol

Ventricular cardiomyocytes were isolated from adult C57BL/6 male mice by perfusion and digestion of ventricles with collagenase, according to a previously described method [487]. The cells were then randomised to receive pre-treatment with either vehicle control or *mdivi-1* treatment at either 10µM or 50µM (N>250 cells per experiment for 4 experiments), before being subjected to 45 minutes of simulated ischaemia followed by 30 minutes of simulated reperfusion, at the end of which cell death was measured by propidium iodide staining [487].

5.7.3 Results

In this specific model of 45 minutes simulated ischaemia against 30 minutes reoxygenation, myocytes treated with 50 µM *mdivi-1* throughout the whole duration of sIR have a significantly reduced percentage of cell death (33.7 ± 1.9% vs. 46.0 ± 1.1% for vehicle control; N=4experiments with 20 cells per treatment group; *P<0.05). Myocytes treated with 10 µM *mdivi-1* showed a percentage of cell death at 48.2 ± 3.2% while treatment with insulin reduces the percentage of myocytes cell death significantly to 25.9 ± 3.3% ; N=4 experiments with 20 cells per treatment group; *P<0.05 (see Figure 5.10).

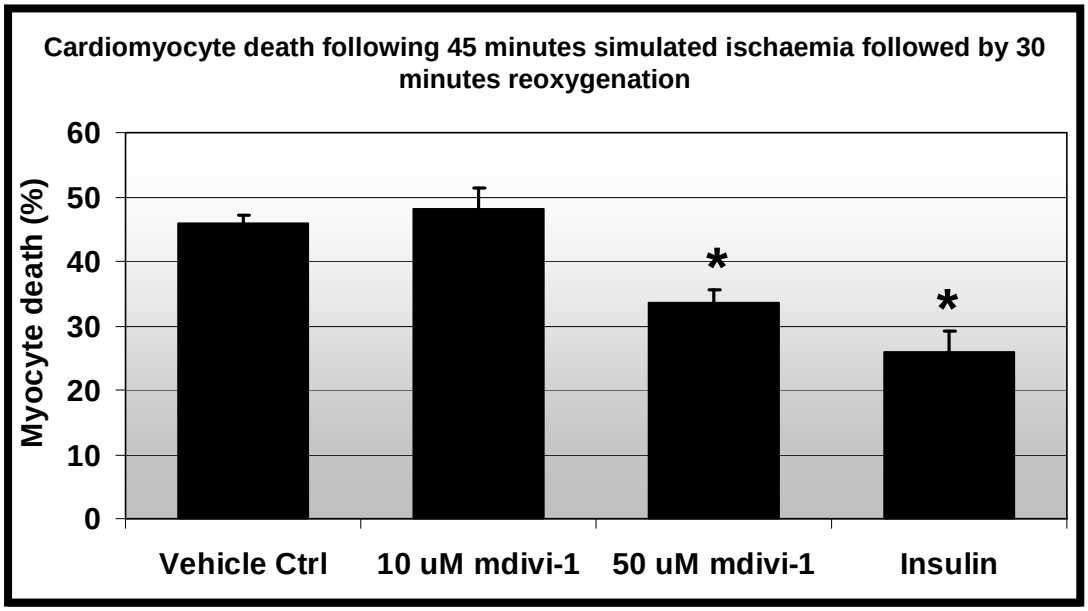

Figure 5.10. Cardiomyocyte death following 45 minutes simulated ischaemia and 30 minutes reoxygenation. Pre-treatment of adult rat cardiomyocytes with EPO or *mdivi-1* at 50 but not 10 mol/L reduced cell death after an episode of SIRI. N=4 experiments with 20 cells per treatment group. *P<0.05.

5.8 Aim (6)

To determine whether modulating mitochondrial morphology by pharmacological manipulation reduces infarct size in the *in vivo* murine model of IR

In this section, we investigated whether the pro-survival effects of *mdivi-1* by inhibition of mitochondrial fragmentation in adult cardiomyocytes can be extrapolated to the settings of the *in vivo* animal model of IR.

5.8.1 Materials

Mdivi-1 drug was purchased from Key Organics Ltd., UK. The drug was dissolved in DMSO to achieve a working concentration of 10 mM and 50 mM and subsequently in saline to achieve a final concentration of 10 µM and 50 µM

5.8.2 Experimental protocol

Mice were randomly assigned to receive by intravenous injection either vehicle control (0.1 mL of 0.1% dimethyl sulfoxide) or *mdivi-1* (at either 0.24 or 1.2 mg/kg, doses that were equivalent to the ex vivo concentrations of 10 and 50 µmol/L, respectively) 15 minutes before myocardial ischaemia (n=6 mice per treatment group).

5.8.3 Results

There were no significant differences in mean arterial blood pressure or heart rate over left ventricular volume with *mdivi-1* treatment in the *in vivo* murine heart compared with control (see Figure 5.11).

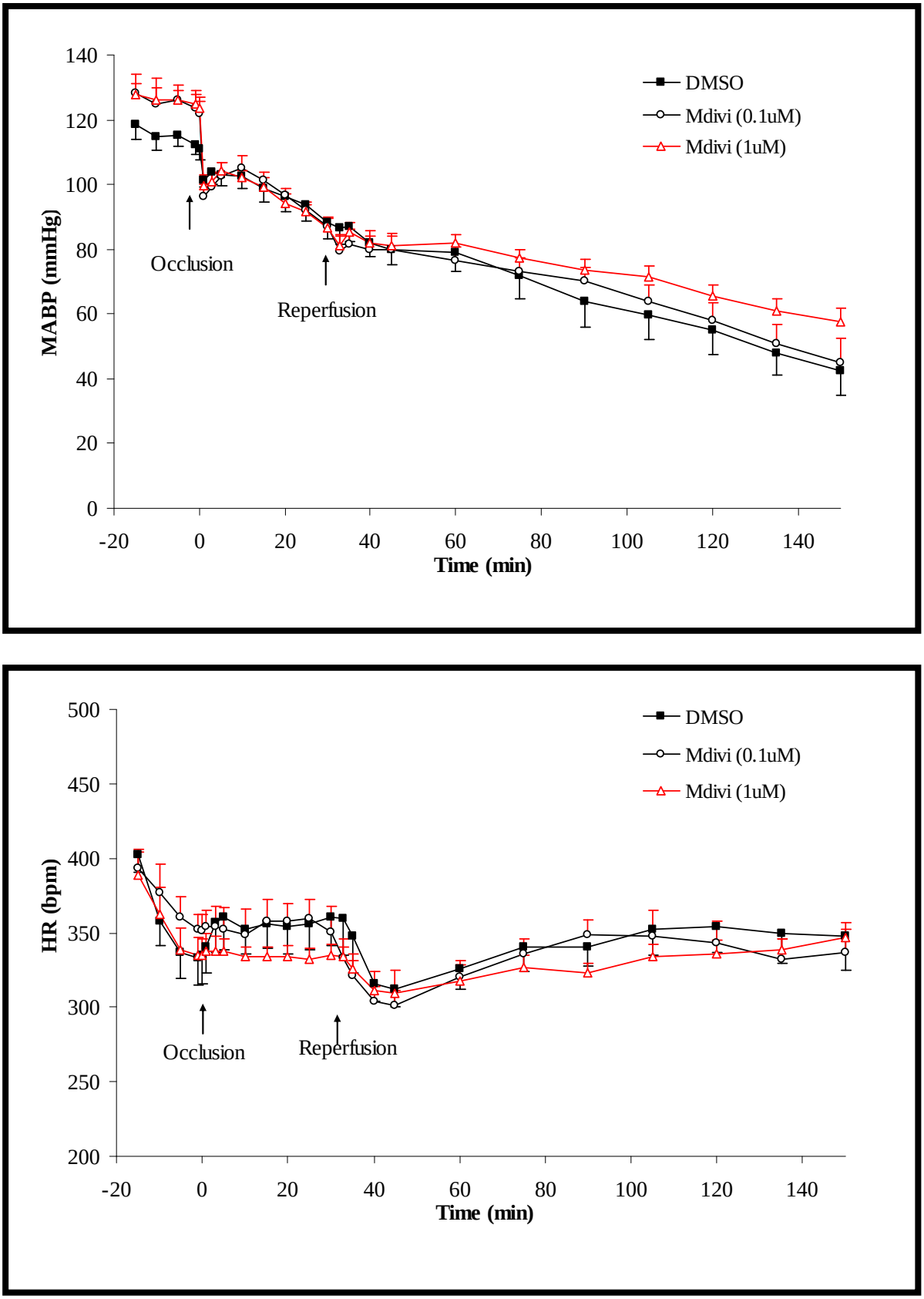

Figure 5.11: Mean arterial blood pressure (MABP) and Heart Rate (HR) for the mice.

Area-at-risk for the mice injected with the vehicle control, 10 µM *mdivi-1* and 50 µM *mdivi-1* are 53.6 ± 5.6%, 55.8 ± 3.9% and 54.5 ± 6.5% respectively (see Figure 5.12) .

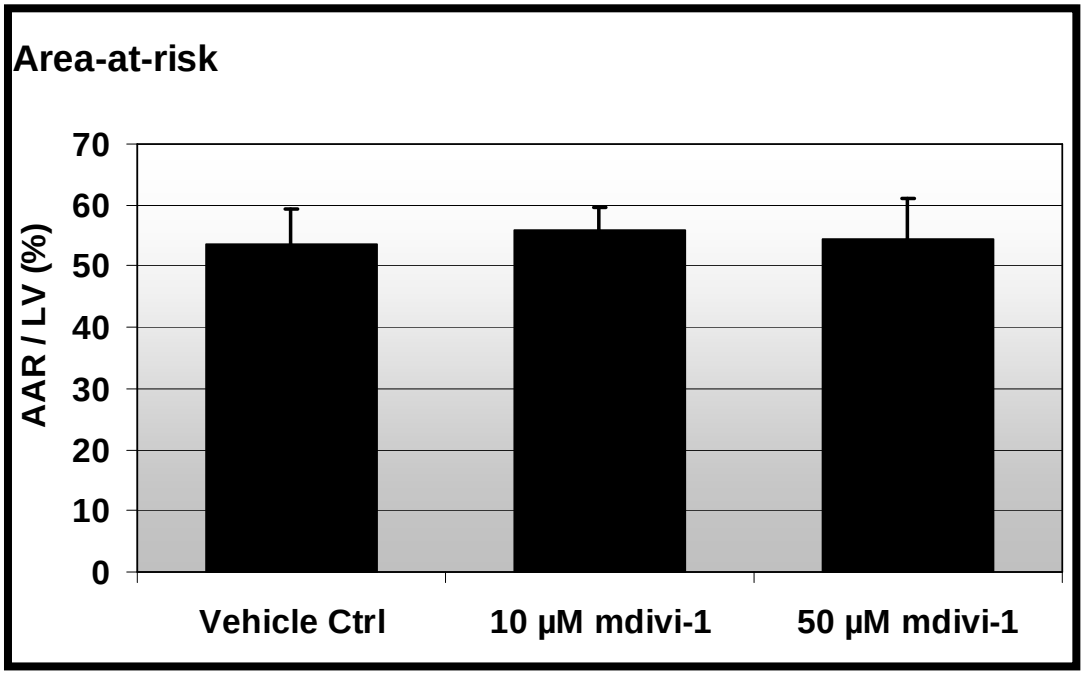

Figure 5.12: Area at risk over left ventricular volume with *mdivi-1* treatment in the *in vivo* murine heart compared with control.

Infarct sizes measured by TTC staining following sIR (see Figure 5.13) were recorded at 48.5 ± 4.5% for vehicle control, 41.9 ± 4.9% for 10 µM *mdivi-1* and a significant reduction to 21.0 ± 2.2% for 50 µM *mdivi-1;* N=6 animals per treatment group. *P<0.05 (see Figure 5.14).

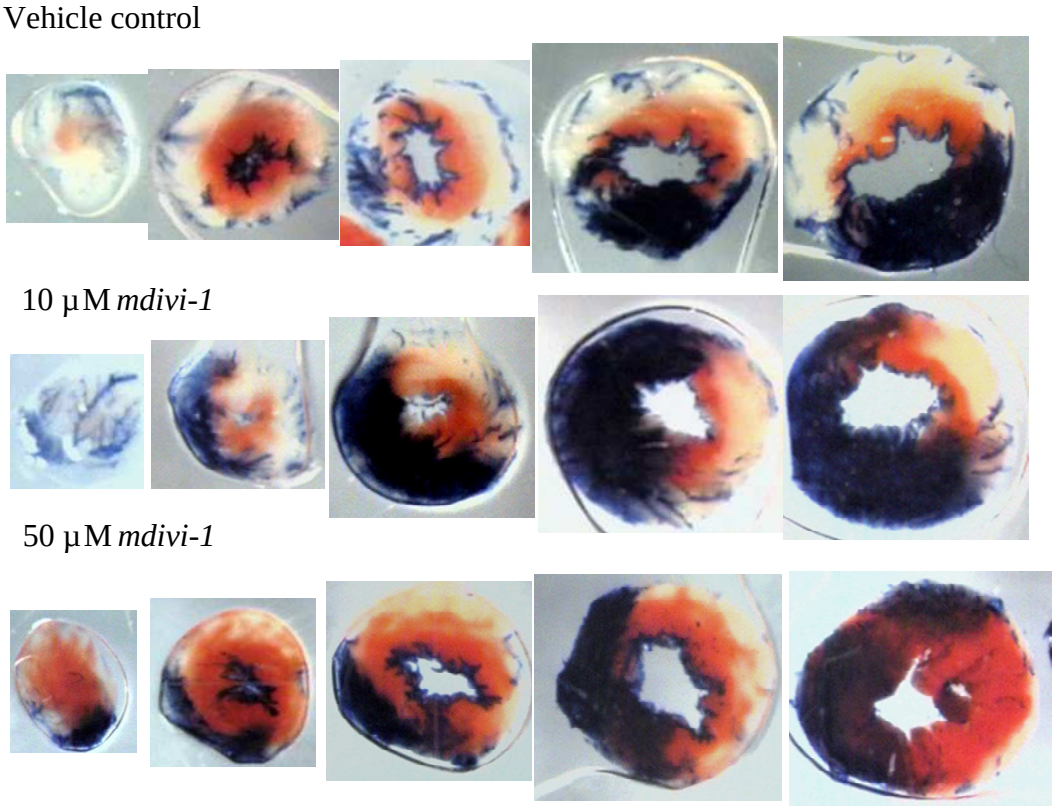

Figure 5.13: Representative transverse slices of hearts treated with control and *mdivi-1* at the 2 doses. The Evan blue area depicts the non-risk zone; tetrazolium-stained area, area at risk; and white area, area of infarction. N=6 animals per treatment group. *P<0.05.

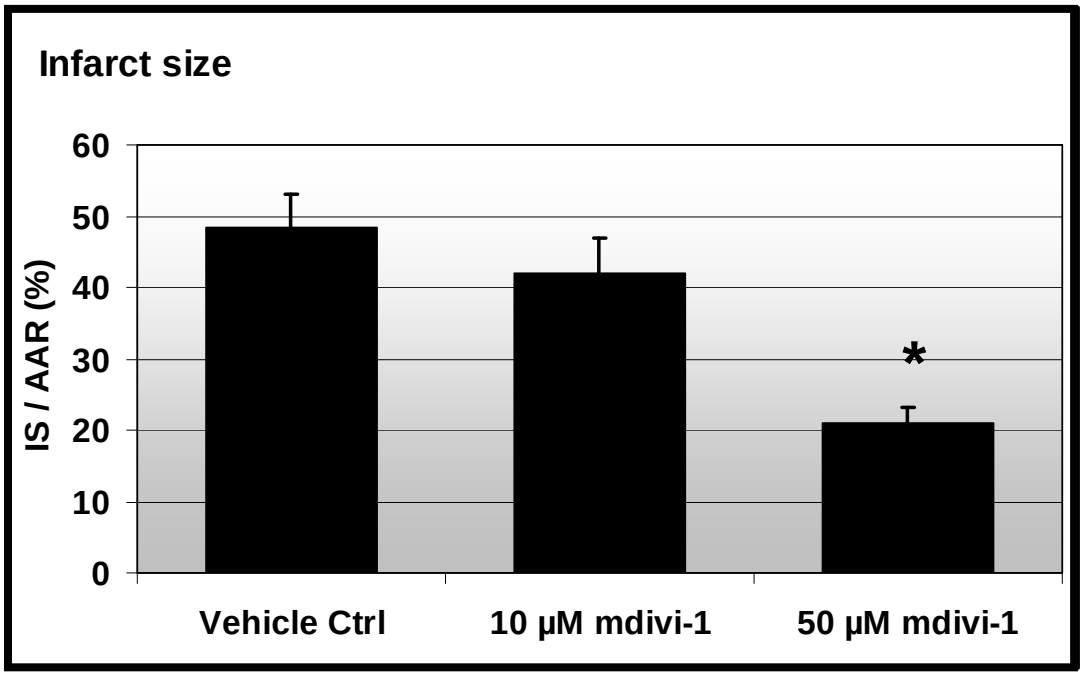

Figure 5.14: Pre-treatment with *mdivi-1* at dose 2 (1.2 mg/kg IV) but not dose 1 (0.24 mg/kg IV) resulted in a significant reduction in myocardial infarct size in the in vivo murine heart. N=6 animals per treatment group. *P<0.05

5.9 Discussion

Effects of sIR on mitochondrial morphology in HL- 1 cells

As shown in this section of the study, 120 minutes of simulated ischaemia fragments the mitochondria of the cells transfected with the empty vector, RcCMV. Cells with an overexpression of the mutant form of the fission protein $Drp1_{K38A}$ however, maintained the fused state of the mitochondria throughout the whole duration of sIR. This result is in line with the phenomenon observed in the study of Brady *et al* in 2006 [488].

This section is of utmost importance as it shows that ischaemia distorts the proper mitochondrial morphology by fragmenting the mitochondria. A previous study by Chen and co-workers in 2009 showed a decrease in OPA1 levels in the settings of heart failure [211]. Following ischaemia, fragmentation of the mitochondria will lead to depolarisation of mitochondrial membrane potential, uncoupling of oxidative phosphorylation and subsequent cell death [160, 207, 417, 489, 490]. For the HL-1

cells, manipulation of mitochondrial morphology can only be carried out and is deemed feasible if the balance of morphology was tilted to one end of the extreme initially.

The duration of simulated ischaemia was also based on the study by Brady *et al* in 2006 [488]. A shorter duration of hypoxia was necessary to track the changes of morphology of mitochondria. The heated perfusion chamber was used as monitoring of mitochondrial morphology in this study was performed 'real-time'. DOG was used to inhibit glycolysis as the cells will revert to glycolysis during a short period of ischaemia. The revertion to glycolysis may enable the cells to maintain normal mitochondrial morphology although this has yet to be proven.

Ischaemia causes fragmentation of the mitochondria probably due to the increase in calcium levels in the mitochondria hence activating the calcium-sensitive phosphatase, calcineurin leading to dephosphorylation and subsequent activation of Drp1 [189]. The activation of Drp1 causes translocation of the protein to the mitochondria to perform fragmenting function. Overexpression of $Drp1_{K38A}$, the mutant form of the fission protein inhibits the function of the endogenous Drp1, by preventing its translocation and hence impairing the mitochondrial fragmenting function of Drp1.

Protecting the HL-1 cells against sIR by modulation of mitochondrial morphology via genetic manipulation

Studies conducted previously have shown that mitochondrial fission precedes cell death in different cell lines caused by various stimuli [408, 491-493]. In our study, we demonstrated that the overexpression of the fusion proteins in HL-1 cardiac cells over a period of 48 hours renders the cells more resistant to 12 hours simulated ischaemia and 1 hour reoxygenation. Conversely, overexpression of the fragmentation-promoting protein, hFis1 renders the cells more susceptible to sIRI. In order to simulate a more relevant clinical setting of a longer period of reoxygenation to a shorter period of ischaemia, we employed the protocol of 24 hours reoxygenation to 12 hours of ischaemia. The 12 hours of simulated ischaemia was

kept constant in both of the protocols because the onset of reoxygenation is when the mitochondrial permeability transition pore (mPTP) starts to open leading to necrotic cell death and therefore, the reoxygenation period is the main injury source. In the 24 hour reoxygenation protocol, the cardioprotective effect was lost for Mfn2 while hFis1 also does not appear to render the cells more susceptible to sIRI. A possible explanation is that following the long period of reoxygenation, the dead cells will have floated off, and we would have under-estimated the percentage of cell death, as can be seen from the ~30% cell death in cells with an overexpression of vector control, RcCMV. Mfn1 still produces significant reduction in cell death in this 24 hour reoxygenation model but we also lost the protection for $Drp1_{K38A}$. The overexpression of hFis1 in this case also did not kill the cells significantly but it should be noted that the percentage of cell death was recorded at ~35% compared to ~65% in the 1 hour reoxygenation model, once again highlighting the possibility that there is an underestimation of cell death. Due to the fact that the dead cells may actually float off following a long period of reoxygenation and possible underestimation of cell death, we decided to use the 12 hours simulated ischaemia followed by 1 hour reoxygenation model for the survival assay.

Protecting the HL-1 cells against sIR by modulation of mitochondrial morphology via pharmacological manipulation

In this section of the study, we demonstrated that pre-treatment of HL1 cardiac cell line with 50 µM of *mdivi-1* prior to simulated ischaemia for 12 hours and 1 hour of reoxygenation in the presence of the same concentration of drug protects the cells against simulated ischaemia-reperfusion injury. Brooks *et al* have shown that using the same dose of drug, they managed to reduce IR-induced tubular damage to renal cortical and outer medulla tissues as well as prevent apoptosis [215]. Different studies using different types of cardioprotective drugs have varied protocols. Some of the studies used the drugs throughout the whole duration of IR with a specific pre-treatment period [494], while there also exist studies where the drugs were administered at the onset of reperfusion [487, 495]. The deciding factor of when to apply the drug depends on the endpoint of the study; whether to test the efficacy of the drug in reducing infarct size, the efficacy of the drug at the onset of reperfusion or reducing injury caused by ischaemia. In our study, the drug was administered throughout the

whole duration of simulated ischaemia and reperfusion to mimic the clinical settings where the drug would have been present throughout surgery and reperfusion. The cardioprotection conferred is probably dependent on the mitochondrial elongation property of the drug, similar to overexpression of mitochondrial fusion-promoting proteins.

Protecting the endothelial cells against sIR by modulation of mitochondrial morphology via genetic manipulation

Using the survival assay generated for HL-1 cardiac cells as a basic model, we attempted to test this model on endothelial cells using the mitofusins to promote mitochondrial fusion and hFis1 to induce fragmentation. Upon embarking on this model, we found that the endothelial cells were extremely hardy toward sIR. We tried several protocols until we finalised on 24 hours of serum starvation followed by 12 hours of simulated ischaemia in the presence of 2.5 mM 2-DOG and 1 hour reoxygenation to achieve approximately 50% of cell death in cells with vector control. DOG was used to inhibit glycolysis which will be initiated during simulated ischaemia. In the model of 24 hours of serum starvation followed by 12 hours of simulated ischaemia in the presence of 2.5 mM DOG and 1 hour reoxygenation, cardioprotection was elicited by the overexpression of the mitofusins. Nevertheless, we did not manage to detect a significant cell death in response to hFis1 overexpression. It is certainly strange to see significant mitochondrial fragmentation with the overexpression of hFis1 in endothelial cells yet failed to detect a significant percentage of cell death following sIR but we should bear in mind that mitochondrial fragmentation pre-disposes the cells to the death pathway but do not definitely lead to cell death. This may hold true for the endothelial cells which are hardy enough to withstand mitochondrial fragmentation in the settings of sIR hence producing a percentage of cell death which was similar to the cells transfected with the vector control alone.

We then investigated a longer period of reoxygenation where the model of 24 hours of serum starvation followed by 12 hours of simulated ischaemia in the presence of

2.5 mM DOG and 24 hours reoxygenation was used. In this model, we lost the cardioprotection by Mfn1 while Mfn2 still protects the cells. We noticed a similar trend to the HL-1 cells in which a long period of reoxygenation leads to an underestimation of cell death.

Protecting the adult cardiomyocytes against sIR by modulation of mitochondrial morphology via pharmacological manipulation

In this part of the study, we determined the cardioprotective effects of the *mdivi-1* drug in adult myocytes. The 45 minutes simulated ischaemia followed by 30 minutes reoxygenation was established by Lim *et al* in 2008 [487]. In this study, only the rod-shaped non-PI stained cardiomyocytes were defined as alive. Cells undergoing hypercontracture were not taken into account. We found that the usage of 10 µM *mdivi-1* drug doesn't protects the cardiomyocytes against sIR in agreement with our previous findings that 10 µM was not the optimum concentration. Only 50 µM showed protection against sIR as this was the optimum concentration to inhibit Drp1 and subsequent mitochondrial fragmentation.

From the results of the previous section, we postulate that the *mdivi-1* drug inhibits mitochondrial fission in the HL-1 cardiac cell line thus increasing the proportion of cells with elongated mitochondria, increases the number of elongated interfibrillar mitochondria in the heart cell, delays the opening of the mPTP in cardiomyocytes following sIR and protects cardiomyocytes against sIR. Our next objective is to determine whether *mdivi-1* reduces the infarct size in a murine model following sIR.

Infarct size reduction in an in vivo murine infarct model by modulation of mitochondrial morphology in the heart

The results obtained show that application of the *mdivi-1* drug at stabilisation for 15 minutes followed by 30 minutes of ischaemia and 120 minutes of reperfusion reduces myocardial injury as can be seen from the reduction in infarct size after TTC staining. The selected protocol was established from the study of Lim *et al* in 2007 [496]. Various types of drugs have been used to demonstrate the cardioprotective

effects using this model; e.g.visfatin [487], rimonobant [497], apelin [498], necrostatin [499]. Selection of C57BL mice was fixed at male mice at the age of 9 – 12 weeks old to standardise the subjects. Male mice were chosen because there have been previous claims of cardioprotective effects of oestrogen in female mice [500, 501]. Compared to 50 µM of *mdivi-1*, 10 µM of *mdivi-1* did not reduced infarct size significantly. This is the first study showing the cardioprotective effects of *mdivi-1* in an *in vivo* setting. Based on the results obtained, we can conclude that the mitochondrial fragmentation inhibiting capability of the *mdivi-1* drug may provide beneficial cardioprotective effects and this effect may be linked to inhibition of mPTP opening

5.10 Conclusion

In this chapter of the thesis, we have demonstrated that modulating mitochondrial morphology by tilting the equilibrium towards a more fused state protects the cardiac cells against sIR. In the next chapter, we will be exploring whether this protective effect is elicited via delaying the opening of the mPTP, a crucial mediator of cell death following sIR.

Chapter Six

MODULATING MITOCHONDRIAL MORPHOLOGY IN THE HEART DELAYS THE OPENING OF THE MITOCHONDRIAL PERMEABLILITY TRANSITION PORE (MPTP)

6.1 Introduction

In the previous chapter, it was demonstrated that modulating mitochondrial morphology in cardiac cells by tilting the balance towards a more fused state protects the cells against ischaemia-reperfusion injury. Previous studies have shown that the cardioprotection elicited by various interventions, particularly IPC and IPost mainly lies in the inhibition of the mPTP opening at the onset of reperfusion [17, 52, 67, 235, 236, 238, 306, 374, 502-508]. In this chapter, the potential role of mitochondrial fusion in delaying the opening of the mPTP was examined to determine whether the cardioprotection conferred by modulation of mitochondrial morphology was linked to delaying of mPTP opening.

Interestingly, the link between mitochondrial morphology and mPTP has never been thoroughly investigated before this, although it has been speculated that these two phenomena may be interrelated. It is well-known that following ischaemia-reperfusion, the function of cardiac myocytes becomes compromised and this is due to mitochondrial damage as a result of calcium overloading [29, 33, 34, 55, 143, 145, 363, 364, 384, 400, 401, 452, 509], elevated ROS levels [23, 31, 32, 35, 62, 137, 408, 457, 510], leading to mPTP opening and subsequent uncoupling of oxidative phosphorylation and release of cytochrome *c* [61, 63, 111, 367, 382, 396, 401, 403, 452, 457, 477]. These factors have been shown to be modified (e.g. reduction of Ca^{2+}, ROS and ATP hydrolysis) by cardioprotective strategies such as IPC induced by ischaemia [17, 49, 52, 234-236, 249, 258, 503, 504, 506, 511], IPost [67, 68, 230, 242, 243, 246, 247, 258, 351, 475, 508] or opening of the mitoK_{ATP} channel [8, 221, 222, 246, 451].

Therefore, protecting the heart against myocardial reperfusion injury can be mediated by attenuation of mitochondrial Ca^{2+} overloading, reduction of ROS levels and preservation of mitochondrial energy production by maintenance of the respiratory chain. These factors, combined prevent the opening of the mPTP at the onset of reperfusion. In this section of the study, we wanted to investigate whether making the mitochondria longer by promoting fusion or inhibiting fragmentation protects the heart by inhibiting the opening of the mPTP as we believe that a longer mitochondria may be more robust and can withstand a higher threshold of Ca^{2+} overloading, ROS while maintaining a competent respiratory chain following IR.

6.2 Hypothesis

Modulating mitochondrial morphology in the heart delays the opening of the mPTP

The first part of the study (section 6.3) was to determine whether promotion of mitochondrial fusion by overexpression of fusion-promoting proteins in HL-1 cells delays the opening of the mPTP using a confocal laser-induced ROS model. The use of CsA serves as an indicator that the mPTP is indeed targeted in this study as CsA binds to the CypD component of the mPTP to inhibit its opening. $Drp1_{K38A}$ serves to verify that it is indeed mitochondrial fusion that is conferring the effects, and eradicating the effects of the presence of the proteins alone.

In the second part of the study (section 6.4), we aimed to investigate whether pharmacological manipulation of the mitochondrial morphology also delays the opening of the mPTP in HL-1 cells. Due to the fact that *mdivi-1* requires a period of pre-treatment to modulate mitochondrial morphology, we pre-treated the cells and subjected them to confocal laser irradiation in the presence of *mdivi-1* to maintain its pharmacological effects.

In section 6.5, similar to the previous sections, we were interested to investigate whether genetic manipulation of mitochondrial morphology in endothelial cells similarly delays mPTP opening.

In the final section of this chapter (section 6.6), we investigated whether pharmacologically inhibiting mitochondrial fragmentation by the use of *mdivi-1* delays the opening of the mPTP in a simulated ischaemia-reperfusion model of mPTP opening.

6.3 Aim (1)

To determine whether modulation of mitochondrial morphology via genetic manipulation delays the opening of the mPTP in HL-1 cardiac cells

Having demonstrated in the previous section that mitochondrial fusion is cardioprotective, we aimed to investigate whether this protection is elicited through the inhibition of mPTP opening. Using HL-1 cells to start off, we investigated whether promotion of mitochondrial fusion using the mitochondrial-shaping proteins delays the opening of the mPTP using confocal laser-induced ROS stress.

6.3.1 Materials

Plasmids: an empty plasmid expression vector (RcCMV); one expressing mitofusin 1(pCB6-MYC-Mfn1); one expressing mitofusin 2 (pCB6-MYC-Mfn2) [165]; one containing $Drp1_{K38A}$ (pcDNA3.1-HA-$_{K38A}$-DRP1), the dominant negative mutant form of the mitochondrial fission protein Drp1 [205]; and one containing hFis1. $Drp1_{K38A}$ has a mutation in the GTPase domain that results in replacement of lysine 38 with alanine (designated as $Drp1_{K38A}$), disabling its ability to induce mitochondrial fission [205]. For the mPTP assay, a ratio of 2:1 plasmid enhanced green fluorescent protein (pEGFP) (Clontech) expression plasmid was included in order to select the cells of interest. All plasmids were a generous gift of Dr Luca Scorrano (Padova, Italy). Krebs buffer comprising (in mM): NaCl 118.0, $NaHCO_3$ 25.0, d-Glucose 11.0, KCl 4.7, $MgSO_4.7H_2O$ 1.2, KH_2PO_4 1.2, $CaCl_2.2H_2O$ 1.8, and HEPES 10.0 (pH 7.4) was used as imaging buffer for confocal studies. TMRM was dissolved in DMSO and added to the Krebs byuffer such that the final concentration is 3 µM.

6.3.2 Experimental protocol

To test the hypothesis that fused mitochondria protects the cells against ischaemia-reperfusion injury by preventing opening of mPTP in the mitochondrial membrane; we subjected the HL-1 cells transfected with either one of the following:

1. RcCMV – empty vector (Vector Control)
2. $Drp1_{K38A}$ – the dominant negative form of the fission protein
3. Mfn1 – fusion-promoting protein
4. Mfn2 – fusion-promoting protein
5. hFis1 - fission-promoting protein

to confocal laser-induced reactive oxygen species release to trigger the opening of the mPTP. For each transfected cell as represented in green, ROI analysis was performed on the section of the cell containing TMRM. For each treatment group, approximately 60 cells were subjected to ROI analysis. The varying fluorescent intensities for the cells were converted to Excel format and subsequently into line graphs, and the half-times to achieve maximum fluorescent intensity determined to compare the time needed for mPTP opening upon lasers-induced release of free oxygen radicals from TMRM.

6.3.3 Results

Overexpression of the fusion proteins delayed the sensitivity of mPTP opening in the HL-1 cardiac cell line in a confocal laser-induced ROS model. Cells which have an overexpression of Mfn1, Mfn2 and the mutant form of the fission protein, $Drp1_{K38A}$ showed a delayed normalised time until mPTP opening (2.4 ± 0.5 fold, 2.3 ± 0.7 fold and 2.4 ± 0.3 fold vs. 1.0 ± 0.1 for vector control; N=4 experiments with 20 cells per treatment group; *P<0.05). The time needed for mPTP opening in HL-1 cells with an over-expresssion of hFis1 was recorded at 0.9 ± 0.7. CsA as a positive control also significantly delayed the time until mPTP opening by 2.2 ± 0.4 fold; N=4 experiments with 20 cells per treatment group; *P<0.05 (see Figure 6.1).

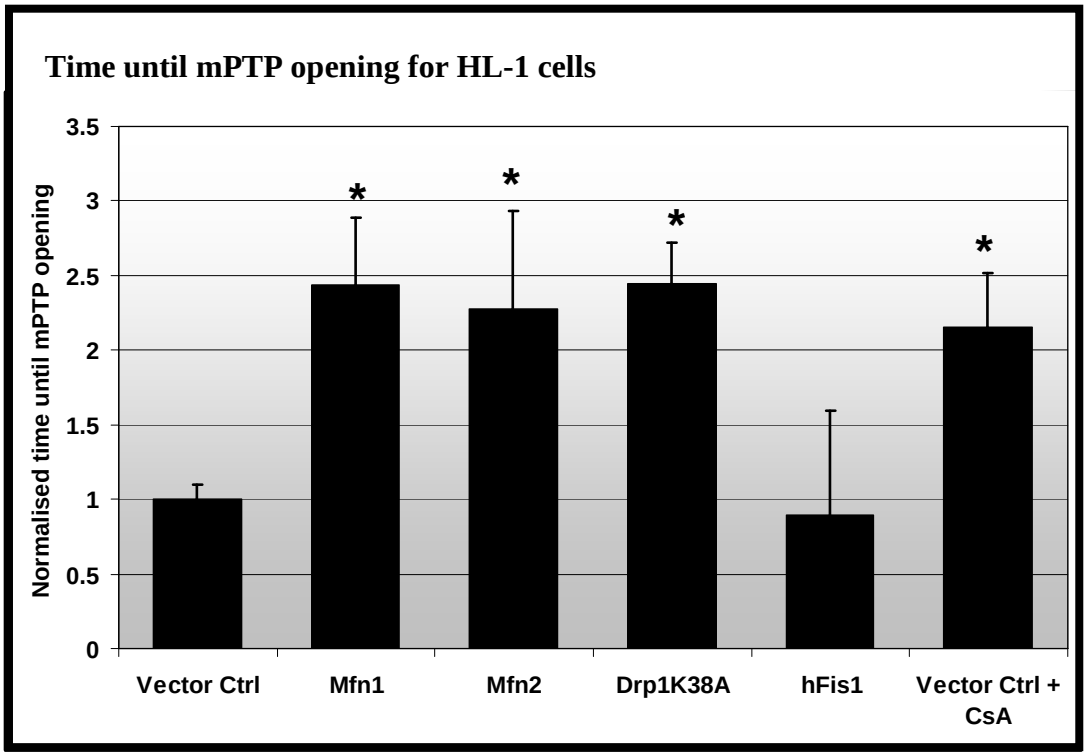

Figure 6.1: Normalised half-times to reach maximum red fluorescent intensity for HL-1 cells transfected with different fusion proteins under confocal-lasers induced oxidative stress. CsA acts as a positive control. Over-expressing Mfn1, Mfn2, or $Drp1_{K38A}$ delayed the time taken to induce mPTP opening, whereas over-expressing hFis1 had no significant effect on mPTP opening sensitivity. As expected, CsA delayed the time taken to induce mPTP opening. N=4 experiments with 20 cells per treatment group. *P<0.05.

Based on the changes in absolute red fluorescent intensities of TMRM over the whole 8 minute cycle of confocal-laser induced ROS, overexpression of the fusion proteins Mfn1, Mfn2, and $Drp1_{K38A}$ caused a significant reduction in the increase of absolute red fluorescent intensities at times 80 seconds (517.3 ± 61.7, 564.7 ± 58.1, 716.9 ± 183.9 respectively) and 160 seconds (745.8 ± 101.9, 951.8 ± 147.3, 1123.8 ± 315.1 respectively) compared to the vector control (1365.2 ± 254.3 at 80 seconds and 1755.1 ± 254.3 at 160 seconds) (N=4 experiments with 20 cells per treatment group; *P<0.05). CsA as a positive control also reduced the amount of increase in red fluorescent intensity at the two time points (571.6 ± 88.0 at time 80 s and 857.6 ± 187.2 at time 160 s) (N=4 experiments with 20 cells per treatment group; *P<0.05) (see Figure 6.2).

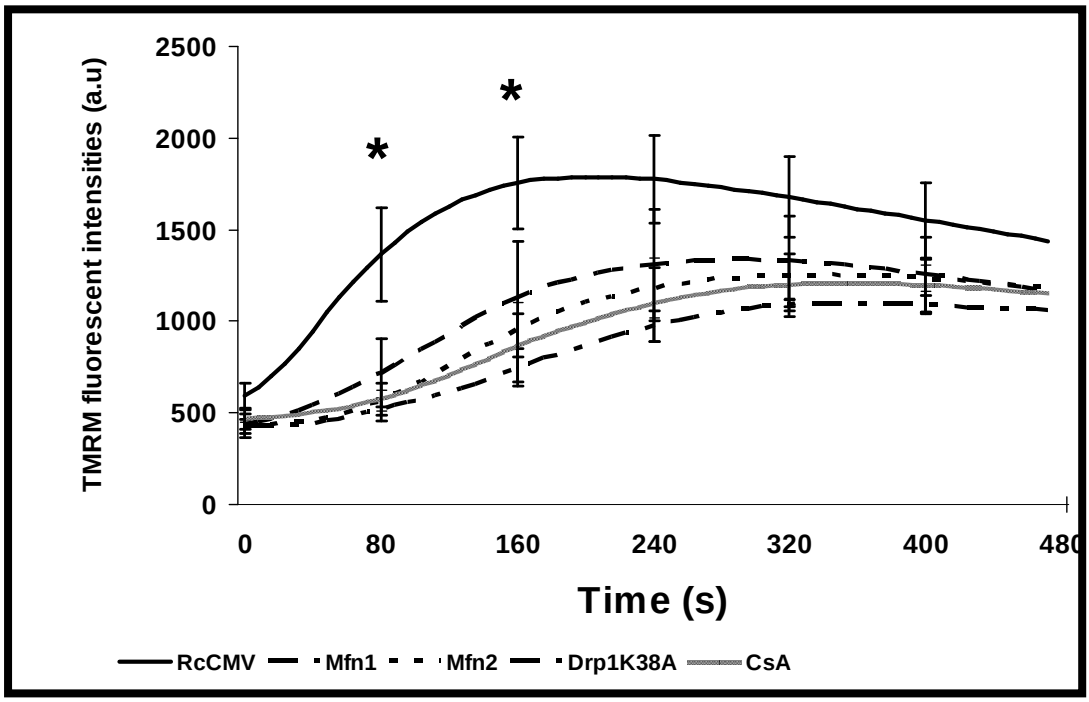

Figure 6.2: Changes in absolute red fluorescent intensities of TMRM over the 8 minute cycle of confocal-lasers induced oxidative stress in HL-1 cells transfected with different proteins. A significant reduction in red fluorescent intensity emmited was observed at time 80 and 160s for cells with an overexpression of Mfn1, Mfn2 and $Drp1_{K38A}$. N=4 experiments with 20 cells per treatment group. *P<0.05.

6.4 Aim (2)

To determine whether modulation of mitochondrial morphology via pharmacological manipulation delays the opening of the mPTP in HL-1 cardiac cells

We have demonstrated the promotion of mitochondrial fusion in HL-1 cells delays the opening of the mPTP in the previous section. In this section, we investigated the effects of pharmacological inhibiting mitochondrial fission in HL-1 cells on mPTP inhibition.

6.4.1 Materials

Mdivi-1 drug was purchased from Key Organics Ltd., UK. The drug was dissolved in DMSO to achieve a working concentration of and subsequently in Claycomb medium or Krebs buffer comprising (in mM): NaCl 118.0, $NaHCO_3$ 25.0, d-Glucose 11.0, KCl 4.7, $MgSO_4$.7H2O 1.2, KH_2PO4 1.2, $CaCl_2$.2H2O 1.8, and HEPES 10.0 (pH 7.4) to achieve a final concentration of 10 µM or 50 µM.

6.4.2 Experimental protocol

HL-1 cells were pre-treated with 50 uM *mdivi-1* for 40 minutes in the 37^{o}C incubator and subjected to confocal-laser induced stress to determine susceptibility to mPTP opening.

6.4.3 Results

HL-1 cells treated with 50 µM *mdivi-1* showed a significant delay in time until mPTP opening by 2.1 ± 0.5 fold vs. 1.0 ± 0.1 for cells treated with vehicle control; N=4 experiments with 20 cells per treatment group; *P<0.05. Time until mPTP opening for cells treated with 10 µM *mdivi-1* was at 0.6 ± 0.1 fold while the positive control, CsA delayed the time until mPTP opening by 2.3 ± 0.5 fold; N=4 experiments with 20 cells per treatment group; *P<0.05 (see Figure 6.3).

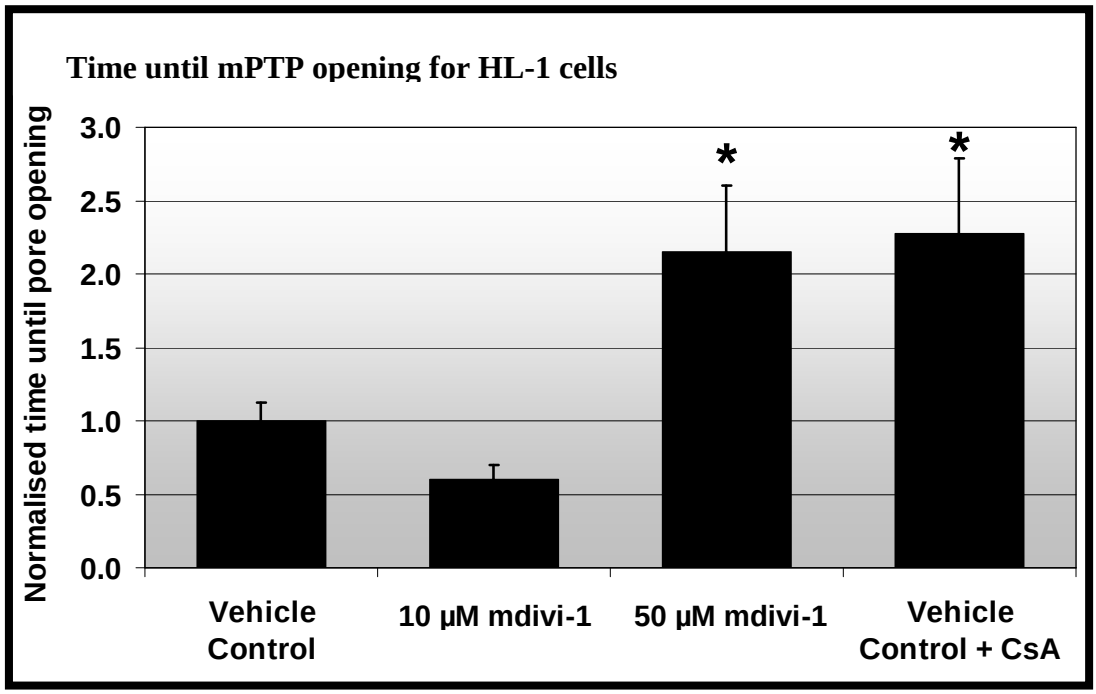

Figure 6.3: **Normalised half-times to reach maximum red fluorescent intensity for HL-1 cells treated with different drugs under confocal-lasers induced oxidative stress. CsA acts as a positive control.** Treatment with *mdivi-1* at 50 but not 10 µM for 40 minutes resulted in a significant delay in the time taken to induce mPTP opening. As expected, CsA delayed the time taken to induce mPTP opening. N=4 experiments with 20 cells per treatment group. *P<0.05

6.5 Aim (3)

To determine whether modulation of mitochondrial morphology via genetic manipulation delays the opening of the mPTP in endothelial cells

In this section, we investigated whether genetically promoting mitochondrial fusion in endothelial cells produces similar results as in HL-1 cells for mPTP inhibition.

6.5.1 Materials

The plasmids used for the endothelial mPTP assay is similar to the ones used in the HL-1 mPTP assay as well as the endothelial morphology study to investigate potential connections between mitochondrial morphology and mPTP sensitivity: an empty plasmid expression vector (RcCMV); one expressing mitofusin 1(pCB6-MYC-Mfn1); one expressing mitofusin 2 (pCB6-MYC-Mfn2) [165]; one containing $Drp1_{K38A}$ (pcDNA3.1-HA-$_{K38A}$-DRP1), the dominant negative mutant form of the mitochondrial fission protein Drp1 [205]; and one containing hFis1. $Drp1_{K38A}$ has a mutation in the GTPase domain that results in replacement of lysine 38 with alanine (designated as $Drp1_{K38A}$), disabling its ability to induce mitochondrial fission [205]. For the mPTP assay, a ratio of 1:2 plasmid enhanced green fluorescent protein (pEGFP) (Clontech) expression plasmid: plasmid of interest was included in order to select the cells of interest. All plasmids were a generous gift of Dr Luca Scorrano (Padova, Italy). Krebs buffer comprising (in mM): NaCl 118.0, $NaHCO_3$ 25.0, d-Glucose 11.0, KCl 4.7, $MgSO_4.7H_2O$ 1.2, KH_2PO_4 1.2, $CaCl_2.2H_2O$ 1.8, and HEPES 10.0 (pH 7.4) was used as imaging buffer for confocal studies. TMRM was dissolved in DMSO and added to the Krebs buffer such that the final concentration is 3 µM.

6.5.2 Experimental Protocol

To test the hypothesis that fused mitochondria protects the cells against ischaemia-reperfusion injury by preventing opening of mPTP in the mitochondrial membrane; we subjected the endothelial cells transfected with either one of the following:

1. RcCMV – empty vector (Vector Control)
2. $Drp1_{K38A}$ – the dominant negative form of the fission protein
3. Mfn1 – fusion-promoting protein
4. Mfn2 – fusion-promoting protein
5. hFis1 – fission-promoting protein

to confocal laser-induced reactive oxygen species release to trigger the opening of the mPTP. For each transfected cell as represented in green, ROI analysis was performed on the section of the cell containing TMRM. For each treatment group, approximately 60 cells were subjected to ROI analysis. The varying fluorescent intensities for the cells were converted to Excel format and subsequently into line graphs, and the half-times to achieve maximum fluorescent intensity determined to compare the time needed for mPTP opening upon lasers-induced release of free oxygen radicals from TMRM.

6.5.3 Results

Endothelial cells transfected with Mfn1 and Mfn2 showed a delay in time until mPTP opening by 1.9 ± 0.4 fold and 2.1 ± 0.4 fold respectively compared to 1.0 ± 0.1 for vector control. Overexpression of the fission protein, hFis1 in endothelial cells recorded a time until mPTP opening at 1.1 ± 0.2 fold whereas CsA as a positive control delayed the time until mPTP opening by 1.7 ± 0.5 fold, albeit not significantly (see Figure 6.4).

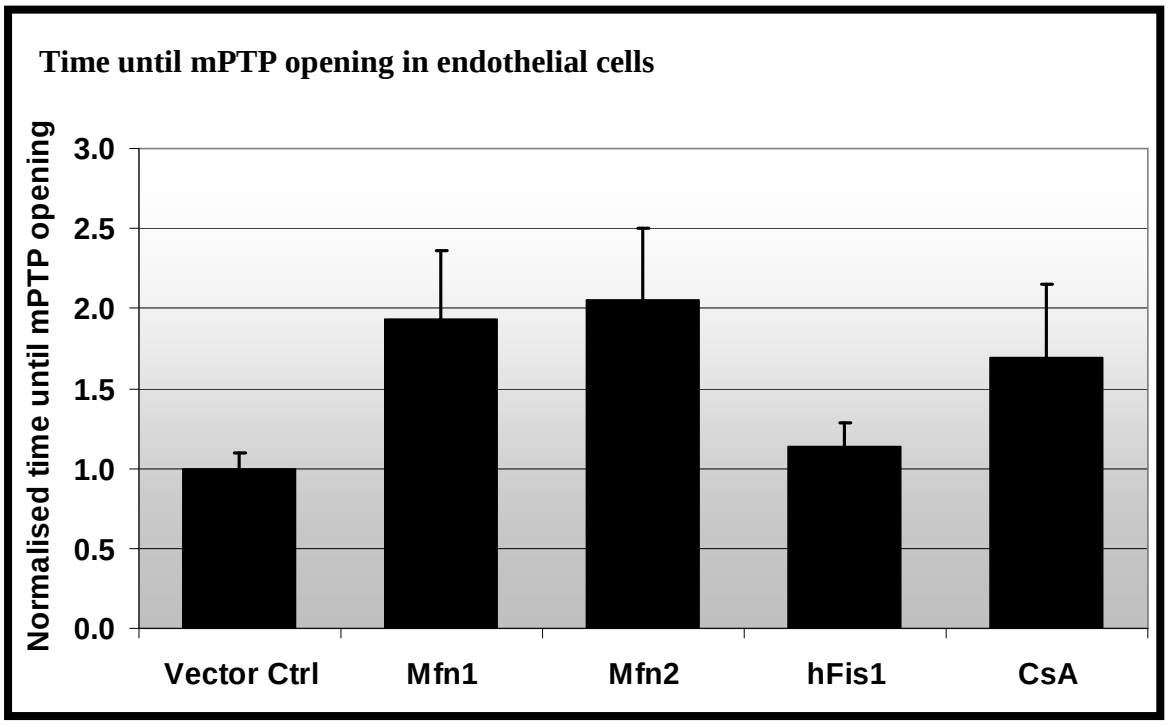

Figure 6.4: Normalised half-times to reach maximum red fluorescent intensity for endothelial cells transfected with different fusion proteins under confocal-lasers induced oxidative stress. CsA acts as a positive control

6.6 Aim (4)

To determine whether modulation of mitochondrial morphology via pharmacological manipulation delays the opening of the mPTP in adult cardiomyocytes

In this section, we aimed to investigate whether the use of *mdivi-1* as a pharmacological agent to inhibit mitochondrial fragmentation in adult cardiomyocytes also delays the opening of the mPTP in an sIR model of mPTP opening.

6.6.1 Materials

Mdivi-1 drug was purchased from Key Organics Ltd., UK. The drug was dissolved in DMSO to achieve a working concentration of 50 mM and subsequently in hypoxic ischaemic buffer to achive a final concentration of 50 µM. Sanglifehrin A (SfA) was dissolved in DMSO to achieve a working concentration of 1 mM and subsequently in hypoxic ischaemic buffer to achieve a final concentration of 1 µM. Simulated ischaemia was performed in hypoxic ischaemic buffer comprising (in mM): KH_2PO_4 1.0, $NaHCO_3$ 10.0, $MgCl_2.6H_2O$ 1.2, NaHEPES 25.0, NaCl 74.0, KCl 16, $CaCl_2$ 1.2 and NaLactate 20 at pH 6.2, bubbled with 100% nitrogen. Reoxygenationwas performed using cardiomyocyte growth medium (M199 buffer: BSA 2 mg/ml, creatine 5 mM, taurine 5 mM, carnitine hydrochloride 1.6 mM, Pencillin-Streptomycin 1%).

6.6.2 Experimental protocol

For the adult cardiomyocytes we used a different model to assess mPTP opening, in which its opening is measured following 45 minutes of simulated ischaemia and 30 minutes of simulated reperfusion by measuring the resultant TMRM fluorescence. Twenty cells were randomly selected for each treatment group, and this was repeated in at least four independent experiments.

6.6.3 Results

Using the hypoxic chamber for mPTP assay in adult cardiomyocytes, the normalised TMRM fluorescent intensity for adult cardiomyocytes following sIR was reduced significantly to 0.8 ± 0.1 compared to 1.0 ± 0.1 for normoxic control; N=4 experiments with 20 cells per treatment group; *P<0.05. sIR in the presence of 50 µM *mdivi-1* maintained the TMRM fluorescent intensity at 1.0 ± 0.1 while sIR in the presence of SfA confers a recorded TMRM intensity at 0.9 ± 0.1 (see Figure 6.5).

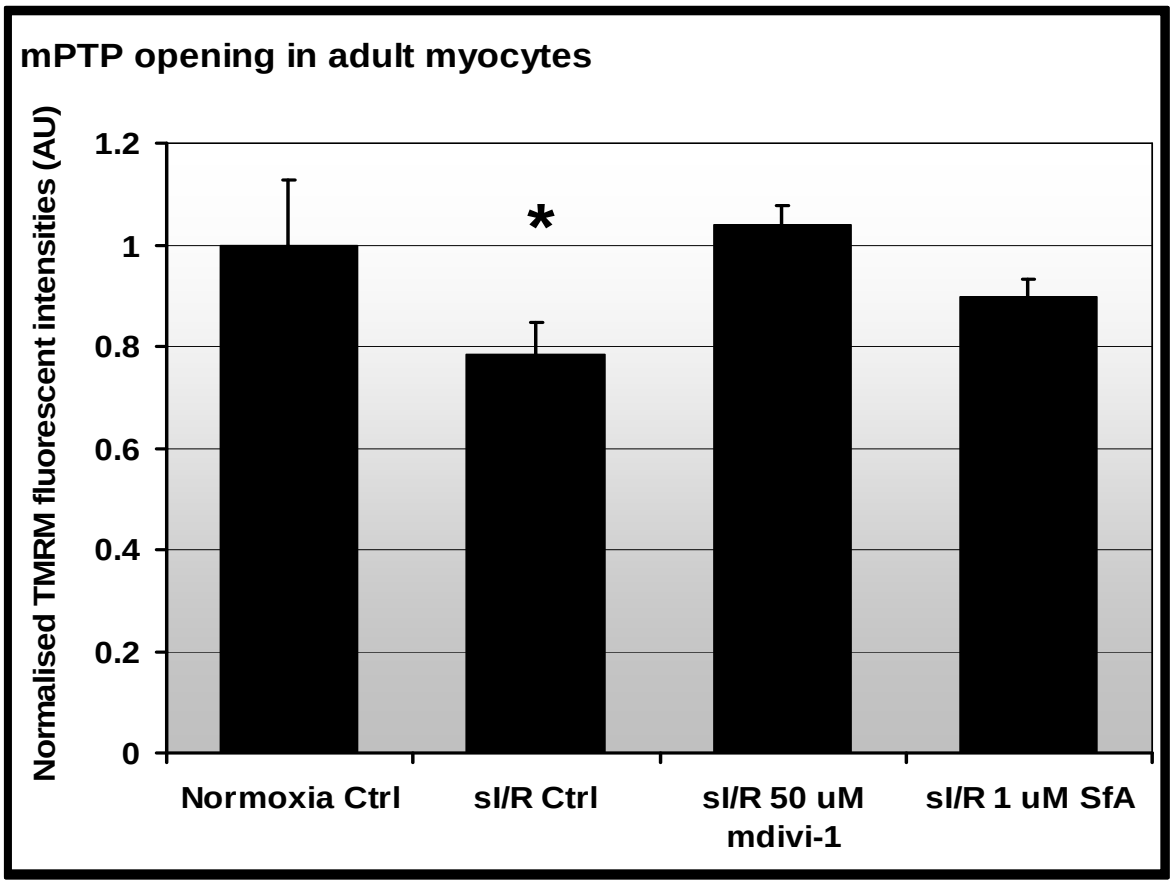

Figure 6.5: Normalised TMRM fluorescent intensities for measurement of mPTP opening in adult cardiomyocytes. Pre-treatment of adult rat cardiomyocytes with *mdivi-1* at 50 µM inhibited mPTP opening as evidenced by the preserved TMRM fluorescence after SIRI. N=4 experiments with 20 cells per treatment group. *P<0.05

6.7 Discussion

Delaying the opening of the mPTP in HL-1 cells by genetic modulation of mitochondrial morphology

In this section of the study, we demonstrated that the overexpression of the fusion proteins that promote mitochondrial elongation delays the sensitivity to mPTP opening. Previous studies conducted have demonstrated the feasibility of this confocal-laser induced ROS model to induce mPTP opening in cultured cells where the increase in overall red fluorescent intensities is due to the de-quenching of the TMRM was used to measure mPTP opening [457, 458, 512] and this has been repeated in subsequent studies [236, 259, 263, 462, 513, 514]. Half-times were taken as the time taken to reach maximum red intensities is very subjective. In addition to that, the 8-minutes period of laser stress produces different maximum values of red intensities for different cells. Therefore, half-times were chosen for data analysis. Normalisation of the half-times to the vector control was also performed to make the data more logical and comprehensible. The efficiency of CsA to delay the sensitivity of mPTP opening shows that the mPTP was indeed targeted in this study instead of other factors that causes the release of TMRM from the mitochondria such as unspecific pores or channels. The mutant form of the fission protein $Drp1_{K38A}$ was included to exclude the effects of the presence of the fusion proteins. CsA was used as a positive control to confirm that the mPTP was indeed targeted in this study as CsA has been proven by various previous studies to be a potent inhibitor of the mPTP [17, 63, 449, 515-517]. The time until mPTP opening was measured as half-time until maximum fluorescence intensity achieved within the specified time period of laser stress. This method was chosen because we had to find a balance between killing the cells with an extended period of laser stress and detecting sufficient pore opening within an optimum time frame. Different methods have been used to quantify opening of the mPTP; e.g. mitochondrial entrapment of 2-deoxy [^{3}H] glucose-6-phosphate ([^{3}H]DOG-6P) or calcein re-distribution. We found that using the TMRM confocal laser-induced ROS model proved practical and efficient. In addition to that, we have also used the re-distribution of calcein to verify our findings. Surprisingly, overexpression of the fission protein, hFis1 did not increase the sensitivity of the mPTP opening in our study. Yet, it has been previously reported that overexpression of either Drp1 or

hFis1 in COS epithelial cells increased the sensitivity of cells towards calcium-induced mPTP opening. The limitation in the resolution of our model to detect sensitivity to mPTP opening may explain our findings. Another alternative explanation is that the cell death caused by hFis1 is independent of the mPTP.

Delaying the opening of the mPTP in HL-1 cells by pharmacological modulation of mitochondrial morphology

In this part of the study, we have demonstrated that the use of 50 µM *mdivi-1* to treat HL-1 cardiac cells for 40 minutes successfully delayed the opening of the mPTP following confocal laser-induced mPTP opening. This was the first time that *mdivi-1* has been shown to inhibit mPTP opening. This suggests that promotion of mitochondrial fusion by either genetic manipulation or pharmacological manipulation can prevent the opening of the mPTP. CsA was used as to indicate that the mPTP was properly targeted in this study. The finding that 10 µM *mdivi-1* did not prevent mPTP opening correlates with results from the previous section where this same concentration of drug was not found to induce mitochondrial elongation.

Delaying the opening of the mPTP in endothelial cells by genetic modulation of mitochondrial morphology

The results obtained from this section showed the trend of delaying the sensitivity of mPTP in endothelial cells, albeit no significance was achieved. This may be achieved if the number of experiments, n number was increased. Similar to the HL-1 cells, overexpression of the hFis1 protein did not increase the sensitivity of the endothelial cells to mPTP opening.

Delaying the opening of the mPTP in adult cardiomyocytes by pharmacological modulation of mitochondrial morphology

In this section, we determined whether treatment of the *mdivi-1* drug at its optimum concentration of 50 µM in cardiomyocytes can reduce the opening of the mPTP following simulated ischaemia-reperfusion. We successfully demonstrated that the use of the *mdivi-1* drug can inhibit mPTP opening following sIR. The positive control for inhibition of mPTP opening was changed from CsA to SfA because SfA

is more potent than CsA. The model in detection of mPTP opening was changed from the confocal laser-induced mPTP opening (quenching concentration of TMRM, 3 µM) to the simulated ischaemia-reperfusion model (non-quenching concentration of TMRM, 100 nM) because:

1) the opening of the mPTP was not delayed significantly by the SfA using the confocal model
2) *mdivi-1* drug seemed to hyperpolarise or increase the membrane potential of the mitochondria in the presence of a quenching concentration of TMRM (3 µM), hence making it difficult to detect any difference in re-distribution of TMRM
3) the simulated ischaemia-reperfusion model is more relevant to the settings of the adult myocytes

To our knowledge, this is the first time that *mdivi-1* has been proven to inhibit mPTP opening in adult myocytes. Compared to the normoxia control, simulated ischaemia-reperfusion causes the mPTP to open and the non-quenching concentration of TMRM to leave the mitochondria and enter the cytosol, hence causing a decrease in red fluorescent intensity. The treatment of *mdivi-1* drug and SfA however, successfully reduced the opening of the mPTP and maintained the TMRM in the mitochondria.

6.8 Conclusion

Opening of the mPTP has been established as the cause of reperfusion injury and inhibition of the mPTP has been shown to alleviate the effects of reperfusion injury. Numerous studies have sought to inhibit the opening of the mPTP; either by pharmacological methods [17, 232, 482, 518-524] or genetic ablation methods such as knocking out the Cyclophilin D component of the mPTP [404, 525-528]. We demonstrate in this chapter that promotion of mitochondrial fusion delays the time until mPTP opening and this delay may underlie the cardioprotective effects of mitochondrial fusion.

Chapter Seven

LINKING PRO-SURVIVAL KINASES TO CARDIOPROTECTION VIA MITOCHONDRIAL DYNAMICS

7.1 Introduction

Kinases and their phosphorylation effects have always been a central focus on studies in cardioprotection, particularly kinases forming the RISK pathway or SAFE pathway [258, 276, 305, 350, 482]. Some of the well-known kinases include Protein Kinase A (PKA), Protein Kinase B (PKB), and Protein Kinase C (PKC). Cardioprotective effects of PKA lies in the fact that PKA can modulate the opening of the mitochondrial Ca^{2+}-activated K^{+} channels [281, 529, 530], while PKB which consist of isoforms Akt1 (PKB-α), 2 (PKB-β) and 3 (PKB-γ) have been known to promote growth and metabolism [287, 288, 531, 532], glucose homeostasis [289, 533-536] and neuronal repair respectively [291, 292]. The story of PKC is controversial with the fact that PKC epsilon protects [10, 360, 537-540] whereas PKC delta is deleterious [495, 541-543].

One of the documented effects of PKA is its ability to phosphorylate and inhibit the fission protein Drp1 [182]. Using an activator of PKA, we intend to find out whether activation of PKA increases the proportion of HL-1 cells with elongated mitochondria, delays opening of mPTP and protects cells against sIR. Similarly, we were also curious to see whether the activation of Akt as a well-known pro-survival kinase (crucial component of the RISK pathway), confers any effect on mitochondrial morphology. Although activation of Akt influences many downstream effectors such as glycogen synthase kinase 3 (GSK3beta) [544, 545], Forkhead family of transcription factors (FOXO) [303, 546, 547] and the pro-apoptotic protein Bcl2 antagonist of cell death (BAD) [297, 298], there is generally a lack of a consensus factor in which the end-effectors of Akt activation act upon. We believe it to be mitochondrial morphology, a notion we seek to investigate in this section. But before we can attempt to investigate the role of Akt in modulation of mitochondrial morphology, we have to prove that the overexpression or activation of Akt in our cardiac cell line also delays the time until mPTP opening and protects the cells against sIR.

7.2 Hypothesis & Objectives

Pro-survival kinases elicit cardioprotection via modulation of mitochondrial morphology in the heart

In the first section of the study, we investigated the documented effects of PKA activation on inhibition of the fission protein, Drp1 in HL-1 cells.

In the second section of the study, we investigated the pro-survival effects of PKA activation in HL-1 cells following sIR.

Following this, we investigated whether the protective effects of PKA activation was based on delaying the opening of the mPTP in HL-1 cells.

In addition to investigating the effects of PKA, we were also interested to investigate the effects of PKB/Akt. First and foremost, we had to determine whether upregulation of Akt protects the cells against sIR as that is a very crucial function of Akt.

Following that, we investigated whether upregulation of Akt delays the opening of the mPTP in HL-1 cells using the confocal laser-induced stress model.

7.3 Aim (1)

To determine whether pharmacologically activating PKA modulates mitochondrial morphology in HL-1 cells

Following the findings from previous sections demonstrating the beneficial effects of modulating mitochondrial morphology in protecting the heart against IRI, we were intrigued to investigate the possible links between pro-survival kinases and cardioprotection. In this section, we investigated the role of PKA in inhibiting the mitochondria fission-promoting protein, Drp1 in HL-1 cells.

7.3.1 Materials

Sp-5, 6-dichloro-1-beta-D-ribofuranosylbenzimidazole-3', 5'-monophosphorothioate (Sp-5, 6 – DCl – cBiMPS) (hereafter referred to as cBiMPS) was purchased from Biomol International. cBiMPS binds to cAMP-binding sites of the cAMP protein kinases hence leading to their activation [419, 548]. The drug was dissolved in water to achieve a working concentration of 1 mM and subsequently in Krebs buffer comprising (in mM): NaCl 118.0, $NaHCO_3$ 25.0, d-Glucose 11.0, KCl 4.7, $MgSO_4.7H_2O$ 1.2, KH_2PO_4 1.2, $CaCl_2.2H_2O$ 1.8, and HEPES 10.0 (pH 7.4) to achieve a final concentration of 0.1 mM.

7.3.2 Experimental protocol

HL-1 cardiac cells were transfected with plasmids encoding for mitochondrial-targeted red fluorescent protein (mtRFP). For a time-response study, 24 hours after transfection, the cells were imaged using confocal microscopy to determine percentage of cells with elongated mitochondria. The cells were then treated with 0.1 mM of cBiMPS and imaged after 20, 40 and 60 minutes to determine percentage of cells with elongated mitochondria.

To verify the optimum duration of incubation determined by the time-response study, a separate batch of cells transfected with mtRFP was imaged using the confocal microscope to determine number of cells with elongated mitochondria and then treated with cBiMPS for the determined duration before re-imaging.

7.3.3 Results

Cells incubated with cBiMPS as a PKA activator had 20% of cells with elongated mitochondria at time 0'. This percentage increases to 96.0% after 20 minutes of incubation, drops slightly to 63.0% at time 40 minutes and increases back to 86.0% after an hour (see Figure 7.1).

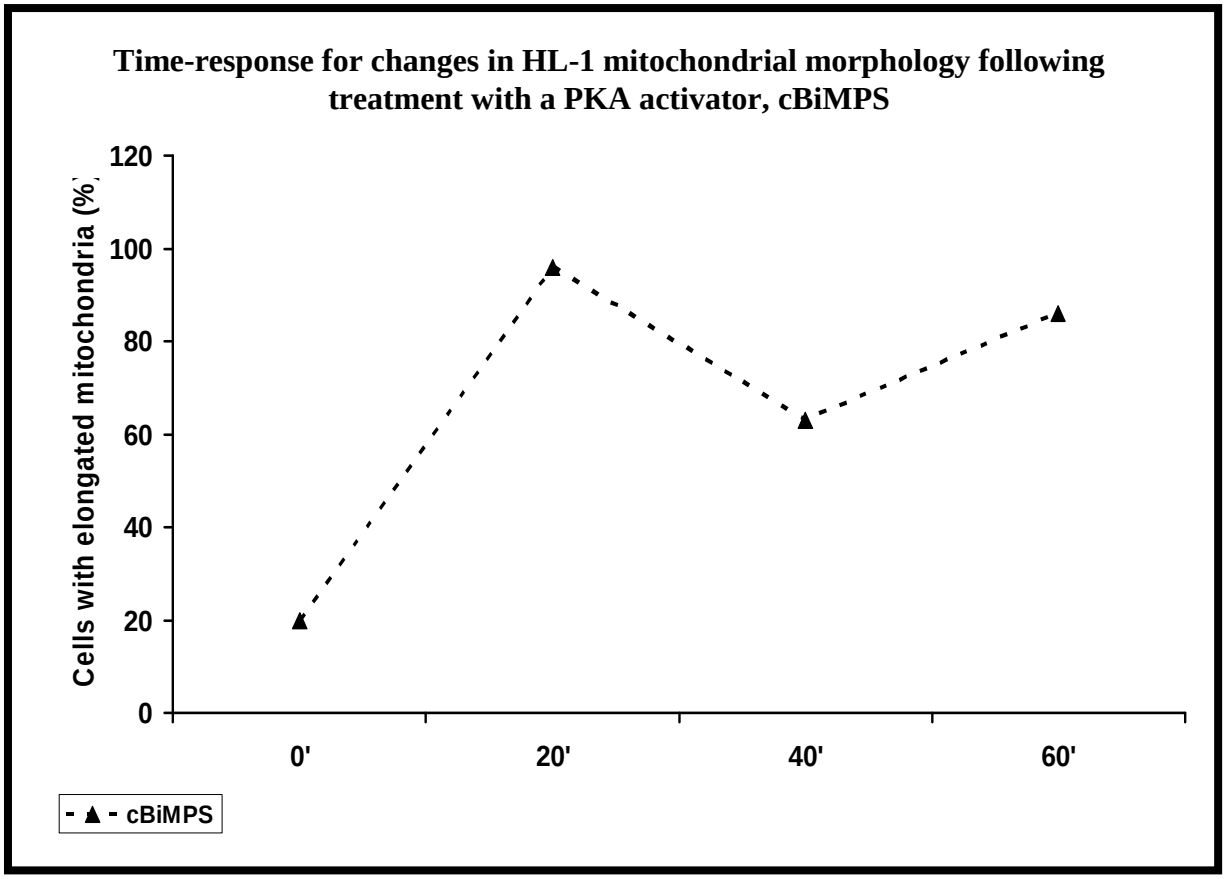

Figure 7.1 Changes in mitochondrial morphology of HL-1 cells following treatment with cBiMPS, a PKA activator. Number of cells with elongated mitochondria (%) increased following cBiMPS treatment as early as 20 minutes.

At time 0', the percentage of cells with elongated mitochondria incubated with vehicle control was 24.2 ± 8.5% while percentage of cells with elongated mitochondria incubated with cBiMPS was 25.7 ± 6.3%. After 40 minutes of incubation with the respective treatments, cBiMPS increased the percentage of cells

with elongated mitochondria to 55.3 ± 11.5% compared to 29.0 ± 8.1% for vehicle control (see Figure 7.2).

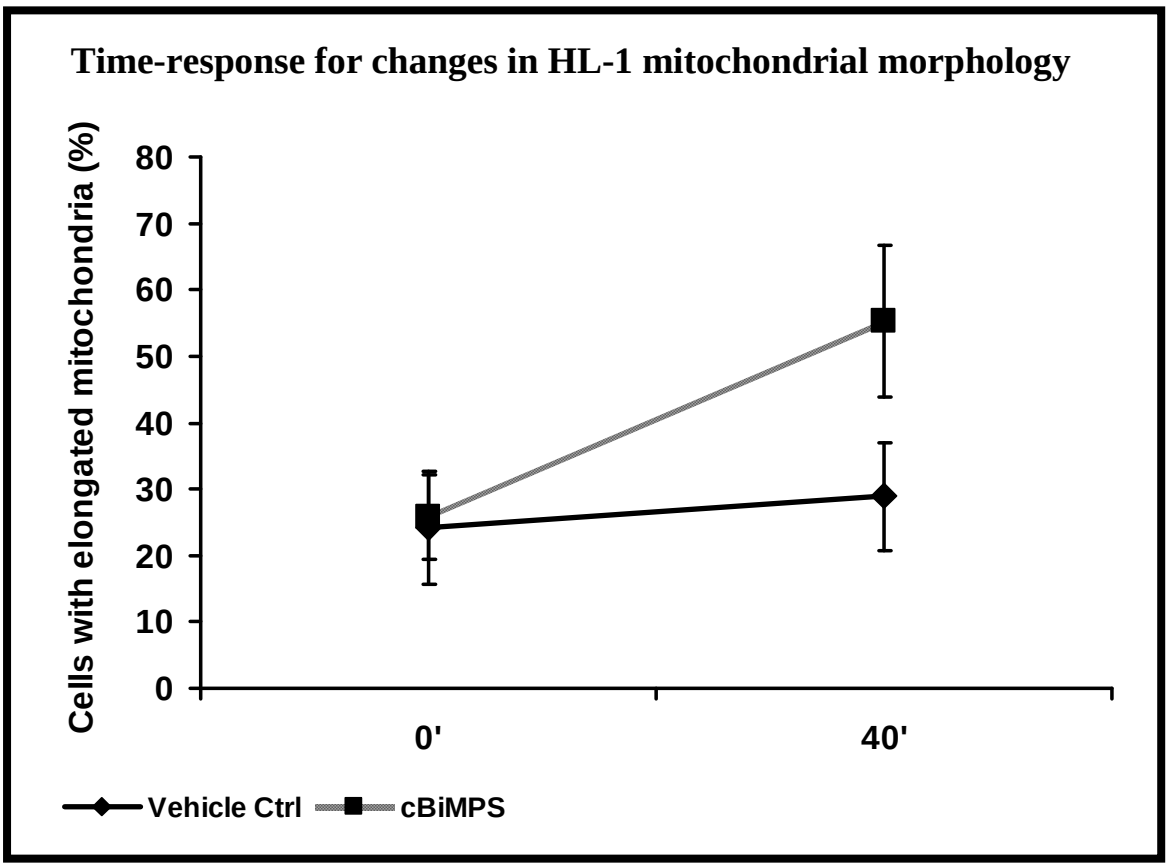

Figure 7.2: Effects of 40 minutes cBiMPS treatment to the morphology of mitochondria in HL-1 cells. In HL-1 cells containing either fragmented or elongated mitochondria under basal conditions, treatment with cBiMPS at 0.1 mM for 40 minutes increased the proportion of cells displaying elongated mitochondria. N=5 experiments with 80 cells per treatment group.

7.4 Aim (2)

To determine whether pharmacologically activating PKA protects the HL-1 cells against sIR

Following the previous sections where we have shown that inhibition of mitochondrial fission by the use of *mdivi-1* protects cells against sIR, we were interested to determine whether upregulation of PKA using an activator of PKA protects the HL-1 cells against sIR by inhibiting mitochondrial fission in this study.

7.4.1 Materials

Sp-5, 6 – DCl – cBiMPS was purchased from Biomol International. The drug was dissolved in water to achieve a working concentration of 1 mM and subsequently in hypoxic ischaemic buffer comprising of (in mM): KH_2PO4 1.0, $NaHCO_3$ 10.0, $MgCl_2.6H_2O$ 1.2, NaHEPES 25.0, NaCl 74.0, KCl 16, $CaCl_2$ 1.2 and NaLactate 20 at pH 6.2, bubbled with 100% nitrogen, or the reoxygenation medium, Claycomb medium to achieve a final concentration of 0.1 mM. EPO (Neorecormon, Roche) was diluted in distilled water to achieve a working concentration of 5000 U / ml. Propidium iodide (PI) (Sigma UK) was dissolved in distilled water and added to the Claycomb medium such that the final concentration was 3 uM.

7.4.2 Experimental protocol

HL-1 cells transfected with mtRFP for 24 hours were treated with cBiMPS for 40 minutes prior to 12 hours of simulated ischaemia followed by 1 hour of reoxygenation in the presence of cBiMPS throughout. Cell death was measured by propidium iodide (PI) staining.

7.4.3 Results

Following pre-treatment of cBiMPS or EPO for 40 minutes prior to 12 hours simulated ischaemia and 1 hour of reoxygenation in the presence of the drugs, cell death for cells treated with cBiMPS or EPO was reduced significantly to 20.5 ± 4.3% and 17.0 ± 2.7% respectively vs. 42.1 ± 4.8% for vehicle control; N=4 experiments with 80 cells per treatment group; *P<0.05 (see Figure 7.3).

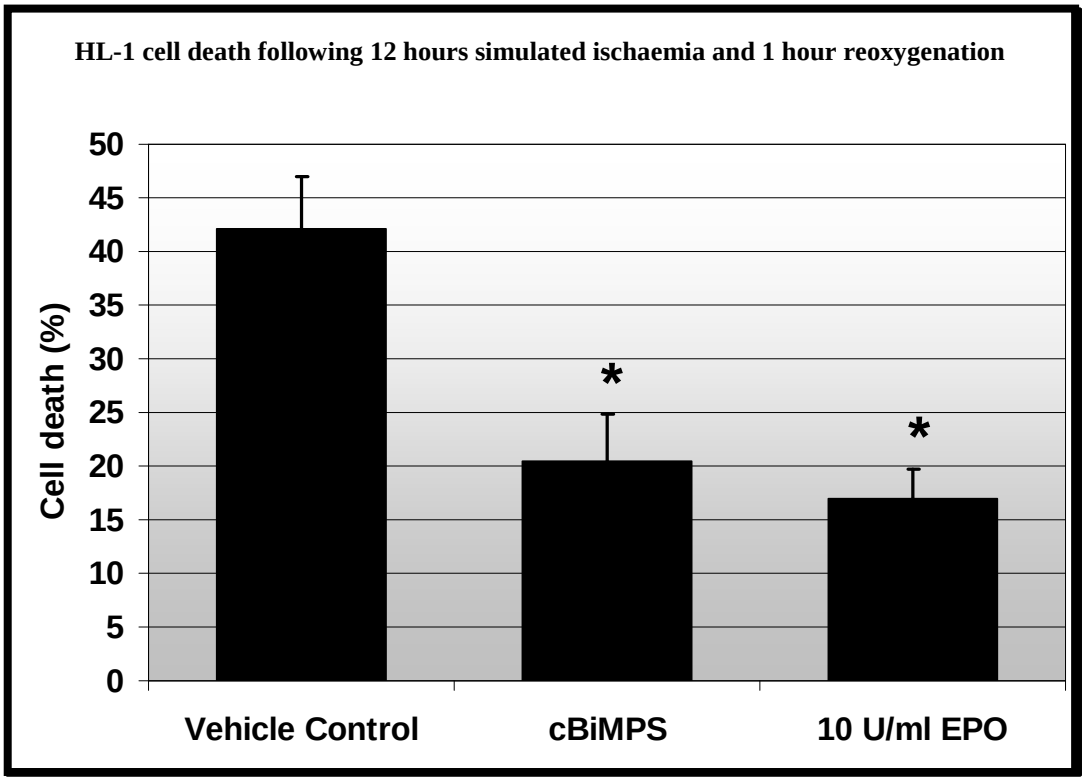

Figure 7.3: Cell death in HL-1 cells treated with different drugs following 12 hours hypoxia and 1 hour reoxygenation. Treatment with cBiMPS at 0.1 mM for 40 minutes resulted in less cell death after SIRI. As expected, EPO also reduced cell death. N=4 experiments with 80 cells per treatment group. *P<0.05 compared to vehicle control.

7.5 Aim (3)

To determine whether pharmacologically activating PKA delays opening of mPTP in HL-1 cells

In previous sections, we have shown that the modulating mitochondrial morphology by tilting the balance towards a more fused state delays the opening of the mPTP. In this section, we were interested to determine whether activating PKA using a PKA activator inhibits mitochondrial fission and delays opening of mPTP in HL-1 cells following confocal laser-induced ROS stress.

7.5.1 Materials

Sp-5, 6 – DCl – cBiMPS was purchased from Biomol International. The drug was dissolved in water to achieve a working concentration of 1 mM and subsequently in Krebs buffer comprising (in mM): NaCl 118.0, $NaHCO_3$ 25.0, d-Glucose 11.0, KCl 4.7, $MgSO_4.7H_2O$ 1.2, KH_2PO_4 1.2, $CaCl_2.2H_2O$ 1.8, and HEPES 10.0 (pH 7.4) to achieve a final concentration of 0.1 mM. EPO (Neorecormon, Roche) was diluted in distilled water to achieve a working concentration of 5000 U / ml.

7.5.2 Experimental protocol

HL-1 cells were treated with vehicle control, EPO, or cBiMPS for 40 minutes in the 37°C incubator. The cells were then loaded with TMRM in Krebs buffer containing cBiMPS for 15 minutes prior to confocal imaging for laser-induced ROS stress in Krebs buffer containing cBiMPS to image mPTP opening.

7.5.3 Results

Normalised times until mPTP opening was delayed slightly to 1.2 ± 0.1 fold. Treatment with the positive controls EPO and CsA significantly delayed the times until mPTP opening by 1.7 ± 0.2 fold and 1.9 ± 0.5 fold respectively, compared to 1.0 ± 0.1 for vehicle control (see Figure 7.4).

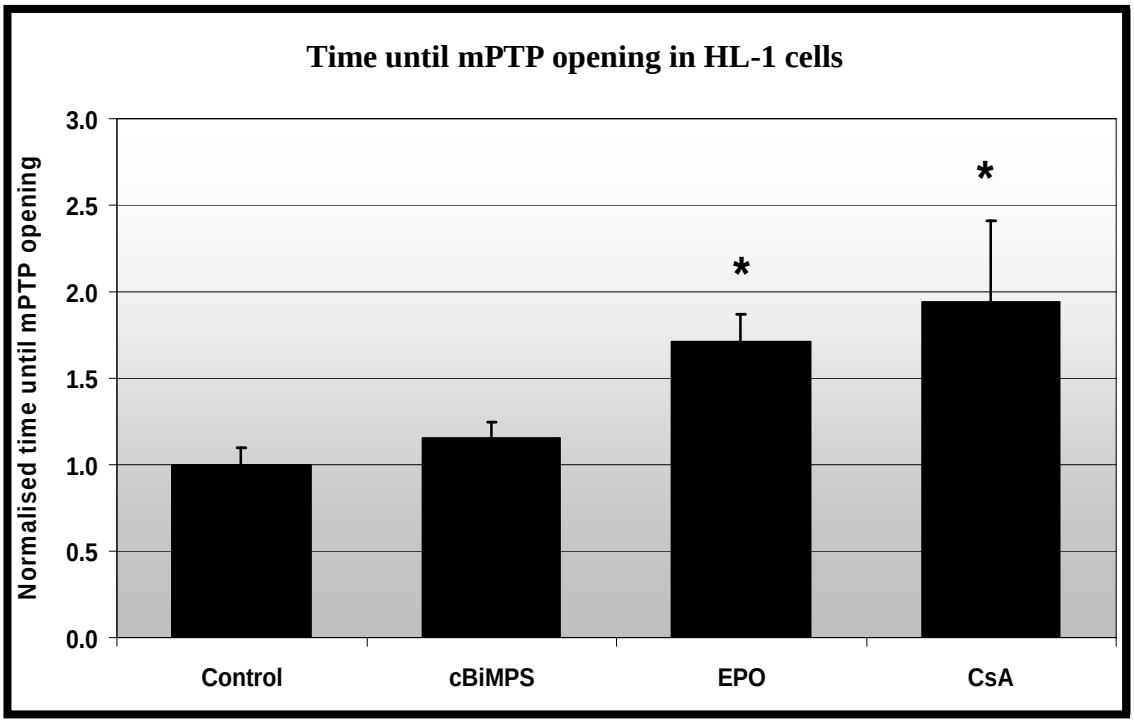

Figure 7.4: **Normalised half-times to reach maximum red fluorescent intensity for HL-1 cells treated with different drugs under confocal-lasers induced oxidative stress. CsA acts as a positive control.** Treatment with cBiMPS at 0.1 mM for 40 minutes showed no difference in the time taken to induce mPTP opening when compared to vehicle control. Treatment with EPO at 10 U/ml delayed the time significantly compared to control. As expected, CsA delayed the time taken to induce mPTP opening. N=4 experiments with 20 cells per treatment group. *P<0.05

7.6 Aim (4)

To determine whether genetic or pharmacological upregulation of Akt protects the HL-1 cells against sIR

Before progressing to investigate effects of Akt on mitochondrial morphology, we had to verify that the genetic overexpression of Akt in HL-1 cells confers cardioprotection against sIR, as it is vital that the pro-survival effects of Akt be maintained in the HL-1 basic model.

7.6.1 Materials

Plasmids: an empty plasmid expression vector (RcCMV); one expressing mitofusin 2 (pCB6-MYC-Mfn2) [165]; one containing $Drp1_{K38A}$ (pcDNA3.1-HA-K38A-DRP1), the dominant negative mutant form of the mitochondrial fission protein Drp1[205]; one expressing constitutively activated Akt (pcDNA3-HA-myrAkt) [346] and one containing the dominant negative form of Akt, Akt-AA (pcDNA3-HA-Akt-AA) [549]. The constitutively active Akt construct has the c-src myristoylation sequence fused in-frame to the N terminus of the HA-Akt (wild-type) coding sequence. The myristolated sequence of Akt targets it to the plasma membrane of the cells where it is constitutively activated [346]. In the N-terminal haemagglutinin (HA)-tagged mutant of Akt1 (PKBα) for the dominant-negative form of Akt, the two major regulatory phosphorylation sites (Thr308 and Ser473) were replaced by alanine residues rendering both endogenous and transfected Akt inactive [549]. $Drp1_{K38A}$ has a mutation in the GTPase domain that results in replacement of lysine 38 with alanine (designated as $Drp1_{K38A}$), disabling its ability to induce mitochondrial fission [205]. For the survival assay, a ratio of 1:2 plasmid enhanced green fluorescent protein (pEGFP) (Clontech) expression plasmid was included in order to permit visual assessment of mitochondrial morphology. All plasmids were a generous gift of Dr Luca Scorrano (Padova, Italy). EPO (Neorecormon, Roche) was diluted in distilled water to achieve a working concentration of 5000 U / ml. Propidium iodide was dissolved in distilled water and added to the Claycomb medium such that the final concentration was 3 μM.

7.6.2 Experimental protocol

HL-1 cells transfected with the vector control, caAkt, Mfn2 or $Drp1_{K38A}$ for a total duration of 48 or 24 hours were subjected to 12 hours of simulated ischaemia in an airtight temperature-controlled hypoxic chamber followed by 1 hour reoxygenation in Claycomb medium at 37°C supplemented with 3 μM PI to determine cell death. EPO and wortmannin were used to confirm the effects of Akt and its relative location in the RISK pathway.

7.6.3 Results

HL-1 cells with an overexpression of caAkt for 48 hours have a cell death percentage of 33.4 ± 1.2% while cells transfected with the vector control have a cell death of 41.8 ± 4.1% following 12 hours simulated ischaemia and 1 hour reoxygenation. Cells which have an overexpression of Mfn2 and $Drp1_{K38A}$ have a significantly reduced cell death of 16.2 ± 3.9% and 12.1 ± 2.9% respectively vs. 41.8 ± 4.1% for vector control; $n = 4$; $*p < 0.05$ compared to vector control.

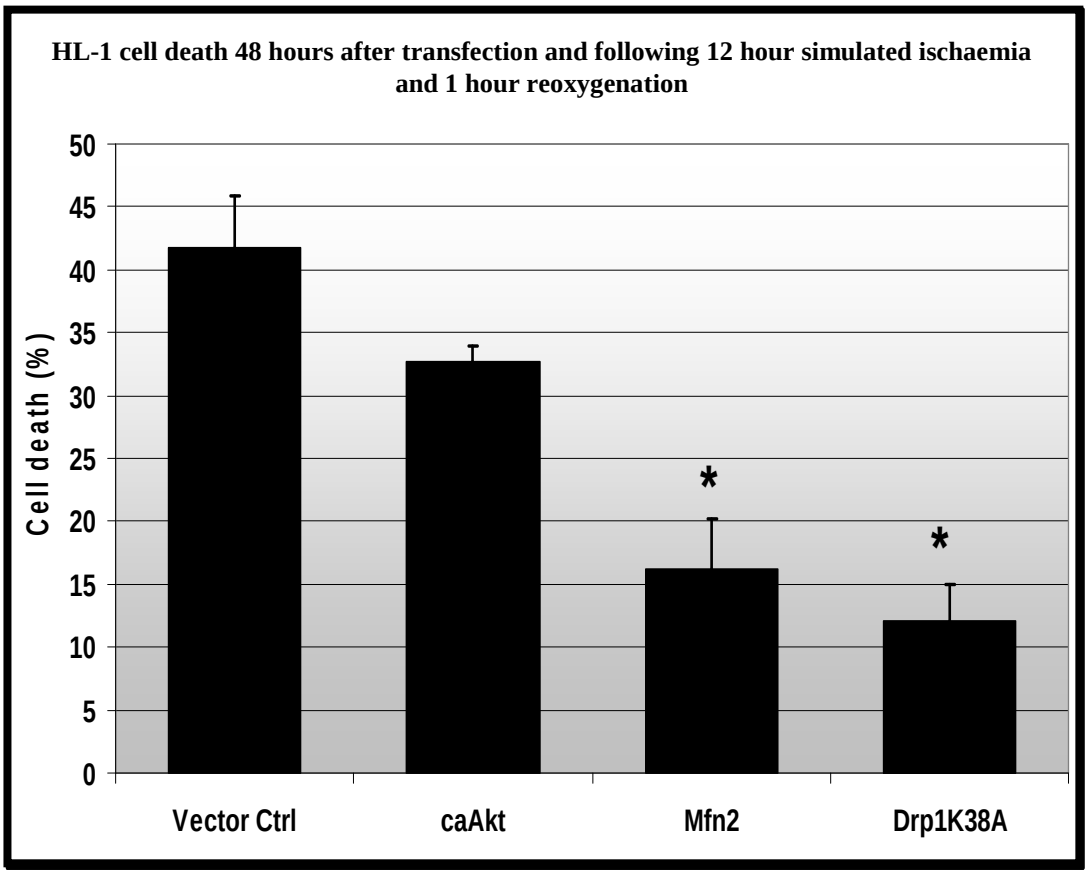

Figure 7.5: Cell death in HL-1 cells 48 hours after transfection with plasmids encoding for different proteins promoting mitochondrial fusion against empty vector, RcCMV following 12 hours hypoxia and 1 hour reoxygenation. Overexpression of HL-1 cells with Mfn2 or $Drp1_{K38A}$ decreased cell death after a period of SIRI; n = 4; *$p < 0.05$ compared to vector control.

HL-1 cells with an overexpression of caAkt for 24 hours has a significantly reduced cell death percentage of 33.0 ± 1.2% vs. 64.0 ± 5.6% for vector control; ; n = 4; *p < 0.05 compared to vector control. Overexpression of the kinase dead form of Akt, Akt-AA has a cell death percentage of 63.0 ± 3.3% (see Figure 7.6).

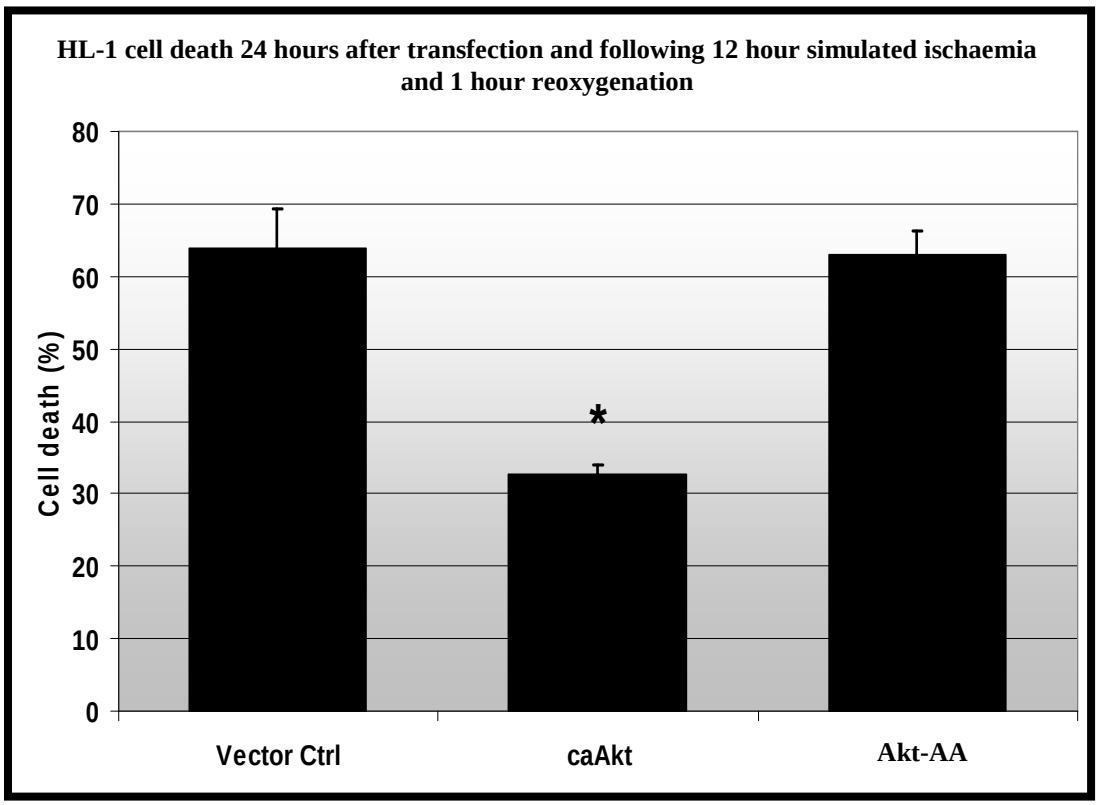

Figure 7.6: Cell death in HL-1 cells 24 hours after transfection with plasmids encoding for different proteins promoting mitochondrial fusion against empty vector, RcCMV following 12 hours hypoxia and 1 hour reoxygenation. Overexpression of HL-1 cells with caAkt decreased cell death after a period of SIRI, compared with control; n = 4; *p < 0.05 compared to vector control.

Treatment of the HL-1 cells with the Akt activator, EPO for 40 minutes prior to simulated ischaemia-reoxygenation significantly reduces cell death to 20.9 ± 3.5% vs. 53.6 ± 3.2% for vehicle control (N=4 experiments with 80 cells per treatment group. *P<0.05 compared to vehicle control) while the PI3K inhibitor, wortmannin maintained the percentage of cell death at 55.5 ± 5.4%. Treating the cells with both EPO and wortmannin together also has a cell death at 53.7 ± 8.3%. EPO treatment with an overexpression of the dominant negative form of the Akt, Akt-AA has a recorded cell death percentage of 62.4 ± 3.3% (see Figure 7.7).

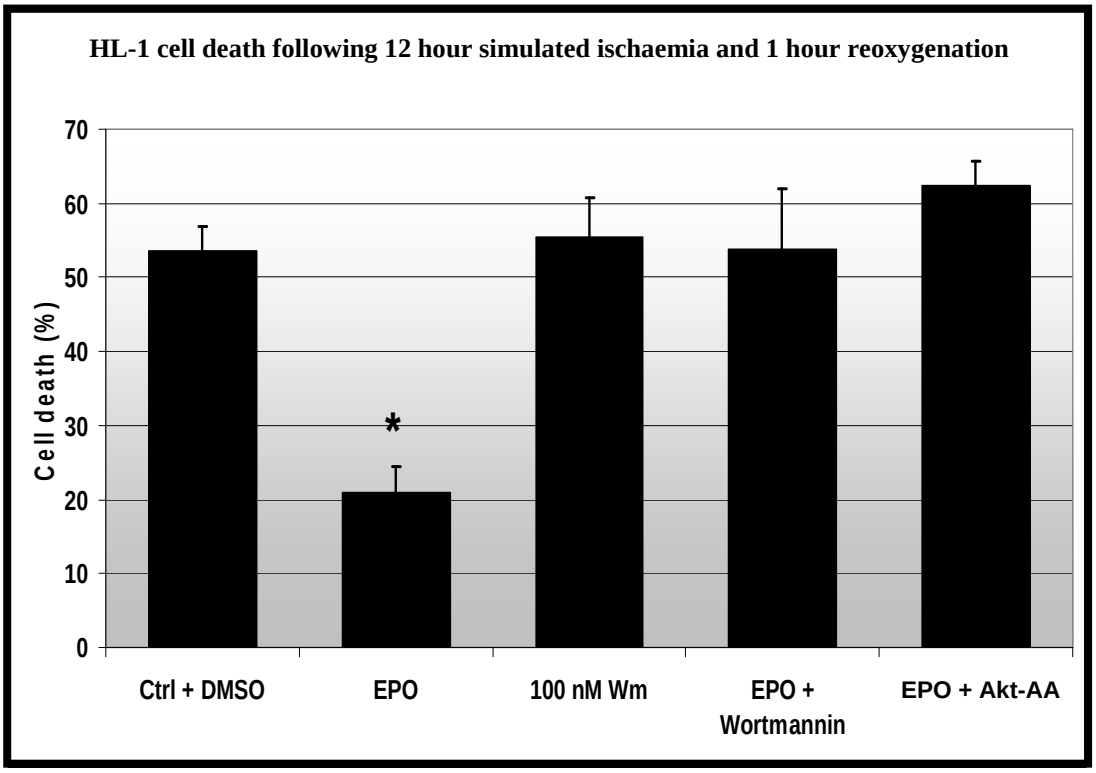

Figure 7.7: Cell death in HL-1 cells treated with different drugs following 12 hours hypoxia and 1 hour reoxygenation. Treatment with EPO at 10 U/ml for 40 minutes resulted in less cell death after SIRI. N=4 experiments with 80 cells per treatment group. *P<0.05 compared to vehicle control.

7.7 Aim (5)

To determine whether genetic or pharmacological upregulation of Akt delays opening of mPTP in HL-1 cells

In this section of the study, we were also interested to know whether overexpression of Akt delays the opening of the mPTP in HL-1 cells using the confocal laser-induced stress model.

7.7.1 Materials

The plasmids used for the mPTP assay is similar to the ones used in the survival study (see Section 7.6) to correlate cell death and mPTP opening: an empty plasmid expression vector (RcCMV); one expressing mitofusin 2 (pCB6-MYC-Mfn2) [165]; one containing $Drp1_{K38A}$ (pcDNA3.1-HA-K38A-DRP1), the dominant negative mutant form of the mitochondrial fission protein Drp1[205]; one expressing constitutively activated Akt (pcDNA3-HA-myrAkt) [346] and one containing the dominant negative form of Akt, Akt-AA (pcDNA3-HA-Akt-AA) [549]. The constitutively active Akt construct has the c-src myristoylation sequence fused in-frame to the N terminus of the HA-Akt (wild-type) coding sequence. The myristolated sequence of Akt targets it to the plasma membrane of the cells where it is constitutively activated [346]. In the N-terminal haemagglutinin (HA)-tagged mutant of Akt1 (PKBα) for the dominant-negative form of Akt, the two major regulatory phosphorylation sites (Thr308 and Ser473) were replaced by alanine residues rendering both endogenous and transfected Akt inactive [549]. $Drp1_{K38A}$ has a mutation in the GTPase domain that results in replacement of lysine 38 with alanine (designated as $Drp1_{K38A}$), disabling its ability to induce mitochondrial fission by sequestering endogenous Drp1 [181, 205]. For the survival assay, a ratio of 1:2 plasmid enhanced green fluorescent protein (pEGFP) (Clontech) expression plasmid: plasmid of interest was included in order to permit visual assessment of mitochondrial morphology. All plasmids were a generous gift of Dr Luca Scorrano (Padova, Italy). EPO (Neorecormon, Roche) was diluted in distilled water to achieve a working concentration of 5000 U / ml. Wortmannin (Tocris) was dissolved in DMSO to

achieve a working concentration of 100 µM. TMRM was dissolved in DMSO and added to the Krebs buffer such that the final concentration is 3 µM.

7.7.2 Experimental protocol

To test the hypothesis that fused mitochondria protects the cells against ischaemia-reperfusion injury by preventing opening of mPTP in the mitochondrial membrane; we subjected the HL-1 cells transfected with either one of the following:

1. RcCMV – empty vector (Vector Control)
2. caAkt – constitutively active Akt
3. $Drp1_{K38A}$ – the dominant negative form of the fission protein
4. Mfn2 – fusion-promoting protein

to confocal laser-induced reactive oxygen species release to trigger the opening of the mPTP. For each transfected cell as represented in green, ROI analysis was performed on the section of the cell containing TMRM. For each treatment group, approximately 60 cells were subjected to ROI analysis. The varying fluorescent intensities for the cells were converted to Excel format and subsequently into line graphs, and the half-times to achieve maximum fluorescent intensity determined to compare the time needed for mPTP opening upon lasers-induced release of free oxygen radicals from TMRM. EPO and wortmannin were used to confirm the effects of Akt and its relative location in the RISK pathway.

7.7.3 Results

Normalised half-time until mPTP opening for cells with an overexpression of caAkt for 48 hours is 2.0 ± 0.4 while cells with an overexpression of Mfn2 for 48 hours have a normalised half time of 2.3 ± 0.7. only cells with an overexpression of $Drp1_{K38A}$ have a significant delay in the normalised half-time until mPTP opening of 2.4 ± 0.3 compared to the vector control at 1.0 ± 0.1; N=4 experiments with 20 cells per treatment group; *P<0.05.

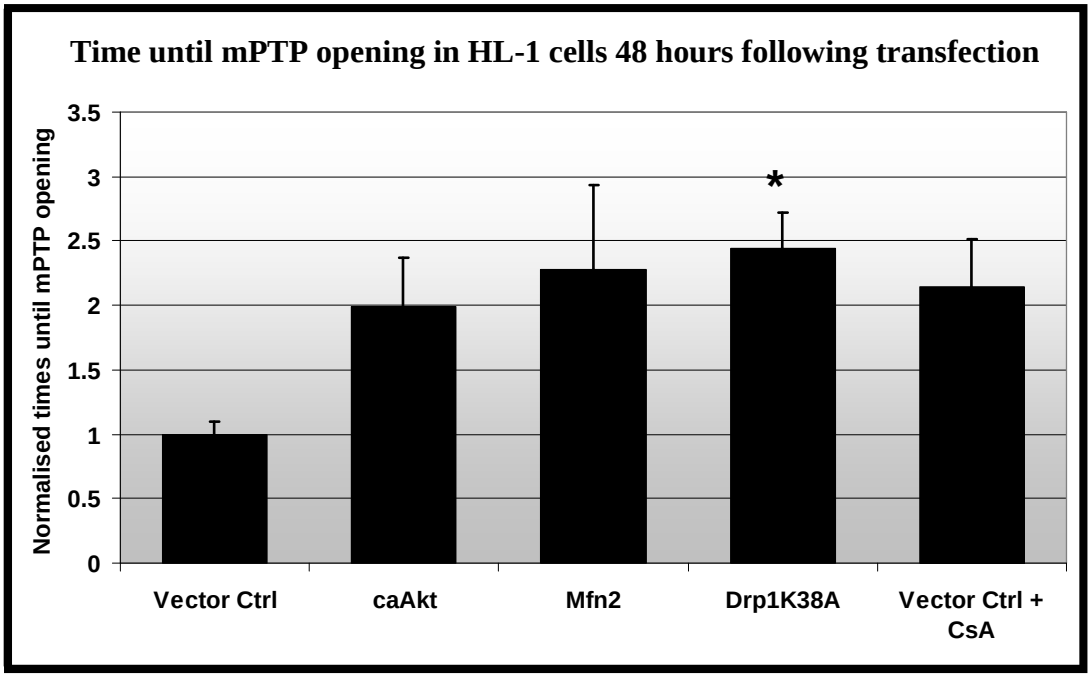

Figure 7.8: Normalised half-times to reach maximum red fluorescent intensity for HL-1 cells transfected with different fusion proteins for 48 hours followed by confocal-lasers induced oxidative stress. CsA acts as a positive control. Over-expressing caAkt, Mfn2, or $Drp1_{K38A}$ delayed the time taken to induce mPTP opening, with only $Drp1_{K38A}$ achieving significance. As expected, CsA delayed the time taken to induce mPTP opening. N=4 experiments with 20 cells per treatment group. *P<0.05.

HL-1 cells with an overexpression of caAkt for 24 hours have a significantly delayed normalised half-time until mPTP opening by 2.4 ± 0.4 fold vs. 1.0 ± 0.1 for vector control; N=4 experiments with 20 cells per treatment group. *P<0.05 vs. vehicle control. Cells with overexpressed Akt-AA have a normalised half-time of 0.5 ± 0.1. Treatment with CsA significantly delayed the time until mPTP opening in cells with an overexpression of vector control for 24 hours by 2.1 ± 0.3 fold; N=4 experiments with 20 cells per treatment group; *P<0.05 vs. vehicle control.

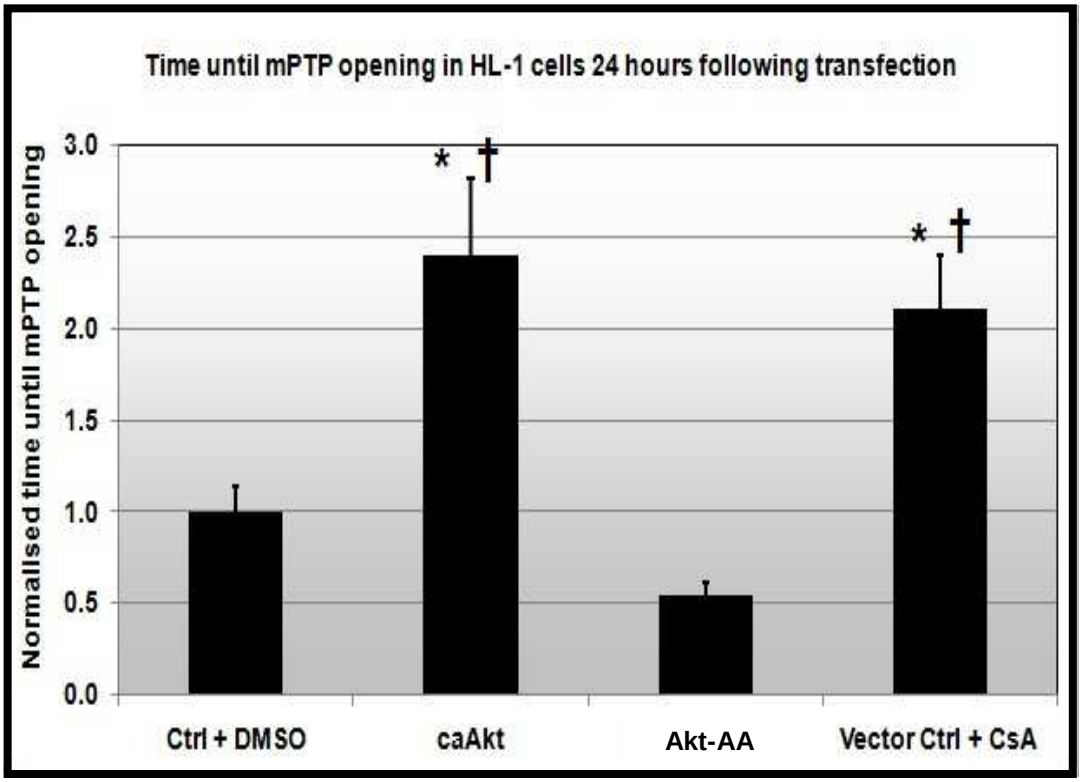

Figure 7.9: Normalised half-times to reach maximum red fluorescent intensity for HL-1 cells transfected with different plasmids for 24 hours followed by confocal-lasers induced oxidative stress. CsA acts as a positive control. Over-expressing caAkt significantly delayed the time taken to induce mPTP opening. As expected, CsA delayed the time taken to induce mPTP opening. N=4 experiments with 20 cells per treatment group. *P<0.05 vs. vehicle control, †p<0.05 compared to Akt-AA.

Treatment with EPO for 40 minutes significantly delayed the normalised half-time until 1.8 ± 0.2 vs. 1.0 ± 0.1 for vehicle control; N=4 experiments with 20 cells per treatment group; *P<0.05. Cells treated with wortmannin have a normalised time until mPTP opening at 1.2 ± 0.3. The beneficial effects of EPO in terms of delaying mPTP opening was blocked by the use of wortmannin (1.1 ± 0.2) and Akt-AA (0.5 ± 0.1). Treatment with CsA delayed the time significantly at 2.1 ± 0.3; N=4 experiments with 20 cells per treatment group; *P<0.05.

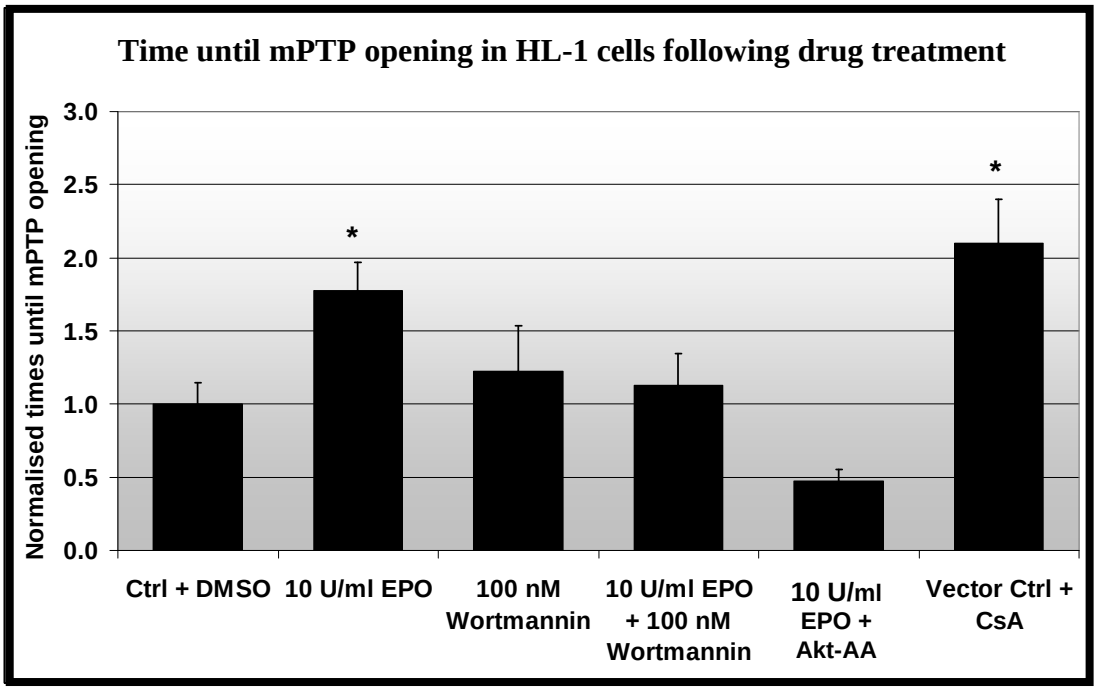

Figure 7.10: **Normalised half-times to reach maximum red fluorescent intensity for HL-1 cells treated with different drugs under confocal-lasers induced oxidative stress. CsA acts as a positive control.** Treatment with EPO at 10 U/ml for 40 minutes resulted in a significant delay in the time taken to induce mPTP opening. As expected, CsA delayed the time taken to induce mPTP opening. N=4 experiments with 20 cells per treatment group. *P<0.05

7.8 Aim (6)

To determine whether genetic or pharmacological upregulation of Akt modulates mitochondrial morphology in HL-1 cells

After demonstrating the pro-survival and delaying of mPTP opening effects of Akt overexpression in previous sections, we investigated the effects of Akt overexpression on the modulation of mitochondrial morphology in HL-1 cells in this section.

7.8.1 Materials

To investigate the changes in mitochondrial morphology in HL-1 cells following up-regulation of Akt, similar plasmids used in the previous sections investigating cell death (see Section 7.6) and mPTP (see Section 7.7) were also used in this study: an empty plasmid expression vector (RcCMV); one expressing mitofusin 2 (pCB6-MYC-Mfn2) [165]; one containing $Drp1_{K38A}$ (pcDNA3.1-HA-K38A-DRP1), the dominant negative mutant form of the mitochondrial fission protein Drp1[205]; one expressing constitutively activated Akt (pcDNA3-HA-myrAkt) [346] and one containing the dominant negative form of Akt, Akt-AA (pcDNA3-HA-Akt-AA) [549]. The constitutively active Akt construct has the c-src myristoylation sequence fused in-frame to the N terminus of the HA-Akt (wild-type) coding sequence. The myristolated sequence of Akt targets it to the plasma membrane of the cells where it is constitutively activated [346]. In the N-terminal haemagglutinin (HA)-tagged mutant of Akt1 (PKBα) for the dominant-negative form of Akt, the two major regulatory phosphorylation sites (Thr308 and Ser473) were replaced by alanine residues rendering both endogenous and transfected Akt inactive [549]. $Drp1_{K38A}$ has a mutation in the GTPase domain that results in replacement of lysine 38 with alanine (designated as $Drp1_{K38A}$), disabling its ability to induce mitochondrial fission [205]. For the survival assay, a ratio of 1:2 plasmid enhanced green fluorescent protein (pEGFP) (Clontech) expression plasmid was included in order to permit visual assessment of mitochondrial morphology. All plasmids were a generous gift of Dr Luca Scorrano (Padova, Italy). EPO (Neorecormon, Roche) was diluted in distilled water to achieve a working concentration of 5000 U / ml. Wortmannin (Tocris) was dissolved in DMSO to achieve a working concentration of 100 μM. Krebs buffer comprising (in

mM): NaCl 118.0, $NaHCO_3$ 25.0, d-Glucose 11.0, KCl 4.7, $MgSO_4.7H_2O$ 1.2, KH_2PO_4 1.2, $CaCl_2.2H_2O$ 1.8, and HEPES 10.0 (pH 7.4) was used as imaging buffer for confocal microscopy studies.

7.8.2 Experimental protocol

Upon reaching confluency of around 50 – 60% (~24 hours after seeding), the cells were transfected with one of the following plasmids:

1. RcCMV – empty vector (Vector Control)
2. caAkt – constitutively active Akt
3. $Drp1_{K38A}$ – the dominant negative form of the fission protein
4. Mfn2 – fusion-promoting protein

mtRFP was always co-transfected to visualise the mitochondria as well as to indicate uptake and expression of the plasmids. As this was the first time that these proteins were overexpressed in a HL-1 cardiac cell line, we had to determine the optimum duration of plasmids expression to induce significant changes in mitochondrial morphology. EPO and wortmannin were used to elucidate the probable pathway linking Akt to the changes in mitochondrial morphology, if any. Images of twenty randomly chosen cells were taken after 24 hours for one set of experiments and 48 hours for another set of cells and this was repeated for each group in at least four independent transfection experiments giving a total number of approximately 80 cells per treatment group. Three investigators, blinded to the initial treatment, independently assigned the cells as displaying either predominantly (>50%) elongated or (>50%) fragmented mitochondria, indicating that either mitochondrial fusion or fission, respectively, was the predominant process in that cell at that particular time, a method which has been adapted from a previously published study [165].

7.8.3 Results

HL-1 cells with an overexpression of caAkt for 48 hours have a percentage of cells with elongated mitochondria of 51.5 ± 4.2% vs. 43.0 ± 6.9% for vector control. Overexpression of Mfn2 and the mutant form of the fission protein, $Drp1_{K38A}$ for 48 hours significantly increases the proportion of cells with elongated mitochondria to 68.0 ± 4.4% and 64.8 ± 6.1% respectively; N=4 experiments with 80 cells per group; *$p < 0.05$ (see Figure 7.11).

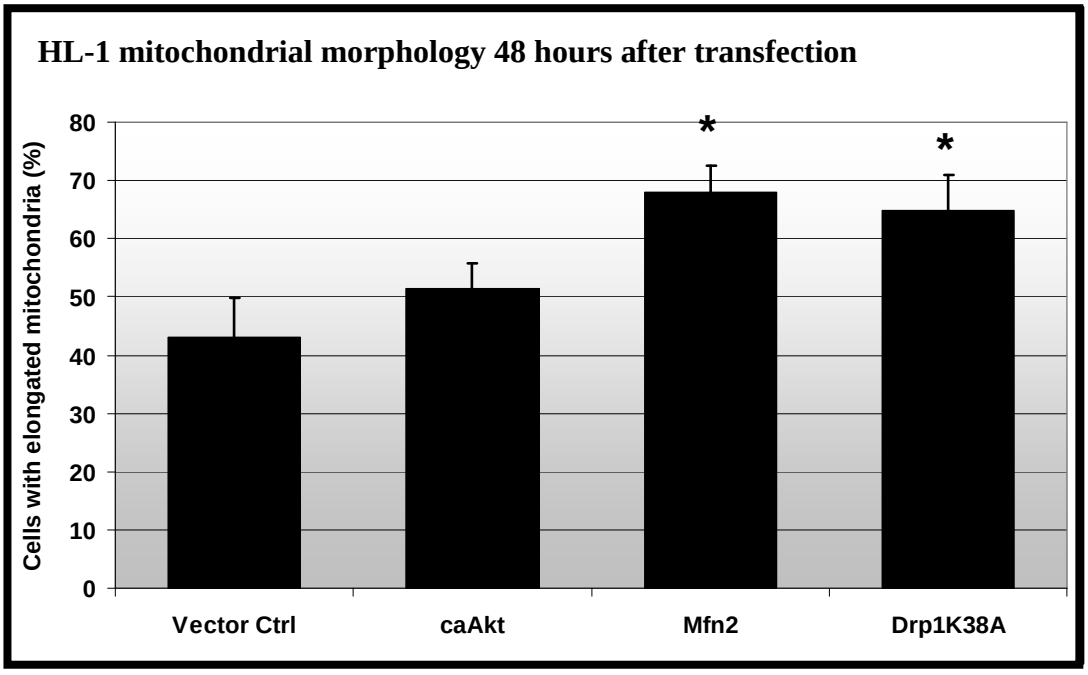

Figure 7.11: Effects of overexpression of different proteins to the morphology of mitochondria in HL-1 cells over a period of 48 hours A significant trend of increasing cells with elongated mitochondria was seen for cells with an overexpression of Mfn2 and $Drp1_{K38A}$. N=4 experiments with 80 cells per group; *$p < 0.05$ compared to Vector Control.

Overexpression of the caAkt construct for 24 hours significantly increased the proportion of HL-1 cells with elongated mitochondria to 73.0 ± 5.0% vs. 49.0 ± 5.8% for vector control; N=4 experiments with 80 cells per group; *$p < 0.05$. Overexpression of the dominant negative construct of Akt, Akt-AA reduces proportion of HL-1 cells with elongated mitochondria to 38.8 ± 16.6% (see Figure 7.12 & 7.13).

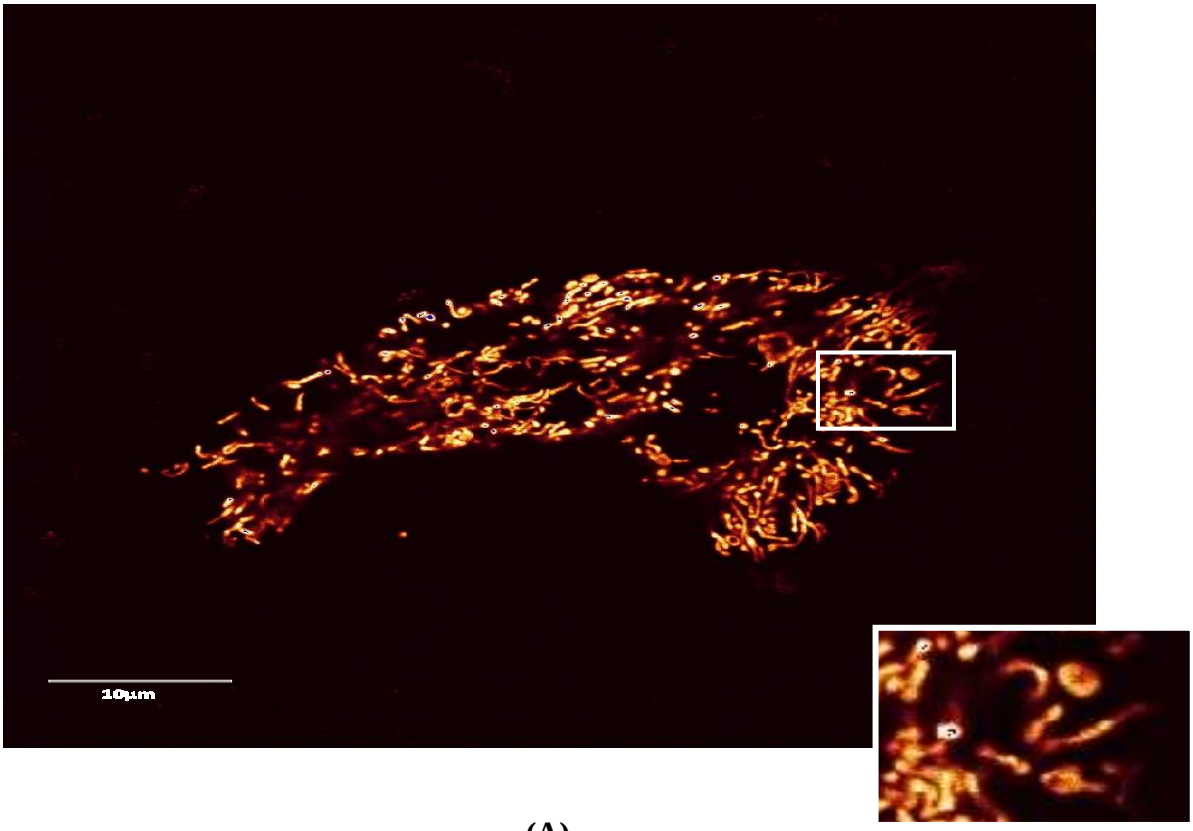

(A)

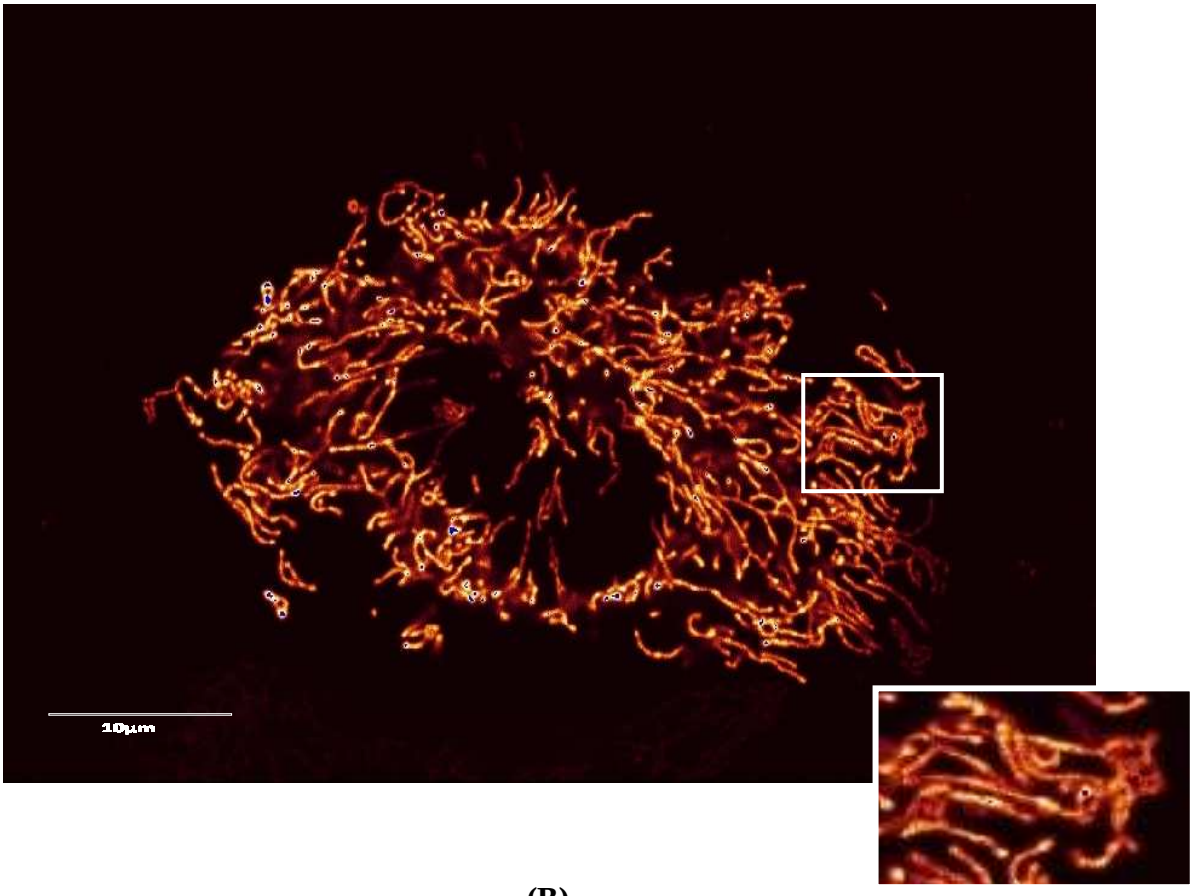

(B)

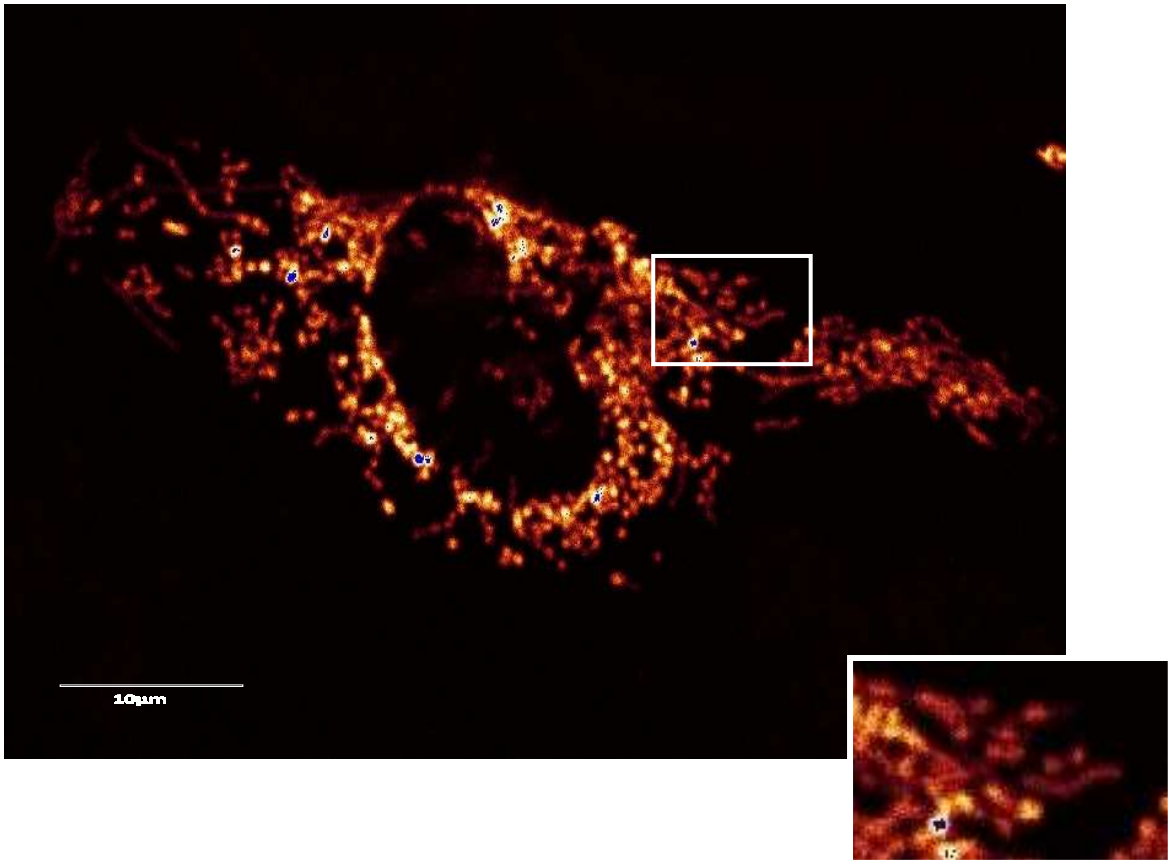

(C)

Figure 7.12: Representative confocal images of HL-1 cells transfected with mtRFP in addition to (A) empty vector control, (B) caAkt, (C) Akt-AA.

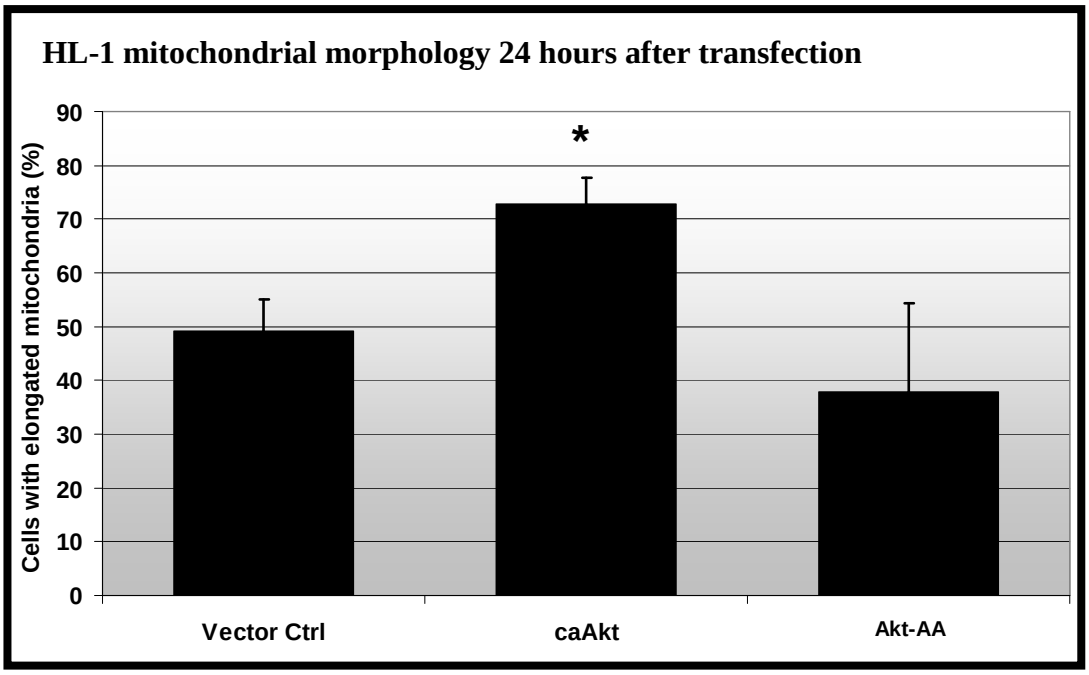

Figure 7.13: Effects of overexpression of different proteins to the morphology of mitochondria in HL-1 cells over a period of 24 hours A significant trend of increasing cells with elongated mitochondria was seen for cells with an overexpression of caAkt. Overexpression of the Akt-AA at 24 hours did not fragment the mitochondria significantly N=4 experiments with 80 cells per group; *p < 0.05 compared to vector control.

Treatment of HL-1 cells with EPO for 40 minutes significantly increased the proportion of cells with elongated mitochondria to 67.0 ±v 3.4% compared to treating the cells with vehicle control at 29.9 ± 3.5%; N=4 experiments with 80 cells per group; *p < 0.05. Percentage of cells with elongated mitochondria in cells treated with wortmannin and EPO + wortmannin for 40 minutes was 27.8 ± 4.8% and 23.9 ± 10.1% respectively. Percentage of cells with elongated mitochondria in cells with an overexpression of the Akt-AA construct with EPO treatment was 41.4 ± 7.8% (see Figure 7.14 & 7.15).

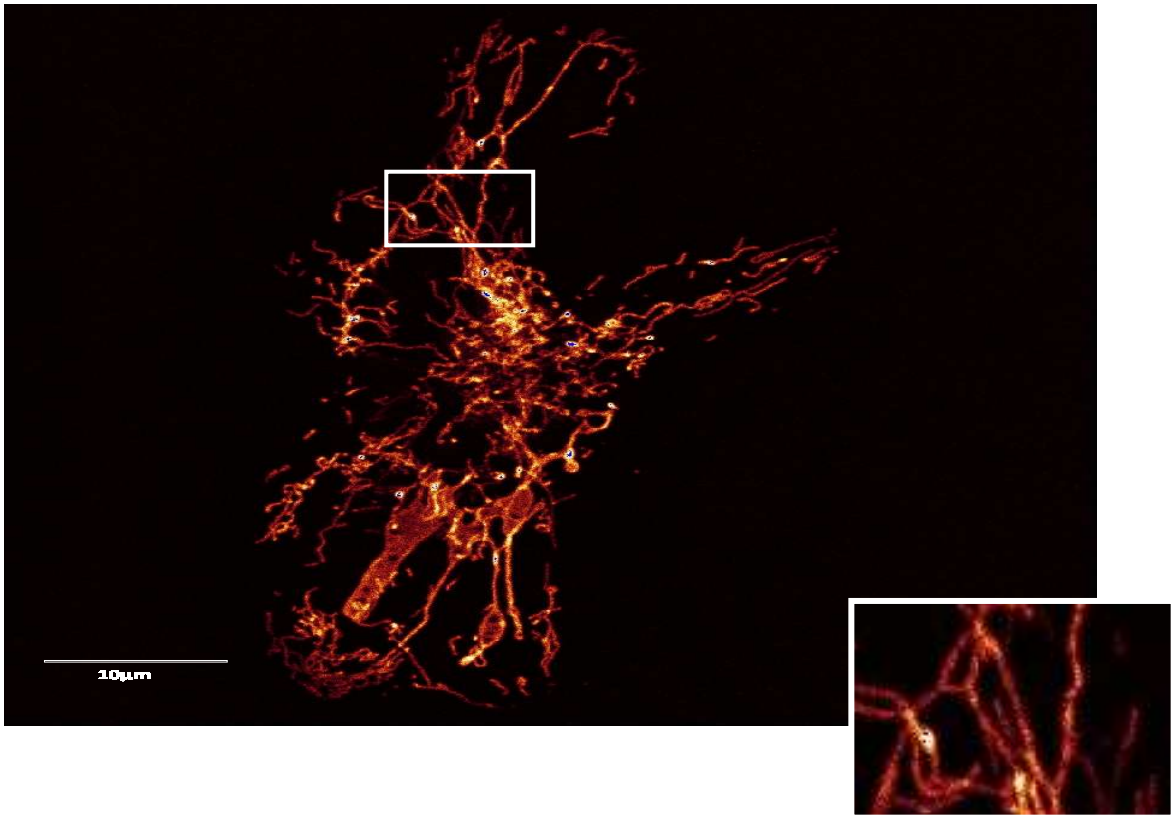

(A)

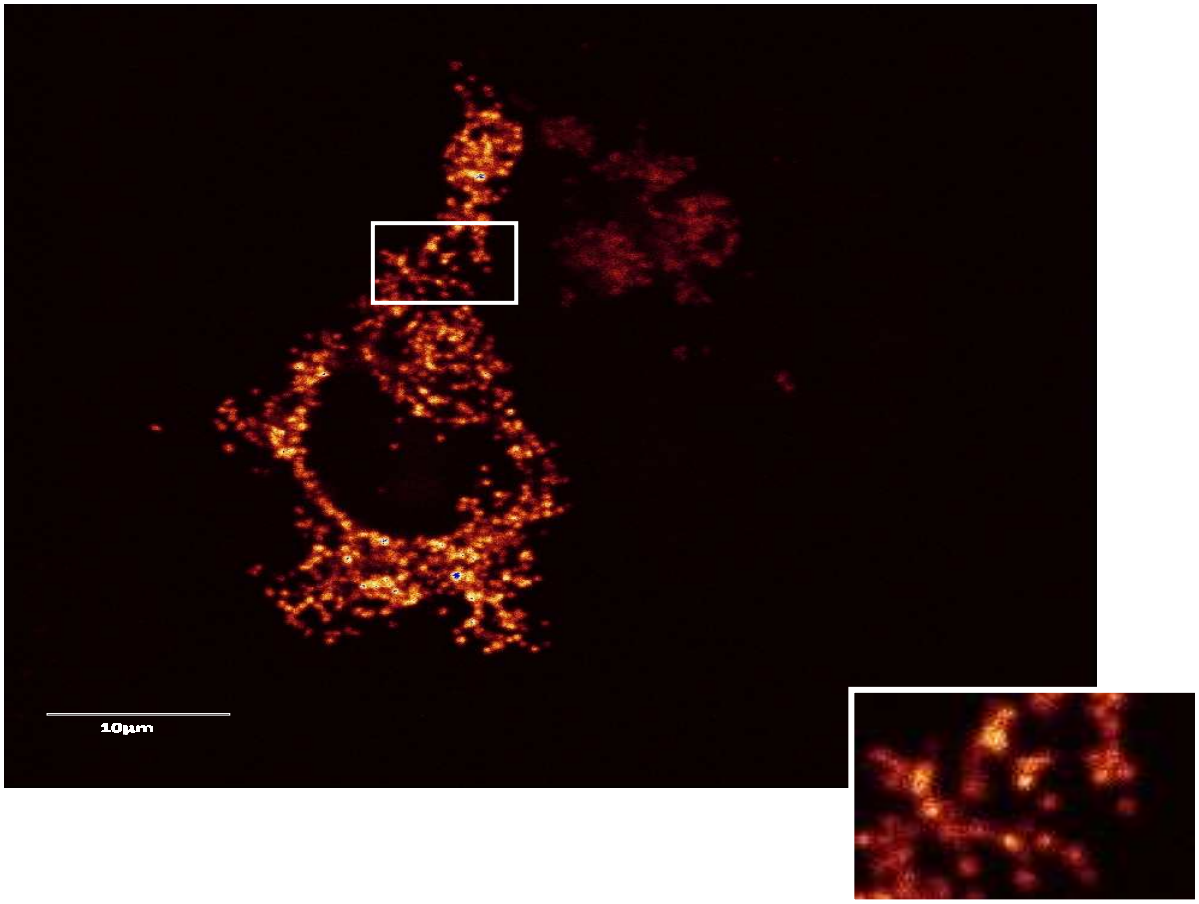

(B)

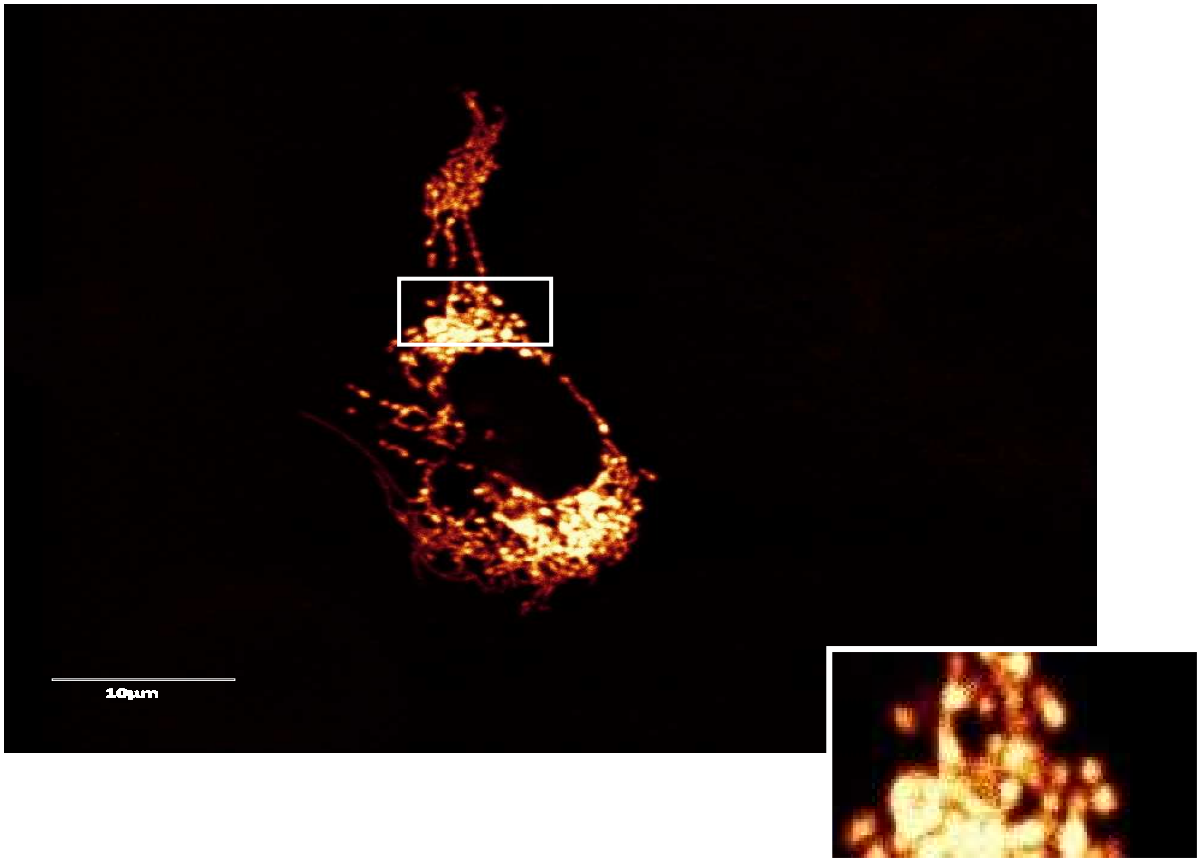

(C)

Figure 7.14: Representative confocal images of HL-1 cells transfected with mtRFP in addition to treatment with (A) EPO, (B) EPO with wortmannin, (C) EPO with co-transfection of Akt-AA

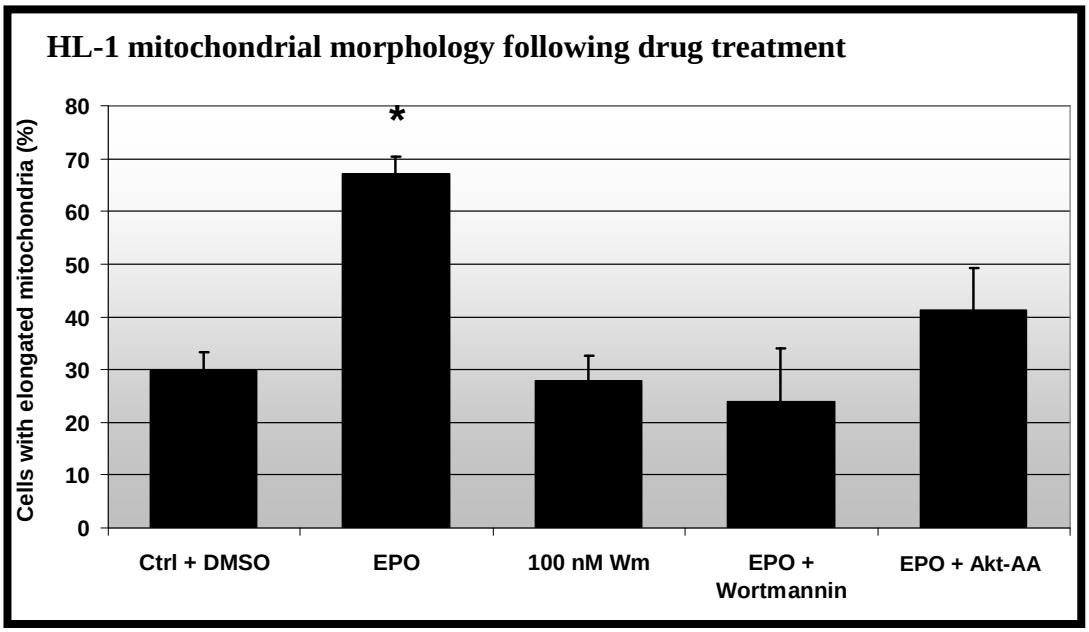

Figure 7.15: Effects of drug treatment to the morphology of mitochondria in HL-1 cells. A trend of increasing cells with elongated mitochondria was seen for cells treated with 10 U/ml EPO for 40 minutes. N=4 experiments with 80 cells per group; *$p < 0.05$ compared to Vector Control.

7.9 Discussion

Modulation of mitochondrial morphology in HL-1 cells by a PKA activator, cBiMPS

The results shown indicate that the use of cBiMPS increase the proportion of cells with elongated mitochondria after a duration of 40 minutes incubation at 37°C, albeit not significantly. cBiMPS is an activator of PKA [419, 550], which has been proven to phosphorylate and inhibit the fission protein, Drp1 [182]. Theoretically, using cBiMPS to activate PKA in the HL-1 cells should also increase proportion of cells with elongated mitochondria significantly. This claim is further supported by Fabio Di Lisa and co-workers where they showed that activation of PKA is very potent in reduction of infarct size (data and details not available). The question remains as to whether the duration of incubation of cells with cBiMPS was too long. According to the time-response study conducted, the increase in proportion of cells would seem to be within the first 15 minutes of incubation. Nevertheless, as the priority at the time this study was conducted was the use of the *mdivi-1* drug, which also phosphorylates and inhibits Drp1, the idea was to incubate the PKA activator, cBiMPS and *mdivi-1* for the same duration to standardise the study. Furthermore, an incubation time of 40 minutes seemed reasonable at that time as there was an increase of proportion of cells with elongated mitochondria up to ~60%. It might also be worthwhile to explore the alternative activators of PKA. There are a few varieties of PKA activators in the market, e.g. 8-CPT-cAMP, 6-MB-cAMP, 6-MBC-cAMP, 8-PIP-cAMP, 8-HA-cAMP and 8-pCPT-2′-O-Me-cAMP. Nevertheless, Sp-5,6-DCl-cBiMPS was considered to be the best option as a PKA activator compared to other activators such as dibutyryl-cAMP or 8-CTP-cAMP [419, 551]. The reason cBiMPS from Biomol was chosen is because it was a new cAMP analogue as well as a potent and specific activator of cAMP-dependent protein kinase. Good cell permeability and resistance to hydrolysation by phosphodiesterases are other factors which make cBiMPS an attractive option. The dosage of cBiMPS is another factor that may be the cause for the failure to achieve significance in this part of the study. We chose the current concentration based on the study by Sandberg and co-workers in 1991 where human platelets were used [419]. It is therefore, our mistake in not realising the differences in cell types used and not performing a proper dose-control study.

Another option is to employ the use of genetic overexpression of PKA in the cells which will need plasmids carrying gene inserts for PKA. In summary, the role of PKA in inhibiting mitochondrial fragmentation and increasing proportion of cells with elongated mitochondria will need further re-investigation.

Protecting the HL-1 cells against sIR by inhibition of mitochondrial fission via pharmacological activation of PKA using cBiMPS

Although the previous section did not show significance in the increase in proportion of cells with elongated mitochondria with treatment of cBiMPS, we still followed on the experiments where cBiMPS was tested to determine whether PKA activation reduces cell death following sIR. In this section, we demonstrated that treatment with cBiMPS reduced cell death significantly following sIR. The cardioprotection elicited by activation of PKA has been shown in a study by Sanada and co-workers where transient activation of PKA during IPC reduces infarct size through Rho-kinase inhibition and actin cytoskeleton deactivation [276]. In that study, PKA was activated using the cell-permeable cAMP analogue dibutyryl-cAMP. Similar to the effects of *mdivi-1*, the phosphorylation and inhibition of Drp1 impairs fragmentation of mitochondria following ischaemia and may increase the proportion of elongated mitochondria hence having a better survival possibility. The lack of significance in the increase in proportion of cells with elongated mitochondria however seems to allude to the possibility that PKA activation may also protect the cells via another mechanism other than modulating mitochondrial morphology.

Delaying the opening of the mPTP in HL-1 cells by activating PKA using cBiMPS

Pre-treatment with cBiMPS for 40 minutes prior to confocal laser-induced ROS release delayed the time until mPTP slightly compared to the use of EPO or CsA. Activation of PKA solely has never been linked to inhibition of mPTP opening in cardiac cells. Yet, the study of Sanada has linked the activation of PKA to cardioprotection from IPC [276]. The inhibition of mPTP has long been known to be

the crucial end effect of IPC hence it would seem probable that activation of PKA may trigger certain mechanisms that can lead to inhibition of the mPTP as well. As shown in previous studies, activation of PKA is part of the framework (e.g. opening of the mitoK$_{Ca}$ channel to prevent calcium overloading) leading to inhibition of mPTP in cardioprotection [529, 530, 552, 553]. In addition, the results from previous sections conducted in our study showed that promotion of mitochondrial elongation protects by inhibiting the opening of the mPTP. In this section, PKA activation did not inhibit the opening of the mPTP which would not be totally unexpected judging from the fact that PKA activation in the previous section of our study also failed to induce a significant increase in fused mitochondria. These studies should be repeated once the timing and doses of cBiMPS have been re-optimised. Another alternative will be to increase the numbers of experiments for this particular mPTP assay using other activators of PKA as a control.

Protecting the HL-1 cells against sIR by genetic overexpression of caAkt

Protein Kinase B (Akt1) has long been identified as a pro-survival kinase in many cell types [299-301, 304, 330, 346, 554]. Results from this section show that the overexpression of Akt1 is also cardioprotective in the HL-1 cardiac cell line. Based on our previous studies using the mitochondrial-shaping proteins such as Mfn1, Mfn2 and Drp1$_{K38A}$, we initially overexpressed caAkt1 for 48 hours before subjecting the cells to sIR. However, we noticed that the cardioprotective effects were not so pronounced compared to caAkt1 that was only expressed for 24 hours prior to sIR. Therefore, we conclude that this may be due to an acute beneficial effect of Akt1 expression where chronic Akt1 expression may abrogate the beneficial effects of Akt1. This phenomenon is in accordance with previous studies conudcted in which they showed that the chronic expression of Akt1 causes hypertrophy in cardiac muscle [338], skeletal muscle [555] and islet beta cell mass [556]. In the *in vivo* system though, Akt1 effects is counteracted by the PTEN, which prevents chronic effects that may be disadvantageous. The overexpression of the dominant negative form of the Akt, Akt-AA also abrogates the cardioprotective effect of Akt.

The use of erythropoietin (EPO), a well known activator of Akt also protects the cells against sIR. EPO is well-known for its survival and proliferative activity and has been used in the cardiac research field for treating patients with arrhythmia [557] and myocardial injury following reperfusion [255, 420, 558-562]. The concentration of EPO (10 U/ml) was determined based on the study by Tramontano *et al* in which neonatal ventricular rat myocytes (NVRM) were used [422]. Pro-survival effects of Akt are conferred via the RISK pathway with EPO acting as an activator of the RISK pathway. Upon activating the receptors, PI3K is activated hence promoting translocation of Akt1 from cytosol to plasma membrane where it is activated and translocates to different locations in the cell to perform various functions. In our study, we attempted to promote cardioprotection by directly over-expressing caAkt1 and also promoting activation of Akt via the upstream activator of the RISK pathway using EPO. From our results, it may seem that the protective effects of EPO is more potent than using caAkt1 alone but there is no significance between the reduction in cell death caused by Akt1 and EPO. This protection conferred by EPO as an activator of endogenous Akt1 can be blocked by using the PI3K inhibitor, wortmannin, which has been shown to inhibit the PI3K by binding to its catalytic subunit, p110 [563]. Concentration of wortmannin used (100 nM) was based on previous studies conducted [487, 563-566]. The nanomolar concentration of wortmannin was deemed suitable in the investigation of the effects of PKB, as it does not interfere with the activity of PKA, PKC or CaMKII [564]. Treatment duration for wortmannin was similar to EPO treatment to standardise the treatment protocol. Overexpression of the dominant negative form of Akt1 also abrogated the protection conferred by EPO hence placing PI3K and Akt downstream of the EPO receptor. This dominant negative construct of Akt acts by inhibiting the endogenous Akt and has been previously used to compare against and verify the results obtained by constitutively active Akt [567-570]. In conclusion, we verified the fact that Akt1 is cardioprotective in the settings of sIR. Our next step is to correlate the cardioprotective effects of Akt1 to inhibition of mPTP opening through which we will investigate the potential mechanism of this inhibition by Akt.

Delaying the opening of the mPTP in HL-1 cells by genetically over-expressing caAkt

Our results obtained from this section show that overexpression of caAkt1 or treatment of the HL-1 cells with EPO successfully delays the opening of the mPTP. CsA was used as a positive control to verify the involvement of the pore in this study. This inhibition of mPTP opening can be abrogated by use of the PI3K inhibitor, wortmannin or overexpression of the dominant negative/kinase dead form of the Akt1, Akt1K178A. The results obtained are in agreement with the previous survival study where both Akt1 and EPO protect the cells against sIR. Previous studies by Davidson *et al* in 2006 also showed the mPTP inhibition capability of Akt1 in the settings of confocal laser-induced ROS stress with HL-1 cells [259]. Nevertheless, a study by Clarke *et al* in 2008 claimed that the inhibition of mPTP is mainly due to reduction of ROS levels rather than protein phosphorylation, though the role of Akt in inhibition of mPTP was still maintained under the caspase-dependent pathway [506]. The use of EPO to inhibit mPTP has been perpetuated in numerous studies but the mechanism of EPO in inhibiting mPTP still remains unresolved. Similarly, there is a lack of a consensus agreement in establishing the primary endpoint of mPTP inhibition by Akt. Most of the studies have implicated the phosphorylation of GSK3β [356, 571, 572] or upregulation of NOS in inhibition of the pore by Akt [573-575]. In the next section, we attempt to investigate the possibility of Akt mediating mPTP inhibition through modulation of mitochondrial dynamics. EPO as an Akt activator therefore should also be able to inhibit the mPTP. Blocking the downstream effectors of EPO by using wortmannin as a PI3K inhibitor blocked the mPTP inhibiting effect. Similarly, inhibiting the Akt directly by use of the AktK178A also prevents the mPTP opening from being delayed. Nevertheless, the use of the dominant negative form of Akt, Akt_{-AA} and wortmannin in investigating the effects on opening of the mPTP has never been explored in previous literature.

Modulation of mitochondrial morphology in HL-1 cells by genetically over-expressing caAkt

In this section, we show that overexpression of caAkt1 increases the proportion of HL-1 cells with elongated mitochondria. Treatment with EPO for 40 minutes also increases the proportion of cells with elongated mitochondria. Conversely, this effect can be blocked by use of wortmannin and overexpression of $Akt1_{-AA}$. We can therefore postulate that Akt plays a role in modulation of mitochondrial dynamics and this may explain the mPTP inhibition effects of Akt1. At this stage, we still cannot infer directly that Akt1 overexpression promotes mitochondrial elongation as the increase in proportion of cells with elongated mitochondria can be either due to promotion of fusion or inhibition of fission. We will therefore need to follow up this study in future using photo-activable green fluorescent protein (PA-GFP) to monitor and detect mitochondrial fusion. If there is significant mitochondrial fusion by overexpression of Akt1, we should expect to see a faster spread of PA-GFP among neighbouring mitochondria. In the case of inhibition of fission however, there should be less of a PA-GFP spread to neighbouring mitochondria. This concept has been explored by the group of Orian Shirihai in which they investigated networking of the mitochondrial network in beta cells [463], COS cells and INS cells [576]. Yet, the clarification of whether Akt promotes mitochondrial fusion or inhibit fission was not investigated. This is the first time that EPO as an Akt activator also increases number of cells with elongated mitochondria, in line with previous sections of our study, cells with elongated mitochondria have a higher resistance towards sIR and delayed opening of the mPTP.

7.10 Conclusion

In this chapter of the study, we have demonstrated that activating the PKA in HL-1 cardiac cells protects against sIR. However, there appears to be no significant effect on mitochondrial morphology or delaying of mPTP opening. Hence, we believe the cardioprotective effects of PKA may be independent of mitochondrial morphology and mPTP opening, although this study has to be repeated. However, genetically oever-expressing the PKB in HL-1 cells protects against sIR, delays opening of the mPTP and increases the proportion of cells with elongated mitochondria.

Chapter Eight: SUMMARY AND DISCUSSION

The main findings of the current study are:

1. Overexpression of the mitochondrial fusion proteins Mitofusin 1 and 2 (Mfn1 and Mfn2), the dominant negative mitochondrial fission protein, $Drp1_{K38A}$, or treatment with *mdivi-1* increased the proportion of HL-1 cells with fused mitochondria, protects against sIR and innibits mPTP opening .
2. Inhibiting mitochondrial fragmentation in adult cardiomyocytes, which has a very different spatial arrangement of mitochondria compared to the HL-1 cell line by the use of *mdivi-1*, the small molecule inhibitor of Drp1, protects against sIRI and delayed the time until mPTP opening.
3. The use of *mdivi-1* in an *in vivo* murine infarct model successfully reduces infarct size following sIR.
4. Genetically over-expressing the pro-survival kinase, Akt or upregulation of endogenous Akt by the use of erythropoietin (EPO) induced an increase in proportion of HL-1 cells with elongated mitochondria and protects the cells against sIR by inhibition of mPTP opening.

We show for the first time that promoting mitochondrial fusion by the overexpression of fusion proteins is able to promote survival of HL-1 cells, a murine atrial-derived cell line in the context of simulated ischaemia-reperfusion injury (IRI) possibly through the inhibition of mPTP opening. Interestingly, the inhibition of the fission protein, Drp1 by the small molecule inhibitor, *mdivi-1*, also seems to protect the cells against sIRI by inhibition of the mPTP. These findings have been extrapolated to the settings of the adult cardiomyocytes where treatment of cells with *mdivi-1* reduced cardiomyocytes death following IR and delays the opening of the mPTP while mice treated with the *mdivi-1* has significantly lesser degree of mitochondrial fragmentation following simulated ischaemia and reduced infarct size.

Fusion of both of the mitochondrial membrane has been previously shown to be beneficial to the cells in terms of preventing apoptotic cell death, albeit the exact reason was not clearly known [489, 490]. Downregulation or impairment of the mitochondrial fusion proteins Mfn1, Mfn2 or OPA1 promote fragmentation of

mitochondria leading to disruption of the mitochondrial respiration system and depolarisation of mitochondrial membrane potential [196]. sIR in renal tissue has been found to fragment the mitochondria through the action of Drp1 leading to cellular apoptosis and renal injury. In our study, we demonstrated that overexpression of Mfn1, Mfn2 and $Drp1_{K38A}$, a mutant form of the fission protein Drp1, or the usage of *mdivi-1* significantly increases the number of cells with elongated mitochondria, by either directly promoting mitochondrial fusion (Mfn1, Mfn2) or inhibition of mitochondrial fragmentation ($Drp1_{K38A}$ and *mdivi-1*). The mutation in the GTPase domain of the Drp1 protein serves to alter the original function of the Drp1 which is to promote mitochondrial fragmentation. The usage of $Drp1_{K38A}$ in our study is particularly important to show that potential effects from mitochondrial fusion derive from fusion itself and not the proteins expressed. Examples highlighting this importance can be shown by the studies of Neuspiel *et al* (2005) [462] who demonstrated that the transgenic overexpression of Mfn2 promotes cell survival by preventing Bax activation and inhibition of mitochondrial cytochrome *c* release while Mfn2 inhibition by siRNA caused the neonatal rat cardiomyocytes to be more prone to ceramide-induced apoptotic cell death [412]. In addition, there are contradicting studies in which Mfn2 has been reported to induce apoptosis in vascular smooth muscle cells and neonatal rat cardiomyocytes by inhibiting the anti-apoptotic pro-survival kinase pathway, PI3K-Akt [577, 578]. Compared to mitochondria of HL-1 cells with the empty vector RcCMV, cells with overexpression of Mfn1, Mfn2 and $Drp1_{K38A}$ have a significantly higher percentage of fused mitochondria.

Another novel finding in our study lies in the fact that EPO actually promotes mitochondrial fusion. The activation of the PI3K pathway and Akt survival kinase by EPO has been well-characterised [255, 309, 420, 480], including the inhibition of mPTP opening by activated Akt [258, 259]. Nevertheless, there exist studies which have placed a reduction in oxidative stress as more relevant rather than the phosphorylation of pro-survival kinases [506]. The crux of the issue at the moment is how Akt plays a role in inhibiting mPTP opening. To answer this question and enhance the understanding of the pro-survival cascade, we postulate that EPO activates Akt which then promotes mitochondrial fusion to inhibit the mPTP opening. Further studies will need to be carried out to elucidate the pathway, possibly by carrying out similar studies using wortmannin as a PI3K inhibitor.

Interestingly, we found that the HL-1 cells with overexpression of fusion proteins or treated with drugs that increase mitochondrial fusion rates such as *mdivi-1* have an increased resistance to simulated ischaemia-reperfusion compared to the cells which were transfected with the empty vector, RcCMV or loaded with Krebs containing DMSO. Overexpression of hFis1 promoted mitochondrial fission as expected in our study. However, the amount of live cells with overexpression of hFis1 was also surprisingly high following 1 hour reoxygenation compared to 24 hour reoxygenation. This might be due to the fact that fission does not always kill as demonstrated by some previous studies [87, 579]. Conversely, fission acts to dissipate the death signal conveyed by the endoplasmic reticulum or calcium overloading. Another important point to note is fission is a normal process in the healthy cell and acts to regulate certain stages in the cell cycle and may actually act as quality control mechanism to remove the unhealthy cells or cells that have reached senescence [172, 196, 411, 489, 580]. Similar patterns have been observed by Parone and colleagues in 2008 where they showed that inhibition of mitochondrial fission by small hairpin RNA (shRNA) targeting the Drp1 actually leads to dysfunction of the mitochondria and loss of mtDNA when measured after 96 hours [581].

The removal and subsequent reintroduction of oxygen through blood flow will cause deleterious results to cells, particularly cardiac cells in the settings of ischaemia-reperfusion [7, 9, 230]. The deprivation of oxygen is an inducer of both apoptotic and necrotic cardiac cell death, all of which converge on the mitochondria as a powerhouse of the cell as well as an apoptotic mediator [75, 540]. The survival rate or ability of a cardiomyocyte depends on the proper functioning of the mitochondrial respiratory mechanisms, which may be influenced by the elongated state of mitochondria. Medical studies have thus placed the mitochondria as a target for myocardial protection [373, 406, 582].

The role of mitochondrial morphology in determining cell fate was first shown by the study of Frank and colleagues in 2001 where they demonstrated that the mitochondria of COS cells changed from a reticulo-tubular interconnected network to a fragmented discrete punctiform phenotype, a process which was dependant on the mitochondrial fission protein, Drp1 in the presence of staurosporine [205]. Conversely, the overexpression of the mutated form of Drp1,

$Drp1_{K38A}$ prevented cytochrome *c* release and ensuing apoptotic cell death. Previous studies have also demonstrated that the inhibition of the fusion proteins Mfn1, Mfn2 or OPA1 promotes mitochondria fission with subsequent impairment of oxygen consumption, reduced mitochondrial membrane potential and decreased respiration [490]. On the contrary, the overexpression of Mfn2 has been shown to promote mitochondrial elongation with enhanced capacity for mitochondrial respiration and hyperpolarisation of the mitochondrial membrane potential [153, 583]. Nevertheless, it has been disputed that this particular effect of mitochondrial fusion is affected by Mfn2 rather than the fusion process because inhibition of Drp1 failed to mediate the same beneficial effects [490].

Following previous studies that implicated the opening of the mPTP in cardiac cell death during ischaemia-reperfusion [232, 374, 377, 584], we were inspired to investigate the possibility that the fusion of mitochondrial inner and outer membrane can actually promote cell survival possibly by inhibiting the opening of the mPTP. The mPTP has been demonstrated by many studies to play a crucial role in mediating the fate of the cardiac myocytes, as opening of the mPTP during the first few minutes of reperfusion causes an influx of solutes less than 1500 Da from the cytosol into the matrix leading to membrane depolarisation, uncoupling of oxidative phosphorylation, organelle swelling and subsequent outer membrane rupture to release pro-apoptotic cytochrome *c* into the cell [11, 477, 509]. Animal studies conducted in the past have shown reduction of myocardial infarct size following pharmacological inhibition of the mPTP opening at the onset of reperfusion, improved recovery in the human atrial trabeculae and reduction of infarct size in patients undergoing primary coronary angioplasty for an acute myocardial infarction [17, 135, 235, 420, 496, 585]. It has also been demonstrated that mice lacking the cyclophilin-D component of the mPTP have a smaller infarct size compared to the wild-type littermate controls [264, 387, 496] indicating the importance of the mPTP as a critical mediator of cell death in the setting of myocardial ischaemia-reperfusion injury. Therefore, inhibiting the opening of the mPTP should theoretically promote the survival of the cells. In our study, we trigger the release of ROS through photoactivation of TMRM loaded and ‘quenched’ in the mitochondria, which consists of an oxygen atom in the chemical structure, by using the high intensity-lasers of the confocal microscope. ROS release in the mitochondria has been shown

to be a major inducer of mPTP opening by increasing the binding of cyclophilin D to the ANT structure of the mPTP as well as to sensitise the PTP to Ca^{2+} by inhibition of adenine nucleotide binding [373, 377, 477, 540]. By subjecting the cells to high-power lasers of the confocal microscope, the pre-loaded TMRM in the mitochondria will be photoactivated and subsequently 'broken-down' into the chemical derivatives, hence releasing the free oxygen radical. The presence of the ROS will induce mPTP opening which can be visualised by the increase in red fluorescent intensity, signifying the 'dequenching' of the TMRM upon release through the pore from the mitochondria into the cytosol. The duration needed for mPTP opening is a very significant factor in the sense that it governs the survival strength of the cardiac cells and successfully delaying the time for mPTP opening provides a desirable breakthrough in the clinical setting where reperfusion to the occluded heart can be extended or even deemed negligible. By measuring the values of the TMRM fluorescent intensities through a course of time and normalising against the cells with the empty vector, we were able to determine when the pores start to open in the mitochondria. The results clearly show that the time needed for mPTP opening in the cells with overexpression of fusion proteins was significantly delayed, similarly to the use of CsA, an immunosuppressive drug which has been previously proven to inhibit mPTP opening.

Using the mtPA-GFP simultaneously with the photosensitive TMRM, we managed to detect mitochondria longer than 2 µm in the adult cardiomyocytes. Interestingly, previous studies have also shown that mitochondria extending up to 2 to 3 sarcomeres (4 to 6 µm) in length can be detected using electron microscopy. Nevertheless, the previous studies may have overlooked the connection between mitochondria length and sarcomere size and the physiological relevance of this finding. Short episodes of hypoxia have also been found to induce elongation of mitochondria, probably as an endogenous defence mechanism against further stress. There have been reports of deformed mitochondria in certain organs of hyperglycaemic patients and animal models of hyperglycaemia [586]. The mitochondria are found to be swollen with disarrayed cristae and reduced electron density of matrix [586]. In obese or Type 2 diabetic subjects, shrinkage of the mitochondria from skeletal muscle with less defined internal structure were observed [587]. The skeletal muscle from obese Zucker rats showed a reduction in levels of Mfn2 as the main

cause of the impairment of the mitochondrial network, leading to pronounced fragmentation [153, 588].

Kong and colleagues reported that overexpression of the fission proteins Drp1 and hFis1 increased the susceptibility of COS epithelial cells to calcium-induced mPTP opening [589]. Conversely, down-regulation of Drp1 in another study showed that the opening of the mPTP induced by mitochondrial oxidative stress generated in hyperglycemia was inhibited [209]. Overexpression of hFis1 in our study did not seem to influence sensitivity of mPTP opening. This may be due to a difference in the models used: e.g. a limitation of the resolution in our model to detect increased sensitivity of mPTP opening. Another possibility is that hFis1 causes cell death independent of the opening of the mPTP. Brady and colleagues showed in 2006 that the mitochondria of HL1 fragment after a 2 hour period of simulated ischaemia and remained in this morphology during the reperfusion period [488]. Interestingly, if the cells were reperfused in the presence of SB203580, a pharmacological inhibitor of p38 MAPK, the mitochondria reverted to a fused morphology [488], further confirming that changes in mitochondrial morphology are relevant to ischaemia-reperfusion injury but also suggesting that mitochondrial morphology may be controlled by protein kinases. In this regard, recent data suggests that protein kinase A may phosphorylate and inhibit the mitochondrial fission protein Drp1, thereby promoting mitochondrial fusion [182, 190]. Oxidative stress is a critical mediator of myocardial ischaemia-reperfusion injury and studies suggest that it too can induce mitochondrial fission [590]. Therefore, based on our study, we postulate that fusion of mitochondrial membrane in HL-1 cells can increase the resistance of the HL-1 cells to simulated ischaemia-reperfusion possibly by delaying the time needed until mPTP opening. Overexpressing proteins that encode for mitochondrial fusion in HL-1 cells delays the time needed for mPTP opening and protect against simulated hypoxia-reoxygenation. This seems to validate and associate the beneficial effects of mitochondrial fusion to inhibition of mPTP opening. It is not clear at the moment how fusion of the mitochondrial membranes prevents the mPTP from opening. Here, we propose a few possibilities; first, the fusion of the inner and outer membranes by the fusion proteins prevents the opening of the mPTP by ‘overlapping’ the potential opening sites or preventing the protein components that make up the pore by joining together. Fusion of mitochondria

involves the outer and inner membrane which occurs separately. Regardless of the exact location of the mPTP spanning the inner and outer membrane, once the outer membrane is fused together, opening of the mPTP will be rendered negligible. The spatial movement or consistent fusion of the membranes may 'cover' the opening sites of a particular mitochondrion prone to mPTP opening as well as to prevent the individual protein components from docking together to form the pore. As long as the individual constituents do not join together, the pore will not be formed and hence depolarisation will not occur. However, due to the fact that the cells were subjected to approximately 8 minutes of high intensity laser stress during measurement of TMRM fluorescence, the pore will eventually open at the end of the time course as can be seen from the line graphs.

Second, fusion of two mitochondria to become one will lead to an increase in the overall size including the volume of the matrix and intermembrane space. This increase in size and volume will enhance the capacity of the mitochondria to accommodate calcium loading, which is an inducer for mPTP opening. The reduction in ratio of individual mitochondria to individual ER may also explain the possible benefits of mitochondrial fusion. An abundant amount of ER relative to the amount of mitochondria may act as Ca^{2+} stores in which calcium is kept in the ER without the need to release into the cytosol and uptake into the mitochondria leading to subsequent mitochondrial calcium overload.

Third, fusion of the inner and outer mitochondrial membrane facilitates the formation of a higher number of individual cristae and possibly the narrow tubular cristae junction which serves to entrap more cytochrome *c* molecules and preventing the release of these apoptotic molecules into the cytosol. It is important to remember that fusion of two mitochondria ensures mixing of the intracellular contents. This fact may also provide an explanation of the increased survival of cells with fused mitochondria in which there is either an increased proportion of the protease PARL to hydrolyse the soluble domain of OPA1 or increase of the OPA1 inner mitochondrial membrane protein itself and hence reducing the diameter of the cristae junction encapsulating the cytochrome *c* present [11]. Compartmentalisation of the mitochondria which occurs with the abundant excess of mitochondrial membranes

following fusion may also assist in maintaining the proper concentrations of oxygen radicals, nitric oxide (reactive species) in the mitochondria.

In line with the possible theory of compartment contents mixing with the fusion of mitochondria, occurrence of mitochondrial DNA (mtDNA) defects can be salvaged by the complementation of a healthy mtDNA, particularly in the cases of missense or deletion mutation. mtDNA mutations and dysfunction have been implicated in cardiovascular (cardiac arrhythmias and cardiomyopathy) and neuronal diseases [591]. The mtDNA is responsible for encoding of certain enzyme complexes (I, III-V) of the oxidative phosphorylation mechanism and the RNAs required for the proper translation of the mitochondrial-encoded genes itself [592].

There is also the argument that upregulation of mitochondrial fusion proteins may conversely reduce the amount of Drp1 protein present in the cytosol, which is responsible for mitochondrial fission and ensuing apoptosis. This effect of reducing the proportion of Drp1 reaching the mitochondria can be explained by the previous phenomenon of reduction in calcium overloading. Elevated levels of calcium in the cell are an activator of calcineurin, a serine/threonine protein phosphatase which is usually bound to Drp1 [146]. Upon activation, calcineurin will dephosphorylate Drp1 hence promoting the translocation of Drp1 to the mitochondria to perform fission [146]. Reduction of calcium overloading may directly translates to reduction of Drp1 to cause mitochondrial fission and cell death.

Fragmentation of the mitochondria falls under the categories of either pathological or physiological events. The classical observation by Hackenbrock [593] that condensed mitochondria are more active with an electron-dense matrix is more relevant in physiological settings, such as mitosis or in the presence of increased substrate. Mitochondrial fragmentation under pathological conditions may alter the fluidity of the matricial contents as well as proper localisation and positioning of the respiratory chain complexes leading to perturbation of ETC activity and ATP production.

Fusion of mitochondria may also enhance the respiratory capacity of cells and enable them to withstand the metabolic and biochemical stresses associated with

IRI. The rate and levels of oxygen consumption, maintenance of mitochondrial membrane potential and respiration of mitochondria in myotubes have been demonstrated to be affected by varying expression levels of fusion proteins.

There are however, certain limitations in our study. We need to investigate the direct role of fusion in the cells during ischaemia and reperfusion. Our study employs three separate studies in which we looked at the morphology, cell survival and mPTP assay of the HL-1 cells. There remains the need to build up a solid link between these three aspects in the field of myocardial protection. Further studies to be carried out include the real-time imaging of the affect of fusion proteins on the mitochondrial morphology before, during and after ischaemia-reperfusion followed by monitoring of the mPTP opening to further establish the role of membrane fusion in inhibiting mPTP opening and promoting cell survival. The cells can be loaded into a simulated ischaemia-reperfusion chamber on a confocal microscope and the hypoxic and normoxic buffer constantly replaced for the determined length of time with the confocal microscope capturing images at the pre-determined set of time. At the moment, our group has already installed and performed a number of experiments on this specialised chamber docked onto the confocal microscope. It will be a matter of time before we achieve the aim of performing the simultaneous studies.

Besides that, a simple yet more accurate method has to be developed to study the morphology of the mitochondria in greater detail. There is variability in our technique where the images of the mitochondria were obtained and saved as TIF files to be read blinded by three different operators. However, it has to be noted that viewing the cells through the lens of the confocal microscope is different from viewing the cells in TIF images where the image can be sometimes blurry hence distorting the judgmental ability of the operators. The averaging tendency of the three operators serves to render a much fairer and near-optimum reading of the morphology of the cells.

Cell death by apoptosis or necrosis can occur simultaneously to the cells in the hypoxic chamber depending on the individual cells susceptibility and positioning of the cells in the wells. The amount of oxygen present in the airtight hypoxic chamber has yet to be measured. However, due to the length of time the nitrogen was

allowed to flow into the chamber (10 minutes forceful flow followed by 10 minutes gentle flow), it will be quite safe to assume that only a very low level (<5%) of oxygen is present in the chamber. Therefore, the cells should theoretically undergo necrosis. The choice of PI was made based on this assumption. It is worth mentioning that PI stains both apoptotic and necrotic cells. A combination of PI and Annexin V may have to be used to differentiate between early apoptotic and necrotic cells. However, regardless of the death pathway, we managed to address the crux of the issue: the cells die following reperfusion as shown by PI staining whereas cells with fused mitochondria were more resistant.

As for the mPTP assays, there has been some controversies as to the components that make up the mPTP but it is irrelevant in our study because we did show that the pores do indeed open following ROS stress with varying intensities and duration as visualised by the increase in TMRM red fluorescent intensity following laser stress. In addition to that, the use of CsA to inhibit mPTP opening prove that the model is working and CypD remains a component of the mPTP.

Questions pertaining to the levels of expression and presence of different proteins in the cells have been raised before. It will be very appropriate to perform Western blots to determine the levels of proteins present in the cells following plasmids transfection and overexpression. Possible additive effects of Mfn1 and Mfn2 have been queried but a consensus agreement has yet to be reached. It has been shown that residual levels of inner membrane fusion exist in single mitofusin knockout cells, whereas double Mfn1-/- or Mfn2-/- cells completely lack mixing of matricial content, an indication of inner membrane fusion [162, 490]. This shows that the presence of a single mitofusin coupled with OPA1 is adequate to promote mitochondrial fusion in cells. Potential deleterious effects of Mfn2 in causing apoptosis, including its interaction with various members of the Bcl-2 family have also been raised by previous studies [206, 577, 578].

The use of *mdivi-1*, cBiMPS and EPO to induce the proportion of cells with elongated mticodhonria was applied throughout the whole duration of simulated ischaemia and reperfusion as these drugs do not confer a ‘memory’ effect in the cardioprotective cascade compared to the use of IPC. The application of IPC and its

subsequent activation of PKG and PKC elicit a cardioprotective response by reduction of ROS and inhibition of mPTP which can be initiated during future episodes of IR. Using the drugs at the onset of reperfusion only may not allow the drugs to have enough time to act.

Genetically over-expressing the caAkt or upregulation of Akt by EPO significantly increases the proportion of cells with elongated mitochondria. Nevertheless, we will need to verify whether this is due to increase of mitochondrial fusion (overexpression of Mfn1 or Mfn2) or inhibition of mitochondrial fragmentation (as in the use of *mdivi-1*, overexpression of $Drp1_{K38A}$ or upregulation of PKA). This can be done using the mtPA-GFP to determine mitochondrial fusion after which the mechanism can be elucidated using different constructs such as monitoring of Drp1 translocation. The study concerning PKC has yet to be performed as planned due to time limitation.

In view of the constant search for interventions to improve clinical outcomes in patients with coronary heart diseases, novel therapeutic strategies are being investigated to protect the heart against IRI. In this present study, we report that modulation of mitochondrial morphology may prove to be a novel cardioprotective strategy against IRI. This is the first time that mitochondrial fusion has been reported to promote cell survival by delaying the time until mPTP opening in HL-1 cardiac cell line. More importantly, this is the first study documenting a proper detection and quantification of elongated mitochodnria (> 2 µm) in adult cardiomyocytes. In addition to that, pharmacological manipulation using *mdivi-1* has been proven to be beneficial in terms of cardioprotection against IRI by inhibiting excessive fragmentation of the mitochondria in the adult heart. This study can be further projected into pharmacological studies where drugs that promote mitochondrial fusion can be used to promote cell survival in the face of acute ischaemia-reperfusion injury. Various possibilities may arise where drugs can be applied at the onset of reperfusion or pre- and post-conditioning to increase the resistance of cells or whole hearts to IRI and subsequently improve clinical outcomes in patients with coronary heart disease.

Chapter Nine: CONCLUSION

9.1 Summary of Findings

This thesis has examined the novel role of modulation of mitochondrial morphology in myocardial protection. We have demonstrated that increasing the proportion of elongated mitochondria by genetic or pharmacological methods protects cardiac cells against ischaemia-reperfusion injury and this can be extrapolated to the animal model where a reduction in infarct size was detected following treatment of the animal with the mitochondrial morphology-modulating drug, *mdivi-1*. We postulated that the inhibition of the mPTP may underlie the protective effect of increased mitochondrial fusion. Interestingly, we also discovered that erythropoietin (EPO) as a known protective agent, also increased the proportion of cells with elongated mitochondria, further supporting our hypothesis.

9.2 Clinical Implications

Current cardioprotective strategies such as ischaemic preconditioning and ischaemic postconditioning converge on the mitochondria by inhibition of the mPTP. Despite this, there have been equivocal speculations pertaining to the mechanism leading to the inhibition of mPTP in these interventions. In this present study, we have provided proof that modulation of mitochondrial morphology can lead to the inhibition of mPTP opening and these findings constitute a novel cardioprotective strategy. Specifically, we have demonstrated that inhibition of mitochondrial fission by pharmacological manipulation using the *mdivi-1*, a small molecule inhibitor of the fission protein, Drp1 reduced myocardial infarct size in the *in vivo* murine infarct model as well as delayed the time until mPTP opening in adult cardiomyocytes. Future research can be directed at other compounds to target the other fission protein, Drp1 or enhancing the levels of the fusion proteins such as Mfn1, Mfn2 and OPA1 to reduce mitochondrial fission in the clinical settings of acute ischaemia-reperfusion injury to improve clinical outcomes in patients with coronary heart disease.

9.3 Future directions

Linking mitochondrial fusion to inhibition of mPTP and cardioprotection

We have demonstrated in the current study that promoting mitochondrial fusion protects the cells against simulated ischaemia-reperfusion injury and mitochondrial fusion delays the time until mPTP opening. Further research needs to be undertaken to conduct the study in real-time to connect mitochondrial fusion, cardioprotection and inhibition of mPTP together. Furthermore, using the real-time heated perfusion chamber, it would be possible to elucidate the underlying mechanism of inhibition of mPTP by mitochondrial fusion. We have speculated that this may be due to enhanced respiratory capability or a better Ca^{2+} retention capacity etc.

Promoting mitochondrial fusion in the adult cardiomyocytes

In the section concerning adult cardiomyocytes, we have demonstrated that using *mdivi-1* to inhibit mitochondrial fission protects cells against IRI, inhibits the mPTP opening and reduced infarct size following IR. *Mdivi-1* is currently the only drug available to inhibit mitochondrial fission. Further studies are required to actually promote mitochondrial fusion in the adult cardiomyocytes. The genes encoding for overexpression of the fusion proteins, Mfn1, Mfn2 or OPA1 can be inserted in the adenoviral vector for transfection into adult cardiomyocytes. Alternatively, it would be interesting to formulate a small molecule activator of the endogenous fusion proteins to be used in the animal model.

Effects of PKCε upregulation or knockdown on the mitochondria

The cardioprotective effects of PKCε have been well-documented. It would be interesting to investigate the effects of PKCε overexpression or knockdown of PKCε on the morphology of mitochondria. Our sister laboratory, the Hatter Institute in Cape Town, South Africa, have sent us some images of PKCε knock-outs mice but due to time limitation, the electron micrographs remains yet to be studied.

Mechanism of mitochondrial elongation by Akt upregulation

We have already demonstrated that activating PKA protects, yet the effects on mitochondrial morphology and inhibition of mPTP remains unresolved. A more

thorough study need to be performed to elucidate the effects of PKA activation on the mitochondria. We have shown that the genetic overexpression or pharmacological upregulation of the Akt by the use of EPO increases the proportion of cells with elongated mtiochohdria, protects against sIRI and inhibits opening of the mPTP. Future studies need to be performed to elucidate the mechanism of the actions of Akt in increasing mitochondrial elongation in the cells.

Chapter Ten: REFERENCES

Reference List

(1) International Cardiovascular Disease Statistics. 2010. American Heart Association. 1-7-2010.
Ref Type: Online Source

(2) Health care and economic costs of CVD and CHD. 2010. British Heart Foundation. 1-7-2010.
Ref Type: Online Source

(3) Luengo-Fernandez R, Leal J, Gray A, Petersen S, Rayner M. Cost of cardiovascular diseases in the United Kingdom. *Heart* 2006 October;92(10):1384-9.

(4) Living With a Heart Condition. 2010. British Heart Foundation. 1-7-2010.
Ref Type: Online Source

(5) Gill C, Mestril R, Samali A. Losing heart: the role of apoptosis in heart disease - a novel therapeutic target? *Faseb Journal* 2002 February;16(2):135-46.

(6) Preventing Heart Disease. 2010. British Heart Foundation. 1-7-2010.
Ref Type: Online Source

(7) Cohen MV, Baines CP, Downey JM. Ischemic preconditioning: From adenosine receptor to K-ATP channel. *Annual Review of Physiology* 2000;62:79-109.

(8) Crisostomo PR, Wairiuko GM, Wang MJ, Tsai BM, Morrell ED, Meldrum DR. Preconditioning versus postconditioning: Mechanisms and therapeutic potentials. *Journal of the American College of Surgeons* 2006 May;202(5):797-812.

(9) Ferdinandy P, Schulz R, Baxter GF. Interaction of cardiovascular risk factors with myocardial ischemia/reperfusion injury, preconditioning, and postconditioning. *Pharmacological Reviews* 2007 December;59(4):418-58.

(10) Baines CP, Song CX, Zheng YT et al. Protein kinase C epsilon interacts with and inhibits the permeability transition pore in cardiac mitochondria. *Circulation Research* 2003 May 2;92(8):873-80.

(11) Gazaryan IG, Brown AM. Intersection between mitochondrial permeability pores and mitochondrial fusion/fission. *Neurochemical Research* 2007 April;32(4-5):917-29.

(12) Fox KAA, Bergmann SR, Sobel BE. Patho-Physiology of Myocardial Reperfusion. *Annual Review of Medicine* 1985;36:125-44.

(13) Jennings RB, Sommers HM, Herdson PB, KALTENBA.JP. Ischemic Injury of Myocardium. *Annals of the New York Academy of Sciences* 1969;156(A1):61-&.

(14) Jennings RB. Early Phase of Myocardial Ischemic Injury and Infarction. *American Journal of Cardiology* 1969;24(6):753-&.

(15) Sommers HM, Jennings RB. Experimental Acute Myocardial Infarction - Histologic + Histochemical Studies of Early Myocardial Infarcts Induced by Temporary 3R Permanent Occlusion of Coronary Artery. *Laboratory Investigation* 1964;13(12):1491-&.

(16) Kloner RA. Does Reperfusion Injury Exist in Humans. *Journal of the American College of Cardiology* 1993 February;21(2):537-45.

(17) Hausenloy DJ, Maddock HL, Baxter GF, Yellon DM. Inhibiting mitochondrial permeability transition pore opening: a new paradigm for myocardial preconditioning? *Cardiovascular Research* 2002 August 15;55(3):534-43.

(18) Maas JE, Wan TC, Figler RA, Gross GJ, Auchampach JA. Evidence that the acute phase of ischemic preconditioning does not require signaling by the A(2B) adenosine receptor. *J Mol Cell Cardiol* 2010 August 24.

(19) Nadtochiy SM, Redman E, Rahman I, Brookes PS. Lysine Deacetylation in Ischemic Preconditioning: The Role of SIRT1. *Cardiovasc Res* 2010 September 7.

(20) Gottlieb RA, Burleson KO, Kloner RA, Babior BM, Engler RL. Reperfusion injury induces apoptosis in rabbit cardiomyocytes. *J Clin Invest* 1994 October;94(4):1621-8.

(21) Talukder MA, Yang F, Shimokawa H, Zweier JL. eNOS is required for acute in vivo ischemic preconditioning of the heart: effects of ischemic duration and sex. *Am J Physiol Heart Circ Physiol* 2010 August;299(2):H437-H445.

(22) Vanden Hoek TL, Qin YM, Wojcik K et al. Reperfusion, not simulated ischemia, initiates intrinsic apoptosis injury in chick cardiomyocytes. *American Journal of Physiology-Heart and Circulatory Physiology* 2003 January;284(1):H141-H150.

(23) Park JL, Lucchesi BR. Mechanisms of myocardial reperfusion injury. *Annals of Thoracic Surgery* 1999 November;68(5):1905-12.

(24) Robicsek F, Schaper J. Reperfusion injury: Fact or myth? *Journal of Cardiac Surgery* 1997 May;12(3):133-7.

(25) Hausenloy DJ, Yellon DM. Time to take myocardial reperfusion injury seriously. *New England Journal of Medicine* 2008 July 31;359(5):518-20.

(26) Di LF, Blank PS, Colonna R et al. Mitochondrial membrane potential in single living adult rat cardiac myocytes exposed to anoxia or metabolic inhibition. *J Physiol* 1995 July 1;486 (Pt 1):1-13.

(27) Jennings RB, Reimer KA, Steenbergen C. Effect of inhibition of the mitochondrial ATPase on net myocardial ATP in total ischemia. *J Mol Cell Cardiol* 1991 December;23(12):1383-95.

(28) Jennings RB, Reimer KA. The cell biology of acute myocardial ischemia. *Annu Rev Med* 1991;42:225-46.

(29) Griffiths EJ, Ocampo CJ, Savage JS et al. Mitochondrial calcium transporting pathways during hypoxia and reoxygenation in single rat cardiomyocytes. *Cardiovasc Res* 1998 August;39(2):423-33.

(30) Miyata H, Lakatta EG, Stern MD, Silverman HS. Relation of mitochondrial and cytosolic free calcium to cardiac myocyte recovery after exposure to anoxia. *Circ Res* 1992 September;71(3):605-13.

(31) Zorov DB, Filburn CR, Klotz LO, Zweier JL, Sollott SJ. Reactive oxygen species (ROS)-induced ROS release: A new phenomenon accompanying induction of the mitochondrial permeability transition in cardiac myocytes. *Journal of Experimental Medicine* 2000 October 2;192(7):1001-14.

(32) Becker LB. New concepts in reactive oxygen species and cardiovascular reperfusion physiology. *Cardiovascular Research* 2004 February 15;61(3):461-70.

(33) Shen AC, Jennings RB. Kinetics of calcium accumulation in acute myocardial ischemic injury. *Am J Pathol* 1972 June;67(3):441-52.

(34) Shen AC, Jennings RB. Myocardial calcium and magnesium in acute ischemic injury. *Am J Pathol* 1972 June;67(3):417-40.

(35) Weiss JN, Korge P, Honda HM, Ping PP. Role of the mitochondrial permeability transition in myocardial disease. *Circulation Research* 2003 August 22;93(4):292-301.

(36) Chambers DE, Parks DA, Patterson G et al. Xanthine-Oxidase As A Source of Free-Radical Damage in Myocardial Ischemia. *Journal of Molecular and Cellular Cardiology* 1985;17(2):145-52.

(37) Weseler AR, Bast A. Oxidative stress and vascular function: implications for pharmacologic treatments. *Curr Hypertens Rep* 2010 June;12(3):154-61.

(38) Landmesser U, Spiekermann S, Dikalov S et al. Vascular oxidative stress and endothelial dysfunction in patients with chronic heart failure: role of xanthine-oxidase and extracellular superoxide dismutase. *Circulation* 2002 December 10;106(24):3073-8.

(39) Mentzer RM, Lasley RD, Jessel A, Karmazyn M. Intracellular sodium hydrogen exchange inhibition and clinical myocardial protection. *Annals of Thoracic Surgery* 2003 February;75(2):S700-S708.

(40) Bedard K, Krause KH. The NOX family of ROS-generating NADPH oxidases: physiology and pathophysiology. *Physiol Rev* 2007 January;87(1):245-313.

(41) Krijnen PA, Meischl C, Hack CE et al. Increased Nox2 expression in human cardiomyocytes after acute myocardial infarction. *J Clin Pathol* 2003 March;56(3):194-9.

(42) Guzik TJ, Sadowski J, Guzik B et al. Coronary artery superoxide production and nox isoform expression in human coronary artery disease. *Arterioscler Thromb Vasc Biol* 2006 February;26(2):333-9.

(43) Meischl C, Krijnen PA, Sipkens JA et al. Ischemia induces nuclear NOX2 expression in cardiomyocytes and subsequently activates apoptosis. *Apoptosis* 2006 June;11(6):913-21.

(44) Alderton WK, Cooper CE, Knowles RG. Nitric oxide synthases: structure, function and inhibition. *Biochem J* 2001 August 1;357(Pt 3):593-615.

(45) Crane BR, Arvai AS, Ghosh DK et al. Structure of nitric oxide synthase oxygenase dimer with pterin and substrate. *Science* 1998 March 27;279(5359):2121-6.

(46) Hemmens B, Mayer B. Enzymology of nitric oxide synthases. *Methods Mol Biol* 1998;100:1-32.

(47) Higashi Y, Sasaki S, Nakagawa K et al. Tetrahydrobiopterin enhances forearm vascular response to acetylcholine in both normotensive and hypertensive individuals. *Am J Hypertens* 2002 April;15(4 Pt 1):326-32.

(48) Stroes E, Kastelein J, Cosentino F et al. Tetrahydrobiopterin restores endothelial function in hypercholesterolemia. *J Clin Invest* 1997 January 1;99(1):41-6.

(49) Dorweiler B, Pruefer D, Andrasi TB et al. Ischemia-reperfusion injury - Pathophysiology and clinical implications. *European Journal of Trauma and Emergency Surgery* 2007 December;33(6):600-12.

(50) Nava E, Noll G, Luscher TF. Nitric-Oxide in Cardiovascular-Diseases. *Annals of Medicine* 1995 June;27(3):343-51.

(51) Szabo G, Liaudet L, Hagl S, Szabo C. Poly(ADP-ribose) polymerase activation in the reperfused myocardium. *Cardiovascular Research* 2004 February 15;61(3):471-80.

(52) Halestrap AP, Kerr PM, Javadov S, Woodfield KY. Elucidating the molecular mechanism of the permeability transition pore and its role in

reperfusion injury of the heart. *Biochimica et Biophysica Acta-Bioenergetics* 1998 August 10;1366(1-2):79-94.

(53) Piper HM, Garcia-Dorado D, Ovize M. A fresh look at reperfusion injury. *Cardiovasc Res* 1998 May;38(2):291-300.

(54) Klein HH, Pich S, Lindert S, Nebendahl K, Warneke G, Kreuzer H. Treatment of reperfusion injury with intracoronary calcium channel antagonists and reduced coronary free calcium concentration in regionally ischemic, reperfused porcine hearts. *J Am Coll Cardiol* 1989 May;13(6):1395-401.

(55) Carry MM, Mrak RE, Murphy ML, Peng CF, Straub KD, Fody EP. Reperfusion injury in ischemic myocardium: protective effects of ruthenium red and of nitroprusside. *Am J Cardiovasc Pathol* 1989;2(4):335-44.

(56) Boden WE, van Gilst WH, Scheldewaert RG et al. Diltiazem in acute myocardial infarction treated with thrombolytic agents: a randomised placebo-controlled trial. Incomplete Infarction Trial of European Research Collaborators Evaluating Prognosis post-Thrombolysis (INTERCEPT). *Lancet* 2000 May 20;355(9217):1751-6.

(57) Zeymer U, Suryapranata H, Monassier JP et al. The Na(+)/H(+) exchange inhibitor eniporide as an adjunct to early reperfusion therapy for acute myocardial infarction. Results of the evaluation of the safety and cardioprotective effects of eniporide in acute myocardial infarction (ESCAMI) trial. *J Am Coll Cardiol* 2001 November 15;38(6):1644-50.

(58) Lemasters JJ, Bond JM, Chacon E et al. The pH paradox in ischemia-reperfusion injury to cardiac myocytes. *EXS* 1996;76:99-114.

(59) Bond JM, Herman B, Lemasters JJ. Protection by acidotic pH against anoxia/reoxygenation injury to rat neonatal cardiac myocytes. *Biochem Biophys Res Commun* 1991 September 16;179(2):798-803.

(60) Avkiran M, Marber MS. Na(+)/H(+) exchange inhibitors for cardioprotective therapy: progress, problems and prospects. *J Am Coll Cardiol* 2002 March 6;39(5):747-53.

(61) Hausenloy DJ, Yellon DM. The mitochondrial permeability transition pore: its fundamental role in mediating cell death during ischaemia and reperfusion. *Journal of Molecular and Cellular Cardiology* 2003 April;35(4):339-41.

(62) Kim JS, Jin Y, Lemasters JJ. Reactive oxygen species, but not Ca2+ overloading, trigger pH- and mitochondrial permeability transition-dependent death of adult rat myocytes after ischemia-reperfusion. *Am J Physiol Heart Circ Physiol* 2006 May;290(5):H2024-H2034.

(63) Crompton M, Andreeva L. On the Involvement of A Mitochondrial Pore in Reperfusion Injury. *Basic Research in Cardiology* 1993 September;88(5):513-23.

(64) Hamacher-Brady A, Brady NR, Gottlieb RA. The interplay hetween pro-death and pro-survival signaling pathways in myocardial ischemia/reperfusion injury: Apoptosis meets autophagy. *Cardiovascular Drugs and Therapy* 2006 December;20(6):445-62.

(65) McCully JD, Wakiyama H, Hsieh YJ, Jones M, Levitsky S. Differential contribution of necrosis and apoptosis in myocardial ischemia-reperfusion injury. *American Journal of Physiology-Heart and Circulatory Physiology* 2004 May;286(5):H1923-H1935.

(66) Bolli R, Becker L, Gross G, Mentzer R, Balshaw D, Lathrop DA. Myocardial protection at a crossroads - The need for translation into clinical therapy. *Circulation Research* 2004 July 23;95(2):125-34.

(67) Zhao ZQ, Corvera JS, Halkos ME et al. Inhibition of myocardial injury by ischemic postconditioning during reperfusion: comparison with ischemic preconditioning. *American Journal of Physiology-Heart and Circulatory Physiology* 2003 August;285(2):H579-H588.

(68) Staat P, Rioufol G, Piot C et al. Postconditioning the human heart. *Circulation* 2005 October 4;112(14):2143-8.

(69) Ahmad A, Ahmad S, Chang LY, Schaack J, White CW. Endothelial Akt activation by hyperoxia: Role in cell survival. *Free Radical Biology and Medicine* 2006 April 1;40(7):1108-18.

(70) Lee YJ, Jeong SY, Karbowski M, Smith CL, Youle RJ. Roles of the mammalian mitochondrial fission and fusion mediators Fis1, Drp1, and Opa1 in apoptosis. *Molecular Biology of the Cell* 2004 November;15(11):5001-11.

(71) Vaux DL, Cory S, Adams JM. Bcl-2 gene promotes haemopoietic cell survival and cooperates with c-myc to immortalize pre-B cells. *Nature* 1988 September 29;335(6189):440-2.

(72) Kranz R, Lill R, Goldman B, Bonnard G, Merchant S. Molecular mechanisms of cytochrome c biogenesis: three distinct systems. *Molecular Microbiology* 1998 July;29(2):383-96.

(73) Gustafsson AB, Gottlieb RA. Bcl-2 family members and apoptosis, taken to heart. *American Journal of Physiology-Cell Physiology* 2007 January;292(1):C45-C51.

(74) Waterhouse NJ, Ricci JE, Green DR. And all of a sudden it's over: mitochondrial outer-membrane permeabilization in apoptosis. *Biochimie* 2002 February;84(2-3):113-21.

(75) Parone PA, James D, Martinou JC. Mitochondria: regulating the inevitable. *Biochimie* 2002 February;84(2-3):105-11.

(76) Lu G, Ren SX, Korge P et al. A novel mitochondrial matrix serine/threonine protein phosphatase regulates the mitochondria permeability transition pore and is essential for cellular survival and development. *Genes & Development* 2007 April 1;21(7):784-96.

(77) Ashkenazi A, Dixit VM. Death receptors: Signaling and modulation. *Science* 1998 August 28;281(5381):1305-8.

(78) Fadok VA, Voelker DR, Campbell PA, Cohen JJ, Bratton DL, Henson PM. Exposure of phosphatidylserine on the surface of apoptotic lymphocytes triggers specific recognition and removal by macrophages. *J Immunol* 1992 April 1;148(7):2207-16.

(79) Vermes I, Haanen C, Steffens-Nakken H, Reutelingsperger C. A novel assay for apoptosis. Flow cytometric detection of phosphatidylserine expression on early apoptotic cells using fluorescein labelled Annexin V. *J Immunol Methods* 1995 July 17;184(1):39-51.

(80) Koopman G, Reutelingsperger CP, Kuijten GA, Keehnen RM, Pals ST, van Oers MH. Annexin V for flow cytometric detection of phosphatidylserine expression on B cells undergoing apoptosis. *Blood* 1994 September 1;84(5):1415-20.

(81) Xu RX, Chen X, Hu SS et al. [Lovastatin protects mesenchymal stem cells against hypoxia and serum deprivation-induced apoptosis through activation of PI3K/Akt and ERK1/2 signaling pathways]. *Zhonghua Xin Xue Guan Bing Za Zhi* 2008 August;36(8):685-90.

(82) Xu R, Chen J, Cong X, Hu S, Chen X. Lovastatin protects mesenchymal stem cells against hypoxia- and serum deprivation-induced apoptosis by activation of PI3K/Akt and ERK1/2. *J Cell Biochem* 2008 January 1;103(1):256-69.

(83) Deng J, Han Y, Yan C et al. Overexpressing cellular repressor of E1A-stimulated genes protects mesenchymal stem cells against hypoxia- and serum deprivation-induced apoptosis by activation of PI3K/Akt. *Apoptosis* 2010 April;15(4):463-73.

(84) Moore A, Donahue CJ, Bauer KD, Mather JP. Simultaneous measurement of cell cycle and apoptotic cell death. *Methods Cell Biol* 1998;57:265-78.

(85) Lecoeur H. Nuclear apoptosis detection by flow cytometry: influence of endogenous endonucleases. *Exp Cell Res* 2002 July 1;277(1):1-14.

(86) Frezza C, Cipolat S, Scorrano L. Organelle isolation: functional mitochondria from mouse liver, muscle and cultured filroblasts. *Nature Protocols* 2007;2(2):287-95.

(87) Alirol E, James D, Huber D et al. The mitochondrial fission protein hFis1 requires the endoplasmic reticulum gateway to induce apoptosis. *Molecular Biology of the Cell* 2006 November;17(11):4593-605.

(88) Rizzuto R, Bernardi P, Pozzan T. Mitochondria as all-round players of the calcium game. *Journal of Physiology-London* 2000 November 15;529(1):37-47.

(89) Chen YQ. [Mechanism of cell damage by hematoporphyrin derivative (HPD) plus light. II. Effect of HPD plus light on respiration and oxidative phosphorylation in hepatoma cells and normal liver mitochondria]. *Zhonghua Zhong Liu Za Zhi* 1988 September;10(5):349-52.

(90) Bereiterhahn J, Voth M. Dynamics of Mitochondria in Living Cells - Shape Changes, Dislocations, Fusion, and Fission of Mitochondria. *Microscopy Research and Technique* 1994 February 15;27(3):198-219.

(91) Okamoto K, Shaw JM. Mitochondrial morphology and dynamics in yeast and multicellular eukaryotes. *Annual Review of Genetics* 2005;39:503-36.

(92) Yaffe MP. The machinery of mitochondrial inheritance and behavior. *Science* 1999 March 5;283(5407):1493-7.

(93) Neupert W. Protein import into mitochondria. *Annual Review of Biochemistry* 1997;66:863-917.

(94) Skarka L, Ostadal B. Mitochondrial membrane potential in cardiac myocytes. *Physiological Research* 2002;51(5):425-34.

(95) Hermann GJ, Thatcher JW, Mills JP et al. Mitochondrial fusion in yeast requires the transmembrane GTPase Fzo1p. *Journal of Cell Biology* 1998 October 19;143(2):359-73.

(96) Hayashi T, Rizzuto R, Hajnoczky G, Su TP. MAM: more than just a housekeeper. *Trends in Cell Biology* 2009 February;19(2):81-8.

(97) Chipuk JE, Bouchier-Hayes L, Green DR. Mitochondrial outer membrane permeabilization during apoptosis: the innocent bystander scenario. *Cell Death and Differentiation* 2006 August;13(8):1396-402.

(98) McMillin JB, Dowhan W. Cardiolipin and apoptosis. *Biochimica et Biophysica Acta-Molecular and Cell Biology of Lipids* 2002 December 30;1585(2-3):97-107.

(99) Barnett DK, Kimura J, Bavister BD. Translocation of active mitochondria during hamster preimplantation embryo development studied by confocal laser scanning microscopy. *Developmental Dynamics* 1996 January;205(1):64-72.

(100) Kayar SR, Claassen H, Hoppeler H, Weibel ER. Mitochondrial Distribution in Relation to Changes in Muscle Metabolism in Rat Soleus. *Respiration Physiology* 1986 April;64(1):1-11.

(101) Kayar SR, Hoppeler H, Howald H, Claassen H, Oberholzer F. Acute Effects of Endurance Exercise on Mitochondrial Distribution and Skeletal-Muscle Morphology. *European Journal of Applied Physiology and Occupational Physiology* 1986;54(6):578-84.

(102) Gamboa JL, Andrade FH. Mitochondrial content and distribution changes specific to mouse diaphragm after chronic normobaric hypoxia. *American Journal of Physiology-Regulatory Integrative and Comparative Physiology* 2010 March;298(3):R575-R583.

(103) Vanekeren GJ, Sengers RCA, Stadhouders AM. Changes in Volume Densities and Distribution of Mitochondria in Rat Skeletal-Muscle After Chronic Hypoxia. *International Journal of Experimental Pathology* 1992 February;73(1):51-60.

(104) Crenshaw AG, Friden J, Thornell LE, Hargens AR. Extreme Endurance Training - Evidence of Capillary and Mitochondria Compartmentalization in Human Skeletal-Muscle. *European Journal of Applied Physiology and Occupational Physiology* 1991 October;63(3-4):173-8.

(105) Chan DC. Dissecting mitochondrial fusion. *Developmental Cell* 2006 November;11(5):592-4.

(106) McBride HM, Neuspiel M, Wasiak S. Mitochondria: More than just a powerhouse. *Current Biology* 2006 July 25;16(14):R551-R560.

(107) Vina J, Gomez-Cabrera MC, Borras C et al. Mitochondrial biogenesis in exercise and in ageing. *Advanced Drug Delivery Reviews* 2009 November 30;61(14):1369-74.

(108) Attardi G, Schatz G. Biogenesis of Mitochondria. *Annual Review of Cell Biology* 1988;4:289-333.

(109) Puigserver P, Wu ZD, Park CW, Graves R, Wright M, Spiegelman BM. A cold-inducible coactivator of nuclear receptors linked to adaptive thermogenesis. *Cell* 1998 March 20;92(6):829-39.

(110) St Pierre J, Drori S, Uldry M et al. Suppression of reactive oxygen species and neurodegeneration by the PGC-1 transcriptional coactivators. *Cell* 2006 October 20;127(2):397-408.

(111) Saraste M. Oxidative phosphorylation at the fin de siecle. *Science* 1999 March 5;283(5407):1488-93.

(112) Takano H, Onoue K, Kawano S. Mitochondrial fusion and inheritance of the mitochondrial genome. *Journal of Plant Research* 2010 March;123(2):131-8.

(113) Zunino R, Braschi E, Xu LQ, McBride HM. Translocation of SenP5 from the Nucleoli to the Mitochondria Modulates DRP1-dependent Fission during Mitosis. *Journal of Biological Chemistry* 2009 June 26;284(26):17783-95.

(114) Boldogh IR, Fehrenbacher KL, Yang HC, Pon LA. Mitochondrial movement and inheritance in budding yeast. *Gene* 2005 July 18;354:28-36.

(115) Taguchi N, Ishihara N, Jofuku A, Oka T, Mihara K. Mitotic phosphorylation of dynamin-related GTPase Drp1 participates in mitochondrial fission. *Journal of Biological Chemistry* 2007 April 13;282(15):11521-9.

(116) Zunino R, Schauss A, Rippstein P, Andrade-Navarro M, McBride HM. The SUMO protease SENP5 is required to maintain mitochondrial morphology and function. *Journal of Cell Science* 2007 April 1;120(7):1178-88.

(117) Chacinska A, Lind M, Frazier AE et al. Mitochondrial presequence translocase: switching between TOM tethering and motor recruitment involves Tim21 and Tim17. *Cell* 2005 March 25;120(6):817-29.

(118) Wiedemann N, Pfanner N, Ryan MT. The three modules of ADP/ATP carrier cooperate in receptor recruitment and translocation into mitochondria. *EMBO J* 2001 March 1;20(5):951-60.

(119) Young JC, Hoogenraad NJ, Hartl FU. Molecular chaperones Hsp90 and Hsp70 deliver preproteins to the mitochondrial import receptor Tom70. *Cell* 2003 January 10;112(1):41-50.

(120) Zara V, Ferramosca A, Robitaille-Foucher P, Palmieri F, Young JC. Mitochondrial carrier protein biogenesis: role of the chaperones Hsc70 and Hsp90. *Biochem J* 2009 April 15;419(2):369-75.

(121) Chacinska A, Pfannschmidt S, Wiedemann N et al. Essential role of Mia40 in import and assembly of mitochondrial intermembrane space proteins. *EMBO J* 2004 October 1;23(19):3735-46.

(122) Hofmann S, Rothbauer U, Muhlenbein N, Baiker K, Hell K, Bauer MF. Functional and mutational characterization of human MIA40 acting during import into the mitochondrial intermembrane space. *J Mol Biol* 2005 October 28;353(3):517-28.

(123) Chacinska A, Koehler CM, Milenkovic D, Lithgow T, Pfanner N. Importing mitochondrial proteins: machineries and mechanisms. *Cell* 2009 August 21;138(4):628-44.

(124) Wiedemann N, Kozjak V, Chacinska A et al. Machinery for protein sorting and assembly in the mitochondrial outer membrane. *Nature* 2003 July 31;424(6948):565-71.

(125) Komiya T, Mihara K. Protein import into mammalian mitochondria - Characterization of the intermediates along the import pathway of the precursor into the matrix. *Journal of Biological Chemistry* 1996 September 6;271(36):22105-10.

(126) Arakaki N, Nishihama T, Owaki H et al. Dynamics of mitochondria during the cell cycle. *Biological & Pharmaceutical Bulletin* 2006 September;29(9):1962-5.

(127) Mitra K, Wunder C, Roysam B, Lin G, Lippincott-Schwartz J. A hyperfused mitochondrial state achieved at G(1)-S regulates cyclin E buildup and entry into S phase. *Proceedings of the National Academy of Sciences of the United States of America* 2009 July 21;106(29):11960-5.

(128) Scarpulla RC. Transcriptional activators and coactivators in the nuclear control of mitochondrial function in mammalian cells. *Gene* 2002 March 6;286(1):81-9.

(129) Mannella CA. The relevance of mitochondrial membrane topology to mitochondrial function. *Biochimica et Biophysica Acta-Molecular Basis of Disease* 2006 February;1762(2):140-7.

(130) Logan DC. The mitochondrial compartment. *Journal of Experimental Botany* 2006 March;57(6):1225-43.

(131) Lea PJ, Temkin RJ, Freeman KB, Mitchell GA, Robinson BH. Variations in Mitochondrial Ultrastructure and Dynamics Observed by High-Resolution Scanning Electron-Microscopy (Hrsem). *Microscopy Research and Technique* 1994 March 1;27(4):269-77.

(132) Mannella CA, Marko M, Penczek P, Barnard D, Frank J. Internal Compartmentation of Rat-Liver Mitochondria - Tomographic Study Using the High-Voltage Transmission Electron-Microscope. *Microscopy Research and Technique* 1994 March 1;27(4):278-83.

(133) HACKENBR.CR. Chemical and Physical Fixation of Isolated Mitochondria in Low-Energy and High-Energy States. *Proceedings of the National Academy of Sciences of the United States of America* 1968;61(2):598-&.

(134) Mannella CA, Marko M, Buttle K. Reconsidering mitochondrial structure: New views of an old organelle. *Trends in Biochemical Sciences* 1997 February;22(2):37-8.

(135) Javadov S, Karmazyn M. Mitochondrial permeability transition pore opening as an endpoint to initiate cell death and as a putative target for cardioprotection. *Cellular Physiology and Biochemistry* 2007;20(1-4):1-22.

(136) Voet D, Voet JG, Pratt CW. *Fundamentals of Biochemistry*. 2nd ed. John Wiley and Sons, Inc; 2006. p. 547.

(137) Huang H, Manton KG. The role of oxidative damage in mitochondria during aging: A review. *Frontiers in Bioscience* 2004 May;9:1100-17.

(138) Mitchell P, Moyle J. Respiration-driven proton translocation in rat liver mitochondria. *Biochem J* 1967 December;105(3):1147-62.

(139) Mitchell P, Moyle J. Chemiosmotic hypothesis of oxidative phosphorylation. *Nature* 1967 January 14;213(5072):137-9.

(140) Mitchell P. Proton current flow in mitochondrial systems. *Nature* 1967 June 24;214(5095):1327-8.

(141) Gunter TE, Buntinas L, Sparagna G, Eliseev R, Gunter K. Mitochondrial calcium transport: mechanisms and functions. *Cell Calcium* 2000 November;28(5-6):285-96.

(142) Gunter TE, Pfeiffer DR. Mechanisms by Which Mitochondria Transport Calcium. *American Journal of Physiology* 1990 May;258(5):C755-C786.

(143) Rizzuto R, Pinton P, Carrington W et al. Close contacts with the endoplasmic reticulum as determinants of mitochondrial Ca2+ responses. *Science* 1998 June 12;280(5370):1763-6.

(144) Gunter KK, Gunter TE. Transport of calcium by mitochondria. *J Bioenerg Biomembr* 1994 October;26(5):471-85.

(145) Halestrap AP. Calcium, mitochondria and reperfusion injury: a pore way to die. *Biochemical Society Transactions* 2006 April;34:232-7.

(146) Dimmer KS, Scorrano L. (De)constructing mitochondria: What for? *Physiology* 2006 August;21:233-41.

(147) Benda C. Ueber dier Spermatogenese de Verbebraten und hoherer Evertebraten, II. Theil: Die Histiogenese der Spermien. *Arch Anat Physiol* 1898;73:393-8.

(148) Bakeeva LE, Chentsov YS, Skulachev VP. Mitochondrial Framework (Reticulum Mitochondrial) in Rat Diaphragm Muscle. *Biochimica et Biophysica Acta* 1978;501(3):349-69.

(149) Nunnari J, Marshall WF, Straight A, Murray A, Sedat JW, Walter P. Mitochondrial transmission during mating in Saccharomyces cerevisiae is determined by mitochondrial fusion and fission and the intramitochondrial segregation of mitochondrial DNA. *Molecular Biology of the Cell* 1997 July;8(7):1233-42.

(150) Hales KG, Fuller MT. Developmentally regulated mitochondrial fusion mediated by a conserved, novel, predicted GTPase. *Cell* 1997 July 11;90(1):121-9.

(151) Rojo M, Legros F, Chateau D, Lombes A. Membrane topology and mitochondrial targeting of mitofusins, ubiquitous mammalian homologs of the transmembrane GTPase Fzo. *Journal of Cell Science* 2002 April 15;115(8):1663-74.

(152) Santel A, Frank S, Gaume B, Herrier M, Youle RJ, Fuller MT. Mitofusin-1 protein is a generally expressed mediator of mitochondrial fusion in mammalian cells. *Journal of Cell Science* 2003 July 1;116(13):2763-74.

(153) Bach D, Pich S, Soriano FX et al. Mitofusin-2 determines mitochondrial network architecture and mitochondrial metabolism - A novel regulatory mechanism altered in obesity. *Journal of Biological Chemistry* 2003 May 9;278(19):17190-7.

(154) Hom J, Sheu SS. Morphological dynamics of mitochondria - A special emphasis on cardiac muscle cells. *Journal of Molecular and Cellular Cardiology* 2009 June;46(6):811-20.

(155) Akepati VR, Muller EC, Otto A, Strauss HM, Portwich M, Alexander C. Characterization of OPA1 isoforms isolated from mouse tissues. *Journal of Neurochemistry* 2008 July;106(1):372-83.

(156) Imoto M, Tachibana I, Urrutia R. Identification and functional characterization of a novel human protein highly related to the yeast dynamin-like GTPase Vps1p. *Journal of Cell Science* 1998 May;111:1341-9.

(157) Stojanovski D, Koutsopoulos OS, Okamoto K, Ryan MT. Levels of human Fis1 at the mitochondrial outer membrane regulate mitochondrial morphology. *Journal of Cell Science* 2004 March 1;117(7):1201-10.

(158) Santel A, Fuller MT. Control of mitochondrial morphology by a human mitofusin. *Journal of Cell Science* 2001 March;114(5):867-74.

(159) Frazier AE, Kiu C, Stojanovski D, Hoogenraad NJ, Ryan MT. Mitochondrial morphology and distribution in mammalian cells. *Biological Chemistry* 2006 December;387(12):1551-8.

(160) Cereghetti GM, Scorrano L. The many shapes of mitochondrial death. *Oncogene* 2006 August;25(34):4717-24.

(161) Chen KH, Guo XM, Ma DL et al. Dysregulation of HSG triggers vascular proliferative disorders. *Nature Cell Biology* 2004 September;6(9):872-U8.

(162) Chen HC, Detmer SA, Ewald AJ, Griffin EE, Fraser SE, Chan DC. Mitofusins Mfn1 and Mfn2 coordinately regulate mitochondrial fusion and are essential for embryonic development. *Journal of Cell Biology* 2003 January 20;160(2):189-200.

(163) Koshiba T, Detmer SA, Kaiser JT, Chen HC, McCaffery JM, Chan DC. Structural basis of mitochondrial tethering by mitofusin complexes. *Science* 2004 August 6;305(5685):858-62.

(164) de Brito OM, Scorrano L. Mitofusin 2 tethers endoplasmic reticulum to mitochondria. *Nature* 2008 December 4;456(7222):605-U47.

(165) Cipolat S, de Brito OM, Dal Zilio B, Scorrano L. OPA1 requires mitofusin 1 to promote mitochondrial fusion. *Proceedings of the National Academy of Sciences of the United States of America* 2004 November 9;101(45):15927-32.

(166) Delettre C, Lenaers G, Griffoin JM et al. Nuclear gene OPA1, encoding a mitochondrial dynamin-related protein, is mutated in dominant optic atrophy. *Nature Genetics* 2000 October;26(2):207-10.

(167) Jones BA, Fangman WL. Mitochondrial-Dna Maintenance in Yeast Requires A Protein Containing A Region Related to the Gtp-Binding Domain of Dynamin. *Genes & Development* 1992 March;6(3):380-9.

(168) Olichon A, ElAchouri G, Baricault L, Delettre C, Belenguer P, Lenaers G. OPA1 alternate splicing uncouples an evolutionary conserved function in mitochondrial fusion from a vertebrate restricted function in apoptosis. *Cell Death and Differentiation* 2007 April;14(4):682-92.

(169) Frezza C, Cipolat S, de Brito OM et al. OPA1 controls apoptotic cristae remodeling independently from mitochondrial fusion. *Cell* 2006 July 14;126(1):177-89.

(170) Alexander C, Votruba M, Pesch UEA et al. OPA1, encoding a dynamin-related GTPase, is mutated in autosomal dominant optic atrophy linked to chromosome 3q28. *Nature Genetics* 2000 October;26(2):211-5.

(171) Cipolat S, Rudka T, Hartmann D et al. Mitochondrial rhomboid PARL regulates cytochrome c release during apoptosis via OPA1-dependent cristae remodeling. *Cell* 2006 July 14;126(1):163-75.

(172) Twig G, Elorza A, Molina AJA et al. Fission and selective fusion govern mitochondrial segregation and elimination by autophagy. *Embo Journal* 2008 January 23;27(2):433-46.

(173) Youle RJ, Karbowski M. Mitochondrial fission in apoptosis. *Nature Reviews Molecular Cell Biology* 2005 August;6(8):657-63.

(174) Szabadkai G, Simoni AM, Chami M, Wieckowski MR, Youle RJ, Rizzuto R. Drp-1-dependent division of the mitochondrial network blocks intraorganellar Ca2+ waves and protects against Ca2+-mediated apoptosis. *Molecular Cell* 2004 October 8;16(1):59-68.

(175) Bleazard W, McCaffery JM, King EJ et al. The dynamin-related GTPase Dnm1 regulates mitochondrial fission in yeast. *Nature Cell Biology* 1999 September;1(5):298-304.

(176) Smirnova E, Shurland DL, Ryazantsev SN, van der Bliek AM. A human dynamin-related protein controls the distribution of mitochondria. *Journal of Cell Biology* 1998 October 19;143(2):351-8.

(177) Smirnova E, Griparic L, Shurland DL, van der Bliek AM. Dynamin-related protein Drp1 is required for mitochondrial division in mammalian cells. *Molecular Biology of the Cell* 2001 August;12(8):2245-56.

(178) Yoon Y, Krueger EW, Oswald BJ, McNiven MA. The mitochondrial protein hFis1 regulates mitochondrial fission in mammalian cells through

an interaction with the dynamin-like protein DLP1. *Molecular and Cellular Biology* 2003 August;23(15):5409-20.

(179) Griffin EE, Graumann J, Chan DC. The WD40 protein Caf4p is a component of the mitochondrial fission machinery and recruits Dnm1p to mitochondria. *Journal of Cell Biology* 2005 July 18;170(2):237-48.

(180) Tieu Q, Okreglak V, Naylor K, Nunnari J. The WD repeat protein, Mdv1p, functions as a molecular adaptor by interacting with Dnm1p and Fis1p during mitochondrial fission. *Journal of Cell Biology* 2002 August 5;158(3):445-52.

(181) Zhu PP, Patterson A, Stadler J, Seeburg DP, Sheng M, Blackstone C. Intra- and intermolecular domain interactions of the C-terminal GTPase effector domain of the multimeric dynamin-like GTPase Drp1. *J Biol Chem* 2004 August 20;279(34):35967-74.

(182) Chang CR, Blackstone C. Cyclic AMP-dependent protein kinase phosphorylation of Drp1 regulates its GTPase activity and mitochondrial morphology. *Journal of Biological Chemistry* 2007 July 27;282(30):21583-7.

(183) Han XJ, Lu YF, Li SA et al. CaM kinase l alpha-induced phosphorylation of Drp1 regulates mitochondrial morphology. *Journal of Cell Biology* 2008 August 11;182(3):573-85.

(184) Harder Z, Zunino R, McBride H. Sumo1 conjugates mitochondrial substrates and participates in mitochondrial fission. *Curr Biol* 2004 February 17;14(4):340-5.

(185) Nakamura N, Kimura Y, Tokuda M, Honda S, Hirose S. MARCH-V is a novel mitofusin 2- and Drp1-binding protein able to change mitochondrial morphology. *EMBO Rep* 2006 October;7(10):1019-22.

(186) Braschi E, Zunino R, McBride HM. MAPL is a new mitochondrial SUMO E3 ligase that regulates mitochondrial fission. *EMBO Rep* 2009 July;10(7):748-54.

(187) Karbowski M, Neutzner A, Youle RJ. The mitochondrial E3 ubiquitin ligase MARCH5 is required for Drp1 dependent mitochondrial division. *J Cell Biol* 2007 July 2;178(1):71-84.

(188) Yonashiro R, Ishido S, Kyo S et al. A novel mitochondrial ubiquitin ligase plays a critical role in mitochondrial dynamics. *EMBO J* 2006 August 9;25(15):3618-26.

(189) Cereghetti GM, Stangherlin A, de Brito OM et al. Dephosphorylation by calcineurin regulates translocation of Drp1 to mitochondria. *Proceedings of the National Academy of Sciences of the United States of America* 2008 October 14;105(41):15803-8.

(190) Cribbs JT, Strack S. Reversible phosphorylation of Drp1 by cyclic AMP-dependent protein kinase and calcineurin regulates mitochondrial fission and cell death. *Embo Reports* 2007 October;8(10):939-44.

(191) Cho DH, Nakamura T, Fang J et al. S-nitrosylation of Drp1 mediates beta-amyloid-related mitochondrial fission and neuronal injury. *Science* 2009 April 3;324(5923):102-5.

(192) James DI, Parone PA, Mattenberger Y, Martinou JC. hFis1, a novel component of the mammalian mitochondrial fission machinery. *Journal of Biological Chemistry* 2003 September 19;278(38):36373-9.

(193) Suzuki M, Jeong SY, Karbowski M, Youle RJ, Tjandra N. The solution structure of human mitochondria fission protein Fis1 reveals a novel TPR-like helix bundle. *Journal of Molecular Biology* 2003 November 28;334(3):445-58.

(194) Dohm JA, Lee SJ, Hardwick JM, Hill RB, Gittis AG. Cytosolic domain of the human mitochondrial fission protein Fis1 adopts a TPR fold. *Proteins-Structure Function and Genetics* 2004 January 1;54(1):153-6.

(195) Jofuku A, Ishihara N, Mihara K. Analysis of functional domains of rat mitochondrial Fis1, the mitochondrial fission-stimulating protein. *Biochemical and Biophysical Research Communications* 2005 July 29;333(2):650-9.

(196) Chen HC, Chan DC. Emerging functions of mammalian mitochondrial fusion and fission. *Human Molecular Genetics* 2005 October 15;14:R283-R289.

(197) Tondera D, Santel A, Schwarzer R et al. Knockdown of MTP18, a novel phosphatidylinositol 3-kinase-dependent protein, affects mitochondrial morphology and induces apoptosis. *Journal of Biological Chemistry* 2004 July 23;279(30):31544-55.

(198) Alto NM, Soderling J, Scott JD. Rab32 is an A-kinase anchoring protein and participates in mitochondrial dynamics. *Journal of Cell Biology* 2002 August 19;158(4):659-68.

(199) Karbowski M, Jeong SY, Youle RJ. Endophilin B1 is required for the maintenance of mitochondrial morphology. *Journal of Cell Biology* 2004 September 27;166(7):1027-39.

(200) Eura Y, Ishihara N, Oka T, Mihara K. Identification of a novel protein that regulates mitochondrial fusion by modulating mitofusin (Mfn) protein function. *Journal of Cell Science* 2006 December 1;119(23):4913-25.

(201) Rizzuto R, Brini M, Murgia M, Pozzan T. Microdomains with High Ca2+ Close to Ip(3)-Sensitive Channels That Are Sensed by Neighboring Mitochondria. *Science* 1993 October 29;262(5134):744-7.

(202) Lamarca V, Scorrano L. When separation means death: killing through the mitochondria, but starting from the endoplasmic reticulum. *Embo Journal* 2009 June 17;28(12):1681-3.

(203) Klee M, Pallauf K, Alcala S, Fleischer A, Pimentel-Muinos FX. Mitochondrial apoptosis induced by BH3-only molecules in the exclusive presence of endoplasmic reticular Bak. *Embo Journal* 2009 June 17;28(12):1757-68.

(204) Verstreken P, Ly CV, Venken KJT, Koh TW, Zhou Y, Bellen HJ. Synaptic mitochondria are critical for mobilization of reserve pool vesicles at Drosophila neuromuscular junctions. *Neuron* 2005 August 4;47(3):365-78.

(205) Frank S, Gaume B, Bergmann-Leitner ES et al. The role of dynamin-related protein 1, a mediator of mitochondrial fission, in apoptosis. *Developmental Cell* 2001 October;1(4):515-25.

(206) Karbowski M, Arnoult D, Chen HC, Chan DC, Smith CL, Youle RJ. Quantitation of mitochondrial dynamics by photolabeling of individual organelles shows that mitochondrial fusion is blocked during the Bax activation phase of apoptosis. *Journal of Cell Biology* 2004 February 16;164(4):493-9.

(207) Estaquier J, Arnoult D. Inhibiting Drp1-mediated mitochondrial fission selectively prevents the release of cytochrome c during apoptosis. *Cell Death and Differentiation* 2007 June;14(6):1086-94.

(208) Parone PA, James DI, Da Cruz S et al. Inhibiting the mitochondrial fission machinery does not prevent Bax/Bak-dependent apoptosis. *Molecular and Cellular Biology* 2006 October;26(20):7397-408.

(209) Yu TZ, Sheu SS, Robotham JL, Yoon YS. Mitochondrial fission mediates high glucose-induced cell death through elevated production of reactive oxygen species. *Cardiovascular Research* 2008 July 15;79(2):341-51.

(210) Mai S, Klinkenberg M, Auburger G, Bereiter-Hahn J, Jendrach M. Decreased expression of Drp1 and Fis1 mediates mitochondrial elongation in senescent cells and enhances resistance to oxidative stress through PINK1. *Journal of Cell Science* 2010 March 15;123(6):917-26.

(211) Chen L, Gong QZ, Stice JP, Knowlton AA. Mitochondrial OPA1, apoptosis, and heart failure. *Cardiovascular Research* 2009 October 1;84(1):91-9.

(212) Zuchner S, Mersiyanova IV, Muglia M et al. Mutations in the mitochondrial GTPase mitofusin 2 cause Charcot-Marie-Tooth neuropathy type 2A. *Nature Genetics* 2004 May;36(5):449-51.

(213) Ong SB, Subrayan S, Lim SY, Yellon DM, Davidson SM, Hausenloy DJ. Inhibiting Mitochondrial Fission Protects the Heart Against Ischemia/Reperfusion Injury. *Circulation* 2010 May 11;121(18):2012-U107.

(214) Chen HC, Vermulst M, Wang YE et al. Mitochondrial Fusion Is Required for mtDNA Stability in Skeletal Muscle and Tolerance of mtDNA Mutations. *Cell* 2010 April 16;141(2):280-9.

(215) Brooks C, Wei Q, Cho SG, Dong Z. Regulation of mitochondrial dynamics in acute kidney injury in cell culture and rodent models. *Journal of Clinical Investigation* 2009 May;119(5):1275-85.

(216) Dagda RK, Cherra SJ, Kulich SM, Tandon A, Park D, Chu CT. Loss of PINK1 Function Promotes Mitophagy through Effects on Oxidative Stress and Mitochondrial Fission. *Journal of Biological Chemistry* 2009 May 15;284(20):13843-55.

(217) Nowikovsky K, Reipert S, Devenish RJ, Schweyen RJ. Mdm38 protein depletion causes loss of mitochondrial K+/H+ exchange activity, osmotic swelling and mitophagy. *Cell Death and Differentiation* 2007 September;14(9):1647-56.

(218) Ishihara N, Nomura M, Jofuku A et al. Mitochondrial fission factor Drp1 is essential for embryonic development and synapse formation in mice. *Nature Cell Biology* 2009 August;11(8):958-U114.

(219) Vinten-Johansen J, Thourani VH, Ronson RS et al. Broad-spectrum cardioprotection with adenosine. *Annals of Thoracic Surgery* 1999 November;68(5):1942-8.

(220) Liu GS, Thornton J, Vanwinkle DM, Stanley AWH, Olsson RA, Downey JM. Protection Against Infarction Afforded by Preconditioning Is Mediated by A1 Adenosine Receptors in Rabbit Heart. *Circulation* 1991 July;84(1):350-6.

(221) Garlid KD, Paucek P, YarovYarovoy V et al. Cardioprotective effect of diazoxide and its interaction with mitochondrial ATP-Sensitive K+ channels - Possible mechanism of cardioprotection. *Circulation Research* 1997 December;81(6):1072-82.

(222) Liu YG, Sato T, O'Rourke B, Marban E. Mitochondrial ATP-dependent potassium channels - Novel effectors of cardioprotection? *Circulation* 1998 June 23;97(24):2463-9.

(223) Yellon DM, Baxter GF. Protecting the ischaemic and reperfused myocardium in acute myocardial infarction: distant dream or near reality? *Heart* 2000 April;83(4):381-7.

(224) Rakhit RD, Marber MS. Nitric oxide: an emerging role in cardioprotection? *Heart* 2001 October;86(4):368-72.

(225) Rakhit RD, Mojet MH, Marber MS, Duchen MR. Mitochondria as targets for nitric oxide-induced protection during simulated ischemia and reoxygenation in isolated neonatal cardiomyocytes. *Circulation* 2001 May 29;103(21):2617-23.

(226) Bolli R, Manchikalapudi S, Tang XL et al. The protective effect of late preconditioning against myocardial stunning in conscious rabbits is mediated by nitric oxide synthase - Evidence that nitric oxide acts both as a trigger and as a mediator of the late phase of ischemic preconditioning. *Circulation Research* 1997 December;81(6):1094-107.

(227) Bolli R, Bhatti ZA, Tang XL et al. Evidence that late preconditioning against myocardial stunning in conscious rabbits is triggered by the generation of nitric oxide. *Circulation Research* 1997 July;81(1):42-52.

(228) Yellon DM, Baxter GF. Reperfusion injury revisited - Is there a role for growth factor signaling in limiting lethal reperfusion injury? *Trends in Cardiovascular Medicine* 1999 November;9(8):245-9.

(229) Hausenloy DJ, Yellon DM. New directions for protecting the heart against ischaemia-reperfusion injury: targeting the Reperfusion Injury Salvage Kinase (RISK)-pathway. *Cardiovascular Research* 2004 February 15;61(3):448-60.

(230) Argaud L, Gateau-Roesch O, Raisky O, Loufouat J, Robert D, Ovize M. Postconditioning inhibits mitochondrial permeability transition. *Circulation* 2005 January 18;111(2):194-7.

(231) Yellon DM, Hausenloy DJ. Mechanisms of disease: Myocardial reperfusion injury. *New England Journal of Medicine* 2007 September 13;357(11):1121-35.

(232) Hausenloy DJ, Duchen MR, Yellon DM. Inhibiting mitochondrial permeability transition pore opening at reperfusion protects against ischaemia-reperfusion injury. *Cardiovascular Research* 2003 December 1;60(3):617-25.

(233) Argenta LC, Morykwas MJ, Mays JJ, Thompson EA, Hammon JW, Jordan JE. Reduction of myocardial ischemia-reperfusion injury by mechanical tissue resuscitation using sub-atmospheric pressure. *J Card Surg* 2010 March;25(2):247-52.

(234) Murry CE, Jennings RB, Reimer KA. Preconditioning with Ischemia - A Delay of Lethal Cell Injury in Ischemic Myocardium. *Circulation* 1986 November;74(5):1124-36.

(235) Hausenloy DJ, Tsang A, Mocanu MM, Yellon DM. Ischemic preconditioning protects by activating prosurvival kinases at reperfusion. *American Journal of Physiology-Heart and Circulatory Physiology* 2005 February;288(2):H971-H976.

(236) Hausenloy DJ, Yellon DM, Mani-Babu S, Duchen MR. Preconditioning protects by inhibiting the mitochondrial permeability transition. *American Journal of Physiology-Heart and Circulatory Physiology* 2004 August;287(2):H841-H849.

(237) DAlonzo AJ, Darbenzio RB, Parham CS, Grover GJ. Effects of Intracoronary Cromakalim on Postischemic Contractile Function and Action-Potential Duration. *Cardiovascular Research* 1992 November;26(11):1046-53.

(238) Hausenloy DJ, Maddock HL, Baxter GF, Yellon DM. Ischemic preconditioning and mitochondrial K-ATP channel activation protect the myocardium by inhibiting mitochondrial permeability transition pore opening. *Circulation* 2002 November 5;106(19):134.

(239) Ma XJ, Zhang XH, Li CM, Luo M. Effect of postconditioning on coronary blood flow velocity and endothelial function in patients with acute myocardial infarction. *Scandinavian Cardiovascular Journal* 2006 December;40(6):327-33.

(240) Thibault H, Piot C, Staat P et al. Long-term benefit of postconditioning. *Circulation* 2008 February 26;117(8):1037-44.

(241) Tsang A, Hausenloy DJ, Mocanu MM, Yellon DM. Postconditioning: A form of "modified reperfusion" protects the myocardium by activating the phosphatidylinositol 3-kinase-Akt pathway. *Circulation Research* 2004 August 6;95(3):230-2.

(242) Sun HY, Wang NP, Kerendi F et al. Hypoxic postconditioning reduces cardiomyocyte loss by inhibiting ROS generation and intracellular Ca2(+) overload. *American Journal of Physiology-Heart and Circulatory Physiology* 2005 April;288(4):H1900-H1908.

(243) Kin H, Zhao ZQ, Sun HY et al. Postconditioning attenuates myocardial ischemia-reperfusion injury by inhibiting events in the early minutes of reperfusion. *Cardiovascular Research* 2004 April 1;62(1):74-85.

(244) Cohen MV, Yang XM, Downey JM. The pH hypothesis of postconditioning - Staccato reperfusion reintroduces oxygen and perpetuates myocardial acidosis. *Circulation* 2007 April 10;115(14):1895-903.

(245) Inserte J, Barba I, Hernando V, Garcia-Dorado D. Delayed recovery of intracellular acidosis during reperfusion prevents calpain activation and determines protection in postconditioned myocardium. *Cardiovascular Research* 2009 January 1;81(1):116-22.

(246) Zhao ZQ, Vinten-Johansen J. Postconditioning: Reduction of reperfusion-induced injury. *Cardiovascular Research* 2006 May 1;70(2):200-11.

(247) Penna C, Perrelli MG, Raimondo S et al. Postconditioning induces an anti-apoptotic effect and preserves mitochondrial integrity in isolated rat hearts. *Biochimica et Biophysica Acta-Bioenergetics* 2009 July;1787(7):794-801.

(248) Kerendi F, Kin H, Halkos ME et al. Remote postconditioning - Brief renal ischemia and reperfusion applied before coronary artery reperfusion

reduces myocardial infarct size via endogenous activation of adenosine receptors. *Basic Research in Cardiology* 2005 September;100(5):404-12.

(249) Przyklenk K, Bauer B, Ovize M, Kloner RA, Whittaker P. Regional Ischemic Preconditioning Protects Remote Virgin Myocardium from Subsequent Sustained Coronary-Occlusion. *Circulation* 1993 March;87(3):893-9.

(250) Pell TJ, Baxter GF, Yellon DM, Drew GM. Renal ischemia preconditions myocardium: role of adenosine receptors and ATP-sensitive potassium channels. *American Journal of Physiology-Heart and Circulatory Physiology* 1998 November;44(5):H1542-H1547.

(251) Gho BCG, Schoemaker RG, vandenDoel MA, Duncker DJ, Verdouw PD. Myocardial protection by brief ischemia in noncardiac tissue. *Circulation* 1996 November 1;94(9):2193-200.

(252) Hausenloy DJ, Mwamure PK, Venugopal V et al. Effect of remote ischaemic preconditioning on myocardial injury in patients undergoing coronary artery bypass graft surgery: a randomised controlled trial. *Lancet* 2007 August 18;370(9587):575-9.

(253) Ali ZA, Callaghan CJ, Lim E et al. Remote ischemic preconditioning reduces myocardial and renal injury after elective abdominal aortic aneurysm repair - A randomized controlled trial. *Circulation* 2007 September 11;116(11):I98-I105.

(254) Bose AK, Mocanu MM, Carr RD, Yellon DM. Glucagon like peptide-1 is protective against myocardial ischemia/reperfusion injury when given either as a preconditioning mimetic or at reperfusion in an isolated rat heart model. *Cardiovascular Drugs and Therapy* 2005 January;19(1):9-11.

(255) Bullard AJ, Govewalla P, Yellon DM. Erythropoietin protects the myocardium against reperfusion injury in vitro and in vivo. *Basic Research in Cardiology* 2005 September;100(5):397-403.

(256) Bell RM, Yellon DM. Atorvastatin, administered at the onset of reperfusion, and independent of lipid lowering, protects the myocardium by up-regulating a pro-survival pathway. *Journal of the American College of Cardiology* 2003 February 5;41(3):508-15.

(257) Yang XM, Philipp S, Downey JM, Cohen MV. Atrial natriuretic peptide administered just prior to reperfusion limits infarction in rabbit hearts. *Basic Research in Cardiology* 2006 July;101(4):311-8.

(258) Hausenloy DJ, Tsang A, Yellon DM. The reperfusion injury salvage kinase pathway: A common target for both ischemic preconditioning and postconditioning. *Trends in Cardiovascular Medicine* 2005 February;15(2):69-75.

(259) Davidson SM, Hausenloy D, Duchen MR, Yellon DM. Signalling via the reperfusion injury signalling kinase (RISK) pathway links closure of the

mitochondrial permeability transition pore to cardioprotection. *International Journal of Biochemistry & Cell Biology* 2006 March;38(3):414-9.

(260) Abdallah Y, Gkatzoflia A, Gligorievski D et al. Insulin protects cardiomyocytes against reoxygenation-induced hypercontracture by a survival pathway targeting SR Ca2+ storage. *Cardiovascular Research* 2006 May 1;70(2):346-53.

(261) Patti G, Pasceri V, Colonna G et al. Atorvastatin pretreatment improves outcomes in patients with acute coronary syndromes undergoing early percutaneous coronary intervention - Results of the ARMYDA-ACS randomized trial. *Journal of the American College of Cardiology* 2007 March 27;49(12):1272-8.

(262) Leung AWC, Varanyuwatana P, Halestrap AP. The mitochondrial phosphate carrier interacts with cyclophilin D and may play a key role in the permeability transition. *Journal of Biological Chemistry* 2008 September 26;283(39):26312-23.

(263) Shanmuganathan S, Hausenloy DJ, Duchen MR, Yellon DM. Mitochondrial permeability transition pore as a target for cardioprotection in the human heart. *American Journal of Physiology-Heart and Circulatory Physiology* 2005 July;289(1):H237-H242.

(264) Baines CP, Kaiser RA, Purcell NH et al. Loss of cyclophilin D reveals a critical role for mitochondrial permeability transition in cell death. *Nature* 2005 March 31;434(7033):658-62.

(265) Stull JT, Buss JE. Phosphorylation of Cardiac Troponin by Cyclic Adenosine 3'=5'-Monophosphate-Dependent Protein-Kinase. *Journal of Biological Chemistry* 1977;252(3):851-7.

(266) Schwartz A, Entman ML, Kaniike K, Lane LK, Vanwinkle WB, Bornet EP. Rate of Calcium-Uptake Into Sarcoplasmic-Reticulum of Cardiac-Muscle and Skeletal-Muscle - Effects of Cyclic Amp-Dependent Protein Kinase and Phosphorylase-B Kinase. *Biochimica et Biophysica Acta* 1976;426(1):57-72.

(267) Fink MA, Zakhary DR, Mackey JA et al. AKAP-mediated targeting of protein kinase A regulates contractility in cardiac myocytes. *Circulation Research* 2001 February 16;88(3):291-7.

(268) Roche KW, Obrien RJ, Mammen AL, Bernhardt J, Huganir RL. Characterization of multiple phosphorylation sites on the AMPA receptor GluR1 subunit. *Neuron* 1996 June;16(6):1179-88.

(269) Walsh DA, VanPatten SM. Multiple Pathway Signal-Transduction by the Camp-Dependent Protein-Kinase. *Faseb Journal* 1994 December;8(15):1227-36.

(270) Niswender CM, Ishihara RW, Judge LM, Zhang C, Shokat KM, McKnight GS. Protein engineering of protein kinase A catalytic subunits results in the acquisition of novel inhibitor sensitivity. *Journal of Biological Chemistry* 2002 August 9;277(32):28916-22.

(271) McKnight GS. Cyclic AMP second messenger systems. *Current Opinion in Cell Biology* 1991;3(2):213-7.

(272) Enns LC, Pettan-Brewer C, Ladiges W. Protein kinase A is a target for aging and the aging heart. *Aging-Us* 2010 April;2(4):238-43.

(273) Brandon EP, Idzerda RL, McKnight GS. PKA isoforms, neural pathways, and behaviour: making the connection. *Current Opinion in Neurobiology* 1997 June;7(3):397-403.

(274) Lochner A, Genade S, Tromp E, Podzuweit T, Moolman JA. Ischemic preconditioning and the beta-adrenergic signal transduction pathway. *Circulation* 1999 August 31;100(9):958-66.

(275) Inserte J, Garcia-Dorado D, Ruiz-Meana M, Agullo L, Pina P, Soler-Soler J. Ischemic preconditioning attenuates calpain-mediated degradation of structural proteins through a protein kinase A-dependent mechanism. *Cardiovascular Research* 2004 October 1;64(1):105-14.

(276) Sanada S, Asanuma H, Tsukamoto O et al. Protein kinase A as another mediator of ischemic preconditioning independent of protein kinase C. *Circulation* 2004 July 6;110(1):51-7.

(277) Sanada S, Kitakaze M, Papst PJ et al. Cardioprotective effect afforded by transient exposure to phosphodiesterase III inhibitors - The role of protein kinase A and p38 mitogen-activated protein kinase. *Circulation* 2001 August 7;104(6):705-10.

(278) Dong JM, Leung T, Manser E, Lim L. cAMP-induced morphological changes are counteracted by the activated RhoA small GTPase and the Rho kinase ROK alpha. *Journal of Biological Chemistry* 1998 August 28;273(35):22554-62.

(279) Shimokawa H. Rho-kinase as a novel therapeutic target in treatment of cardiovascular diseases. *Journal of Cardiovascular Pharmacology* 2002 March;39(3):319-27.

(280) Oeseburg H, de Boer RA, Buikema H, van der Harst P, an Gilst WH, Silljé HH. Glucagon-like peptide 1 prevents reactive oxygen species-induced endothelial cell senescence through the activation of protein kinase A. *Arterioscler Thromb Vasc Biol* 2010;30(7):1407-14.

(281) Sato T, Saito T, Saegusa N, Nakaya H. Mitochondrial Ca2+-activated K+ channels in cardiac myocytes - A mechanism of the cardioprotective effect and modulation by protein kinase A. *Circulation* 2005 January 18;111(2):198-203.

(282) Marx SO, Reiken S, Hisamatsu Y et al. PKA phosphorylation dissociates FKBP12.6 from the calcium release channel (ryanodine receptor): Defective regulation in failing hearts. *Cell* 2000 May 12;101(4):365-76.

(283) Miyamoto N, Tanaka R, Shimosawa T et al. Protein kinase A-dependent suppression of reactive oxygen species in transient focal ischemia in adrenomedullin-deficient mice. *Journal of Cerebral Blood Flow and Metabolism* 2009 November;29(11):1769-79.

(284) Ma Y, Cheng WT, Wu S, Wong TM. Oestrogen confers cardioprotection by suppressing Ca2+/calmodulin-dependent protein kinase II. *British Journal of Pharmacology* 2009 July;157(5):705-15.

(285) Downward J. Mechanisms and consequences of activation of protein kinase B/Akt. *Current Opinion in Cell Biology* 1998 April;10(2):262-7.

(286) Shiojima I, Walsh K. Regulation of cardiac growth and coronary angiogenesis by the Akt/PKB signaling pathway. *Genes & Development* 2006 December 15;20(24):3347-65.

(287) Chen WS, Xu PZ, Gottlob K et al. Growth retardation and increased apoptosis in mice with homozygous disruption of the akt1 gene. *Genes & Development* 2001 September 1;15(17):2203-8.

(288) Cho H, Thorvaldsen JL, Chu QW, Feng F, Birnbaum MJ. Akt1/PKB alpha is required for normal growth but dispensable for maintenance of glucose homeostasis in mice. *Journal of Biological Chemistry* 2001 October 19;276(42):38349-52.

(289) Cho H, Mu J, Kim JK et al. Insulin resistance and a diabetes mellitus-like syndrome in mice lacking the protein kinase Akt2 (PKB beta). *Science* 2001 June 1;292(5522):1728-31.

(290) Garofalo RS, Orena SJ, Rafidi K et al. Severe diabetes, age-dependent loss of adipose tissue, and mild growth deficiency in mice lacking Akt2/PKB beta. *Journal of Clinical Investigation* 2003 July;112(2):197-208.

(291) Easton RM, Cho H, Roovers K et al. Role for Akt3/Protein kinase B gamma in attainment of normal brain size. *Molecular and Cellular Biology* 2005 March;25(5):1869-78.

(292) Tschopp O, Yang ZZ, Brodbeck D et al. Essential role of protein kinase B gamma (PKB gamma/Akt3) in postnatal brain development but not in glucose homeostasis. *Development* 2005 July;132(13):2943-54.

(293) Shiraishi I, Melendez J, Ahn Y et al. Nuclear targeting of Akt enhances kinase activity and survival of cardiomyocytes. *Circulation Research* 2004 April 16;94(7):884-91.

(294) Walsh K. Akt signaling and growth of the heart. *Circulation* 2006 May 2;113(17):2032-4.

(295) Sun JF, Phung T, Shiojima I et al. Microvascular patterning is controlled by fine-tuning the Akt signal. *Proceedings of the National Academy of Sciences of the United States of America* 2005 January 4;102(1):128-33.

(296) Phung TL, Ziv K, Dabydeen D et al. Pathological angiogenesis is induced by sustained Akt signaling and inhibited by rapamycin. *Cancer Cell* 2006 August;10(2):159-70.

(297) Datta SR, Dudek H, Tao X et al. Akt phosphorylation of BAD couples survival signals to the cell-intrinsic death machinery. *Cell* 1997 October 17;91(2):231-41.

(298) del PL, Gonzalez-Garcia M, Page C, Herrera R, Nunez G. Interleukin-3-induced phosphorylation of BAD through the protein kinase Akt. *Science* 1997 October 24;278(5338):687-9.

(299) Dudek H, Datta SR, Franke TF et al. Regulation of neuronal survival by the serine-threonine protein kinase Akt. *Science* 1997 January 31;275(5300):661-5.

(300) Kauffmann-Zeh A, Rodriguez-Viciana P, Ulrich E et al. Suppression of c-Myc-induced apoptosis by Ras signalling through PI(3)K and PKB. *Nature* 1997 February 6;385(6616):544-8.

(301) Kennedy SG, Wagner AJ, Conzen SD et al. The PI 3-kinase/Akt signaling pathway delivers an anti-apoptotic signal. *Genes Dev* 1997 March 15;11(6):701-13.

(302) Stambolic V, Suzuki A, de la Pompa JL et al. Negative regulation of PKB/Akt-dependent cell survival by the tumor suppressor PTEN. *Cell* 1998 October 2;95(1):29-39.

(303) Brunet A, Bonni A, Zigmond MJ et al. Akt promotes cell survival by phosphorylating and inhibiting a Forkhead transcription factor. *Cell* 1999 March 19;96(6):857-68.

(304) Miao WF, Luo ZY, Kitsis RN, Walsh K. Intracoronary, adenovirus-mediated Akt gene transfer in heart limits infarct size following ischemia-reperfusion injury in vivo. *Journal of Molecular and Cellular Cardiology* 2000 December;32(12):2397-402.

(305) Jonassen AK, Sack MN, Mjos OD, Yellon DM. Myocardial protection by insulin at reperfusion requires early administration and is mediated via Akt and p70s6 kinase cell-survival signaling. *Circulation Research* 2001 December 7;89(12):1191-8.

(306) Hausenloy DJ, Mocanu MM, Yellon DM. Activation of the pro-survival kinases (PI3 kinase-Akt and Erk 1/2) at reperfusion is essential for preconditioning-induced protection. *Circulation* 2003 October 28;108(17):62.

(307) Hausenloy DJ, Mocanu MA, Yellon DM. Cross-talk between the survival kinases during early reperfusion: its contribution to ischemic preconditioning. *Cardiovascular Research* 2004 August 1;63(2):305-12.

(308) Hausenloy DJ, Yellon DM. Reperfusion injury salvage kinase signalling: taking a RISK for cardioprotection. *Heart Failure Reviews* 2007 December;12(3-4):217-34.

(309) Kobayashi H, Miura T, Ishida H et al. Limitation of infarct size by erythropoietin is associated with translocation of Akt to the mitochondria after reperfusion. *Clin Exp Pharmacol Physiol* 2008 July;35(7):812-9.

(310) Franke TF. PI3K/Akt: getting it right matters. *Oncogene* 2008 October 27;27(50):6473-88.

(311) Bellacosa A, Testa JR, Staal SP, Tsichlis PN. A Retroviral Oncogene, Akt, Encoding A Serine-Threonine Kinase Containing An Sh2-Like Region. *Science* 1991 October 11;254(5029):274-7.

(312) Coffer PJ, Woodgett JR. Molecular-Cloning and Characterization of A Novel Putative Protein-Serine Kinase Related to the Camp-Dependent and Protein-Kinase-C Families. *European Journal of Biochemistry* 1991 October 15;201(2):475-81.

(313) Jones PF, Jakubowicz T, Hemmings BA. Molecular-Cloning of A 2Nd Form of Rac Protein-Kinase. *Cell Regulation* 1991 December;2(12):1001-9.

(314) Foster FM, Traer CJ, Abraham SM, Fry MJ. The phosphoinositide (PI) 3-kinase family. *Journal of Cell Science* 2003 August 1;116(15):3037-40.

(315) Wymann MP, Zvelebil M, Laffargue M. Phosphoinositide 3-kinase signalling - which way to target? *Trends in Pharmacological Sciences* 2003 July;24(7):366-76.

(316) Kovacic S, Soltys CLM, Barr AJ, Shiojima I, Walsh K, Dyck JRB. Akt activity negatively regulates phosphorylation of AMP-activated protein kinase in the heart. *Journal of Biological Chemistry* 2003 October 10;278(41):39422-7.

(317) Alessi DR, Andjelkovic M, Caudwell B et al. Mechanism of activation of protein kinase B by insulin and IGF-1. *Embo Journal* 1996 December 2;15(23):6541-51.

(318) Stephens L, Anderson K, Stokoe D et al. Protein kinase B kinases that mediate phosphatidylinositol 3,4,5-trisphosphate-dependent activation of protein kinase B. *Science* 1998 January 30;279(5351):710-4.

(319) Yang J, Cron P, Thompson V et al. Molecular mechanism for the regulation of protein kinase B/Akt by hydrophobic motif phosphorylation. *Molecular Cell* 2002 June;9(6):1227-40.

(320) Toker A, Newton AC. Akt/protein kinase B is regulated by autophosphorylation at the hypothetical PDK-2 site. *Journal of Biological Chemistry* 2000 March 24;275(12):8271-4.

(321) Balendran A, Casamayor A, Deak M et al. PDK1 acquires PDK2 activity in the presence of a synthetic peptide derived from the carboxyl terminus of PRK2. *Current Biology* 1999 April 22;9(8):393-404.

(322) Persad S, Attwell S, Gray V et al. Regulation of protein kinase B/Akt-serine 473 phosphorylation by integrin-linked kinase - Critical roles for kinase activity and amino acids arginine 211 and serine 343. *Journal of Biological Chemistry* 2001 July 20;276(29):27462-9.

(323) Kawakami Y, Nishimoto H, Kitaura J et al. Protein kinase C beta II regulates Akt phosphorylation on Ser-473 in a cell type- and stimulus-specific fashion. *Journal of Biological Chemistry* 2004 November 12;279(46):47720-5.

(324) Feng JH, Park J, Cron P, Hess D, Hemmings BA. Identification of a PKB/Akt hydrophobic motif Ser-473 kinase as DNA-dependent protein kinase. *Journal of Biological Chemistry* 2004 September 24;279(39):41189-96.

(325) Viniegra JG, Martinez N, Modirassari P et al. Full activation of PKB/Akt in response to insulin or ionizing radiation is mediated through ATM. *Journal of Biological Chemistry* 2005 February 11;280(6):4029-36.

(326) Sarbassov DD, Guertin DA, Ali SM, Sabatini DM. Phosphorylation and regulation of Akt/PKB by the rictor-mTOR complex. *Science* 2005 February 18;307(5712):1098-101.

(327) Andjelkovic M, Maira SM, Cron P, Parker PJ, Hemmings BA. Domain swapping used to investigate the mechanism of protein kinase B regulation by 3-phosphoinositide-dependent protein kinase 1 and ser473 kinase. *Molecular and Cellular Biology* 1999 July;19(7):5061-72.

(328) Deprez J, Vertommen D, Alessi DR, Hue L, Rider MH. Phosphorylation and activation of heart 6-phosphofructo-2-kinase by protein kinase B and other protein kinases of the insulin signaling cascades. *Journal of Biological Chemistry* 1997 July 11;272(28):17269-75.

(329) Catalucci D, Condorelli G. Effects of Akt on cardiac myocytes - Location counts. *Circulation Research* 2006 August 18;99(4):339-41.

(330) Gottlob K, Majewski N, Kennedy S, Kandel E, Robey RB, Hay N. Inhibition of early apoptotic events by Akt/PKB is dependent on the first committed step of glycolysis and mitochondrial hexokinase. *Genes & Development* 2001 June 1;15(11):1406-18.

(331) Nagoshi T, Matsui T, Aoyama T et al. PI3K rescues the detrimental effects of chronic Akt activation in the heart during ischemia/reperfusion injury

(vol 115, pg 2128, 2005). *Journal of Clinical Investigation* 2006 February;116(2):548.

(332) Haq SE, Choukroun G, Grazette L et al. Differential regulation of the signaling pathways of the MAPKs, calcineurin and AKT in the failing human heart. *Circulation* 2000 October 31;102(18):289-90.

(333) Haq S, Choukroun G, Lim H et al. Differential activation of signal transduction pathways in human hearts with hypertrophy versus advanced heart failure. *Circulation* 2001 February 6;103(5):670-7.

(334) Nagoshi T, Matsui T, Aoyama T et al. PI3K rescues the detrimental effects of chronic Akt activation in the heart during ischemia/reperfusion injury. *Journal of Clinical Investigation* 2005 August;115(8):2128-38.

(335) Shiojima I, Sato K, Izumiya Y et al. Disruption of coordinated cardiac hypertrophy and angiogenesis contributes to the transition to heart failure. *Journal of Clinical Investigation* 2005 August;115(8):2108-18.

(336) Matsui T, Nagoshi T, Hong EG et al. Effects of chronic Akt activation on glucose uptake in the heart. *American Journal of Physiology-Endocrinology and Metabolism* 2006 May;290(5):E789-E797.

(337) Li JP, Defea K, Roth RA. Modulation of insulin receptor substrate-1 tyrosine phosphorylation by an Akt/phosphatidylinositol 3-kinase pathway. *Journal of Biological Chemistry* 1999 April 2;274(14):9351-6.

(338) Matsui T, Li L, Wu JC et al. Phenotypic spectrum caused by transgenic overexpression of activated Akt in the heart. *Journal of Biological Chemistry* 2002 June 21;277(25):22896-901.

(339) Huber M, Helgason CD, Damen JE et al. The role of SHIP in growth factor induced signalling. *Progress in Biophysics & Molecular Biology* 1999;71(3-4):423-34.

(340) Andjelkovic N, Zolnierowicz S, vanHoof C, Goris J, Hemmings BA. The catalytic subunit of protein phosphatase 2A associates with the translation termination factor eRF1. *Faseb Journal* 1996 April 30;10(6):1456.

(341) Gao TY, Furnari F, Newton AC. PHLPP: A phosphatase that directly dephosphorylates akt, promotes apoptosis, and suppresses tumor growth. *Molecular Cell* 2005 April 1;18(1):13-24.

(342) Freude B, Masters TN, Robicsek F et al. Apoptosis is initiated by myocardial ischemia and executed during reperfusion. *Journal of Molecular and Cellular Cardiology* 2000 February;32(2):197-208.

(343) Hausenloy DJ, Yellon DM. Preconditioning and postconditioning: United at reperfusion. *Pharmacology & Therapeutics* 2007 November;116(2):173-91.

(344) Bell RM, Yellon DM. Bradykinin limits infarction when administered as an adjunct to reperfusion in mouse heart: the role of PI3K, Akt and eNOS. *Journal of Molecular and Cellular Cardiology* 2003 February;35(2):185-93.

(345) Schulman D, Latchman DS, Yellon DM. Urocortin protects the heart from reperfusion injury via upregulation of p42/p44 MAPK signaling pathway. *American Journal of Physiology-Heart and Circulatory Physiology* 2002 October;283(4):H1481-H1488.

(346) Fujio Y, Nguyen T, Wencker D, Kitsis RN, Walsh K. Akt promotes survival of cardiomyocytes in vitro and protects against ischemia-reperfusion injury in mouse heart. *Circulation* 2000 February 15;101(6):660-7.

(347) Fryer RM, Pratt PF, Hsu AK, Gross GJ. Differential activation of extracellular signal regulated kinase isoforms in preconditioning and opioid-induced cardioprotection. *Journal of Pharmacology and Experimental Therapeutics* 2001 February;296(2):642-9.

(348) Behrends M, Schulz R, Post H et al. Inconsistent relation of MAPK activation to infarct size reduction by ischemic preconditioning in pigs. *American Journal of Physiology-Heart and Circulatory Physiology* 2000 September;279(3):H1111-H1119.

(349) Solenkova N, Cohen MV, Downey JM. PI3 kinase supports the preconditioned heart through a critical convalescent period. *Journal of Molecular and Cellular Cardiology* 2005 May;38(5):848.

(350) Yang XM, Krieg T, Cui L, Downey JM, Cohen MV. NECA and bradykinin at reperfusion reduce infarction in rabbit hearts by signaling through PI3K, ERK, and NO. *Journal of Molecular and Cellular Cardiology* 2004 March;36(3):411-21.

(351) Yang XM, Proctor JB, Cui L, Krieg T, Downey JM, Cohen MV. Multiple, brief coronary occlusions during early reperfusion protect rabbit hearts by targeting cell signaling pathways. *Journal of the American College of Cardiology* 2004 September 1;44(5):1103-10.

(352) Downey JM, Cohen MV. We think we see a pattern emerging here. *Circulation* 2005 January 18;111(2):120-1.

(353) Kin H, Zatta AJ, Lofye MT et al. Postconditioning reduces infarct size via adenosine receptor activation by endogenous adenosine. *Cardiovascular Research* 2005 July 1;67(1):124-33.

(354) Philipp S, Yang XM, Cui L, Davis AM, Downey JM, Cohen MV. Postconditioning protects rabbit hearts through a protein kinase C-adenosine A(2b) receptor cascade. *Cardiovascular Research* 2006 May 1;70(2):308-14.

(355) Brookes PS, Salinas EP, Darley-Usmar K et al. Concentration-dependent effects of nitric oxide on mitochondrial permeability transition and cytochrome c release. *Journal of Biological Chemistry* 2000 July 7;275(27):20474-9.

(356) Juhaszova M, Zorov DB, Kim SH et al. Glycogen synthase kinase-3 beta mediates convergence of protection signaling to inhibit the mitochondrial permeability transition pore. *Journal of Clinical Investigation* 2004 June;113(11):1535-49.

(357) Gross ER, Hsu AK, Gross GJ. Opioid-induced cardioprotection occurs via glycogen synthase kinase beta inhibition during reperfusion in intact rat hearts. *Circulation Research* 2004 April 16;94(7):960-6.

(358) Chen L, Hahn H, Wu GY et al. Opposing cardioprotective actions and parallel hypertrophic effects of delta PKC and epsilon PKC. *Proceedings of the National Academy of Sciences of the United States of America* 2001 September 25;98(20):11114-9.

(359) Roy SS, Madesh M, Davies E, Antonsson B, Danial N, Hajnoczky G. Bad Targets the Permeability Transition Pore Independent of Bax or Bak to Switch between Ca2+-Dependent Cell Survival and Death. *Molecular Cell* 2009 February 13;33(3):377-88.

(360) Malhotra A, Begley R, Kang BPS et al. PKC-epsilon-dependent survival signals in diabetic hearts. *American Journal of Physiology-Heart and Circulatory Physiology* 2005 October;289(4):H1343-H1350.

(361) Khaliulin I, Clarke SJ, Lin H, Parker J, Suleiman MS, Halestrap AP. Temperature preconditioning of isolated rat hearts - a potent cardioprotective mechanism involving a reduction in oxidative stress and inhibition of the mitochondrial permeability transition pore. *Journal of Physiology-London* 2007 June 15;581(3):1147-61.

(362) Cohen MV, Downey JM. Adenosine: trigger and mediator of cardioprotection. *Basic Research in Cardiology* 2008 May;103(3):203-15.

(363) Chappell JB, Crofts AR. Calcium Ion Accumulation and Volume Changes of Isolated Liver Mitochondria - Calcium Ion-Induced Swelling. *Biochemical Journal* 1965;95(2):378-&.

(364) Crofts AR, Chappell JB. Calcium Ion Accumulation and Volume Changes of Isolated Liver Mitochondria - Reversal of Calcium Ion-Induced Swelling. *Biochemical Journal* 1965;95(2):387-&.

(365) Hunter DR, Haworth RA. Ca-2+-Induced Membrane Transition in Mitochondria .1. Protective Mechanisms. *Archives of Biochemistry and Biophysics* 1979;195(2):453-9.

(366) Haworth RA, Hunter DR. Ca-2+-Induced Membrane Transition in Mitochondria .2. Nature of the Ca-2+ Trigger Site. *Archives of Biochemistry and Biophysics* 1979;195(2):460-7.

(367) Crompton M, Costi A, Hayat L. Evidence for the Presence of A Reversible Ca-2+-Dependent Pore Activated by Oxidative Stress in Heart-Mitochondria. *Biochemical Journal* 1987 August 1;245(3):915-8.

(368) Kroemer G, Reed JC. Mitochondrial control of cell death. *Nature Medicine* 2000 May;6(5):513-9.

(369) Baines CP, Kaiser RA, Sheiko T, Craigen WJ, Molkentin JD. Voltage-dependent anion channels are dispensable for mitochondrial-dependent cell death. *Nature Cell Biology* 2007 May;9(5):550-U122.

(370) Leung AWC, Halestrap AP. Recent progress in elucidating the molecular mechanism of the mitochondrial permeability transition pore. *Biochimica et Biophysica Acta-Bioenergetics* 2008 July;1777(7-8):946-52.

(371) Kokoszka JE, Waymire KG, Levy SE et al. The ADP/ATP translocator is not essential for the mitochondrial permeability transition pore. *Nature* 2004 January 29;427(6973):461-5.

(372) Alcala S, Klee M, Fernandez J, Fleischer A, Pimental-Muinos F. A high-throughput screening for mammalian cell death effectors identifies the mitochondrial phosphate carrier as a regulator of cytochrome c release. *Oncogene* 2008 January 3;27(1):44-54.

(373) Suleiman MS, Halestrap AP, Griffiths EJ. Mitochondria: a target for myocardial protection. *Pharmacology & Therapeutics* 2001 January;89(1):29-46.

(374) Xu MF, Wang YG, Hirai K, Ayub A, Ashraf A. Calcium preconditioning inhibits mitochondrial permeability transition and apoptosis. *American Journal of Physiology-Heart and Circulatory Physiology* 2001 February;280(2):H899-H908.

(375) Halestrap AP, Brenner C. The adenine nucleotide translocase: A central component of the mitochondrial permeability transition pore and key player in cell death. *Current Medicinal Chemistry* 2003 August;10(16):1507-25.

(376) Halestrap AP, Davidson AM. Inhibition of Ca-2+-Induced Large-Amplitude Swelling of Liver and Heart-Mitochondria by Cyclosporine Is Probably Caused by the Inhibitor Binding to Mitochondrial-Matrix Peptidyl-Prolyl Cis-Trans Isomerase and Preventing It Interacting with the Adenine-Nucleotide Translocase. *Biochemical Journal* 1990 May 15;268(1):153-60.

(377) Halestrap AP, Mcstay GP, Clarke SJ. The permeability transition pore complex: another view. *Biochimie* 2002 February;84(2-3):153-66.

(378) Da Cruz S, Xenarios I, Langridge J, Vilbois F, Parone PA, Martinou JC. Proteomic analysis of the mouse liver mitochondrial inner membrane. *Journal of Biological Chemistry* 2003 October 17;278(42):41566-71.

(379) Halestrap AP. Dual role for the ADP/ATP translocator? *Nature* 2004 August 26;430(7003).

(380) Halestrap AP. What is the mitochondrial permeability transition pore? *Journal of Molecular and Cellular Cardiology* 2009 June;46(6):821-31.

(381) Crompton M, Virji S, Ward JM. Cyclophilin-D binds strongly to complexes of the voltage-dependent anion channel and the adenine nucleotide translocase to form the permeability transition pore. *European Journal of Biochemistry* 1998 December 1;258(2):729-35.

(382) Crompton M, Ellinger H, Costi A. Inhibition by Cyclosporin-A of A Ca-2+-Dependent Pore in Heart-Mitochondria Activated by Inorganic-Phosphate and Oxidative Stress. *Biochemical Journal* 1988 October 1;255(1):357-60.

(383) Connern CP, Halestrap AP. Purification and N-Terminal Sequencing of Peptidyl-Prolyl Cis-Trans-Isomerase from Rat-Liver Mitochondrial Matrix Reveals the Existence of A Distinct Mitochondrial Cyclophilin. *Biochemical Journal* 1992 June 1;284:381-5.

(384) Tanveer A, Virji S, Andreeva L et al. Involvement of cyclophilin D in the activation of a mitochondrial pore by Ca2+ and oxidant stress. *European Journal of Biochemistry* 1996 May;238(1):166-72.

(385) Johnson N, Khan A, Virji S, Ward JM, Crompton M. Import and processing of heart mitochondrial cyclophilin D. *European Journal of Biochemistry* 1999 July;263(2):353-9.

(386) Schreiber SL, Crabtree GR. The Mechanism of Action of Cyclosporine-A and Fk506. *Immunology Today* 1992 April;13(4):136-42.

(387) Nakagawa T, Shimizu S, Watanabe T et al. Cyclophilin D-dependent mitochondrial permeability transition regulates some necrotic but not apoptotic cell death. *Nature* 2005 March 31;434(7033):652-8.

(388) Basso E, Fante L, Fowlkes J, Petronilli V, Forte MA, Bernardi P. Properties of the permeability transition pore in mitochondria devoid of cyclophilin D. *Journal of Biological Chemistry* 2005 May 13;280(19):18558-61.

(389) Clarke SJ, Mcstay GP, Halestrap AP. Sanglifehrin A acts as a potent inhibitor of the mitochondrial permeability transition and reperfusion injury of the heart by binding to cyclophilin-D at a different site from cyclosporin A. *Journal of Biological Chemistry* 2002 September 20;277(38):34793-9.

(390) Bernardi P, Krauskopf A, Basso E et al. The mitochondrial permeability transition from in vitro artifact to disease target (vol 273, pg 2077, 2006). *Febs Journal* 2006 June;273(11):2578.

(391) Di Lisa F, Bernardi P. A CaPful of mechanisms regulating the mitochondrial permeability transition. *Journal of Molecular and Cellular Cardiology* 2009 June;46(6):775-80.

(392) Kroemer G, Galluzzi L, Brenner C. Mitochondrial membrane permeabilization in cell death. *Physiological Reviews* 2007 January;87(1):99-163.

(393) Zorov DB, Juhaszova M, Yaniv Y, Nuss HB, Wang S, Sollott SJ. Regulation and pharmacology of the mitochondrial permeability transition pore. *Cardiovascular Research* 2009 July 15;83(2):213-25.

(394) Halestrap AP. Regulation of Mitochondrial Metabolism Through Changes in Matrix Volume. *Biochemical Society Transactions* 1994 May;22(2):522-9.

(395) Mcstay GP, Clarke SJ, Halestrap AP. Role of critical thiol groups on the matrix surface of the adenine nucleotide translocase in the mechanism of the mitochondrial permeability transition pore. *Biochemical Journal* 2002 October 15;367:541-8.

(396) Crompton M, Costi A. Kinetic Evidence for A Heart Mitochondrial Pore Activated by Ca-2+, Inorganic-Phosphate and Oxidative Stress - A Potential Mechanism for Mitochondrial Dysfunction During Cellular Ca-2+ Overload. *European Journal of Biochemistry* 1988 December 15;178(2):489-501.

(397) Lenartowicz E, Bernardi P, Azzone GF. Phenylarsine Oxide Induces the Cyclosporine-A-Sensitive Membrane-Permeability Transition in Rat-Liver Mitochondria. *Journal of Bioenergetics and Biomembranes* 1991 August;23(4):679-88.

(398) Petronilli V, Cola C, Massari S, Colonna R, Bernardi P. Physiological Effectors Modify Voltage Sensing by the Cyclosporine A-Sensitive Permeability Transition Pore of Mitochondria. *Journal of Biological Chemistry* 1993 October 15;268(29):21939-45.

(399) Petronilli V, Costantini P, Scorrano L, Colonna R, Passamonti S, Bernardi P. The Voltage Sensor of the Mitochondrial Permeability Transition Pore Is Tuned by the Oxidation-Reduction State of Vicinal Thiols - Increase of the Gating Potential by Oxidants and Its Reversal by Reducing Agents. *Journal of Biological Chemistry* 1994 June 17;269(24):16638-42.

(400) Halestrap AP. Calcium-Dependent Opening of A Nonspecific Pore in the Mitochondrial Inner Membrane Is Inhibited at Ph Values Below 7 - Implications for the Protective Effect of Low Ph Against Chemical and Hypoxic Cell-Damage. *Biochemical Journal* 1991 September 15;278:715-9.

(401) Bernardi P, Vassanelli S, Veronese P, Colonna R, Szabo I, Zoratti M. Modulation of the Mitochondrial Permeability Transition Pore - Effect of Protons and Divalent-Cations. *Journal of Biological Chemistry* 1992 February 15;267(5):2934-9.

(402) Petronilli V, Cola C, Bernardi P. Modulation of the Mitochondrial Cyclosporine A-Sensitive Permeability Transition Pore .2. the Minimal Requirements for Pore Induction Underscore A Key Role for Transmembrane Electrical Potential, Matrix Ph, and Matrix Ca2+. *Journal of Biological Chemistry* 1993 January 15;268(2):1011-6.

(403) Bernardi P. Modulation of the Mitochondrial Cyclosporine-A-Sensitive Permeability Transition Pore by the Proton Electrochemical Gradient - Evidence That the Pore Can be Opened by Membrane Depolarization. *Journal of Biological Chemistry* 1992 May 5;267(13):8834-9.

(404) Basso E, Petronilli V, Forte MA, Bernardi P. Phosphate is essential for inhibition of the mitochondrial permeability transition pore by cyclosporin A and by cyclophilin D ablation. *Journal of Biological Chemistry* 2008 September 26;283(39):26307-11.

(405) Halestrap AP, Woodfield KY, Connern CP. Oxidative stress, thiol reagents, and membrane potential modulate the mitochondrial permeability transition by affecting nucleotide binding to the adenine nucleotide translocase. *Journal of Biological Chemistry* 1997 February 7;272(6):3346-54.

(406) Scheffler IE. Mitochondria make a come back. *Advanced Drug Delivery Reviews* 2001 July 2;49(1-2):3-26.

(407) Mozdy AD, McCaffery JM, Shaw JM. Dnm1p GTPase-mediated mitochondrial fission is a multi-step process requiring the novel integral membrane component Fis1p. *Journal of Cell Biology* 2000 October 16;151(2):367-79.

(408) Mancini M, Anderson BO, Caldwell E, Sedghinasab M, Paty PB, Hockenbery DM. Mitochondrial proliferation and paradoxical membrane depolarization during terminal differentiation and apoptosis in a human colon carcinoma cell line. *J Cell Biol* 1997 July 28;138(2):449-69.

(409) Gottlieb RA. Mitochondria and apoptosis. *Biological Signals and Receptors* 2001 May;10(3-4):147-61.

(410) Santel A. Get the balance right: Mitofusins roles in health and disease. *Biochimica et Biophysica Acta-Molecular Cell Research* 2006 May;1763(5-6):490-9.

(411) Detmer SA, Chan DC. Functions and dysfunctions of mitochondrial dynamics. *Nat Rev Mol Cell Biol* 2007 November;8(11):870-9.

(412) Parra V, Eisner V, Chiong M et al. Changes in mitochondrial dynamics during ceramide-induced cardiomyocyte early apoptosis. *Cardiovascular Research* 2008 January 15;77(2):387-97.

(413) Zorzano A, Liesa M, Palacin M. Role of mitochondrial dynamics proteins in the pathophysiology of obesity and type 2 diabetes. *International Journal of Biochemistry & Cell Biology* 2009 October;41(10):1846-54.

(414) Beraud N, Pelloux S, Usson Y et al. Mitochondrial dynamics in heart cells: very low amplitude high frequency fluctuations in adult cardiomyocytes and flow motion in non beating Hl-1 cells. *J Bioenerg Biomembr* 2009 April;41(2):195-214.

(415) Hom J, Sheu SS. Morphological dynamics of mitochondria--a special emphasis on cardiac muscle cells. *J Mol Cell Cardiol* 2009 June;46(6):811-20.

(416) Westermann B. Merging mitochondria matters - Cellular role and molecular machinery of mitochondrial fusion. *Embo Reports* 2002 June;3(6):527-31.

(417) Olichon A, Baricault L, Gas N et al. Loss of OPA1 perturbates the mitochondrial inner membrane structure and integrity, leading to cytochrome c release and apoptosis. *Journal of Biological Chemistry* 2003 March 7;278(10):7743-6.

(418) Cassidy-Stone A, Chipuk JE, Ingerman' E et al. Chemical inhibition of the mitochondrial division dynamin reveals its role in Bax/Bak-dependent mitochondrial outer membrane permeabilization. *Developmental Cell* 2008 February;14(2):193-204.

(419) Sandberg M, Butt E, Nolte C et al. Characterization of Sp-5,6-Dichloro-1-Beta-D-Ribofuranosyl-Benzimidazole-3',5'-Monophosphorothioate (Sp-5,6-Dcl-Cbimps) As A Potent and Specific Activator of Cyclic-Amp-Dependent Protein-Kinase in Cell-Extracts and Intact-Cells. *Biochemical Journal* 1991 October 15;279:521-7.

(420) Mudalagiri NR, Mocanu MM, Di Salvo C et al. Erythropoietin protects the human myocardium against hypoxia/reoxygenation injury via phosphatidylinositol-3 kinase and ERK1/2 activation. *British Journal of Pharmacology* 2008 January;153(1):50-6.

(421) Parsa CJ, Matsumoto A, Kim J et al. A novel protective effect of erythropoietin in the infarcted heart. *Journal of Clinical Investigation* 2003 October;112(7):999-1007.

(422) Tramontano AF, Muniyappa R, Black AD et al. Erythropoietin protects cardiac myocytes from hypoxia-induced apoptosis through an Akt-dependent pathway. *Biochemical and Biophysical Research Communications* 2003 September 5;308(4):990-4.

(423) Cyclosporin A, Tolypocladium inflatum. 2010. Merck Chemicals UK. 16-9-2010.
Ref Type: Online Source

(424) Propidium Iodide. 2010. Sigma-Aldrich UK. 16-9-2010.
Ref Type: Online Source

(425) Tetramethylrhodamine methyl ester perchlorate. 2010. Sigma-Aldrich UK. 16-9-2010.

Ref Type: Online Source

(426) Sp-5,6-Dichloro-cBIMPS. 2010. Enzo Life Sciences UK. 16-9-2010.
Ref Type: Online Source

(427) mdivi-1. 2010. Sigma-Aldrich UK. 16-9-2010.
Ref Type: Online Source

(428) pRc/CMV Vector Map. 2010. Invitrogen. 16-9-2010.
Ref Type: Online Source

(429) White SM, Constantin PE, Claycomb WC. Cardiac physiology at the cellular level: use of cultured HL-1 cardiomyocytes for studies of cardiac muscle cell structure and function. *American Journal of Physiology-Heart and Circulatory Physiology* 2004 March;286(3):H823-H829.

(430) Claycomb WC. Long-Term Culture and Characterization of the Adult Ventricular and Atrial Cardiac-Muscle Cell. *Basic Research in Cardiology* 1985;80:171-4.

(431) Claycomb WC, Lanson N. Isolation and Culture of the Terminally Differentiated Adult Mammalian Ventricular Cardiac-Muscle Cell. *In Vitro-Journal of the Tissue Culture Association* 1984;20(8):647-51.

(432) Claycomb WC, Lanson NA, Stallworth BS et al. HL-1 cells: A cardiac muscle cell line that contracts and retains phenotypic characteristics of the adult cardiomyocyte. *Proceedings of the National Academy of Sciences of the United States of America* 1998 March 17;95(6):2979-84.

(433) Delcarpio JB, Lanson NA, Field LJ, Claycomb WC. Morphological Characterization of Cardiomyocytes Isolated from A Transplantable Cardiac Tumor Derived from Transgenic Mouse Atria (At-1 Cells). *Circulation Research* 1991 December;69(6):1591-600.

(434) Markwald RR. Distribution and Relationship of Precursor Z Material to Organizing Myofibrillar Bundles in Embryonic Rat and Hamster Ventricular Myocytes. *Journal of Molecular and Cellular Cardiology* 1973;5(4):341-&.

(435) Sagazio A, Xiao X, Wang Z, Martari M, Salvatori R. A single injection of double-stranded adeno-associated viral vector expressing GH normalizes growth in GH-deficient mice. *J Endocrinol* 2008 January;196(1):79-88.

(436) Flierl A, Chen Y, Coskun PE, Samulski RJ, Wallace DC. Adeno-associated virus-mediated gene transfer of the heart/muscle adenine nucleotide translocator (ANT) in mouse. *Gene Ther* 2005 April;12(7):570-8.

(437) Date T, Mochizuki S, Belanger AJ et al. Expression of constitutively stable hybrid hypoxia-inducible factor-1alpha protects cultured rat cardiomyocytes against simulated ischemia-reperfusion injury. *Am J Physiol Cell Physiol* 2005 February;288(2):C314-C320.

(438) Nagata M, Takahashi M, Muramatsu S et al. Efficient gene transfer of a simian immuno-deficiency viral vector into cardiomyocytes derived from primate embryonic stem cells. *J Gene Med* 2003 November;5(11):921-8.

(439) Faneca H, Simoes S, de Lima MCP. Evaluation of lipid-based reagents to mediate intracellular gene delivery. *Biochimica et Biophysica Acta-Biomembranes* 2002 December 23;1567(1-2):23-33.

(440) Kiefer K, Clement J, Garidel P, Peschka-Suss R. Transfection efficiency and cytotoxicity of nonviral gene transfer reagents in human smooth muscle and endothelial cells. *Pharmaceutical Research* 2004 June;21(6):1009-17.

(441) Haider HK, Elmadbouh I, Jean-Baptiste M, Ashraf M. Nonviral vector gene modification of stem cells for myocardial repair. *Molecular Medicine* 2008 January;14(1-2):79-86.

(442) Cornelis S, Vandenbranden M, Ruysschaert JM, Elouahabi A. Role of intracellular cationic liposome-DNA complex dissociation in transfection mediated by cationic lipids. *Dna and Cell Biology* 2002 February;21(2):91-7.

(443) Neuhuber B, Huang DI, Daniels MP, Torgan CE. High efficiency transfection of primary skeletal muscle cells with lipid-based reagents. *Muscle & Nerve* 2002 July;26(1):136-40.

(444) Jacobsen LB, Calvin SA, Colvin KE, Wright M. FuGENE 6 Transfection Reagent: the gentle power. *Methods* 2004 June;33(2):104-12.

(445) FuGENE®6 Transfection Reagent. 2009. Roche Diagnostics GmbH . 2-7-2010.
Ref Type: Online Source

(446) Dailey M, Marrs G, Satz J, Waite M. Concepts in imaging and microscopy exploring biological structure and function with confocal microscopy. *Biological Bulletin* 1999 October;197(2):115-22.

(447) Semwogerere D, Weeks ER. Confocal Microscopy. *Encyclopedia of Biomaterials and Biomedical Engineering* 2005;1-10.

(448) Paddock SW. Principles and practices of laser scanning confocal microscopy. *Molecular Biotechnology* 2000 October;16(2):127-49.

(449) Griffiths EJ, Halestrap AP. Protection by Cyclosporine-A of Ischemia Reperfusion-Induced Damage in Isolated Rat Hearts. *Journal of Molecular and Cellular Cardiology* 1993 December;25(12):1461-9.

(450) Shanmuganathan S, Hausenloy DJ, Duchen MR, Yellon DM. Inhibiting mitochondrial permeability transition pore opening protects the human myocardium from ischemia-reperfusion injury. *Circulation* 2004 October 26;110(17):235.

(451) Korge P, Honda HM, Weiss JN. Protection of cardiac mitochondria by diazoxide and protein kinase C: Implications for ischemic preconditioning. *Proceedings of the National Academy of Sciences of the United States of America* 2002 March 5;99(5):3312-7.

(452) Crompton M. The mitochondrial permeability transition pore and its role in cell death. *Biochemical Journal* 1999 July 15;341:233-49.

(453) O'Reilly CM, Fogarty KE, Drummond RM, Tuft RA, Walsh JV. Quantitative analysis of spontaneous mitochondrial depolarizations. *Biophysical Journal* 2003 November 1;85(5):3350-7.

(454) Fontaine E, Ichas F, Bernardi P. A ubiquinone-binding site regulates the mitochondrial permeability transition pore. *Journal of Biological Chemistry* 1998 October 2;273(40):25734-40.

(455) Boengler K, Gres P, Dodoni G et al. Mitochondrial respiration and membrane potential after low-flow ischemia are not affected by ischemic preconditioning. *Journal of Molecular and Cellular Cardiology* 2007 November;43(5):610-5.

(456) Scaduto RC, Jr., Grotyohann LW. Measurement of mitochondrial membrane potential using fluorescent rhodamine derivatives. *Biophys J* 1999 January;76(1 Pt 1):469-77.

(457) Huser J, Rechenmacher CE, Blatter LA. Imaging the permeability pore transition in single mitochondria. *Biophys J* 1998 April;74(4):2129-37.

(458) Huser J, Blatter LA. Fluctuations in mitochondrial membrane potential caused by repetitive gating of the permeability transition pore. *Biochem J* 1999 October 15;343 Pt 2:311-7.

(459) Zhang H, Huang HM, Carson RC, Mahmood J, Thomas HM, Gibson GE. Assessment of membrane potentials of mitochondrial populations in living cells. *Anal Biochem* 2001 November 15;298(2):170-80.

(460) Shaw JM, Nunnari J. Mitochondrial dynamics and division in budding yeast. *Trends in Cell Biology* 2002 April;12(4):178-84.

(461) Karbowski M, Youle RJ. Dynamics of mitochondrial morphology in healthy cells and during apoptosis. *Cell Death and Differentiation* 2003 August;10(8):870-80.

(462) Neuspiel M, Zunino R, Gangaraju S, Rippstein P, McBride H. Activated mitofusin 2 signals mitochondrial fusion, interferes with Bax activation, and reduces susceptibility to radical induced depolarization. *Journal of Biological Chemistry* 2005 July 1;280(26):25060-70.

(463) Molina AJA, Wikstrom JD, Stiles L et al. Mitochondrial Networking Protects beta-Cells From Nutrient-Induced Apoptosis. *Diabetes* 2009 October;58(10):2303-15.

(464) Kim MJ, Kang KH, Kim CH, Choi SY. Real-time imaging of mitochondria in transgenic zebrafish expressing mitochondrially targeted GFP. *Biotechniques* 2008 September;45(3):331-4.

(465) Sun CN, Dhalla NS, Olson RE. Formation of Gigantic Mitochondria in Hypoxic Isolated Perfused Rat Hearts. *Experientia* 1969;25(7):763-&.

(466) Dimmer KS, Navoni F, Casarin A et al. LETM1, deleted in Wolf-Hirschhorn syndrome is required for normal mitochondrial morphology and cellular viability. *Human Molecular Genetics* 2008 January;17(2):201-14.

(467) Gomes LC, Scorrano L. High levels of Fis1, a pro-fission mitochondrial protein, trigger autophagy. *Biochimica et Biophysica Acta-Bioenergetics* 2008 July;1777(7-8):860-6.

(468) de Brito OM, Scorrano L. Mitofusin-2 regulates mitochondrial and endoplasmic reticulum morphology and tethering: The role of Ras. *Mitochondrion* 2009 June;9(3):222-6.

(469) Romanello V, Guadagnin E, Gomes L et al. Mitochondrial fission and remodelling contributes to muscle atrophy. *Embo Journal* 2010 May 19;29(10):1774-85.

(470) Cui M, Tang XN, Christian WV, Yoon Y, Tieu K. Perturbations in Mitochondrial Dynamics Induced by Human Mutant PINK1 Can Be Rescued by the Mitochondrial Division Inhibitor mdivi-1. *Journal of Biological Chemistry* 2010 April 9;285(15):11740-52.

(471) Shimada T, Horita K, Murakami M, Ogura R. Morphological-Studies of Different Mitochondrial Populations in Monkey Myocardial-Cells. *Cell and Tissue Research* 1984;238(3):577-82.

(472) Bakeeva LE, Chentsov YS, Skulachev VP. Intermitochondrial Contacts in Myocardiocytes. *Journal of Molecular and Cellular Cardiology* 1983;15(7):413-20.

(473) Arbustini E, Diegoli M, Fasani R et al. Mitochondrial DNA mutations and mitochondrial abnormalities in dilated cardiomyopathy. *Am J Pathol* 1998 November;153(5):1501-10.

(474) Kraus B, Cain H. Giant mitochondria in the human myocardium--morphogenesis and fate. *Virchows Arch B Cell Pathol Incl Mol Pathol* 1980;33(1):77-89.

(475) Tsang A, Hausenloy DJ, Yellon DM. Myocardial postconditioning: reperfusion injury revisited. *American Journal of Physiology-Heart and Circulatory Physiology* 2005 July;289(1):H2-H7.

(476) Yu TZ, Robotham JL, Yoon Y. Increased production of reactive oxygen species in hyperglycemic conditions requires dynamic change of mitochondrial morphology. *Proceedings of the National Academy of Sciences of the United States of America* 2006 February 21;103(8):2653-8.

(477) Halestrap AP. The mitochondrial permeability transition: its molecular mechanism and role in reperfusion injury. *Mitochondria and Cell Death* 1999;(66):181-203.

(478) Zorov DB, Filburn CR, Klotz LO, Zweier JL, Sollott SJ. Reactive oxygen species (ROS)-induced ROS release: a new phenomenon accompanying induction of the mitochondrial permeability transition in cardiac myocytes. *J Exp Med* 2000 October 2;192(7):1001-14.

(479) Hausenloy DJ, Yellon DM. The mitochondrial permeability transition pore as a critical determinant of cell death. *Journal of Molecular and Cellular Cardiology* 2005 June;38(6):1027.

(480) Riksen NP, Hausenloy DJ, Yellon DM. Erythropoietin: ready for prime-time cardioprotection. *Trends in Pharmacological Sciences* 2008 May;29(5):258-67.

(481) Paschos N, Lykissas MG, Beris AE. The role of erythropoietin as an inhibitor of tissue ischemia. *International Journal of Biological Sciences* 2008;4(3):161-8.

(482) Davidson SM, Hausenloy D, Duchen MR, Yellon DM. Insulin inhibits opening of the mitochondrial permeability transition pore via the reperfusion injury salvage kinase (RISK) pathway. *Circulation* 2004 October 26;110(17):29.

(483) Tsang A, Hausenloy DJ, Mocanu MM, Carr RD, Yellon DM. Preconditioning the diabetic heart - The importance of Akt phosphorylation. *Diabetes* 2005 August;54(8):2360-4.

(484) Ludman A, Hausenloy DJ, Venugopal V, Yellon DM. Can high-dose atorvastatin provide cardioprotection during coronary artery bypass surgery? *Journal of Molecular and Cellular Cardiology* 2008 April;44(4):729.

(485) Ludman A, Venugopal V, Yellon DM, Hausenloy DJ. Statins and cardioprotection - More than just lipid lowering? *Pharmacology & Therapeutics* 2009 April;122(1):30-43.

(486) Iliodromitis EK, Papalois A, Gritsopoulos G, Kremastinos DT, Yellon DM, Hausenloy DJ. Remote Ischaemic Preconditioning and Postconditioning and the Reperfusion Injury Salvage Kinase Pathway. *Heart* 2009 June;95:A11.

(487) Lim SY, Davidson SM, Paramanathan AJ, Smith CCT, Yellon DM, Hausenloy DJ. The novel adipocytokine visfatin exerts direct cardioprotective effects. *Journal of Cellular and Molecular Medicine* 2008 August;12(4):1395-403.

(488) Brady NR, Hamacher-Brady A, Gottlieb RA. Proapoptotic BCL-2 family members and mitochondrial dysfunction during ischemia/reperfusion

injury, a study employing cardiac HL-1 cells and GFP biosensors. *Biochim Biophys Acta* 2006 May;1757(5-6):667-78.

(489) Bossy-Wetzel E, Barsoum MJ, Godzik A, Schwarzenbacher R, Lipton SA. Mitochondrial fission in apoptosis, neurodegeneration and aging. *Curr Opin Cell Biol* 2003 December;15(6):706-16.

(490) Chen HC, Chomyn A, Chan DC. Disruption of fusion results in mitochondrial heterogeneity and dysfunction. *Journal of Biological Chemistry* 2005 July 15;280(28):26185-92.

(491) Desagher S, Martinou JC. Mitochondria as the central control point of apoptosis. *Trends Cell Biol* 2000 September;10(9):369-77.

(492) De VK, Goossens V, Boone E et al. The 55-kDa tumor necrosis factor receptor induces clustering of mitochondria through its membrane-proximal region. *J Biol Chem* 1998 April 17;273(16):9673-80.

(493) Zhuang J, Dinsdale D, Cohen GM. Apoptosis, in human monocytic THP.1 cells, results in the release of cytochrome c from mitochondria prior to their ultracondensation, formation of outer membrane discontinuities and reduction in inner membrane potential. *Cell Death Differ* 1998 November;5(11):953-62.

(494) Alloatti G, Arnoletti E, Bassino E et al. Obestatin affords cardioprotection to the ischemic/reperfused isolated rat heart and inhibits apoptosis in cultures of similarly stressed cardiomyocytes. *Am J Physiol Heart Circ Physiol* 2010 June 4.

(495) Sivaraman V, Hausenloy DJ, Kolvekar S et al. The divergent roles of protein kinase C epsilon and delta in simulated ischaemia-reperfusion injury in human myocardium. *Journal of Molecular and Cellular Cardiology* 2009 May;46(5):758-64.

(496) Lim SY, Davidson SM, Hausenloy DJ, Yellon DM. Preconditioning and postconditioning: The essential role of the mitochondrial DC permeability transition pore. *Cardiovascular Research* 2007 August 1;75(3):530-5.

(497) Lim SY, Davidson SM, Yellon DM, Smith CC. The cannabinoid CB1 receptor antagonist, rimonabant, protects against acute myocardial infarction. *Basic Res Cardiol* 2009 November;104(6):781-92.

(498) Simpkin JC, Yellon DM, Davidson SM, Lim SY, Wynne AM, Smith CC. Apelin-13 and apelin-36 exhibit direct cardioprotective activity against ischemia-reperfusion injury. *Basic Res Cardiol* 2007 November;102(6):518-28.

(499) Smith CC, Davidson SM, Lim SY, Simpkin JC, Hothersall JS, Yellon DM. Necrostatin: a potentially novel cardioprotective agent? *Cardiovasc Drugs Ther* 2007 August;21(4):227-33.

(500) Gabel SA, Walker VR, London RE, Steenbergen C, Korach KS, Murphy E. Estrogen receptor beta mediates gender differences in ischemia/reperfusion injury. *J Mol Cell Cardiol* 2005 February;38(2):289-97.

(501) Zhai P, Eurell TE, Cooke PS, Lubahn DB, Gross DR. Myocardial ischemia-reperfusion injury in estrogen receptor-alpha knockout and wild-type mice. *Am J Physiol Heart Circ Physiol* 2000 May;278(5):H1640-H1647.

(502) Argaud L, Gateau-Roesch O, Muntean D et al. Specific inhibition of the mitochondrial permeability transition prevents lethal reperfusion injury. *J Mol Cell Cardiol* 2005 February;38(2):367-74.

(503) Hausenloy DJ, Wynne AM, Yellon DM. Ischemic preconditioning targets the reperfusion phase. *Basic Research in Cardiology* 2007 September;102(5):445-52.

(504) Shiang-Yong L, Hausenloy D, Davidson S, Yellon D. Preconditioning and postconditioning: The mitochondrial permeablity transition pore as the common end-effector. *Heart* 2007 June;93:A18.

(505) Hausenloy DJ, Yellon DM. Preconditioning and postconditioning: new strategies for cardioprotection. *Diabetes Obesity & Metabolism* 2008 June;10(6):451-9.

(506) Clarke SJ, Khaliulin I, Das M, Parker JE, Heesom KJ, Halestrap AP. Inhibition of mitochondrial permeability transition pore opening by ischemic preconditioning is probably mediated by reduction of oxidative stress rather than mitochondrial protein phosphorylation. *Circ Res* 2008 May 9;102(9):1082-90.

(507) Hausenloy DJ, Yellon DM. Preconditioning and postconditioning: Underlying mechanisms and clinical application. *Atherosclerosis* 2009 June;204(2):334-41.

(508) Hausenloy DJ, Ong SB, Yellon DM. The mitochondrial permeability transition pore as a target for preconditioning and postconditioning. *Basic Research in Cardiology* 2009 March;104(2):189-202.

(509) Crompton M, Virji S, Doyle V, Johnson N, Ward JM. The mitochondrial permeability transition pore. *Biochem Soc Symp* 1999;66:167-79.

(510) Graziewicz MA, Day BJ, Copeland WC. The mitochondrial DNA polymerase as a target of oxidative damage. *Nucleic Acids Research* 2002 July 1;30(13):2817-24.

(511) Davidson SM, Lim SY, Yellon DM, Hausenloy DJ. The Mitochondrial Permeability Transition Pore As A Mediator of Ischaemic Preconditioning. *Heart* 2009 June;95:A11-A12.

(512) Duchen MR, Leyssens A, Crompton M. Transient mitochondrial depolarizations reflect focal sarcoplasmic reticular calcium release in single rat cardiomyocytes. *J Cell Biol* 1998 August 24;142(4):975-88.

(513) De GF, Lartigue L, Bauer MK et al. The permeability transition pore signals apoptosis by directing Bax translocation and multimerization. *FASEB J* 2002 April;16(6):607-9.

(514) Bhamra GS, Hausenloy DJ, Davidson SM et al. Metformin protects the ischemic heart by the Akt-mediated inhibition of mitochondrial permeability transition pore opening. *Basic Research in Cardiology* 2008 May;103(3):274-84.

(515) Halestrap AP, Connern CP, Griffiths EJ, Kerr PM. Cyclosporin A binding to mitochondrial cyclophilin inhibits the permeability transition pore and protects hearts from ischaemia/reperfusion injury. *Mol Cell Biochem* 1997 September;174(1-2):167-72.

(516) Nazareth W, Yafei N, Crompton M. Inhibition of anoxia-induced injury in heart myocytes by cyclosporin A. *J Mol Cell Cardiol* 1991 December;23(12):1351-4.

(517) Duchen MR, McGuinness O, Brown LA, Crompton M. On the involvement of a cyclosporin A sensitive mitochondrial pore in myocardial reperfusion injury. *Cardiovasc Res* 1993 October;27(10):1790-4.

(518) Routhu KV, Tsopanoglou NE, Strande JL. Parstatin(1-26): the putative signal peptide of protease-activated receptor 1 confers potent protection from myocardial ischemia-reperfusion injury. *J Pharmacol Exp Ther* 2010 March;332(3):898-905.

(519) Yao Y, Li L, Li L, Gao C, Shi C. Sevoflurane postconditioning protects chronically-infarcted rat hearts against ischemia-reperfusion injury by activation of pro-survival kinases and inhibition of mitochondrial permeability transition pore opening upon reperfusion. *Biol Pharm Bull* 2009 November;32(11):1854-61.

(520) Hausenloy DJ, Mani-Babu S, Duchen MR, Yellon DM. Mitochondrial KATP channel activation protects the myocyte against oxidative stress by inhibiting mitochondrial permeability transition pore opening. *Circulation* 2002 November 5;106(19):230.

(521) Hausenloy DJ, Yellon DM. Adenosine-induced second window of protection is mediated by inhibition of mitochondrial permeability transition pore opening at the time of reperfusion. *Cardiovascular Drugs and Therapy* 2004 January;18(1):79-80.

(522) Hausenloy D, Wynne A, Mocanu M, Yellon D. Glimepiride treatment facilitates the protective effect of ischaemic preconditioning in the diabetic heart. *Heart* 2007 June;93:A17.

(523) Hausenloy D, Bhamra G, Davidson S, Carr R, Mocanu M, Yellon D. Metformin given at time of reperfusion reduces myocardial infarct size through the Akt-mediated inhibition of mitochondrial permeability transition pore opening. *Heart* 2007 June;93:A15-A16.

(524) Hausenloy D, Shiang-Yong L, Paramanathan A, Davidson S, Smith C, Yellon D. The adipocytokine, visfatin, reduces myocardial infarct size, when given at time of reperfusion, by inhibiting the mitochondrial permeability transition pore. *Heart* 2007 June;93:A15.

(525) Devalaraja-Narashimha K, Diener AM, Padanilam BJ. Cyclophilin D gene ablation protects mice from ischemic renal injury. *Am J Physiol Renal Physiol* 2009 September;297(3):F749-F759.

(526) Li V, Brustovetsky T, Brustovetsky N. Role of cyclophilin D-dependent mitochondrial permeability transition in glutamate-induced calcium deregulation and excitotoxic neuronal death. *Exp Neurol* 2009 August;218(2):171-82.

(527) Palma E, Tiepolo T, Angelin A et al. Genetic ablation of cyclophilin D rescues mitochondrial defects and prevents muscle apoptosis in collagen VI myopathic mice. *Hum Mol Genet* 2009 June 1;18(11):2024-31.

(528) Fujimoto K, Chen Y, Polonsky KS, Dorn GW. Targeting cyclophilin D and the mitochondrial permeability transition enhances beta-cell survival and prevents diabetes in Pdx1 deficiency. *Proc Natl Acad Sci U S A* 2010 June 1;107(22):10214-9.

(529) Nishida H, Sato T, Miyazaki M, Nakaya H. Infarct size limitation by adrenomedullin: protein kinase A but not PI3-kinase is linked to mitochondrial KCa channels. *Cardiovasc Res* 2008 January 15;77(2):398-405.

(530) Fukasawa M, Nishida H, Sato T, Miyazaki M, Nakaya H. 6-[4-(1-Cyclohexyl-1H-tetrazol-5-yl)butoxy]-3,4-dihydro-2-(1H)quinolinone (cilostazol), a phosphodiesterase type 3 inhibitor, reduces infarct size via activation of mitochondrial Ca2+-activated K+ channels in rabbit hearts. *J Pharmacol Exp Ther* 2008 July;326(1):100-4.

(531) Cui XW, Zhao FJ, Liu J et al. Suppression of Akt1 expression by small interference RNA inhibits SGC7901 cell growth in vitro and in vivo. *Oncol Rep* 2009 December;22(6):1305-13.

(532) Antico Arciuch VG, Galli S, Franco MC et al. Akt1 intramitochondrial cycling is a crucial step in the redox modulation of cell cycle progression. *PLoS One* 2009;4(10):e7523.

(533) Ueki K, Yamamoto-Honda R, Kaburagi Y et al. Potential role of protein kinase B in insulin-induced glucose transport, glycogen synthesis, and protein synthesis. *J Biol Chem* 1998 February 27;273(9):5315-22.

(534) Kohn AD, Summers SA, Birnbaum MJ, Roth RA. Expression of a constitutively active Akt Ser/Thr kinase in 3T3-L1 adipocytes stimulates glucose uptake and glucose transporter 4 translocation. *J Biol Chem* 1996 December 6;271(49):31372-8.

(535) Tanti JF, Grillo S, Gremeaux T, Coffer PJ, Van OE, Le Marchand-Brustel Y. Potential role of protein kinase B in glucose transporter 4 translocation in adipocytes. *Endocrinology* 1997 May;138(5):2005-10.

(536) Bae SS, Cho H, Mu J, Birnbaum MJ. Isoform-specific regulation of insulin-dependent glucose uptake by Akt/protein kinase B. *J Biol Chem* 2003 December 5;278(49):49530-6.

(537) Wynne AM, Hausenloy D. Reperfusion signaling in preconditioned hearts: Role for Pkc, the Mkatp channel, oxidative stress and transient acidosis. *Journal of Molecular and Cellular Cardiology* 2007 June;42:S173.

(538) Mackay K, Mochly-Rosen D. Arachidonic acid protects neonatal rat cardiac myocytes from ischaemic injury through epsilon protein kinase C. *Cardiovasc Res* 2001 April;50(1):65-74.

(539) Cross HR, Murphy E, Bolli R, Ping P, Steenbergen C. Expression of activated PKC epsilon (PKC epsilon) protects the ischemic heart, without attenuating ischemic H(+) production. *J Mol Cell Cardiol* 2002 March;34(3):361-7.

(540) Kim MH, Jung YS, Moon CH et al. Isoform-specific induction of PKC-epsilon by high glucose protects heart-derived H9c2 cells against hypoxic injury. *Biochem Biophys Res Commun* 2003 September 12;309(1):1-6.

(541) Bright R, Raval AP, Dembner JM et al. Protein kinase C delta mediates cerebral reperfusion injury in vivo. *J Neurosci* 2004 August 4;24(31):6880-8.

(542) Basu A. Involvement of protein kinase C-delta in DNA damage-induced apoptosis. *J Cell Mol Med* 2003 October;7(4):341-50.

(543) Brodie C, Blumberg PM. Regulation of cell apoptosis by protein kinase c delta. *Apoptosis* 2003 January;8(1):19-27.

(544) Barillas R, Friehs I, Cao-Danh H, Martinez JF, del Nido PJ. Inhibition of glycogen synthase kinase-3beta improves tolerance to ischemia in hypertrophied hearts. *Ann Thorac Surg* 2007 July;84(1):126-33.

(545) Clodfelder-Miller B, De SP, Zmijewska AA, Song L, Jope RS. Physiological and pathological changes in glucose regulate brain Akt and glycogen synthase kinase-3. *J Biol Chem* 2005 December 2;280(48):39723-31.

(546) Nakae J, Park BC, Accili D. Insulin stimulates phosphorylation of the forkhead transcription factor FKHR on serine 253 through a Wortmannin-sensitive pathway. *J Biol Chem* 1999 June 4;274(23):15982-5.

(547) Rena G, Guo S, Cichy SC, Unterman TG, Cohen P. Phosphorylation of the transcription factor forkhead family member FKHR by protein kinase B. *J Biol Chem* 1999 June 11;274(24):17179-83.

(548) Dostmann WR, Taylor SS, Genieser HG, Jastorff B, Doskeland SO, Ogreid D. Probing the cyclic nucleotide binding sites of cAMP-dependent protein kinases I and II with analogs of adenosine 3',5'-cyclic phosphorothioates. *J Biol Chem* 1990 June 25;265(18):10484-91.

(549) Kotani K, Ogawa W, Hino Y et al. Dominant negative forms of Akt (protein kinase B) and atypical protein kinase Clambda do not prevent insulin inhibition of phosphoenolpyruvate carboxykinase gene transcription. *J Biol Chem* 1999 July 23;274(30):21305-12.

(550) Schaap P, van Ments-Cohen M, Soede RD et al. Cell-permeable non-hydrolyzable cAMP derivatives as tools for analysis of signaling pathways controlling gene regulation in Dictyostelium. *J Biol Chem* 1993 March 25;268(9):6323-31.

(551) Laychock SG. Sp-5,6-dichloro-1-beta-D-ribofuranosylbenzimidazole-3',5'-cyclic monophosphorothioate is a potent stimulus for insulin release. *Endocr Res* 1993;19(2-3):113-22.

(552) Shintani Y, Node K, Asanuma H et al. Opening of Ca2+-activated K+ channels is involved in ischemic preconditioning in canine hearts. *J Mol Cell Cardiol* 2004 December;37(6):1213-8.

(553) Xu W, Liu Y, Wang S et al. Cytoprotective role of Ca2+- activated K+ channels in the cardiac inner mitochondrial membrane. *Science* 2002 November 1;298(5595):1029-33.

(554) Songyang Z, Baltimore D, Cantley LC, Kaplan DR, Franke TF. Interleukin 3-dependent survival by the Akt protein kinase. *Proc Natl Acad Sci U S A* 1997 October 14;94(21):11345-50.

(555) Bodine SC, Stitt TN, Gonzalez M et al. Akt/mTOR pathway is a crucial regulator of skeletal muscle hypertrophy and can prevent muscle atrophy in vivo. *Nat Cell Biol* 2001 November;3(11):1014-9.

(556) Bernal-Mizrachi E, Wen W, Stahlhut S, Welling CM, Permutt MA. Islet beta cell expression of constitutively active Akt1/PKB alpha induces striking hypertrophy, hyperplasia, and hyperinsulinemia. *J Clin Invest* 2001 December;108(11):1631-8.

(557) Burger DE, Xiang FL, Hammoud L, Jones DL, Feng Q. Erythropoietin protects the heart from ventricular arrhythmia during ischemia and reperfusion via neuronal nitric-oxide synthase. *J Pharmacol Exp Ther* 2009 June;329(3):900-7.

(558) Mihov D, Bogdanov N, Grenacher B et al. Erythropoietin protects from reperfusion-induced myocardial injury by enhancing coronary endothelial nitric oxide production. *Eur J Cardiothorac Surg* 2009 May;35(5):839-46.

(559) Chan CY, Chen YS, Lee HH et al. Erythropoietin protects post-ischemic hearts by preventing extracellular matrix degradation: role of Jak2-ERK pathway. *Life Sci* 2007 August 9;81(9):717-23.

(560) Ferrario M, Arbustini E, Massa M et al. High-dose erythropoietin in patients with acute myocardial infarction: A pilot, randomised, placebo-controlled study. *Int J Cardiol* 2009 November 9.

(561) Lipsic E, Schoemaker RG, van der Meer P, Voors AA, van Veldhuisen DJ, van Gilst WH. Protective effects of erythropoietin in cardiac ischemia: from bench to bedside. *J Am Coll Cardiol* 2006 December 5;48(11):2161-7.

(562) Lipsic E, van der Meer P, Voors AA et al. A single bolus of a long-acting erythropoietin analogue darbepoetin alfa in patients with acute myocardial infarction: a randomized feasibility and safety study. *Cardiovasc Drugs Ther* 2006 April;20(2):135-41.

(563) Yano H, Nakanishi S, Kimura K et al. Inhibition of histamine secretion by wortmannin through the blockade of phosphatidylinositol 3-kinase in RBL-2H3 cells. *J Biol Chem* 1993 December 5;268(34):25846-56.

(564) Park YC, Lee CH, Kang HS, Chung HT, Kim HD. Wortmannin, a specific inhibitor of phosphatidylinositol-3-kinase, enhances LPS-induced NO production from murine peritoneal macrophages. *Biochem Biophys Res Commun* 1997 November 26;240(3):692-6.

(565) Arcaro A, Wymann MP. Wortmannin is a potent phosphatidylinositol 3-kinase inhibitor: the role of phosphatidylinositol 3,4,5-trisphosphate in neutrophil responses. *Biochem J* 1993 December 1;296 (Pt 2):297-301.

(566) Berger J, Hayes N, Szalkowski DM, Zhang B. PI 3-kinase activation is required for insulin stimulation of glucose transport into L6 myotubes. *Biochem Biophys Res Commun* 1994 November 30;205(1):570-6.

(567) Cong LN, Chen H, Li Y et al. Physiological role of Akt in insulin-stimulated translocation of GLUT4 in transfected rat adipose cells. *Mol Endocrinol* 1997 December;11(13):1881-90.

(568) Kulik G, Weber MJ. Akt-dependent and -independent survival signaling pathways utilized by insulin-like growth factor I. *Mol Cell Biol* 1998 November;18(11):6711-8.

(569) Lee CW, Lin CC, Lin WN et al. TNF-alpha induces MMP-9 expression via activation of Src/EGFR, PDGFR/PI3K/Akt cascade and promotion of NF-kappaB/p300 binding in human tracheal smooth muscle cells. *Am J Physiol Lung Cell Mol Physiol* 2007 March;292(3):L799-L812.

(570) Doronin S, Shumay E, Wang HY, Malbon CC. Akt mediates sequestration of the beta(2)-adrenergic receptor in response to insulin. *J Biol Chem* 2002 April 26;277(17):15124-31.

(571) Park SS, Zhao H, Mueller RA, Xu Z. Bradykinin prevents reperfusion injury by targeting mitochondrial permeability transition pore through glycogen synthase kinase 3beta. *J Mol Cell Cardiol* 2006 May;40(5):708-16.

(572) Nishihara M, Miura T, Miki T et al. Modulation of the mitochondrial permeability transition pore complex in GSK-3beta-mediated myocardial protection. *J Mol Cell Cardiol* 2007 November;43(5):564-70.

(573) Wang G, Liem DA, Vondriska TM et al. Nitric oxide donors protect murine myocardium against infarction via modulation of mitochondrial permeability transition. *Am J Physiol Heart Circ Physiol* 2005 March;288(3):H1290-H1295.

(574) Gao F, Gao E, Yue TL et al. Nitric oxide mediates the antiapoptotic effect of insulin in myocardial ischemia-reperfusion: the roles of PI3-kinase, Akt, and endothelial nitric oxide synthase phosphorylation. *Circulation* 2002 March 26;105(12):1497-502.

(575) Kim JS, Ohshima S, Pediaditakis P, Lemasters JJ. Nitric oxide protects rat hepatocytes against reperfusion injury mediated by the mitochondrial permeability transition. *Hepatology* 2004 June;39(6):1533-43.

(576) Twig G, Graf SA, Wikstrom JD et al. Tagging and tracking individual networks within a complex mitochondrial web with photoactivatable GFP. *Am J Physiol Cell Physiol* 2006 July;291(1):C176-C184.

(577) Guo X, Chen KH, Guo Y, Liao H, Tang J, Xiao RP. Mitofusin 2 triggers vascular smooth muscle cell apoptosis via mitochondrial death pathway. *Circ Res* 2007 November 26;101(11):1113-22.

(578) Shen T, Zheng M, Cao C et al. Mitofusin-2 is a major determinant of oxidative stress-mediated heart muscle cell apoptosis. *J Biol Chem* 2007 August 10;282(32):23354-61.

(579) Pauleau AL, Galluzzi L, Scholz SR, Larochette N, Kepp O, Kroemer G. Unexpected role of the phosphate carrier in mitochondrial fragmentation. *Cell Death Differ* 2008 March;15(3):616-8.

(580) Tatsuta T, Langer T. Quality control of mitochondria: protection against neurodegeneration and ageing. *EMBO J* 2008 January 23;27(2):306-14.

(581) Parone PA, Da CS, Tondera D et al. Preventing mitochondrial fission impairs mitochondrial function and leads to loss of mitochondrial DNA. *PLoS One* 2008;3(9):e3257.

(582) Szewczyk A, Wojtczak L. Mitochondria as a pharmacological target. *Pharmacol Rev* 2002 March;54(1):101-27.

(583) Pich S, Bach D, Briones P et al. The Charcot-Marie-Tooth type 2A gene product, Mfn2, up-regulates fuel oxidation through expression of OXPHOS system. *Hum Mol Genet* 2005 June 1;14(11):1405-15.

(584) Lemasters JJ, Qian T, Trost LC et al. Confocal microscopy of the mitochondrial permeability transition in necrotic and apoptotic cell death. *Biochem Soc Symp* 1999;66:205-22.

(585) Sivaraman V, Mudalagiri NR, Di Salvo C et al. Postconditioning protects human atrial muscle through the activation of the RISK pathway. *Basic Research in Cardiology* 2007 September;102(5):453-9.

(586) Vanhorebeek I, De VR, Mesotten D, Wouters PJ, De Wolf-Peeters C, Van den Berghe G. Protection of hepatocyte mitochondrial ultrastructure and function by strict blood glucose control with insulin in critically ill patients. *Lancet* 2005 January 1;365(9453):53-9.

(587) Kelley DE, He J, Menshikova EV, Ritov VB. Dysfunction of mitochondria in human skeletal muscle in type 2 diabetes. *Diabetes* 2002 October;51(10):2944-50.

(588) Bach D, Naon D, Pich S et al. Expression of Mfn2, the Charcot-Marie-Tooth neuropathy type 2A gene, in human skeletal muscle - Effects of type 2 diabetes, obesity, weight loss, and the regulatory role of tumor necrosis factor alpha, and interleukin-6. *Diabetes* 2005 September;54(9):2685-93.

(589) Kong D, Xu L, Yu Y et al. Regulation of Ca2+-induced permeability transition by Bcl-2 is antagonized by Drpl and hFis1. *Mol Cell Biochem* 2005 April;272(1-2):187-99.

(590) Skulachev VP, Bakeeva LE, Chernyak BV et al. Thread-grain transition of mitochondrial reticulum as a step of mitoptosis and apoptosis. *Mol Cell Biochem* 2004 January;256-257(1-2):341-58.

(591) Wallace DC. Mitochondrial diseases in man and mouse. *Science* 1999 March 5;283(5407):1482-8.

(592) Ballinger SW. Mitochondrial dysfunction in cardiovascular disease. *Free Radic Biol Med* 2005 May 15;38(10):1278-95.

(593) Hackenbrock CR. Ultrastructural bases for metabolically linked mechanical activity in mitochondria. I. Reversible ultrastructural changes with change in metabolic steady state in isolated liver mitochondria. *J Cell Biol* 1966 August;30(2):269-97.